Vrije Universiteit Brusseld
Faculty of Applied Sciencesd
Laboratory of Hydrologyd

MODELING THREE-DIMENSIONAL GROUNDWATER FLOW AND TRANSPORT BY HEXAHEDRAL FINITE ELEMENTS

ByA

MohammedAAdilASBAIA

Thesis!submitted!in!fulfillment!of!
the!requirements!for!the!award!
of the degree of Doctor of Philosophy in !
Applied!Sciences!

September, 1999A

'Say "O my lord ! advance me in knowledge'

The!Holy!Quran,!chapter!16,!verse!114.!

Dedicationd

To my lovely mother,7
and all my teachers.7

Author's Thesis Committeed

Promoter: *Prof. F. De Smedt (Freey University ofy Brussels)*

Members of the Jury:

Prof. R. Ababou (University ofy Toulouse)	Member!
Prof. W. Bauwens (Free University of Brussels)	Member!
Prof A. Larabi (Mohammedy V University ofy Rabat)	Member!
Prof. J. Vereecken (Freey University ofy Brussels)	Vice-Chairman!
Prof. K. Walraevens (University ofy Ghent)	Member!
Prof. A. Van der Beken (Freey University ofy Brussels)	Chairman!

Acknowledgmentsd

Financial! support! for! this! research! work! was! granted! by! VUB! scholarships! from! the! AVICENNE! project! funds,! given! by! the! commission! of! the! European! Union! under! contract! No.! CT93AVI2073,! entitled:! 'Development! of! water! resources! management! tools! for! problems! of! seawater! intrusion! and! contamination! of! freshwater! resources! in! coastal! aquifers'.! The! author! is! also! thankful! to! 'David! et! Alice! Van! Beuren'! foundation! for! their! financial! aid! for! the! academic! year! 1998-1999! enabling! him! to! finish! successfully! his! doctoral! thesis.!

My! deep! gratitude! goes! to! my! promoter! Prof.! Dr.! ir.! F.! De! Smedt,! chairman! of! the! InterUniversity! Program! of! Water! Resources! Engineering! (IUPWARE),! for! his! unconditional! contribution! to! the! success! of! this! thesis,! by! giving! moral,! financial! and! human! support.! I'm! indebted! to! his! wide! scientific! skills,! talent,! kindness,! and! patience.! He! remains! to! me! the! first! source! of! inspiration! during! this! study! leave,! by! sharing! his! knowledge! with! me,! all! his! former! students! and! co-workers!.!

I'am! very! thankful! to! Prof.! Dr.! ir.! A.! Van! der! Beken,! director! of! the! Laboratory! of! Hydrology,! for! the! positive! support! and! encouragements! throughout! my! Ph.D.! roads.!

Extended! thanks! to! Prof.! Dr.! ir.! A.! Larabi! from! M.! V.! University,! Ecole! Moham-! madia! d'Ingénieurs,! Hydrogeology! Section,! Rabat,! Morocco.! As! a! former! Ph.D.! at! the! Laboratory! of! Hydrology,! he! inspired! my! skills! at! many! stages,! and! was! always! avail-! able! and! eager! to! help.! I! appreciated! gratefully! his! sense! of! criticism! on! the! contents! of! a! primary! version! of! this! thesis! dissertation! which! he! kindly! accept! to! revise.!

My! thanks! to! all! the! members! of! Jury,! for! accepting! to! be! a! part! of! the! author's! the-! sis! committee,! and! for! providing! many! suggestions,! and! useful! comments! which! surely! rises! the! standard! of! this! thesis.! Any! remaining! mistakes! are! my! own! responsibility.!

I'm! so! afraid! to! forget! somebody's! name! of! all! IUPWARE! technical! and! scientific! staff,! and! Ph.D's! I! have! meet! since! my! arrival! in! July! 1995.! Thanks! to! all! of! you! guys! for! your! help! and! making! the! working! environment! as! pleasant! as! possible.!

Finally,! my! heartfelt! thanks! goes! to! all! members! of! my! family,! for! their! love! and! support.! My! parents! moral! principles! and! philosophy! was! the! first! catalyzer! to! end! up! four! years! of! hard! work.! Staying! abroad! in! difficult! conditions,! whiled! away! days! (and! nights!)! looking! for! a! particular! problem! solution,! frustrated! over! extended! periods! of! time,! combined! with! lack! of! sleep,! too! much! coffee,! and! heatburn! pizza! was! the! price! to! pay! for! this! Ph.D.! degree.!

M.AA. SBAI

Brussels, September 1999w

Abstractd

Modeling Threey Dimensional Groundwatery Flowy and Transporty by Hexahedral Finitey Elementsy

By

MohammedyAdilySBAIy

Doctor of Philosophy in Applied Sciencesw

Free University of Brusselsw

Faculty of Applied Sciencesw

This!research!work!deals!with!three-dimensional!modeling!of!groundwater!flow!and! solute! transport! problems! in! groundwater! aquifer! systems,! with! several! complexities,! heterogeneities! and! variable! conditions! as! encountered! in! the! field.! Finite! element! methods!are!used!throughout!to!solve!a!range!of!different!problems,!using!in!particular! the!Galerkin!weighted!residual!approach!based!on!trilinear!hexahedral!elements.!

Special! emphasis! is! made! on! transient! and! non-linear! groundwater! flow! problems! with! moving! interfaces,! such! as! the! water! table! and! the! freshwater-saltwater! sharp! interface.! A!generalized!Fast!Updating!Procedure!technique!is!developed!for!these!sit-! uations,! which! presents! a! number! of! advantageous! features! in! comparison! to! classic! computational!techniques!used!to!deal!with!such!problems.! One!of!the!important!con-! tributions!is!the!automatic!construction!of!the!generic!soils!characteristic!curves,!which! are!dynamically!dependent!upon!the!overall!system!water!status.! Several!test!examples! are!successfully!worked!out!for!validating!this!technique!in!different!aquifer!configura-! tions,!and!under!different!initial!and!boundary!conditions.! These!test!cases!show!that! the! proposed! method! is! cheap,! numerically! stable! and! accurate.! Numerical! stability! is! guaranteed! through! a! developed! solver,! which! is! obtained! by! using! state! of! the! art!

methods! for! robust! preconditioning! and! efficient! numerical! implementation.! The! ac-! curacy!is!demonstrated!by!comparison!against!analytical,!other!numerical!approaches,! and!laboratory!experimental!solutions.!

The!usefulness!of!the!method!is!clearly!shown!by!the!application!of!the!3-D!sharp! interface!finite!element!model!'GEO-SWIM'!to!the!coastal!aquifer!system!of!Martil!in! the! north! of! Morocco.! Several! efficient! runs! are! made,! leading! to! a! calibrated! man-! agement!model!for!the!study!area,!giving!a!clear!picture!of!the!salinization!risk!in!the! aquifer!due!to!saltwater!encroachment.!

Three-dimensional! modeling! of! solute! transport! problems! in! groundwater! aquifer! systems! is! equally! investigated.! It! is! concluded! that! the! standard! Galerkin! finite! el-! ement! method! is! computationally! intensive,! since! the! obtained! system! of! numerical! equations! is! very! large,! sparse,! none! symmetric! and! usually! difficult! to! solve! with! standard!iterative!techniques.! Hence,!preconditioning!is!necessary!to!improve!the!con-! vergence! behavior! of! ill-conditioned! systems.! In! this! work,! we! propose! an! M! matrix! type!of!transformation!on!the!general!transport!matrix!which!guarantees!the!existence! of! the! preconditioning! schemes,! and! hence! improves! the! overall! solvers! performance! and!robustness.! The!usefulness!of!the!method!is!demonstrated!by!solving!several!test! examples! with! different! complexities,! including! hypothetical! and! field! applications! in! Belgium.! Different!solvers!are!tested!as!the!minimal!residual!method!and!the!stabilized! biconjugate! gradient! method,! in! combination! with! different! preconditioning! schemes,! as! diagonal! scaling! and! incomplete! factorization.! It! is! concluded! that! M! matrix! pre-! conditioning!is!very!simple!to!implement,!and!proves!to!be!very!efficient!and!robust.!

An! effort! is! put! on! packaging! the! computer! programs,! by! giving! modern! visual! support! to! many! modules.! Therefore,! several! GUI! programs! are! provided! as! comple-! mentary! tools! to! support! the! developed! models,! enabling! their! friendly! use,! and! the! possibility!for!future!extensions.!

Contentsg

List of Figures

List of Tables

List of Mathematical Notations and Symbolsd

Symbol	Description
$\|.\|$	Absolute!value!
ψ_a	Air-entry!pressure!head!value![L]!
b_i, b_j	Basis!functions!
$\mathbf{B}$, $\mathbf{B}^*$	Boundary!conditions!vector!
C!	Concentration!of!dissolved!matter![ML^{-3}]!
Ω_i	Control!volume!of!node!i![L^3]!
c!	Normalized!concentration![dimensionless]!
C_D	Source!distribution!function![ML^{-3}]!
$\mathbf{Cy}$	Unknown!concentration!vector![ML^{-3}]!
C_w	Water!capacity![L^{-1}]!
∇	Del!operator!
δ	Density!difference!ratio![dimensionless]!
$\mathbf{Dy}$	Diagonal!matrix!
dV	Differential!volume!
μ	Dynamic!viscosity!of!water![$ML^{-1}T^{-1}$]!
$\mathbb{D}$	Hydrodynamic!dispersion!tensor![L^2T^1]!
$erfc$	Complementary!error!function!
erf	Error!function!
exp	Exponential!function!
e^m_{max4}	Maximum!error!at!iteration!level!m
Γ_i	Finite!element!patch!of!node!i in!the!surface!xy!plane!
λ	First-order!decay!coefficient!
$\forall$	For! all! values! of!
ρ_f	Freshwater!density![ML^{-3}]!
g	Acceleration!of!gravity!constant!($= 9.81 m^2/s$)A

(x, y, z)A	Global!coordinate!system![L]!
$\mathbf{G}, \mathbf{G}^*$	Global!flow!conductance!matrix!
G_{ij}, G_{ii}	Global!flow!conductance!matrix!entries!
$\mathbf{G}^T$	Transpose!of!matrix!$\mathbf{Gy}$
$\widehat{h}$	Approximate!groundwater!potential![L]!
h_s	Equivalent!saltwater!potential![L]!
h	Groundwater!head![L]!
$\mathbf{hy}$	Unknown!groundwater!head!vector!
h_i, h_j	Unknown!nodal!groundwater!head!at!nodes!i!and!j![L]!
$\mathbf{Iy}$	Identity!matrix!
$\eta(t)$A	Interface!depth!below!datum!level!at!time!t [L]!
$it_{\max 4}$	Maximum number of linear PCG !terations !
[$\mathbf{J}$]A	Jacobian!matrix!
K_d	Adsorption!distribution!coefficient![$\mathrm{L}^3\mathrm{M}^{-1}$]!
$\mathbf{Ky}$	Hydraulic!conductivity!tensor![LT^{-1}]!
$\mathbf{k}_r$	Relative!hydraulic!conductivity!tensor![LT^{-1}]!
$\mathbf{Ky}$	Saturated!hydraulic!conductivity!tensor![LT^{-1}]!
$\mathbf{ky}$	Unsaturated!permeability!tensor![L^2]!
δ_{ij}	Kronecker!symbol!
$\mathbb{K}^i(\mathbf{G}, \mathbf{r}^0)$A	Krylov!subspace!of!dimension!i for!$\mathbf{Gy}$and!$\mathbf{r}^{04}$
L(.)!	Differential!operator!
(ξ, η, ζ)A	Local!finite!element!coordinate!system![L]!
α_L	Longitudinal!dispersivity![L]!
$\mathbf{Ly}$	Lower!triangular!matrix!
$\mathbf{My}$	Mass!transport!matrix!
$\omega_{\max 4}$	Maximum!underrelaxation!factor!
$\omega_{\min 4}$	Minimum!underrelaxation!factor!
n_e	Effective!porosity![dimensionless]!
$ln(.)$A	Natural!logarithm!function!
nn	Number!of!nodes!

$\mathbf{n}$	Outward unit vector perpendicular to curve tangent
n	Porosity [dimensionless]
$\frac{\partial}{\partial x}, \frac{\partial}{\partial y}, \frac{\partial}{\partial z}$	Partial derivatives with respect to global coordinates
$\frac{\partial}{\partial \xi}, \frac{\partial}{\partial \eta}, \frac{\partial}{\partial \zeta}$	Partial derivatives with respect to local coordinates
$\mathbb{P}_i$	Polynomial of degree i
$\mathbf{P}$	Preconditioning matrix
ψ	Pressure head [L]
p	Water pressure [$\mathrm{ML^{-1}T^{-2}}$]
q_n	Prescribed Neuman or Cauchy flux type [$\mathrm{LT^{-1}}$]
q	Specific discharge rate [$\mathrm{LT^{-1}}$]
Q	Total inflow/outflow [$\mathrm{L^3T^{-1}}$]
$\mathbf{Q}$	Transport matrix
R	Internal flow source/sink term [$\mathrm{T^{-1}}$]
$\mathbf{r}$	Residual vector
R	Retardation factor [dimensionless]
R_c	Solute transport source/sink [$\mathrm{MT^{-1}L^{-3}}$]
S_C	Cauchy type concentration boundary
S_{ii}	Diagonal term of the storage matrix
S_1	Dirichlet-type boundary
S_D	Dirichlet type concentration boundary
S_p	Elastic storage coefficient [dimensionless]
S_2	Neuman-type boundary
S_N	Neuman type concentration boundary
ρ_s	Saltwater density [$\mathrm{ML^{-3}}$]
θ_s	Saturated water content [dimensionless]
ε	Small positive number
S_s	Specific storage coefficient [$\mathrm{L^{-1}}$]
S^e	Storage coefficient of element e
$\mathbf{S}$	Storage matrix
S_w	Water saturation [dimensionless]

$\sum$	Sigma!sum!notation!
$T_{\max 4}$	Maximum!calculation!time![T]!
$tolw$	Prescribed!groundwater!head!tolerance![L]!
t_p	Target!time!value![T]!
Δt	Time!step![T]!
t	Time!variable![T]!
T	Transmissivity![L^2T^{-1}]!
α_{Th}	Transverse!horizontal!dispersivity![L]!
α_{Tv}	Transverse!vertical!dispersivity![L]!
ω^m	Underrelaxation!factor!at!iteration!level!m
$\mathbf{Uy}$	Upper!triangular!matrix!
Δt_{user}	User-specified!time!step![T]!
V_i^e	Control!volume!contribution!of!element!e at!node!i [L^3]
V_F	Freshwater!zone!volume![L^3]!
$\mathbf{vy}$	Groundwater!seepage!velocity![L^2T^{-1}]!
V_S	Saltwater!zone!volume![L^3]!
V	Space!volume![L^3]!
z	Elevation!head![L]!
θ	Volumetric!water!content![dimensionless]!
ρ	Water!density![ML^{-3}]!

List of Abbreviations

Abbreviation	Description
1-D, 2-D, 3-D	M One, two, and three-dimensional
ANSI	M American National Standards Institute
API	M Application Programming Interface
BCM	Boundary conditions
BICGM	Biconjugate Gradient Solver
BI-CGSTAB	M Biconjugate Gradient Stabilized Solver
BI-CGSTAB (l)	M Biconjugate Gradient Stabilized Solver of order l
CAD	M Computer Aided Design
CF90	M Cray Fortran 90 compiler system
CGM	Conjugate Gradient Solver
CG-like	M Conjugate Gradient-like Solver
CGS	M Conjugate Gradient Squared Solver
CPU	M Central Processing Unit
Cr	M Courant number
Cray J916/8-1024	M Super Computer architecture
CSR	M Compressed Sparse Row matrix storage format
CVFEM	Control Volume Finite Element
DCSR	M Diagonal Compressed Sparse Row matrix storage format
DSM	Diagonal Scaling preconditioner
DXF	M Data Exchange file Format
FDM	Finite Differences
FEM	M Finite Elements
FDM	Finite Difference Method
FEM	M Finite Element Method

FEMWATER	Finite Element Ground Water flow and transport model
FUP	Fast Updating Procedure
GEO-PROFM	Geohydrological Professional Groundwater Flow and transport model
GEO-SWIM	Geohydrological Saltwater Intrusion odel
GHM	Ghyben-Herzberg elationship
GISM	Geographical Information System
GMRES	Generalized inimal Residual olver
GUI	Graphic User Interface
HISM	Hydrogeological Information System
IF0	Incomplete Factorization preconditioner of order 0
IF0-M	-matrix Incomplete Factorization preconditioner of order 0
IFDM	Integrated Finite Difference ethod
MB	Mega Bytes
MBE	Mass Balance Error
MCSR	Modified Compressed Sparse Row matrix storage format
MFEM	ixed Finite Elements
MIF0	Modified Incomplete Factorization preconditioner of order 0
MIF0-M	-matrix odified Incomplete Factorization preconditioner of order 0
MIPS	Multiple Instruction Processor Systems
MOCM	odified Method of Characteristics
MODFLOWM	odular groundwater flow model
MR	Minimal Residual solver
MT3D	Modular Transport Three-Dimensional finite difference model
NIM	Number of Iterations
PCM	Personal Computer
PCGM	Preconditioned Conjugate Gradient
PDEM	Partial Differential Equation

Pe!	Peclet!Number!
Quasi-3D!	Quasi!Three-Dimensional!
RAM!	Random!Access!Memory!
USGS!	United!States!Geological!Survey!

Chapter 1

Introductiony

Contentsy

1.1 Generaly

In the past few decades, modeling has become an important and powerful toolA in many branches of science. Models allow engineers and scientists a way to testA hypotheses in a manner that is nondestructive to the actual problem. ComputerA modeling has become a necessity and a meaningful way of improving our qualityA ofAlife, andAthatAofAtheAfutureAgenerations, rather than a '*luxury*' solely offered for A the experts at the academicAand laboratory environment level.A

The astonishing development of computer hardware and software technolo-A gies, and the significant increase of computational power, has contributedAwidelyA inAsolvingAcomplex engineeringAproblemsAin severalAfields. Although, it seems thatA

there will be no limits for such developments, it turns out that at the same timeA needsAforAfuture man civilizationsAwillAput moreAdemands, andAmoreAdelicateAcom-A putationalAproblems to be manageable by digital or/and '*interactive*' computers.A NumericalAmodelersAand engineers are therefore always in a challenge to designA andAimplementAbetterAstrategies, inAtermsAofAbothAcostAandAefficiency.AWhich, at the same time may prove very useful for an improved understanding of theA world'sAsurrounding physical phenomena.A

1.2y ProblemyDefinitiony

Protection of freshwater resources against contamination and toxic pollution isA ofAbroadAinterestAforAtheAgroundwaterAcommunity, including modelers, practition-A ersAorAtechnicalAexperts, andAdecisionAmakersAorAmanagers.ADifferentAsourcesAofA groundwater contamination are man made actions modifying the natural envi-A ronment process, asAillustratedAin Fig. 1.1. MathematicalAmodelingAplays an everA increasingAroleAin theAquantitative analysisAofAthe actual behaviorAofAgroundwaterA in terms of quantity and quality, and in the design of efficient protection andA remediation scenarios.A

Mathematical models are classified in two broad categories: stochastic and de-A terministic. Stochastic models are useful when our total ignorance of the actualA situation reach a sufficient level to assume a '*statistically*' random realizationsA of the unknown problem parameters.ADeterministic models are by far the mostA commonAinAuseAtoday.ASystemsAofApartialAdifferentialAequationsAthatArelateApa-A rametersAsuchAasApotentialAhead, waterAflowAand concentrationAofAdissolvedAmatterA are commonly utilized by this type of numerical models.A

The typesAofAmethods commonly usedAfor numericalAmodeling areAfiniteAdiffer-A ence methods (FDM), and finite element methods (FEM). The system of equa-A tionsAthat resultsAasAsolvedAsimultaneouslyAtoAdetermine necessaryAflow parametersA

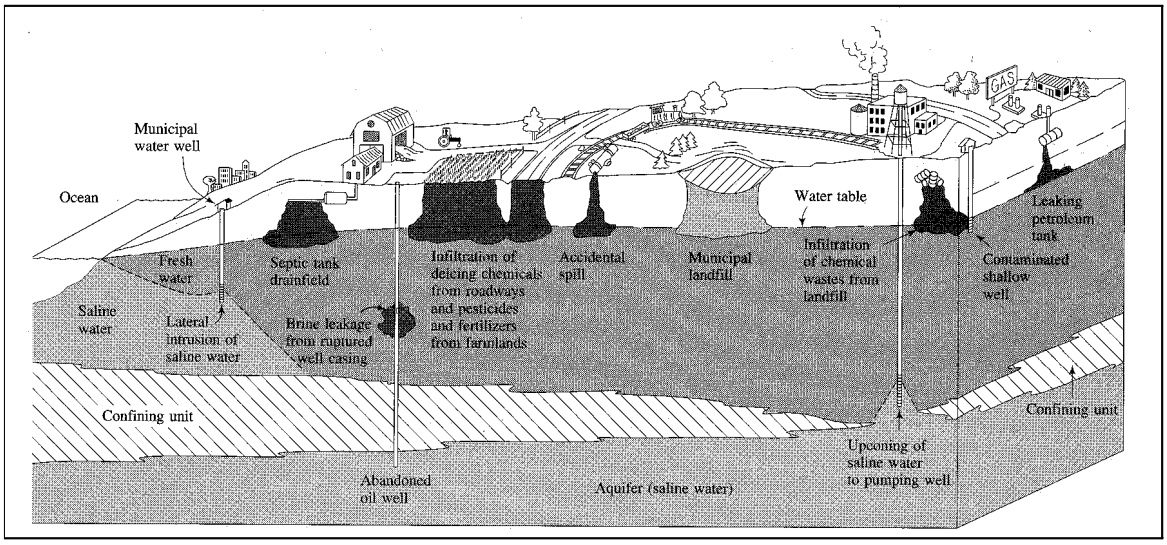

Figure 1.1:ADifferent sources of groundwater contamination (Fetter, 1998).w

at specific nodes.AIn this manner, the hydraulic characteristics are found at spe-A cific points throughout the system.AFinite element methods, unlike finite differ-A ence which require orthogonal grid elements, utilize elements of various size andA shape, enabling these methods to better handle irregular shapes, and complexA domains with various heterogeneities, and curvilinear boundaries, allowing alsoA better AimplementationAofAcharacterizedAtimeAvaryingAconditions.ADespiteAtheseA FEM advantages, FDMAisAstillAcompetitive, andAsomewhat moreAstableAin dealingA with practical field applications, where the simulation cost becomes an impor-A tant objective of the project itself, which explains the encountered success andA widespread use of these kind of models.A

These conclusions become more evident in case of fully three dimensional mod-A els.A three dimensional model does not only permit the simulated independentA variable to be calculated everywhere in the real world physical domain, but itA removes many underlying AassumptionsAwhenAformulating theAoriginalAmodel. Ex-A amples of these assumptions are the well-known Dupuit horizontal flow in aquifersA and vertical flow in aquitards, leading to quasi-3D models; And the Baden-GhybenA (1888) and Herzberg (1901) approximation for the salt-freshwater interface nearA

the sea coast.AThese assumptions have been proven to be physically unrealisticA for a full range of situations (Bear, 1972).A

Moreover, for transient groundwater flow problems, the PDE's are more del-A icate to solve, since four independent variables are involved (space coordinatesA andAtime). InAunconfined aquifersAinvolvingAvariablyAsaturatedAflow, a traditionalA model can not encompass many additional parameters related to the soil charac-A teristics, most of these parameters are found using some mathematical niceties, for which it is often hard to find a physically based interpretation. These limita-A tions shorten the applicability of this kind of models, especially for groundwaterA systems with a high variability of soils andAheterogeneities. UnsaturatedAsystemsA often involve variable and moving boundaries in time, like the water table de-A limiting the saturatedAand variably saturated zones, the salt-freshwater interfaceA separating the assumed immiscible freshwater and saltwater zones.A

Saltwater Intrusion, or encroachment, defined by Freeze and Cherry (1979)A as:A*the migration of saltwater into freshwater aquifers under the influence of groundwater development*, becomes a problem in coastal areas where freshwa-A ter aquifers are hydraulicallyAconnected with seawater.AWhen large amounts ofA freshwater are withdrawn from these aquifers, hydraulic gradients encourage theA flowAofAseawaterAtowardAtheApumpedAwellAorAwells.AOneAcommonAgoalAofAtheseA models is to predictAand characterize the movement of the transition zone in theA aquifer where freshwater and saltwater meet. Another purpose of modeling is toA predict the behavior, degree, and extent of mixing that occurs in this transitionA region. TheseAare twoAsimpleAexamplesAofAhow models areAusedAtoAquicklyApredictA the future conditions of situations that may actually take many years to occur.A

Mathematical groundwater modelsAof this class are complex, andAtheAexistingA numericalAapproachesAare notAapplicableAforAfield applicationsAofAlargeAdimensionsA requiringAhighAresolution. MostAofAtheAexisting threeAdimensionalAsaltwaterAintru-A sion models are miscible density dependent solute transport models, which faceA

data availability problems and a need of large amount of computer hardware re-A sources. Two-phase sharp interface models are 2-DAor at most quasi-3D, becauseA the traditional approach requiring the solution of coupled system of freshwaterA and saltwater governing equations is very demanding.AHence, there is still prac-A ticalAlimitationsAinAapplicationAofAtheseAmodelsAinAfieldAconditions.AMoreover, boundaryAconditions relevant to the saltwater phase are not always easily acces-A sibleAorAknown in caseAof movingAinterfaces. ToAourApresent knowledge, thereAis noA three-dimensional model based on a '*cheap*' embedded sharp interface approachA available.A

Three dimensional modeling of solute transport is readily accessible today.A ButAstillAsomeAcomputationalAlimitationsAareAexistingAforAenhancingAtheAscopeA of the numerical methods knownAtoAbe standardAin use for this typeAofAprob-A lems.AIndeed, finiteAelementAdiscretizationsAleadAtoAlargeAsparseAmatricesAwhichA are often ill-conditioned and hence an iterative solution method even when it isA robust may fail to provide an acceptable solution. For transport problems theseA difficulties are augmented by the possibility of other typical errors arising in theA computational process, such as numerical dispersion, numerical oscillations andA overshootsAleadingAtoAsmearingAconcentrationsAfronts.ADifferentAstrategiesAhaveA been adopted in theApast decades to exclude or minimize at best these numericalA errors.AWeAprovideAhereAanotherAmethodologyAbasedAonArobustAnumericalApre-A conditioning of the FE algebraic equations, based on physical interpretation ofA the different terms in the numerical formulation leading to an anticipated massA conservation of the numerical process.A

For most modeling applications, the time and effort spent on pre-processingA andApost-processingAofAdata far exceedAthatAspent on otherAproject activities. ThisA work can be tedious for three dimensional simulations which require more inputA dataAand more nicely presented results in easily understood graphic form.AThisA explains the new trends towardsAstandardization of graphic interface tools, andA

the motivationAofAdeveloping comprehensiveAvisual interfacesAenvironments forA more interactivity andAfriendly use.A

1.3y ScopeyandyObjectivesy

This work focuses on contributing to computationally efficient three dimensionalA groundwater flow and solute transport models and additional set of tools based onA new techniques and methodologies, which enhance significantly standard conceptsA knownAtoApresent. SpecialAemphasisAisAmadeAtoAtransient andAnonlinearAproblems, which are more difficult toAinvestigate andAto model effectively. Before a detailedA expositionAof theAmainAobjectives taken into account in thisAresearch, weAstillA separateAtheAinvestigatedAproblemsAintoAthreeArelatedAcategories:A(i)AtransientA variablyAsaturatedAgroundwaterAflowAwith a movingAwaterAtable, (ii) theAsameAbutA including a moving fresh-saltwater interface, and (iii) solute transport problems.A

Respectively, theAobjectives for each of these three main topics areAasAfollows:A

1.ADevelop a robust and efficient time dependent solver, based on linearizedA equations.AThe trade-off between the global cost in memory storage, CPUA requirements, and theAgeneralAsolution accuracyAshouldAbeAquiteAreasonable;A

2.ATheALinearization process should be mass conservative, smooth, andAeffi-A cient;A

3.AProvide built-in generic representation of the soils characteristic curves, toA relax the numericalAsolutionAprocedure. ItAshouldAuse a minimum setAofAsoilA physical parameters;A

4.ATesting of the codes efficiency and robustness under various platforms andA with different test examples, to ensure numerical accuracy;A

5. ApplicationAofAtheAcomputerAprogramsAtoAstudyAtheAactualAbehavior, andA futureAmanagementAplansAinAselectedAfieldAsites.ATheseAincludeAanAaquiferA

system from Morocco for seawater intrusion analysis, and two field sitesA from Belgium subject to groundwater pollution;A

6.A Development of user interface program packages to be used as a front end7 to the simulation codes.7

One of the important addressed goals in the development stage was the codeA portability issue, such that the model will run on any hardware provided that aA FortranAcompilerAisAavailable.AToAachieveAthisAgoal, weAdevelopedAaAFortranA90A compatibleAcodeAfreeAofAhardwareAdependentAcompilerAdirectives.ATheAcodeAhasA been tested by running test examples including academic, hypothetical and fieldA scenarios on the following platforms:A

- ±Cray J916/8-1024Asupercomputer (UNIX-based UNICOS 9.0.2.1Aand CF90A Fortran compiling systems)A
- ±SiliconAGraphicsAChallenge-L workstationA(UNIX-based IRIX 5.3AandAMIPSA Fortran90 compiler)A
- ±Sun UltraSparc2Aworkstation(UNIX-based SOLARIS 5.2.1Aand F90ASPAR-A Cworks Pro Fortran compiler)A
- ±Personal computers with Intel Pentium processors (MS DOS- Win95/Win98/NT), provided that a 32-bit compiler is available.A

1.4y Organizationy

The dissertation text is organized in eight chapters including the introductoryA and theAconcludingAremarks chapters. Separate chapters discussing theAresultsAorA the application of the methods and concepts described in other chapters are notA given.ATherefore,AallAthingsArelatedAtoAaAspecificAtopic, includingAtheAtheoreticalA

developments, applicationsAandAdiscussions areAput togetherAin oneAconsistentA chapter.A

Chapter 2 is an introduction to several aspects of computational hydrogeology, including the model classification, and the computational techniques such as theA finite element method, and their practical application. Throughout the text, theA correspondingAliteratureAisAreviewed.AThisAisAnotAintendedAtoAgiveAaAcompleteA review of the numerical methodsAused for modeling groundwater flow and soluteA transport in aquifer systems.AIt only introduces the reader to this field throughA numerous hints and by providing standard references.AState of the art methodsA forAeachAproblemAareAdescribed inAtheAliteratureAreviewsAgiven at theAbeginningAofA the respective chapter.A

In chapter 3, the review is extended to more specific aspects of three-dimensionalA modeling of groundwater flow in aquifer systems.AWe start by a general discus-A sionAofAseveralAformsAofAtheAgroundwaterAflowAgoverningAequations.A fterwards, a detailed exposition of the finite element matrix equations derivation is given, this constitutes the core of the chapter, and sets up the necessary foundationsA forAtheAnumericalAmodels.ASeveralAotherAaspectsAareAdiscussed, suchAasAtheAnu-A merical implementation of boundaryAconditionsAand the sparse matrix storageA scheme.AOnce the algebraic FE equations are derived, several solution methodsA andAstrategies areApresentedAin theAlastAparagraph, aimingAtoAintroduce theAreaderA to the concepts and methodologiesAused in the next chapter.A

Chapter 4 focuses onAvariably saturatedAgroundwaterAflowAwithAmovingAwaterA table profiles.A general discussion on the subject is followed by the conceptualA development of theAFUP technique, theAdifferent stepsAinvolvedAinAitsAapplication, andAhowAdifficultiesAsubjectedAtoAseveralAnon-linearitiesAareAavoided.ATheAper-A formances of the inner linear numerical solver andApreconditioner are discussedA inAdetail, andAtheirAuseAisAjustified.AOtherAstepsAandAtechniquesAinvolvingAtheA constructionAofAtheAnon-linearAsolverAinAtimeAoverlayAareApresented.ATheAFUPA based model is verified using four test examples.AThe first example is quite sim-A

pleAandAdescribesAtheAdrainageAthroughAaAverticalAsoilAcolumn.AThe AsecondAisA basically similar to the first except that a leaky soil is placed at the exit of theA soil column, retarding the vertical flow.AThe third example is important for theA transient drainageAstudies in water table aquifers.AThe last validation sample isA mostAinterestingAin theAscopeAof thisAstudy, it showsAclearlyAtheAperformancesAandA capabilitiesAof theA3-D model. ThisAstudyAcomparesAthe modelApredictionsAagainstA theAlaboratory experimentsAdesigned and performed byABaseghi andADesaiA(1987, 1990), in a 3-D earth model with several complex configurations.A

Generalization of the FUP approach for problems with freshwater-seawaterA movingAinterfacesAisAdiscussedAinAchapterA5.ATheAconceptualAproblemAproperAtoA thisAmore complicated problems is formulated. This is smoothly adapted from theA developments already performed in chapter 4.AHere again, a series of test prob-A lemsAareArelevantAtoAcheckAtheAnumericalAsolutionAaccuracy.AFiveAexamplesAareA considered, includingAlateralAseawaterAintrusionAin (i)Aconfined and A(ii)AunconfinedA aquifers; (iii) seawater intrusion control with recharging wells; (iv) saltwater in-A trusionAin a multilayer aquiferAsystem;AandAfinallyA(v) a movingAsharpAinterfaceAinA a 3-DAlaboratory sand box model as designed by Sugio and Rahim (1992), whichA is the most challenging problem. Except for the fifth test all numerical solutionsA are compared with available analytical solutions, additionally for the fourth testA the results are compared to the numerical solution computed by Huyakorn et al.A (1996).ASatisfactoryAagreementsAareAnoticedAinAthisAoverallAcomparativeAstudy.A

last paragraph is devoted to the model application to seawater intrusion inA Martil aquifer system in Morocco, for studying the actual behavior of the sharpA interface, and establishing future risk to salinization scenarios.A

Chapter 6 deals with numerical aspects of three-dimensional modeling of so-A lute transport problems, using the common-place Galerkin finite element tech-A nique.AModelAgoverningAequationsAareApresented, followedAbyAtheirAmatrix FEA equivalent form.ALimitations related to this approach are shown andAexplained. An alternative throughAthe useAofArobust numericalAmethodsAisAproposed. ThisAn-A

volvesAusingAstateAofAtheartAsolversAforAparticularAnone-symmetricAsystemsAarisingA fromAtheFEAdiscretizationAoftheAglobalAsystem,namelyAtheAbiconjugateAgradientA stabilized method (Van der Vorst, 1992).AThis is followed by applying the bestA preconditioner for a particular situation, meaning the multiplicity of choice fromA aArangeAofAtheAexistingAones.AMotivationsAforApreferringAattractiveAschemesAareA explained andAreinforced by giving examples from the state of the art literature.A The performances of possible mixtures of the selected solvers andAprecondition-A ers are comparedAbased on CPU's, the convergence behavior, and accuracy. FiveA problems are studiedAincluding two field situations from Belgium.A

Chapter 7 describes how several of the developed models are implementedA from software point of view. Thus, a brief explanation of many computer packagesA andAadditional toolsAisAgiven. OneAshould keep inAmind that, this chapterAdoes notA intendAtoAbe a user manualAforAtheAsoftware, neither a technicalAreport explainingA theAdevelopment process moreArelatedAtoAsoftwareAengineeringAdesignAin computerA science. These detailed aspects are specifically hidden.A

Finally, in chapterA8 theAoverall conclusionsAareAdiscussed andAideasAforAfutureA research are formulated.A

Chapter 2

An Introduction to Computational Hydrogeology

Contents

2.1 Introduction

In this chapter, we attempt to present a short and concise coverage of key aspects of modeling groundwater flow and solute transport in aquifer systems. An effort

is made to mix theoretical and practical aspects together, such that it will be fruitful from the developer and practitioner points of view.

We start by a short discussion on the terminology, explaining the difference between '*subsurface hydrology modeling*' and '*computational hydrogeology*', which is a more general and appealing definition. Next, we discuss different kind of groundwater flow and solute transport models. Section 2.4 describes the different steps usually involved during a classical modeling approach, starting from the conceptual model development to building a reliable predictive model. Emphasis is made on practical aspects and precautions to take in this process. Section 2.5 gives a brief introduction to structured mesh generation in simple domains, and the extension to complex domains using multiblock methods (Ho-Le, 1988). The next section sets up the basics of the standard Galerkin finite element method, and its theory useful throughout the upcoming chapters. Section 2.7 introduces advanced finite element methods, and other discretization methods becoming common place in use by the groundwater community. Particular features of these alternative methods are briefly described and commented. Finally, we give a brief overview of iterative methods, which are the heart of any numerical solver.

2.2 What is Computational Hydrogeology ?

Computational hydrogeology is an emerging multi-disciplinary scientific discipline. It has its roots in broad branches of science as illustrated in Fig. 2.1. These are, *Groundwater Hydrology*, *Applied Mathematics and Computational Methods*, and *Computer Science*.

Additional fields resulting from other interactions between these areas (see Fig. 2.1) have specific orientations. Nevertheless, they have several aspects in common, and a sharp distinction cannot be made. It is clear however, that computational hydrogeology has a much broader significance than modeling, because usually a sound understanding and detailed know-how in several other fields are

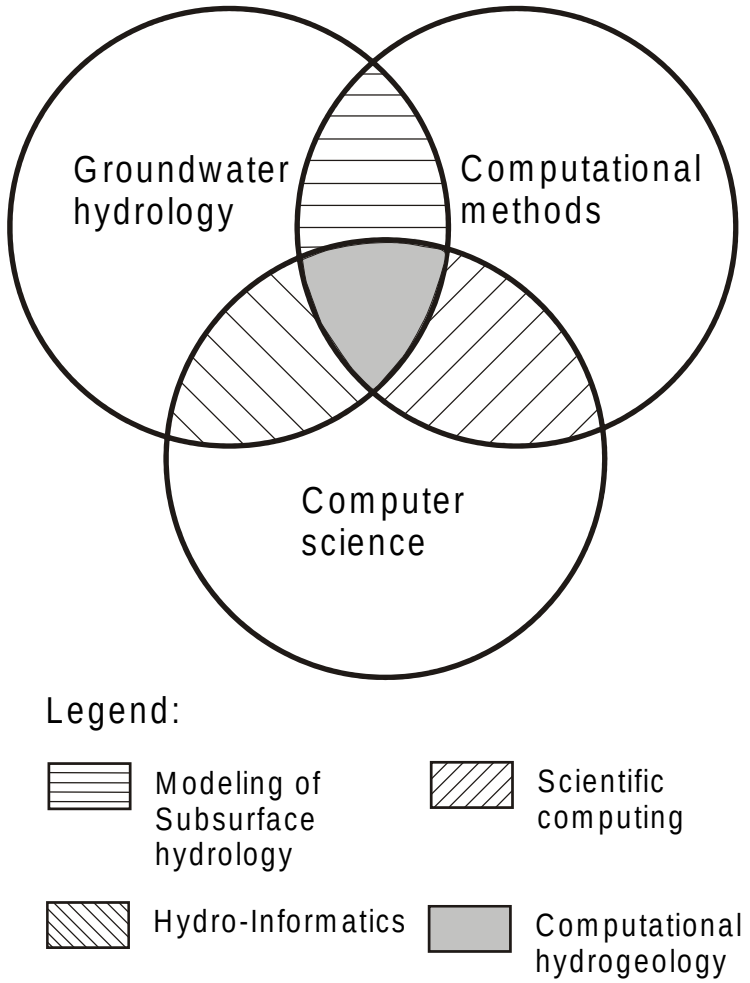

Figure 2.1: Definition of computational hydrogeology.w

needed for solving computational hydrogeology problems efficiently. A

2.3 Classification of Groundwater Flow and Transport Models

Groundwater and transport models can be categorized into three broad categories (Anderson and Woessner, 1992; Kresic, 1997) numerical, physical, and analytical. Of these three, numerical models are by far the most commonly used today, with

the availability of high speed computers that can solve many systems of equations in a short amount of time. Physical models find unique applications as visual aids that allow the actual problem to be scaled down to a size that is manageable and controllable. Analytical models involve solving equations where a definite closed answer is reached at the end of calculations, offering ease of calculation and a simplified version of the real problem. Each of these three types of models will be discussed further below.

2.3.1 Physicaly Modelsy

Physical models consist of miniature physical analogs of the geology and/or hydrology of the situation being studied. Custodio (1987) describes physical models as an analog which is scaled down from the prototype, and in which every prototype element is reproduced, differing only in size. Physical models often come into use in situations where numerical and analog models are inappropriate, due to insufficient historic and hydrogeologic data. Physical models have the advantage of providing a means of visually understanding the problem being studied. One simple type of physical model is a sand box type model. A container is filled with a porous media, such as sand or glass beads, and the movement of fluids through the media is observed. Another type is the ion-motion analog. In this type of model, the movement of ions, under an electrical gradient, through an electrolytic solution is used to model the movement of fluids through porous media. By introducing other electrically charged probes into the system, hydraulic phenomena such as impermeable layers and pumping wells can be simulated in the system. Another commonly used physical model is the Hele-Shaw analog (Bear and Dagan, 1964; Segol, 1994). This model is used to represent two dimensional flow in groundwater systems and consists of two clear plates placed close together with a porous media in between. Flow of fluid between the two plates under different hydraulic gradient is observed and studied.

2.3.2 Analytical Models

The first analytical models that accurately represented hydrogeologic conditions appeared in the 1960's. Analytical models are similar to numerical models, except that the equations involved can be solved exactly at any point of the space flow domain, without the use of approximation methods. In order to arrive at equations that provide an exact solution, many simplifying assumptions must generally be made. Therefore, these models are not suited for systems that involve complex flows and geometries. For this reason, analytical models have limited use in groundwater flow and transport modeling. However, when analytical models are suitable, they provide solutions that are relatively simple to calculate and understand.

2.3.3 Numerical Models

Numerical models consist of mathematical algorithms that represent the hydraulic and/or chemical aspects of the situation being studied. Systems of partial differential equations that relate parameters such as head, concentration and water flow are commonly utilized by this type of model. Studies involving the numerical modeling of groundwater flow started in the early 1960's, most of these formulations solve the two-dimensional depth integrated equations using comprehensive approximations, such as Dupuit-Forchheimer for saturated flows, and Ghyben-Herzberg in coastal aquifers. Finite difference was the method of choice during this era; a numerical solution of equations with a range of thousand unknowns was difficult to obtain. During the 1970's advances were made for applications of the finite element method to groundwater models, while in the 1980's many algorithms have been detailed and made much powerful and efficient. The 1990's era is marked by the development and evolvement of three-dimensional models to simulate realistic flow and transport phenomena as they would occur in reality, thus most research efforts are focussing on improving the

existing algorithms, or their adaptation for greater efficiency and robustness.

2.4 The Computery Modeling Paradigm

For every modeling work, many steps are involved to build up a complete representative model of the situation being studied. Usually, many stages of the model setup follow the logic presented in Fig. 2.2. These steps are grouped into three categories, pre-processing, model run or processing involving application of the numerical method and the model embedded numerical solver, and finally post-processing tasks related, which are useful as tools for results verification and visualization. A strong link exists between different tasks during the model calibration and verification stage, which is illustrated by the dashed lines in Fig. 2.2. These generic model construction steps are discussed in detail below.

2.4.1 Conceptual Model Development

The development of a model concept stands the origin of any modeling effort, and plays a key role in the success of the following steps. A carefully designed and understood conceptual model can save months of man work. A thorough analysis of the global hydrogeological situation, the flow direction and its seasonal variation, the system communication with other water resources, etc, are required at this level. All the information is presented in a form of simplified maps and cross-sections of the aquifer, though a better management (in space and time) is performed by storing and organizing these data in a computerized database, linked with a general Geographic Information System (GIS) or at the best a custom GIS or a Hydrogeological Information System (HIS), managing all the data in easily graphic understood form.

It is always a common practice to revise the conceptual model design during the calibration process. As an example, model results may indicate that a neigh-

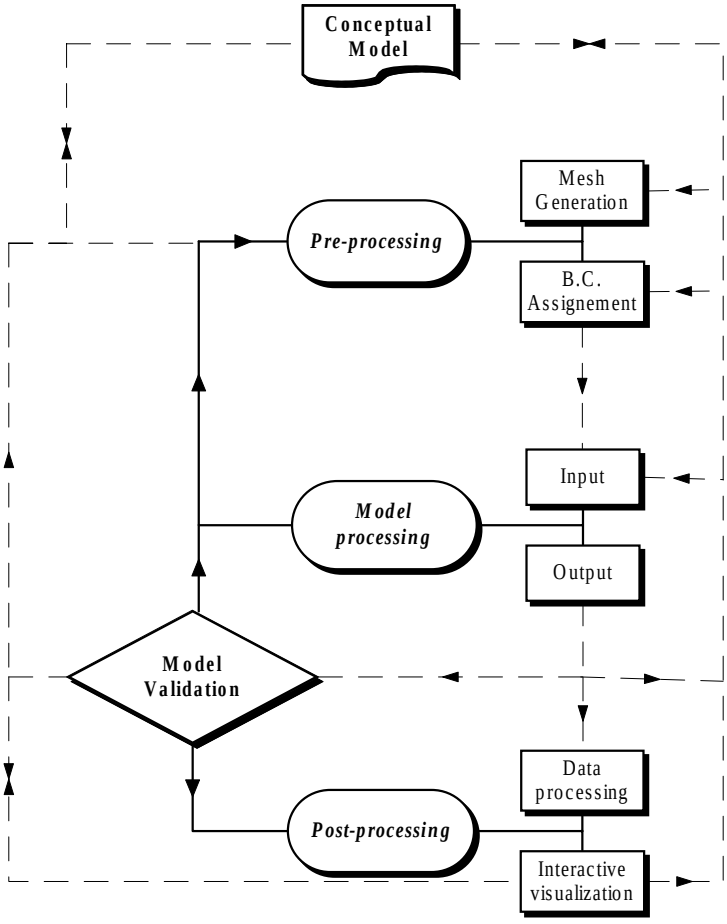

Figure 2.2: Simplified flow chart representation of the computer modeling paradigm.

boring hydrogeological unit having lateral contact with the initial model, should be a part of the final model.

2.4.2 Model Selection

The selection of a computer code is certainly one of the most challenging tasks. Within the objective to simulate effectively the conceptual developed in the previous phase, a good knowledge and sufficient level of expertise are needed to choose the most appropriate model for a given situation. However, it should be mentioned that besides the 'technical' requirements other socio-economic decisive factors

take much importance. Special care should be taken for understanding the code functionality, and the limitations and approximations used in the built-in numerical approach. An example is the case of modeling saltwater encroachment in aquifer systems, where decision ambiguity exists.

Miscible/Density Dependent/or/Sharp Interface?

Two conceptually different approaches governing the saltwater intrusion, namely the sharp interface and the density dependent flow coupled with miscible salt transport, are widely accepted by the groundwater community (Segol et al., 1975; Galeati et al., 1992; Xue et al., 1995; Yeh et al., 1997). However, in many situations decisive factors determining the choice of the best approach and eventually the numerical code as well, should be defined precisely. For instance, in a situation where regional analysis are required in an advective dominated flow field, the use of a fully coupled miscible and density dependent transport model will just increase the simulation cost, and make the problem more complex, whereas this level of complexity is not desired.

Nowadays, several computer codes are either freely available, or are packaged and distributed by several vendors with other utilities and auxiliary programs, especially pre and post-processors. Most of these programs are different distributions of the USGS MODFLOW code (McDonald and Harbaugh, 1988; Harbaugh and McDonald, 1996). An example of a finite element code put in the public-domain is FEMWATER (Yeh and Ward, 1981; Yeh et al., 1997), capable of solving coupled 3-D groundwater flow, and transport. A detailed review of this computer codes is beyond the scope of this work.

2.4.3 Mesh Generation

To perform simulations of the partial differential equations governing groundwater flow and solute transport systems on a computer, these continuum equations

need to be discretized, resulting in a finite number of points in space (and time) at which variables such as groundwater head, velocity, density, and solute concentration are calculated. The usual methods of discretization, finite differences, finite volumes and finite elements, use neighboring points to calculate derivatives, and so there is the concept of a mesh or grid on which the computation is performed. There are two mesh types, characterized by the connectivity of the points. *Structured meshes* have a regular connectivity, which means that each point has the same number of neighbors (for some grids a small number of points will have a different number of neighbors). *Unstructured meshes* have irregular connectivity: each point can have a different number of neighbors. Fig. 2.3 gives an example of each type of grid. In some cases part of the grid is structured and part unstructured.

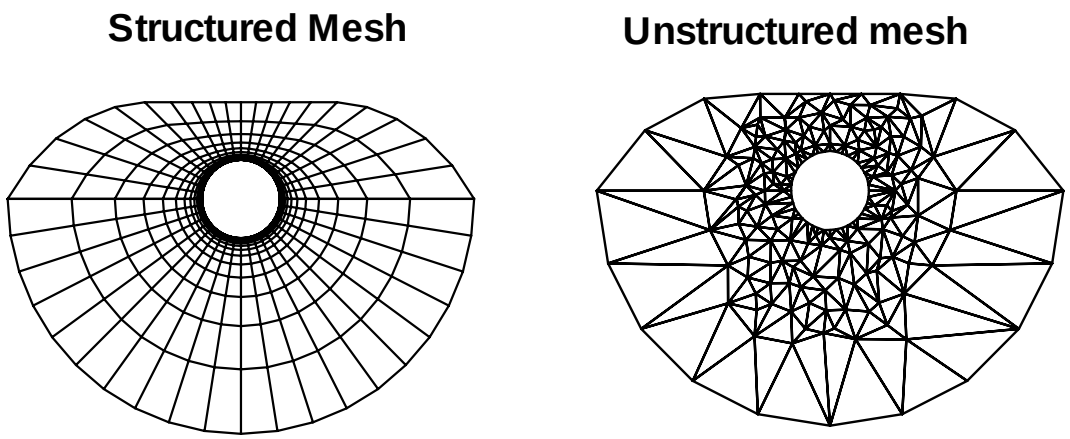

Figure 2.3: Structured mesh (left) and unstructured mesh (right) for the same physical domain.

For all types of meshes, there are certain characteristics that we want to control:

- The local density of points: high density gives more accuracy, but computation takes longer. This leads to adaptive meshing methods;

- ±The smoothness of the point distribution:Alarge variations in gridAdensityA or shape can cause numerical diffusion or/andAdispersion. This can lead toA inaccurate results or instability;A

- ±TheAshape of the grid volumes: when the finite element method usesAquadri-A lateralAelements theAmaximum angle mustAbeAboundedAstrictlyAbelow toA enable convergence of the method as the element size is reduced.A

For simple domains, the choice between regular or irregular meshes is governedA mainlyAbyAtheAdiscretizationAmethod.AHowever, forAcomplex domains, irregularA meshAgenerationA(at leastAforAtriangularAorAtetrahedralAelements) can beAfullyA automatic and fast. Regular mesh generation requires the domain to be split upA into simple blocks which are then meshed automatically.A

2.4.4y Boundary Conditionsy

BoundaryAconditionsA(BC)Aexpress theAinkAbetweenAhe conceptualAmodel andAtsA surrounding environment, including external stresses and water flow at domainA boundaries. ItAsAimportant toAaddressAspecificallyAeachAcondition andAbetterAesti-A mate the needed related parameters. These are given in many forms, e.g., waterA headAhydrographs, varyingApumpingArates, etc.ATheAmodelerAhasAtoAdealAquiteA oftenAwithAuncertaintiesAwhich are related toApoor initialAestimates of theABCA parameters, in such case the start up values should be improved in the modelA calibrationAprocess.ADifficultAandAnonlinearABC, suchAasAdrainage, seepage, orA evapotranspiration are very particular and require special concern, their imple-A mentation isAbasedAonAvariousAtechniques different fromAoneAsituation to another.A

In manyAfinite element models, the conditions are attributedAdirectlyAtoAnodes, byAmeansAof an integerAindex or code, andAoptionallyAanotherAsub-index indicatingA the nodeAbehaviorAwhenAt is necessaryAtoAdistinguishAbetweenAdifferent situationsA (e.g., a drainage node is switching from saturated to unsaturated, or the otherA way).A

2.4.5 Model Parameters

These are classified in two main categories: time and physical model parameters. Time parameters (for transient models) required could be reduced to a bear minimum if only values corresponding to the simulation time, and an array of output time levels are given. However, other input is required usually, because each model uses its own time steeping scheme. An example is given in chapter 4 for GEO-PROF (De Smedt, 1995) and GEO-SWIM (Sbai and De Smedt, 1997a) models. Another example is the MODFLOW's time control, which subdivides the maximum simulation time into intervals defined as '*stress periods*' over which BC are considered to be constant, afterwards computational time steps are internally estimated, and are adjusted at each nonlinear iterate to fit output at target time values.

Other physical input for groundwater models are hydraulic conductivities (or transmissivities) of all soil types, porosity, and specific yield. It might also be necessary to specify other input in the framework of other computational solvers, like soil curves fitted parameters or characteristics of the unsaturated flow (water capacity, etc ...). Solute transport problems need additionally the longitudinal, horizontal and vertical transverse dispersivities, the diffusion, decay, and sorption coefficients when the corresponding mechanisms are taken into account. Other parameters depends on the water phase properties, e.g., density, and viscosity.

2.4.6 Model Run

Before any model run, it is worth the time to check the validity of the input, to probe possible errors and incompatibilities. Indeed, for large applications it can save hours of expensive and useless computations. In this context, visual mapping of the distributed input would be a valuable assisting tool. It is also a good practice to perform a preliminary steady state simulation from bulk data sets, without introducing changing conditions, e.g. recharge and lateral inflows. This

can give insightful understanding and guidelines for the future work. Afterwards, introduction of existing conditions in the developed model can be performed smoothly.

2.4.7 Calibration and Sensitivity Analysis

Sensitivity analysis of input data sets constitute another step towards completion of the model calibration. However, these two tasks are often combined simultaneously as one. This is the most tedious and time consuming phase, and could be a real hassle for the modeler to perform a good calibrated model. Therefore, it is always suggested to setup guidelines to better characterize uncertainties, by determining more sensitive model parameters. Model integrated or independent tools able to help in this task are suggested, however, this can be at the best semi-automatic and recent advances show that user-interaction and skills are always needed for a clean interpretation of the results.

2.4.8 Interactive Scientific Visualization

In general, scientists and engineers need efficient, reliable and powerful tools to better express their ideas, and illustrate their research findings. Scientific visualization techniques play an ever increasing role in today's simulation projects. Many software packages have reached a high level of stability and versatility, such that their use become easier even to non professionals. This is especially true for interactive 3-D modeling, which required expensive budgets and highly qualified people a few years ago. One should keep in mind that advanced tools enable not only quality presentation of the simulated results. Advantageously, they accelerate the model calibration phase, and are also useful for checking the input field data.

2.4.9 Verification and Prediction

This is the final stage of the modeling study, and these two processes are often linked together. Because, verification and future predictions require transient conditions, and hence an extended set of model parameters, which is often not included in the calibrated (steady state) model, there will be other uncertainties in the predictive model, caused by the parameters not being calibrated (and hence estimated).

However, a clear distinction must be made between verification of a given model, and predictive scenarios. Verification is achieved on a previously calibrated model with an extended or different data sets, while predictive models assume an hypothetical situation, which is projected or possibly available in the future. Popular examples are, projection of abstraction well fields, dispersion of a dissolved chemical matter due to waste migration from a disposal site nearby a pumping station. Hence, predictive models are never thoroughly verified.

2.5 Structured Meshes Generation

This section begins with a discussion of boundary-fitted grids and the discretization of PDE's on them, and then introduces the multiblock concept used for more complicated domains. Thompson et al. (1985), Knupp and Steinberg (1993), are detailed expositions of structured mesh generation.

2.5.1 Boundary-Fitted Meshes

Structured meshes are characterized by regular connectivity, i.e., the points of the grid can be indexed (by 2 indices in 2D, 3 indices in 3D) and the neighbors of each point can be calculated rather than looked up (e.g., the neighbors of the point are at $(i+1, j)$, $(i-1, j)$, etc.). Meshes on a rectangular domain are trivial to generate (though some care needs to be taken in the discretization

at convex corners) and structured mesh generation techniques concentrate on meshing domains with irregular boundaries. Generally, the meshes are generated so that they fit the boundaries, with one coordinate surface forming (part of) the boundary. This gives accurate solutions near the boundary and enables the use of fast and accurate solvers.

For groundwater flow these grids allow the easy application of groundwater models, which usually require the grid to be aligned with the boundary. The alternative is to use a rectangular grid which is clipped at the boundary, with local grid refinement near sharp features on the boundary (Cartesian grids). This will reduce the truncation order at the boundary and will require the mesh cells to be clipped at the boundary, increasing the complexity of the solver. Cartesian grid generation is very fast, but it does not appear to be applicable to general situations. The most common method of generating boundary-fitting grids is to have one continuous grid that fits to all the boundaries. The effect is to fit a contiguous set of rectangular computational domains to a physical domain with curved boundaries.

It is difficult to fit complex domains with one mapping from a rectangular computational domain without generating excessively skewed grids. To get around this problem the domain is split up into blocks and each block is gridded, with some continuity requirements at the block interfaces; this is a multiblock. The decomposition of the domain into blocks is usually done manually using CAD techniques and is slow. An alternative to continuous boundary-fitted grids with multiple blocks is to use a boundary fitting grid near each boundary, and simple rectangular grid in the interior, and interpolate between them. These are called overset or chimera grids, as discussed by Chesshire and Henshaw (1990).

This type of grid is easier to generate than a multiblock grid since each grid is local and does not need to match the others. The individual grids will generally be of high quality (low distortion). However, the interpolation can be difficult, especially with more than two grids overlapping, and it increases the solver time.

The overlapping grids cannot be too different in resolution and this can cause problems with the grids required for solute transport problems. Chimera grids are very useful for moving boundaries, e.g., the water table and the salt-freshwater interface, or multiple boundaries. Most of the grid remains fixed but the interpolation changes as the grids move with the boundaries. Chimera grids also have certain advantages, and the recent work by Chesshire and Henshaw (1994) on conservative interpolation methods have increased their usefulness. However, the bulk of structured grid generation is based on multiblock type grids.

2.5.2 Multiblock Boundary-Fitted Grids

In theory, complex geometries can be mapped to one rectangular region, but this will lead to unacceptable distortion of the grid cells. In practice, the physical region is broken up into pieces that each have a simple mapping from a rectangular grid.

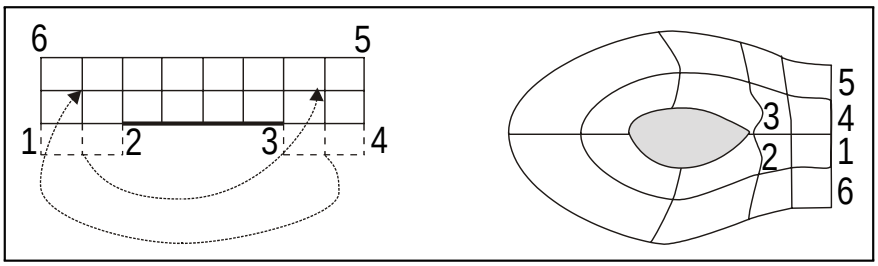

Figure 2.4: Example of a single multiblock grid component.

These blocks are fitted together with some degree of grid continuity at their interfaces as shown in Fig. 2.4, ranging from none to complete, such that the final mesh looks like a single grid with no slope or spacing discontinuities. So, the grid generation process splits into two parts, the decomposition of the physical domain into blocks and the gridding of each block. The decomposition process has not yet been fully automated, and requires considerable user interaction for choosing block edges to align with object edges, aiming to produce good meshes.

The meshing of the blocks can proceed automatically, using one of the methodsA devoted to one single block.A

2.6y TheyFiniteyElementyMethody

2.6.1 Generaly

Continuous physical systems, such as the airflow around an aircraft, the stressA concentration in a dam, the electric field in an integrated circuit, or the concen-A tration of reactants in a chemical reactor, are generally modelled using PDE's.A The quality of a numerically approximated solution of any PDE depends mainlyA onAtheAgeometryAdiscretization, and the numerical approximationAschemeAbuiltAonA theAdiscretizedAdomain. TheAlinksAbetween these two aspectsAareAveryAstrong, andA in the context of a given problem the domain discretization and the numericalA scheme which is applied should be considered together.A

Finite difference and finite element based methods are the most commonlyA usedAnumericalAapproximationAtechniques.A Basically, inAaAdiscreteAnumberAofA nodal points, finite difference based methods approximate the function deriva-A tives, whileAfiniteAelementAmethodsAapproximateAtheAfunctionAitself.ATherefore, finite difference methods produce solutions at a discrete number of points, whileA finiteAelementAmethodsAyieldAspatialAsolutions.AFurthermore, theAfiniteAelementA method has following advantages over finite difference methods:A

- Aquifers anisotropy and heterogeneity are easily considered in the approx-A imate formulation;A
- ±Irregular boundaries are easily incorporated;A
- ±Less nodal points are neededAto have the same level of accuracy in a regionA of interest, thus core computer storage and computational time are saved;A

- The integral formulation used in this method permits the flux type of boundary conditions to come out about naturally (Yeh and Ward, 1980)

This does not diminish the importance of finite difference related methods as one of the most used numerical methods worldwide. For the interested reader, a comparison between the two methods have been discussed in detail by Anderson and Woessner (1992), and Gray (1984). However, in this study the finite element method is preferred. The theoretical background of the finite element method will be briefly presented further below.

2.6.2 Basic Concepts

The finite element method envisions the flow domain as non overlapping smaller elements called '*finite elements*'. The dependent variable is spatially approximated by an interpolating function which is continuous to a specified order. The elements are defined by a discrete number of nodal points. Each element is identified by its number and local nodes numbers, coded by following a given numbering sequence.

The finite elements used in this study are irregular hexahedrons, defined by eight nodes as shown in Fig. 2.5. The numbering sequence is first anti clockwise in the base plane and then, starting above the first node, anti clockwise in the top plane.

Consider the continuum problem governed by the PDE

$$L(h) = 0 \quad (2.1)$$

where L is a differential operator and h is the dependent variable.

The mathematical concept leading to the FE formulation can be accomplished via the use of either a variational or a weighted residual approach. For more details see Zienkiewics and Taylor (1989), and Lapidus and Pinder (1982). The

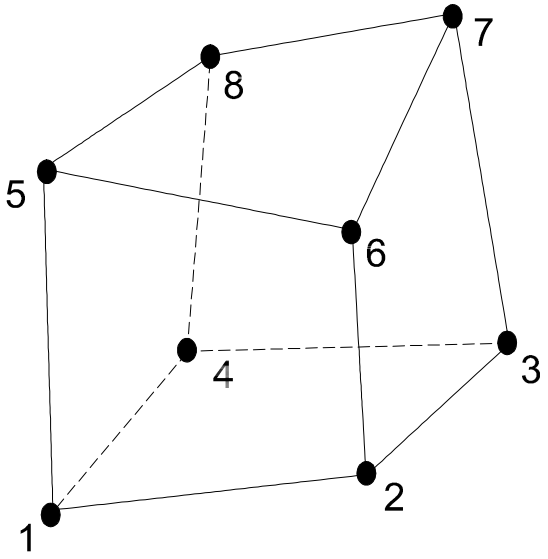

Figure 2.5:AHexahedral finite element.w

so-called Galerkin weighted residual scheme is employed in the models presentedA in chapters 4, 5, and 6.A

2.6.3y TheyGalerkinyWeightedyResidualyMethod

Among the existing methods, the Galerkin scheme is one of the most popularA weightedAresidual methodsAbecomingAstandardAin use. In generalAthe method canA beAachievedAfollowingAaAstraightforwardAprocedure:A

1.ADefineAtheA*trialysolutiony*asAaAfiniteAseriesAapproximationA

$$\widehat{h} \approx \sum_{j=14}^{nn} b_j h_j \tag{2.2}$$A

whereA$\widehat{h}$ isAtheAapproximateAdependentAvariableAtoAestimate, e.g.AgroundwA-ter potential, h_j are the unknown nodal values, b_j are linearly independentA basis functions defined over the entire domainAandAnn is the total numberA of nodes over the hole domain.ASinceA$\widehat{h}$ is only an approximated solution,

residuals occur when replacing it in equation (2.1), this results in an error

$$r = L(\widehat{h}) \neq 0 \quad (2.3)$$

2. Formulate the *integraly equationsy*

The purpose is to minimize the residual over the problem domain, which is accomplished using the set of the n basis functions b_i, orthogonal to the residual

$$\int_V b_i r \, dV = 0 \quad \text{for } i = 1, 2, ..., nn \quad (2.4)$$

or equivalently

$$\int_V b_i \, L(\sum_j b_j h_j) \, dV = 0 \quad \text{for } i = 1, 2, ..., nn \quad (2.5)$$

2.6.4y Basisy and Weightingy Functionsy

The element basis functions commonly employed take the form of polynomials. Their construction is best accomplished using the local coordinates (ξ, η, ζ). The dependence between the local and the global coordinates will be derived in the next paragraph. In local coordinates, the original hexahedral element is mapped into a cube whose corners are located at $\xi = \pm 1, \eta = \pm 1, \zeta = \pm 1$, as shown in Fig. 2.6.

The eight basis functions for trilinear hexahedral elements are obtained as a product of three orthogonal Lagrange polynomials in three dimensional isoparameteric coordinates

$$b_i(\xi, \eta, \zeta) = \frac{1}{8}(1 + \xi\xi_i)(1 + \eta\eta_i)(1 + \zeta\zeta_i) \qquad \text{for } i = 1, 2, ..., 8 \quad (2.6)$$

2.6.5y Numericaly Integrationy

Since the derived algebraic system of finite element equations is expressed on an integral basis, one may encounter difficulties to evaluate integrals with respect

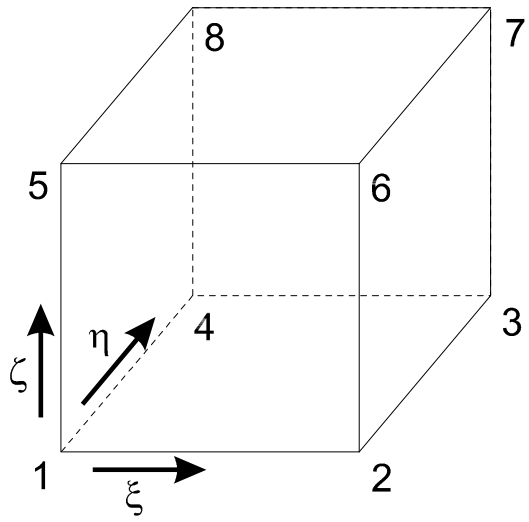

Figure 2.6:Aisoparametric hexahedral element.w

to global coordinates, and because base functions are expressed in local coordi-A nates, a transformationAisArequired. ThisAtransformationAisAobtainedAviaAtheAbasisA functions asA

$$x = \sum_{j=14}^{8} x_j \; b_j(\xi,\eta,\zeta) \qquad (2.7)$$

$$y = \sum_{j=14}^{8} y_j \; b_j(\xi,\eta,\zeta) \qquad (2.8)$$

$$z = \sum_{j=14}^{8} z_j \; b_j(\xi,\eta,\zeta) \qquad (2.9)$$

Using this transformation, firstAorderAderivativesAofAtheAbasisAfunctionsAversusA global coordinates can be changed to their equivalent with respect to local coor-A dinates byA

$$\begin{pmatrix} \frac{\partial b_i}{\partial x}S \\ \frac{\partial b_i}{\partial y}S \\ \frac{\partial b_i}{\partial z}S \end{pmatrix} = [J]^{-14} \begin{pmatrix} \frac{\partial b_i}{\partial \xi}S \\ \frac{\partial b_i}{\partial \eta} \\ \frac{\partial b_i}{\partial \zeta}S \end{pmatrix} \qquad (2.10)$$

$$[J] = \begin{pmatrix} \frac{\partial x}{\partial \xi} & \frac{\partial y}{\partial \xi} & \frac{\partial z}{\partial \xi} \\ \frac{\partial x}{\partial \eta} & \frac{\partial y}{\partial \eta} & \frac{\partial z}{\partial \eta} \\ \frac{\partial x}{\partial \zeta} & \frac{\partial y}{\partial \zeta} & \frac{\partial z}{\partial \zeta} \end{pmatrix} \tag{2.11}$$

where $[J]$ is the Jacobian of the transformation.

The encountered integrals arising out from the finite element approximation of the groundwater flow equations may take the forms

$$\Lambda = \int_V F(x, y, z)\, dx\ dy\ dz \tag{2.12}$$

where $F(x, y, z)$ is a continuous function over the volume V. Equation (2.12) can be transformed to

$$\Lambda = \int_{-14}^{+14} \int_{-14}^{+14} \int_{-14}^{+14} F(\xi, \eta, \zeta) J\ d\xi\ d\eta\ d\zeta \tag{2.13}$$

where $J = \det [J]$. Λ can be easily computed by a Gaussian quadrature.

2.7 Advanced Finite Element Methods

2.7.1 Mixed Finite Element Method

The mixed finite element method (MFE) was first introduced to the groundwater community by the works of Meissner (1972), and Douglas et al. (1983). Since then, the method has been extensively studied and compared to more classical techniques (Brezzi and Fortin, 1991; Chavent and Roberts, 1991; Cordes and Putti, 1997; Durlofsky, 1993). However, the state of the art is attained for 2-D delaunay unstructured triangulations (Durlofsky, 1993), and fundamental research is still needed to extend it to a full range of 3-D problems.

The MFE formulation leads to continuous flux approximations (first order accurate) across the element edges, whereas the conforming finite element method fails (discontinuous fluxes). This is achieved by adding additional degrees of

freedom at the elements mid-edges. The flow equation is discretized using un-known groundwater heads at the nodes, and unknown Darcian velocity vectors at the mid-edges. The typical scheme employed for this type of problem is the Raviart-Thomas (RT0) approach that uses piecewise constant basis functions for the groundwater head and linear vector basis functions for the Darcian velocity. As a consequence the solution is more accurate even for the flow field. There is an expensive price to pay for such accuracy; the MFE formulation generates about twice as many degrees of freedom as standard finite elements of the same order.

By generating high accuracy velocity fields, the MFE is an attractive method for modeling coupled flow and transport problems. In particular, The method has been effectively used in conjunction with the finite volume method for the transport equation (Durlofsky, 1993).

2.7.2 Control Volume Finite Element Method

The essence of the control volume finite element method (CVFE) is to use the finite element basis functions to approximate the groundwater heads at the nodes, whereas the conservation equations are applied to control-volumes (Forsyth, 1989). The control-volumes definition is highly flexible, they may be patches centered around the nodes as illustrated in Fig 2.7, or coincide completely with the fi-nite element cells. For more general triangulations, control volumes are general polygons spanning more or fewer elements and which are not necessarily convex.

Here again, recent works have focussed on 2-D triangular elements (even if 3-D extensions are straightforward, at least for tetrahedrals) though there exists some restrictions with respect to the triangulation used (Forsyth, 1989; Jie and Van Quy, 1992; Gottardi and Venutelli, 1993).

The cell-volume CVFE dual discretization approach can be used in order to improve the approximation of fluid velocities, computed at the basis of groundwa-

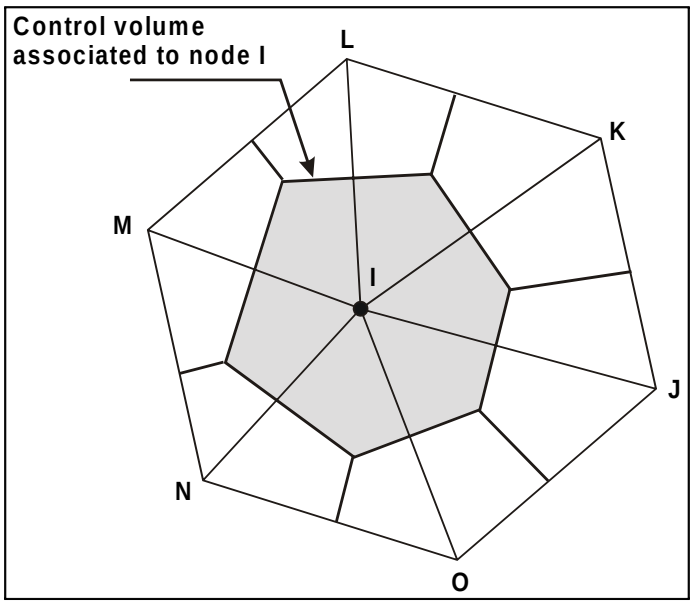

Figure 2.7:AControl volumes versus finite element cells for 2-D triangulations.w

terAheadAvaluesAresultingAfromAstandard FEAformulationsA(Durlofsky, 1993; Tracy, 1994).A

2.8y IterativeyMethodsy

2.8.1 IterativeyMethodsyVersusyDirectyMethodsy

The discretization of PDE's using numerical approximation methodsAleads to aA system of algebraic equations which is in most cases expressed in matrix form.A The problemAreduces toAsolving the given systemAof equationsAforAn unknowns (n is the matrix order).A

Regardless of the structure of the system, e.g., linear or nonlinear, dense orA sparse, one has to choose between direct or iterative solution methods.A

The present state of the art in numerical methods is that direct methods canA be used as black boxes. This is by far not the case for iterative methods, at leastA not if we do not know the specific properties of the matrix of the linear systemA

to be solved. And even then it is no trivial matter to decide when to stop the iteration process and to obtain a reasonable estimate of the approximation error in the result.

The simplest direct method is probably the well-known Gaussian elimination procedure, unfortunately this popular method leads to fill-in, which makes the method often expensive. Usually large sparse matrices are related to some grid or network, and it is highly desirable to exploit this 'nice' property efficiently.

For large 3-D problems, iterative methods are preferable, for this class of problems Van der Vorst and Chan (1998) estimated the flops count for a direct solution method in the order of n^3, and the number of flops for an iterative solver in the order of $n^{7/3}$. Also the requirements for memory space for the iterative methods are typically smaller by orders of magnitude. This is often the argument for the usage of iterative methods in 2D situations, when flop counts for both classes of methods are more or less comparable. Finally it should be noted that iterative methods can exploit good initial guesses, e.g., in time dependent problems. The preconditioner can often be chosen to adapt to the machine architecture.

The above given arguments are quite nicely illustrated by observations made by Simon (1989). For linear problems with some $5x10^{94}$ unknowns, he has estimated the CPU time required by the most economic direct method, as 520,040 years, provided that the computation can be carried out at a speed of 1 TFLOP. On the other hand, he estimates the CPU time for preconditioned conjugate gradients, assuming still a processing speed of 1 TFLOPS, as 575 seconds. Though we should not take it for granted that in particular a very sparse preconditioning part can be carried out at that high processing speed (for the direct solver this is more likely), and the CPU values may change, we see that the differences in CPU time requirements are gigantic.

2.8.2 A Basic Iterative Method

The very basic idea, that leads to many effective iterative solvers, is to split the matrix of a given linear system as the sum of two matrices, one of which leading to a system that can easily be solved. The most simple splitting we can think of is $\mathbf{G} = \mathbf{I} - (\mathbf{I} - \mathbf{G})$. Given the linear system $\mathbf{G}\mathbf{h} = \mathbf{B}$, this splitting leads to the well-known Richardson iteration

$$\mathbf{h}^{i+1} = \mathbf{B} + (\mathbf{I} - \mathbf{G})\mathbf{h}^i = \mathbf{h}^i + \mathbf{r}^i$$

Multiplication by $-\mathbf{G}$ and adding $\mathbf{B}$ gives

$$\mathbf{B} - \mathbf{G}\mathbf{h}^{i+1} = \mathbf{B} - \mathbf{G}\mathbf{h}^i - \mathbf{G}\mathbf{r}^i$$

or

$$\mathbf{r}^{i+1} = (\mathbf{I} - \mathbf{G})\mathbf{r}^i = (\mathbf{I} - \mathbf{G})^{i+1}\mathbf{r}^0 = \mathbb{P}_{i+1}(\mathbf{G})\mathbf{r}^0$$

or, in terms of the error

$$\begin{aligned} \mathbf{G}(\mathbf{h} - \mathbf{h}^{i+1}) &= \mathbb{P}_{i+1}(\mathbf{G})\mathbf{G}(\mathbf{h} - \mathbf{h}^0) \\ \mathbf{h} - \mathbf{h}^{i+1} &= \mathbb{P}_{i+1}(\mathbf{G})(\mathbf{h} - \mathbf{h}^0) \end{aligned}$$

In these expressions $\mathbb{P}_{i+1}$ is a (special) polynomial of degree $i + 1$. Note that $\mathbb{P}_{i+1}(0) = 1$.

Results obtained for the standard splitting can be easily generalized to other splittings, since the more general splitting $\mathbf{G} = \mathbf{M} - \mathbf{N} = \mathbf{M} - (\mathbf{M} - \mathbf{G})$ can be rewritten as the standard splitting $\mathbf{B} = \mathbf{I} - (\mathbf{I} - \mathbf{B})$ for the preconditioned matrix $\mathbf{P} = \mathbf{M}^{-1}\mathbf{G}$. Other more powerful iteration methods can be viewed as accelerated versions of the basic iteration methods. In the context of these accelerated methods, the matrix splittings become important in another way, since the matrix $\mathbf{M}$ of the splitting is often used to precondition the given system. That is, the iterative method is applied to, e.g., $\mathbf{M}^{-1}\mathbf{G}\mathbf{h} = \mathbf{M}^{-1}\mathbf{B}$.

For the simple Richardson iteration it follows that

$$h^{i+1} = \mathbf{r}^0 + \mathbf{r}^1 + \mathbf{r}^2 + .. + \mathbf{r}^i = \sum_{j=0}^{i} (\mathbf{I} - \mathbf{G})^j \mathbf{r}^0$$
$$\in \{\mathbf{r}^0, \mathbf{G}\mathbf{r}^0, ..., \mathbf{G}^i\mathbf{r}^0\} \equiv \mathbb{K}^{i+1}(\mathbf{G}; \mathbf{r}^0)$$

$\mathbb{K}^{i+1}(\mathbf{G}; \mathbf{r}^0)$ is a subspace of dimension $i+1$, generated by $\mathbf{r}^0$ and $\mathbf{G}$, and is called the *Krylov subspace* for $\mathbf{G}$ and $\mathbf{r}^0$. Apparently, the Richardson iteration delivers elements of Krylov subspaces of increasing dimension. Note that the Richardson iteration generates a basis for the Krylov subspace, and this basis can be used to construct other approximations for the solution of $\mathbf{G}\mathbf{h} = \mathbf{B}\mathbf{y}$ as well.

2.8.3 Linear Symmetric and Nonsymmetric Systems

When the system matrix is symmetric and positive definite, which is the case for the conductance matrix derived from the FE discretization of the governing equations for groundwater flow, powerful and efficient preconditioned iterative solvers are available, and become widespread. The most attractive feature of many of these solvers is the mathematically guaranteed convergence in an arithmetic number of iterations. This is however, not the case in practice, where several difficulties might be encountered whenever the positive transmissibility (PT) condition is not fulfilled (Putti and Cordes, 1996). We refer to section 4.3 for a more detailed explanation.

For matrices that are not positive definite symmetric the situation can be more problematic. It is often difficult to find the proper iterative method or a suitable preconditioner. However, projection type methods, like GMRES, Bi-CG, CGS, and Bi-CGSTAB are used as alternatives, even if extreme care should be taken when choosing the most appropriate solver to a given class of systems. Despite CG-like algorithms for symmetric matrices, the convergence is neither guaranteed for such accelerators. Section 6.3 details these aspects, and discuss several examples of preconditioning showing their strenghts and weaknesses.

Chapter 3G

Numerical Formulationy of Mathematicaly Groundwatery Flowy Modelsy

Contentsy

3.1 Introductiony

The mathematical formulation of the governing groundwater flow equations and different steps involved in their derivation are highlighted, while most of the discussion focuses on the distinction of the different flow situations encountered

in practice. Of special concern in the next chapters, will be the case of variably saturated flow and saltwater intrusion. Next, conforming Galerkin finite element discretizations of these equations are derived and presented in their general form as used and implemented in the numerical groundwater flow models discussed further. The numerical algorithms used to handle each of the equations are left for the upcoming chapters. So, herein only classical derivations as found in the relevant literature are applied. Interesting issues such as treatment of different boundary conditions from numerical point of view, and different implementation techniques are discussed in more detail. A clear picture of different strategies for solving the finite element equations system is given, in which different methods used during the last decades are compiled, compared and commented.

3.2 Governing Equations for 3-D Groundwater Flow

3.2.1 Basic Equations

The governing equations for variable saturated flow in heterogeneous porous medium are derived based on the *mass conservation* equation and the generalized *Darcy* law relating flux to potential gradient.

In general, local mass conservation in compressible and variable saturated porous media is expressed as

$$\frac{\partial}{\partial t}\left[S_p(p)+\theta(p)\right] = -\nabla\mathbf{q}+R \tag{3.1}$$

where p is the water pressure [M/LT^2] relative to atmospheric pressure, negative in the unsaturated zone and positive in the saturated zone, S_p is the elastic storage coefficient due to the combined effect of water and solid porous matrix compressibility, and saturated or unsaturated conditions [dimensionless], θ is the volumetric water content [dimensionless], $\mathbf{q}$ is the specific discharge rate

[LT^{-1}], R is the internal source/sink term [T^{-1}], and ∇ is the del operator [L^{-1}], $(\partial/\partial x, \partial/\partial y, \partial/\partial z)^T$, where $\mathbf{x} = (x, y, z)^T$ is the location vector [L].

The generalized *Darcy* law for variable saturated flow in heterogeneous porous media is given by

$$\mathbf{q} = -\frac{\mathbf{k}(p)}{\mu} \left[\nabla p + \rho g \nabla z\right] \tag{3.2}$$

where $\mathbf{k}$ is the unsaturated permeability tensor [L^2], μ is the dynamic viscosity [M/LT], g is the acceleration due to gravity [L^2T^{-1}], ρ is the fluid density [M/L^3], and the z-axis is taken vertical and positive upwards.

Introducing the hydraulic head or groundwater potential h, as

$$h = z + \frac{p}{\rho g} = z + \psi \tag{3.3}$$

Where ψ is the pressure head [L]. *Darcy's* law can be written in an equivalent form

$$\mathbf{q} = -\mathbf{K}(h)\ \nabla h \tag{3.4}$$

where $\mathbf{K} = \mathbf{k}\rho g/\mu$ is the hydraulic conductivity tensor [LT^{-1}].

3.2.2 Saturated Groundwater Flow

Under saturated conditions, the porous medium compressibility depends upon the water pressure, or groundwater potential, such that we can assume the elastic storage coefficient, S_p, proportional to the pressure head, p

$$S_p = S_s\, p \qquad \text{if} \quad p \geqslant 0 \tag{3.5}$$

where the coefficient of proportionality, S_s, is called the specific storage coefficient [L^{-1}], depending only upon compressibility characteristics of the porous medium and the fluid, S_s represents the volume of water produced per unit saturated volume of the porous medium, per unit decline of groundwater potential.

Note also that the saturated water content, θ_s, and the corresponding con-A ductivityA**K**y, do not depend on pressure. Inserting equation (3.4) andA(3.5) intoA equation (3.1) yields a linear partial differential equation governing saturated flowA in a 3-D heterogeneous porous mediumA

$$S_s \frac{\partial h}{\partial t} =A\nabla (\mathbf{K}y\nabla h) + R \tag{3.6}$$A

3.2.3y UnsaturatedyGroundwateryFlowy

In this case, it is assumed that the storage due to compression of the medium orA the fluid can be ignored in comparison to storage resulting from changes in theA water content (Freeze and Cherry, 1979), i.e,

$$S_p = 0 \text{ A} \quad \text{if A} p < 0\text{A} \tag{3.7}$$A

inserting equation (3.4)Aand (3.7) into equation (3.1)Ayields a nonlinear partialA differential equation governing unsaturated flow, namely theA*Richardy*equationA

$$\frac{\partial \theta}{\partial t} =A\nabla(\mathbf{K}y\nabla h) + R \tag{3.8}$$A

Notice that this equation contains the groundwater potentialAh, and the water A contentθ, which are a-priori the unknowns of the problem, therefore additionalA relationships relating these variables and the hydraulic conductivity should beA formulated.A ExamplesAofAtheseAconstitutiveArelationshipsAareAgivenAinAsectionA 3.2.6.A

Using the chain ruleA$\frac{\partial \theta}{\partial t} =A\frac{d\theta}{dh}\frac{\partial h}{\partial t}$ we obtain the following equationA

$$C \frac{\partial h}{\partial t} =A\nabla (\mathbf{K}y\nabla h) + R \tag{3.9}$$A

whereA$C(h)$ is the water capacity [L^{-1}], given asA

$$C = \frac{d\theta}{dh} =A\theta_s \frac{dS_w}{dh} \tag{3.10}$$A

C represents the amount of water released per unit volume of unsaturated porous medium, per unit decline of the groundwater potential, and S_w $(= \theta/\theta_s)$ is the saturation of water $(0 \leq S_w \leq 1)$ [dimensionless].

In the general case, where the elastic storage coefficient is not neglected, the exact derivation leads to a general storage term in the left hand side of equation (3.9) which is given by (see Huyakorn and Pinder, 1983)

$$S(h) = S_w S_s + C \tag{3.11}$$

Hence, the general equation governing the flow in 3-D variably saturated porous media may be written as

$$S(h)\ \frac{\partial h}{\partial t} = \nabla(\mathbf{K}_s \mathbf{k}_r\ \nabla h) + R \tag{3.12}$$

where $\mathbf{k}_r$ is the relative hydraulic conductivity tensor [dimensionless]. This form of the governing equation is the so-called *h-based Richards* equation, while other forms are the *θ-based* and *pressure head-based Richards* equations, where the dependent variables are substituted for θ and ψ respectively. However, the h-based form presents some advantages, as it can be used for saturated and unsaturated soils, as well for layered soils.

3.2.4 Steady State Groundwater Flow

Another possibility arising from the use of equations (3.6), (3.9) or (3.12) is when the variables become independent of time, the flow equation can be reduced to

$$\nabla(\mathbf{K}_s \mathbf{k}_r\ \nabla h) + R = 0 \tag{3.13}$$

The nonlinearity in the groundwater flow equation is still not removed, but decreased by an order of magnitude, since dependencies on the groundwater heads are shortened to $\mathbf{k}_r = \mathbf{k}_r(h)$ relationship. Water contents are not involved in the steady state groundwater potentials, meaning implicitly that steady saturation profiles have a sharp distribution ($\theta = 1$ in the saturated zone, and $\theta = 0$ in the unsaturated zone).

3.2.5y UnconfinedyGroundwateryFlowy

In modeling unconfined aquifer systems, care should be taken of theAvadoze zoneA above the saturated region.ATThe two regions can be distinguished from physicalA point of view by the variability of the water content denoted here by θ $(0A< \theta < n)$, which equals the porosity, n, or saturated water content, θ_s, in the saturated zone.A In between an abrupt water table delimits sharply the vadose and saturated zones.A Neuman and Witherspoon (1970)Aderived the exact mathematical expression forA the water table as a boundary condition, given byA

$$(R - \theta_s \frac{\partial \zeta}{\partial t}).\mathbf{n}_{34} = \sum_{i=14}^{3} (\mathbf{K}y\nabla h).\mathbf{n}_i \qquad (3.14)A$$

whereA$\mathbf{n}_i$ are components of the outward unit vector, andAζ represents the waterA tableAelevation aboveAtheAdatum level. ThisAis a directAconclusion of theAfactAthatA the water table is a streamline satisfying the kinematic conditionA$\frac{dF}{dt} = 0$, whereA $F(\mathbf{x}, t) = \zeta A(x, y, t)A - z$ representsAtheAgeometryAofAtheAwaterAtable.AInAadditionA it is necessary to prescribe the atmospheric pressure, taken as a reference, to theA water table boundary, such thatA

$$h(\mathbf{x}, t) = zA \qquad (3.15)A$$

3.2.6y ConstitutiveyRelationshipsy

In general, for variably saturated flow, relative hydraulicAconductivity and volu-A metricAmoisture content depend on the pressure head; theseAwell-known relation-A shipsAareAtheAsoilAcharacteristicAcurvesA(Fig.A3.1), whichAshouldAbeAidentifiedAinA order toAsolveAthe mathematicalAproblem. The tremendousAvariabilityAofAtheAsoilsA compounds, theirAcomplex behavior underAsaturation andAdesaturationAprocesses, andAtheAhystereticAnatureAofAtheseAchangesA(seeAFig.A3.2), makesAexactAquanti-A tativeAdescriptionAofAtheAsoilAcurvesAveryAdifficult.APractically, theseAcurvesAareA obtained from laboratory experimental analysis, by fitting appropriate parame-A ters of semi-empirical expressions.A

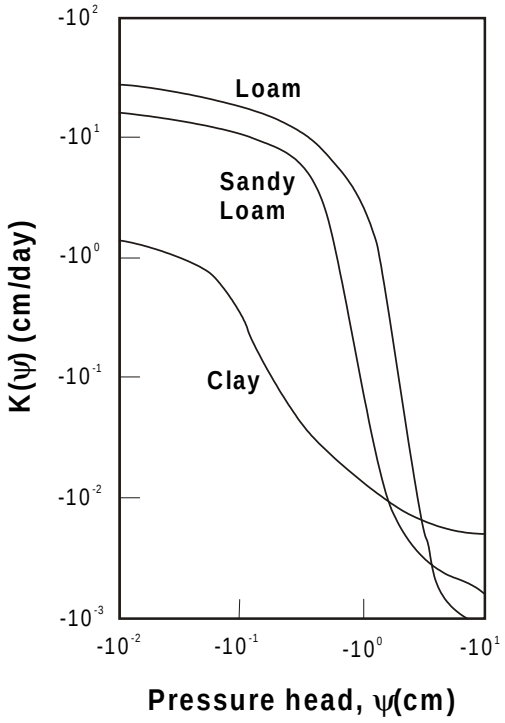

Figure 3.1: Representative unsaturated hydraulic conductivity curves for given soil types.

Among the most popular ones, the Van Genuchten and Nielsen (1985) equations are given by

$$\theta(\psi) = \begin{cases} \theta_r + (\theta_s - \theta_r)[1 + \beta]^{-\gamma} & \text{if } \psi < 0 \\ \theta_s & \text{if } \psi \geq 0 \end{cases} \tag{3.16}$$

$$k_r(\psi) = \begin{cases} (1+\beta)^{-5\gamma/2}[(1+\beta)^{\gamma} - \beta^{\gamma}]^2 & \text{if } \psi < 0 \\ 1 & \text{if } \psi \geq 0 \end{cases} \tag{3.17}$$

where $\beta = \left(\frac{\psi}{\psi_a}\right)^n$, ψ_a (≤ 0) is the capillary or air-entry pressure head value [L], n is a constant, and $\gamma = 1 - \frac{1}{n}$ for n approximately in the range $1.25 < n < 6$.

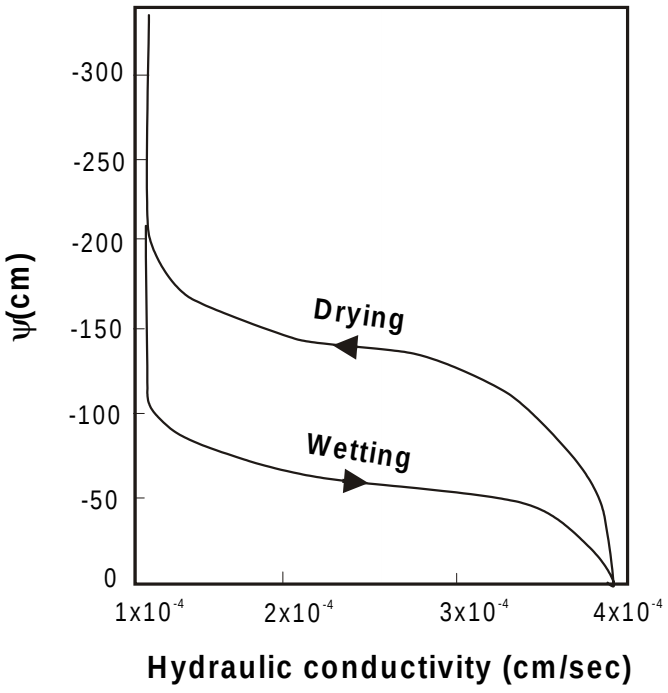

Figure 3.2:AHysterisiseffectswinwthew ettingwandwdryingwcycleswofwthewunsaturatedw hydraulic conductivity (After Fetter, 1998).w

Paniconi et al.A(1991) have suggested the following substitutionA

$$\theta(\psi) = \begin{cases} \theta_r + (\theta_s - \theta_r)[1 + \beta]^{-\gamma} & \text{ifA } \psi < \psi_{04} \\ \theta_r + (\theta_s - \theta_r)[1 + \beta_0]^{-\gamma} + S_s(\psi - \psi_0) & \text{ifA } \psi \geq \psi_{04} \end{cases} \tag{3.18}$$

whereA$\psi_{04}$is a continuity parameter, β_{04}=A$\beta(\psi_0) = \left(\dfrac{\psi_{04}}{\psi_a}\right)^n$.

Other widely used functions are given by Brooks and Corey (1964)A

$$\theta(\psi) = \begin{cases} \theta_r + (\theta_s - \theta_r)\left(\dfrac{\psi}{\psi_a}\right)^{\lambda} & \text{forA } \psi \geq \psi_a \\ \theta_s \qquad \text{ifA } \psi < \psi_a \end{cases} \tag{3.19}$$

$$k_r(\psi) = \begin{cases} \left(\dfrac{\theta - \theta_r}{\theta_s - \theta_r}\right)^m & \text{ifA } \psi < 0\text{A} \\ 1 \qquad \text{ifA } \psi \geq 0\text{A} \end{cases} \tag{3.20}$$

whereAλ is a constant, andAm is a conductivity shape parameter.7

Fuentes et al. (1992) showed that the combination of the Van Genuchten water retention equation (3.16) and the Brooks and Corey conductivity equation (3.20) yields the most consistent approximation for a large number of soil types encountered in practice. Therefore, we recommend using such a combination for the model to be developed afterwards. However, a major difficulty in applying such equations on large scale is that 'point' scale measurements are only in-situ quantities of the real representative field parameters, which make this approach a subject of many uncertainties and inadequate for large scale field studies. Notice that, for each soil type a significant number of related parameters is involved, some dimensionless parameters are usually obtained based on curve fitting techniques rather than a physical meaning based approach (Haverkamp et al., 1999).

3.2.7 Boundary and Initial Conditions

The specification of appropriate boundary conditions is essential in groundwater modeling. Each set of boundary conditions defines one unique solution of the mathematical problem. These conditions need to be well understood from physical point of view, and their mathematical formulation and numerical implementation should be worked out in an efficient way.

Conditions at the flow domain boundaries are classified from mathematical point of view either as Dirichlet, Neuman, Cauchy or variable conditions.

Dirichlet Boundary Conditions

Also known as first type boundary condition, because the potential value is prescribed on a given boundary S_1

$$h = h_0(\mathbf{x}, t) \qquad \text{on} \quad S_1 \tag{3.21}$$

Dirichlet boundary conditions are usually applied to soil-water interfaces, such as streams, rivers (draining or feeding), reservoirs, trenches, lakes, wells, coastal lines and infiltration ponds.

Neumany Boundary Conditionsy

This is a second type boundary condition, involving a prescribed flux normal toA the boundary, or a prescribed gradient of the potentialA

$$q_n(\mathbf{x},t) = A(\mathbf{K}y\nabla h)A\,\mathbf{n}y = A-q_0(\mathbf{x},t) \qquad \text{on} \quad S_24A \tag{3.22}$$

whereA**n**yis the outward unit vector normal to boundaryAS_{24} $q_0(\mathbf{x},t)$ is considered A positiveAwhenAenteringAtheAdomainAandAnegativeAotherwise.ANeumanAboundaryA conditions are typically encountered at the boundaries of aquifer systems whereA either Arecharge Aor Adrainage Aoccurs, or Ano Aflow A(q_n =A0) Ain caseAof Aimpervious A boundaries. Other examples are water divide lines, pumping or recharging wells, infiltration, effective rainfall, water outflow to the sea, and ground water inflowA or outflow through a boundary from a part of the aquifer that is not consideredA in the simulation, etc.A

Cauchy Boundary Conditionsy

The third type of boundary condition, which is also known as head dependent fluxA boundary condition, involves prescribing theAtotal normalAflux due to the gradientA in the boundary in response to changes in head within the aquifer adjacent toA this boundaryA

$$q_n(\mathbf{x},t) = A\lambda\,[h_0(\mathbf{x},t) - h] = Aq_0(\mathbf{x},t) \qquad \text{on} \quad S_34A \tag{3.23}$$

whereAλ isAaAconstant.AThisAtypeAofAboundaryAcanAbeAillustratedAbyAtheAupperA surface of an aquifer overlain by a semi-confining bed that is in turn overlain byA a body of surface water.AThe flux, q_{04} across the semi-confining bed entering theA aquifer, is given by A*Darcy's y*law asA

$$q_{04} = AK'\,\frac{h_{04} - h}{d} = AC_{04}(h_{04} - h)A \tag{3.24}$$

where K' is the hydraulic conductivity of the semi-confining bed, d is its thickness, $C_{04}$is the specific conductance of the resisting layer, $h_{04}$is the head in the surfaceA water body, andAh is the head in the aquifer.A

Examples of such a boundary condition are artificial injection of water or pumping of ground water, where the transfer is subjected to a certain resistance, as a sedimented infiltration pond or a clogged well, or a stream with a muddy bed.

Initial Conditions

For variable groundwater flow problems initial conditions have to be specified, given by

$$h = h_0(\mathbf{x}) \qquad \text{in} \quad V \tag{3.25}$$

where h_0 is the prescribed initial value for the groundwater potential, and V is the region of interest.

3.3 Governing Equations for Saltwater Intrusion

3.3.1 Basics

The flow in both saltwater and freshwater zones is modeled via an abrupt interface assumption (Bear and Verruijt, 1987) as shown in Fig. 3.3. This approach is successfully applied in case the transition zone is thin relative to the thickness of the freshwater lens. The exact position of this interface is initially unknown; in fact this is part of the solution, such that the sharp interface constitutes a free nonlinear boundary of the problem.

With the abrupt interface approximation, only the flow equations of both fluids need to be solved, i.e., salt concentrations in the freshwater zone V_F, and the saltwater zone V_S are respectively given by

$$\begin{cases} C = 0 & \text{in } V_F \\ C = C_s & \text{in } V_S \end{cases} \tag{3.26a}$$

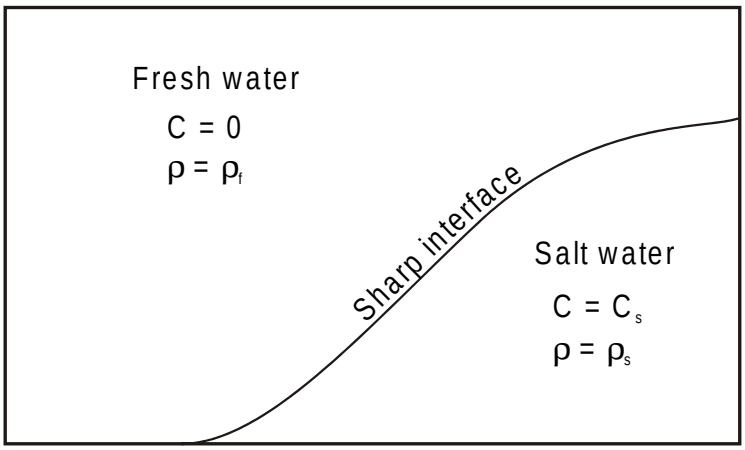

Figure 3.3:ASchematicwrepresentationwofwthewsaltwaterwintrusionwsharpwinterfacewap-wproach.w

Notice that consequently the density of each flow phase becomes constant,

$$\begin{cases} \rho = \rho_f & \text{in } V_F \\ \rho = \rho_s & \text{in } V_S \end{cases} \tag{3.27a}$$

This is easily deduced from the empirical formula suggesting density to be linearly dependent upon concentration, and given by

$$\rho = \rho_f(1 + \delta c) \tag{3.28}$$

where, ρ_f is taken as a reference density, c $(= C/C_s)$ is a normalized concentration, and $\delta = (\rho_s - \rho_f)/\rho_f$ is the density difference ratio, such that ρ_s is the density at the maximum concentration $(c = 1)$.

3.3.2 The Multiphase Sharp Interface Approach

Under these assumptions, the flow equations governing the flow in each phase are stated independently as in Bear (1979), Volker (1980) and Huyakorn and Pinder

(1983)

$$S(h^{(f)})\,\frac{\partial h^{(f)}}{\partial t} = \nabla\left(\mathbf{K}^{(f)}\nabla h^{(f)}\right) + R^{(f)} \tag{3.29a}$$

$$S(h^{(s)})\,\frac{\partial h^{(s)}}{\partial t} = \nabla\left(\mathbf{K}^{(s)}\nabla h^{(s)}\right) + R^{(s)} \tag{3.29b}$$

where (f) and (s) superscripts on the equation variables denote fresh and salt water phases respectively. The general storage coefficient for the saltwater phase is rigorously required in case of special conditions. For instance, the saltwater phase may overlap with the unsaturated zone, a salt cone of depression may develop in contact with the unsaturated zone, or infiltration of salty water from irrigation parcels need to be simulated.

The coupled equations (3.29a) and (3.29b) are solved for a given problem if unique boundary conditions are specified. These include in particular the fresh-saltwater interface as a physical boundary condition for the two equations simultaneously. Volker (1980) used a similarity between the water table and the fresh-saltwater interface, leading to a generalized form of equation (3.14), and given by

$$-\theta_s\frac{\partial \eta}{\partial t}.\mathbf{n}_{34} = \sum_{i=14}^{3}(\mathbf{K}^{(f)}\nabla h^{(f)}).\mathbf{n}_i \tag{3.30a}$$

$$-\theta_s\frac{\partial \eta}{\partial t}.\mathbf{n}_{34} = \sum_{i=14}^{3}(\mathbf{K}^{(s)}\nabla h^{(s)}).\mathbf{n}_i \tag{3.30b}$$

where η is the interface depth below the datum level, given by Hubbert (1940) as

$$\eta = \frac{\rho_s}{\rho_s - \rho_f}h^{(s)} - \frac{\rho_f}{\rho_s - \rho_f}h^{(f)} \tag{3.31}$$

This leads to the following equations relating the change of the position of the interface with time to potential gradient (or Darcian velocity) components

$$\frac{\partial \eta}{\partial t} = \frac{K^{(f)}}{\theta_s}\left(\frac{\partial h^{(f)}}{\partial x}\frac{\partial \eta}{\partial x} + \frac{\partial h^{(f)}}{\partial y}\frac{\partial \eta}{\partial y} - \frac{\partial h^{(f)}}{\partial z}\right) \tag{3.32a}$$

$$\frac{\partial \eta}{\partial t} = \frac{K^{(s)}}{\theta_s}\left(\frac{\partial h^{(s)}}{\partial x}\frac{\partial \eta}{\partial x} + \frac{\partial h^{(s)}}{\partial y}\frac{\partial \eta}{\partial y} - \frac{\partial h^{(s)}}{\partial z}\right) \tag{3.32b}$$

The equation for freshwater potential (3.32a) is derived by several authors, amongA which BearA(1972), Sugio andADesai (1987) implemented it in a 2-D seawaterA intrusionAfiniteAelement model, andABakkerA(1998) usedAit forAsolving theAtransientA *Dupuity*interface with the analytic element method.A

3.3.3y AySimplifiedyApproachy

Solving theAcoupledAsystemAofAequationsA(3.29a) andA(3.29b)AsubjectAtoAboundaryA conditionsAincludingA(3.32a)AandA(3.32b), isAdelicateAandAfarAexpensive.ASolvingA suchAproblemAfor a fullyAthreeAdimensionalAflowAfieldAwillAinduceAfurtherAunneededA complexity.AInstead, a simplified approach is developed to determine the sharpA interfaceAposition, assuming a quasi-stationaryAsaltwater zone, with a hydrostaticA pressure distributionA

$$p = -\rho_s g z \tag{3.33}$$A

by using the expression in equation (3.3)A

$$h = -\delta z \tag{3.34}$$

AssumingAthatAtheAhydraulicAhead changesAin theAsaltwater zone areAsmallAduringA the saltwater displacement (Hantush, 1968;A nderson, 1976) it is only necessaryA toAsolveAequationA(3.29a)Afor theAfreshwaterAheads, andAhenceAthe couplingAisA removed, whichAisAverysuitableAandAcheap.AThus, theAequationAgoverningAtheA flow for saltwater intrusion in 3-D heterogeneous aquifer systems is the same asA equation (3.12), except that an additional unknown free boundary, namely theA sharp interface is to be determined.A

Differentiation of equation (3.31) givesA

$$\frac{\partial \eta}{\partial t} = -\frac{1}{\delta}\frac{\partial h}{\partial t} \tag{3.35}$$

Equation (3.35) shows explicitly that the variations of the interface position areA dependent on the density difference and the groundwater heads in the flow field,

while in equation (3.32a) these variations are implicit. It turns out that, the latest equation is more suitable for numerical implementation in a computer model to estimate the differential saltwater interface displacement over a given time interval, knowing the residuals of the groundwater potential distributions.

3.4 Application of The Finite Element Method

For the sake of simplicity, we first shall approximate the steady groundwater flow equation (3.13), since the right hand side of equation (3.12) is the same. The left hand side of the transient variably saturated flow equation, which expresses the time dependence will be approximated later on by a fully implicit finite difference technique.

3.4.1 Galerkin Spacial Approximation

By applying the FEA approach already described in the previous chapter, the groundwater potential h is approximated by a finite series as

$$\widehat{h} \approx \sum_{j=1}^{nn} b_j(\mathbf{x}) h_j \tag{3.36}$$

where h_j is the nodal value of the groundwater potential, $b_j(\mathbf{x})$ is a trilinear nodal basis function and nn is the number of the nodes in the problem domain. Using equation (3.36) in equation (3.13) and applying the orthogonality condition in equation (2.5) results on the following equation

$$\int_V \{\nabla\ [\mathbf{K}\nabla(\sum_j b_j h_j)] + R\}\ b_i\ dV = 0 \quad \text{for } i = 1, 2, ..., nn \tag{3.37}$$

by applying the *Green's* theorem on the first term and integrating over all ele-ments and then summing over the domain, we obtain the FE equations in matrix form, which are linear for saturated flow and nonlinear for unsaturated flow

$$[\mathbf{G}]\{\mathbf{h}\} = \{\mathbf{B}\} \tag{3.38}$$

where $\{\mathbf{h}\}$ is the unknown vector containing the nodal potentials, $[\mathbf{G}]$ is the globalA conductance matrix depending on the geometrical and conductive properties ofA the flow domain andA$\{\mathbf{B}\}$ is a vector containing all boundaryAconditions, andA sources and sinks terms.A

In section 3.5 some important properties of the conductance matrix are ex-A plored for an efficient use by the solver. The entries of $[\mathbf{G}]$ are given by A

$$G_{ij} = \sum_e G_{ij}^e = \sum_e \int_{V^e} \nabla b_i^e \; \mathbf{K}^e \nabla b_j^e \; dV^e \tag{3.39}$$

where the local element contributions, G_{ij}^e, are calculated in local coordinatesA (ξ, η, ζ) by means of equations (2.7) through (2.13).A

The boundary conditions, together with sources and sinks, are incorporatedA in the entries of vectorA$\{\mathbf{B}\}$ given byA

$$B_i = \int_S q_n \; b_i \; dS + \int_V R \; b_i \; dV \tag{3.40}$$A

whereAq_n is the outer normal flux through the boundary surface, S.A

3.4.2y FiniteyDifferenceyApproximationyinyTimey

finite difference method is used for approximating the time derivative.A fullyA implicit method or backwardAdifference is adopted in the presented groundwaterA flow model because it is unconditionally stable and quite resistant to oscillatoryA nonlinear instability (Huyakorn andAPinder, 1983), even if the method is onlyA first order accurate.A

Considering the governing equation (3.12), the matrix system is written inA the formA

$$\frac{[\mathbf{S}]}{\Delta t}[\{\mathbf{h}\}^{t+\Delta t} - \{\mathbf{h}\}^t] + [\mathbf{G}]\{\mathbf{h}\}^{t+\Delta t} = \{\mathbf{B}\} \tag{3.41}$$A

where $[\mathbf{S}]$ is the diagonalized storage matrix having the following entriesA

$$S_{ij} = \delta_{ij} \sum_e \int_{V^e} S^e \; b_i^e \; dV^e \tag{3.42}$$A

whereAδ_{ij} is the Kronecker symbol, andAS^e is the storage coefficient of elementAe as defined in equation (3.11).

Assuming that the element storage quantityAS^e is averaged over each elementA volume, and that the value is attributed to the 3-D element centroid, we mayA express the diagonal matrix storage terms asA

$$S_{ii} = \sum_e S^e \int_{V^e} b_i^e \, dV^e = \sum_e S^e V_i^e \tag{3.43}$$

whereAV_i^e is the control volume contribution of elementAe at nodeAi as shown inA Fig.A3.4. Hence, The storage term does only increase the diagonal dominance ofA the global matrix.A

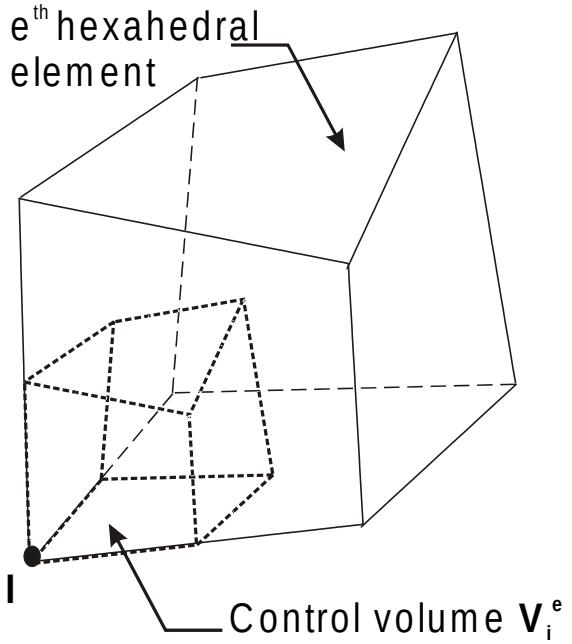

Figure 3.4:AThree-dimensional control volume contribution of the element e at nodew i.w

Finally, equation (3.41) can be transformed to a similar form as in equationA (3.38), but in this case with a global matrix $[\mathbf{G}^\star]$ and the boundary vectorA$\{\mathbf{B}^\star\}$

having respectively the following entriesA

$$G^{\star}_{ij} = \sum_{e} \int_{V^e} \nabla b_i^e \; \mathbf{K}^e \nabla b_j^e \; dV^e + \frac{S_{ij}}{\Delta t} \tag{3.44}$$

$$B^{\star}_{i} = \int_{S} q_n \; b_i \; dS + \int_{V} R \; b_i \; dV + \frac{S_{ii}}{\Delta t} h_i^t \tag{3.45}$$

So, in the remainder sections, $\mathbf{G}$ and $\mathbf{B}$ will refer to entries given by equations (3.44) and (3.45) respectively.

3.4.3 Numerical Implementation of Boundary Conditions

Basically, for a general groundwater flow problem there are different boundary conditions possible, depending upon the type of flow: confined, unconfined, or unsaturated-saturated flow. In the presented FE numerical model, a wide range of boundary conditions were implemented to allow for either natural or artificial stresses that might be encountered in practice. All conditions are attributed to the nodes of the finite element mesh, by means of a boundary condition code.

Fixed Potentials

In such nodes the potentials are given a fixed value in the left-hand side of equation (3.41) and are not anymore calculated by the model. As a consequence, for such nodes located on the boundary S_{14} the finite element equations are not needed. A simple substitution of equation (3.21) in the matrix system leads to an unsymmetrical global matrix, which is an undesirable property for solving the matrix system. Therefore, in the remaining equations all known fixed potential terms are moved to the right-hand side of equation (3.41) in order to conserve symmetry, and the equations corresponding to a prescribed potential nodes are simply skipped in the computational routines (Larabi and De Smedt, 1994), this method is efficient because it diminish the dimension or the number of unknowns of the matrix system. It is also robust, because prescribed potential values are preserved at their initial fixed values.

Fixed Flux or Flow

Here, the flux or flow rate of inflow or outflow of water in a node or at a series of nodes is fixed in the right-hand side of the matrix system. Hence, boundary conditions prescribed at Neuman boundaries S_{24} are explicit, except for nodes with a prescribed flux value, and for which the nodal surface normal to the flux vector must be calculated. This is practically feasible for vertical fluxes, as recharge or seepage, otherwise this becomes tricky or difficult to implement. Furthermore, the nodal horizontal surface areas are needed in other computational finite element routines, such that the cost of this implementation is reduced.

Leakage Flux or Flow

In nodes of mixed type boundary conditions as described previously in section 3.2.7, the resisting layer characteristics are described by one parameter, which can be considered as a global conductance, AC_{04} or as a nodal specific conductance, C_{04} depending on which condition (flux or flow) is prescribed, respectively. If the conductance is large, h will be nearly equal to h_{04} but in the opposite case no much flow is possible and the potential will be different from h_0. Nodes at boundary S_{34} are explicitly included in the matrix system, and diagonal dominance of the general matrix will increase at rows corresponding to this condition, i.e. global conductance terms are added to some of the matrix diagonal entries.

Seepage Face

This condition applies to the case of a seepage face. Outflow can occur under athmospheric conditions, this means zero pressure, or h equal to z, but no inflow is possible. This is expressed as

$$\begin{cases} h = z & \text{if } Q < 0 \\ Q = 0 & \text{otherwise} \end{cases} \tag{3.46}$$

The position of this boundary is known, but its extent is initially unknown.AToA handle the complexity of such situation, an iteratively based procedure is imple-A mented in the computer model which determines nodal points of this kind, thisA is an improved version of the Neuman's procedure (1973).A ll the nodes whichA can possibly be on the seepage face are treated initially as prescribed potentialA boundaries, with the potential equal to the elevation.A fter every iteration step, the flux values of the nodes are checked, and if an inflowing flux is encountered, thisAnodeAsAreatedAas an imperviousAboundaryAin theAnextAterationAstep. OnAtheA other hand, if a positive value of pressure is encountered at a boundary node inA the unsaturated zone, such node is treated in the next iteration step respectivelyA as node located on a seepage face node boundary.A

OutflowySea Facey

This condition applies at boundaries of either confined or unconfined aquifers, having a physical contact with a sea and through which the freshwater outflowA toAtheAseaAisApossible.AThisAconditionAisAsimilarAtoAtheAseepageAfaceAconditionA except that here the density gradient of salt and freshwater needs to be takenA into account, it is given byA

$$\begin{cases} h = -\delta z & \text{if } Q < 0 \\ Q = 0 & \text{otherwise} \end{cases} \qquad (3.47)$$

where z is the elevation referenced to the sea water level, and h is the freshwaterA potentialAatAtheAoutflowAnodes. AllAtheAnodesAwhichAcanApossiblyAbeAonAtheA outflowAfaceAareAtreatedAinitially asAprescribedApotentialAboundaries, withAtheA potential equal to the sea water level corrected for density difference, andAduringA theAterationAprocessAf a negativeAoutflowAlux isAencountered at a boundaryAnodeA in the saltwater zone, in the next iteration step the flow rate at such nodes willA put equal to zero.A

Variable Boundary Conditions

Because boundary conditions are subject to sharp temporal changes, and to the large variability of the medium properties which influence in turn the flow field, variable conditions give powerful capabilities to simulate situations as they would occur naturally. Examples are, horizontal infiltration where the flow rate specified at the soil surface infiltrate in the unsaturated zone above the water table surface; abstraction wells becoming dry at unsaturated depths where no water can be pumped; drainage systems, where the collected water is removed by an overflow system set at a given elevation. Such boundary conditions (Infiltration, drainage or abstraction) are efficiently implemented and given a special attention in the groundwater model routines as well.

Special nodes are also involved in many situations, such as isolated nodes which are completely surrounded by 'empty' elements, i.e. where no soil type is considered. These nodes are excluded from the system of equations and computational routines, and no flow can be calculated at their locations. Typical examples are man-made holes such as mining excavations, galleries, and drainage systems.

3.5 Finite Element Matrix Analysis

Repeatedly generated systems of FE equations are ideally solved by an iterative solver for large dimensions. But, the choice of this solver depends mainly on the particular properties of the global matrix which should be used efficiently to gain in memory use and CPU consumption. Investigation of FE matrix properties also clarifies many numerical issues related to the solvers efficiency and the preconditioners existence.

3.5.1 PropertiesyofytheyGeneralyMatrixy

It is of great importance to investigate the shape of the conductance matrix re-A sultingAfromAtheAuseAofAhexahedralAfiniteAelements.AIndeedAtheAGymatrix hasA some properties that make preconditioning possible and enhance the solver per-A formance.AGysatisfies following the conditions:A

1.AGyisAsparse, becauseAG_{ij} isAzeroAifAiandAjareAnotAnodesAof theAsameAelementA

2.AGyis symmetric, as can be concluded from equations (3.39 andA3.44)A

3.AGyis positive semi-definite (Axelsson and Barker, 1984).A

desiredAproperty Aforthe conductanceAmatrix isAtheAso-calledAM-matrix prop-A erty, which means that theAfollowing conditionsAhave toAbeAsatisfiedA(AxelssonandA Barker,y1984)A

- $G_{ii} > 0$ fo$\quad i =$A1, 2, ..., nn
- $G_{ij} \leq 0$ fo$\quad i \neq$AjS
- $\mathbf{G}^{-1} \geq 0$7

In case of symmetrical matrices these conditions are less restrictive, and areA equivalent to the following (Gustafson,y1984):A

- Gyis positive definiteA
- $G_{ij} \leq 0$ fo$\quad i \neq$AjS

From equation (3.44) it is clear that,7

$$G_{ii} = \int_V \nabla b_i \, \mathbf{K} \nabla b_i \, dV + \sum_e \int_{V^e} S^e \, b_i^e \, dV^e \qquad (3.48)$$

is always positive, and using the basis functions properties

$$\sum_{j=14}^{nn} b_j = 1 \tag{3.49a}$$

$$\sum_{j=14}^{nn} \nabla b_j = 0 \tag{3.49b}$$

it follows that,

$$\sum_{j=14}^{nn} G_{ij} = \sum_{e} \int_{V^e} S^e \; b_i^e \; dV^e \tag{3.50}$$

$$G_{ii} = -\sum_{j \neq i} G_{ij} + \sum_{e} \int_{V^e} S^e \; b_i^e \; dV^e \tag{3.51}$$

Substituting equation 3.48 to G_{ii} yields

$$\sum_{j \neq i} G_{ij} = -\int_{V} \mathbf{K} y (\nabla b_i)^{24} dV < 0 \tag{3.52}$$

This implies that some but not necessarily all of the off-diagonal terms are negative. For trilinear hexahedral elements, Larabi and De Smedt (1994) showed that the conductance matrix satisfies an M-matrix property if and only if all finite elements are cubes.

First and second type boundary conditions do not affect the general structure of G. Third type boundary conditions only increase the diagonal dominance of some rows.

3.5.2 Sparsey Matrix Storagey Schemey

conventional array storage of the conductance matrix composed of n^{24} elements, requires usually more core computer storage than the hardware can handle. Therefore, use is made of the symmetry and sparsity of G. y matrix and only non zero entries in the lower triangular part of G. y are stored via an indexing algorithm that keeps element positions within the original matrix. Several compressed storage schemes have been developed for sparse matrices (Saad, 1994),

with the aim of gain in efficiency both in terms of memory utilization and arith-A metic operations. It seems that the Compressed Sparse Row (CSR) format, andA its variants as the Modified CSR (MCSR) and Diagonal CSR (DCSR) are theA most Apopular Abecause Athey Aare Aimplemented An many Acomputer Apackages. SimilarA schemes referred as the forward and backward structures, have been describedA by Nawalany (1986), and Zijl and Nawalany (1993). AHerein, a DCSR variant isA used, and which is described as follows:A

compact row-wise real vector **gy** is used to represents the conductance matrixA **G**, all non zero entries existing in subsequent rows along the lower triangularA submatrix of A**G**.A direct Arelationship can be Aestablished Abetween Athe Adimensions A of A**G** yand A**g**, respectively denoted by Ann and An_g, as A

$$n_g = \sum_{i=14}^{nn} k_i \qquad (3.53)\text{A}$$

where Ak_i is Athe number Aof non Azero Aelements An Athe Ai^{th} row Aof the Alower triangularA part of A**G**.A

Two Ainteger Apointer Avectors A**pcy** and A**pdy** are used to Astore Arespectively theA numbers of the columns of subsequent non zero elements, and the positions ofA the diagonal elements, of A**G** yin vector A**g**, such that A

$$pd_j = \sum_{i=14}^{j} k_i \qquad (3.54)\text{A}$$

$$G_{i,pc_j} = g_j \qquad (3.55)\text{A}$$

Since a two Away correspondence Abetween **G** yand Its Acompressed Arepresentation A(**g**, **pc**, **pd**) is needed, this has to be clarified Aand established.A non zero elementA G_{ij} $(i \leq j)$ is retrieved as follows A

- For A$i = 1$ and Aj = 1 A G_{114} = A$g(1)$A

- For $i > 1$, a search is performed on the elements of pc to determine the element that is equal to a given j. The search can be limited to the range

$$k \in (pd_{i-1}, pd_i), \text{ when } pc_k = j, \text{ we find } G_{ij} = g_k$$

Reciprocally, to find the element G_{ij} corresponding to a given element g_k, its column number is directly obtained from pc_k, and its row number is the maximum i, such that $pd_i < k$.

3.6 Solution Strategies

The finite element system is usually solved by mesh-free iterative techniques, since the number of unknowns involved may be very large. The choice of a particular solver must suit the special system properties to gain in efficiency and robustness, the shape of the matrix stays the most decisive factor, i.e, symmetric or unsymmetrical, dense or sparse, banded or random, etc. More discussions on the solver to be used within the computer packages being under study will be given in the next chapter.

Besides the numerical solver, several strategies exist for solving unsaturated flow problems in unconfined or multilayer aquifers, the choice of a given method involves a number of underlying approximations and limitations, but the application goals and interests remain the general guidelines for such compromise. For instance, the moving mesh procedure is quite efficient, practical, and economical for prediction of the water table fluctuations in a regional groundwater aquifer system. In contrast, for seasonal variations study of the saturation soil profiles involving infiltration and ponding, the unsaturated zone plays a key role, and the more general variably saturated groundwater flow formulation including the unsaturated soils parameters is more appropriate.

3.6.1 TheyMovingyMeshyMethody

This technique involves an adaptive finite element mesh fitting the geometry ofA the external flow domain boundaries.AThe most naturally encountered free andA moving boundaries in groundwater flow problems being the water table and theA fresh-saltwaterAinterface.AThe AtechniqueAhasAbeenAsuccessfullyAusedAbyAseveralA groundwaterAflowAmodelersAworldwideA(France, 1974;ADesaiAet al., 1983; BearAandA Verruijt, 1987; Larabi and De Smedt, 1993; Crowe et al., 1998).A

nice feature of the method is that soil unsaturated properties are not needed, such that we may escape from the use of the waterAretention and theArelativeAy-A draulic conductivity curvesAin theAmodel, whichAwillAdecreaseAtheAproblemAnonlin-A earity.AHowever, a price is paid for such approximations, because under certainA conditions unacceptable errors could be introduced to the solution, or conver-A gence difficulties are present. To better illustrate these limitations, the followingA two descriptive examples are given.A

1.yAyFirstyExampley

Recharge from effective rainfall in an homogeneous shallow unconfined aquiferA isAprescribed at the most upperAlayer, whichAis theAfirstAlayer toAbe adjustedA duringAtheAsolutionAprocedure.ARetardationAeffectsAinAtheAunsaturatedAzoneAareA anAimportantAissueAespeciallyAifAtheApercolationAzoneAisAbecomingAthick.AThisA scenario not being taken into account in the moving mesh based simulators, theA numerical solution is inaccurate in consequence, especially for time dependentA scenarios involving a number of consecutive series of humidAandAdry periods.A

2.yAySecondyExampley

partially penetrating well pumping a fixed amount of water flow, Q_0, is placedA inAanAunconfinedAaquiferAasAillustratedAinAFigA3.5.AThe AtopAsectionAofAtheAwellA filterAofAlength$A l_F$, isAplaced at a givenAdepth, d_{FT}, fromAtheAsoilAsurface.AIfA

the water level at the well, h_w, is beneath the top filter section, the distributedA pumpingArateAover theAmovingApumpingAnodes at theAwellAfaceAshouldAbeAupdatedA in parallel, this amount of water depends on the length of the saturated part ofA the filter, this adaptive procedure at the boundary nodes is tricky to implement.A The problem still remains when the well becomes completely dry, because a userA intervention is still required.A

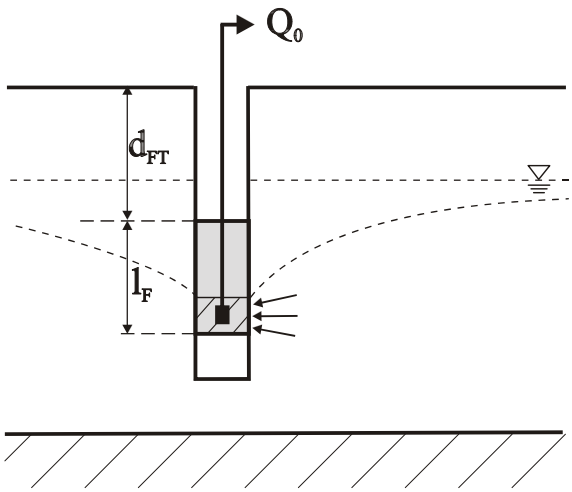

Figure 3.5:AExample of a partially penetrating pumpingw ell withdrawingw ater overw a portion of the filtered part.w

Hence, unexpected problems may occur with the moving mesh strategy. TheA modeler experience plays a very important role here, since the interpretation ofA the model obtained in many situations should be performed with care.A

3.6.2y TheyFixedyMeshyMethod

Another possibility consists on adopting a fixed or 'rigid' network of elements, invariantAinAspaceAandAtime.A ThisAconceptAisAmoreAwidelyAusedAforAmodelingA groundwater flow problems in unconfined aquifers (Cooley, 1983;AHuyakorn etA al., 1986; Paniconi et al., 1996), but in all these models the traditional approachA

considers the characteristicAsoilAcurvesAtoAresolve theAnonlinearitiesAin theAun-A saturatedAzone.ADrawbacksArelatedAtoAsuchAapproachAareAclassifiedAinAtwoAmainA points:A

1.ANumerical instabilities: due to the irregular shape of the characteristic soilA curves, and the difficulties surrounding an accurate representation of theA capacitance terms. These effects are best described in the next chapterA

2.AInefficiency: most of computer codes using a compact matrix based solver, needAtoArecompute allAmatrix entries termsAfor theAfixedAmeshAsizeAelements, which needAexcessiveAcomputerAtimeAto achieve an accurateAsolution. TheseA kind of problems for large 3-D problems has been the domain of high-endA supercomputersAandAmainframeAworkstationsAforAaAlongAtimeAago.AEvenA if several ports are existing nowadays for cheap desktop computers, CPUA costAisAstillAveryAhigh. LarabiandADeASmedtA(1997)AhaveAshowed that the **G**·**y** matrix entries depends upon the soil medium properties and the elementsA geometry which remains constant along the iterative process, they demon-A strate that important computer time saving is achieved when keeping theA fixed contribution the same all the time, so the relative hydraulicAconduc-A tivityAisAtheAuniqueAparameterAwhichAhasAtoAbeAadapted.AHowever, thisA previous study was limited to steady state conditionsAand will be furtherA extended for transient problems.A

Chapter 4G

Modeling 3-D Transient Variably Saturatedy Groundwatery Flowy withy Movingy Interfacesy

Contentsy

4.1 Introductiony

The problem of unconfined groundwater seepage is of a great interest in manyA fields such as in hydrogeology, civil and agricultural engineering, and hydrology.A Practical applications are for example, seepage flow in earth dams for stabilityA

analysis; prediction of water table levels in a phreatic aquifer bounding an adja-A cent water bodyA(river, canal, lake, stream, reservoir)AwhoseAwaterAlevelAfluctuatesA with time; performance of trenches which intercept contaminated groundwater;A bank storage due to fluctuations of water levels in rivers.A

The solution of these problems is often complicated owing to the occurrenceA of a free or moving water table and seepage face which are unknown a-priori, andAshouldAthereforeAbeAdeterminedAasAaApartAofAtheAsolutionAprocedure. Ana-A lytical solutions for such problems are derived for two-dimensional groundwaterA flow (in vertical cross-section) under theA*Dupuit-Forchhemeiry*assumption, whichA neglects the vertical flow component.AClassic solutions for initial and boundaryA value problems of this kind are found in the works of Harr (1962), Polubarinova-A Kochina (1962), Bear (1972, 1979) and Bear and Veruijt (1987); these solutionsA are limited to simple situations where hydraulic properties are uniform andAdo-A mainAgeometriesAareAregular.ATheseAlimitationsAhaveAledAtoAtheAdevelopmentAofA numericalAtechniquesAusingAtheAFDMA(Rubin, 1968;AFreeze, 1971).AHowever, itA is not possible to construct a finite difference grid which fits exactly the curvedA water table position.AThe IFDM brings a further improvement, this method canA handle easily domains of complex shape by constructing an irregular fitted net-A work of elements, but the drawback of the method is that the elements shouldA satisfy a given number of orthogonality conditions, which restricts its flexibility.A InAcontrast, the FEMAasAmoreAflexibleAinAhandlingAsuchAdifficulties, whichAexplainsA its popular use and implementation in many groundwater flow numerical codes, asAthoseApresentedAbyANeuman (1973), YehAandAWardA(1980), CooleyA(1983), HuyakornAetAal.A(1984), PaniconiAandAPuttiA(1996), andALarabiAandADeASmedtA (1997).A

However, it is our point of view that more research is needed to implement aA powerful and cost-effective solver for three-dimensional modeling with the stan-A dardAfiniteAelement method, becauseAof theAhighlyAinvolvedAcostAinAconstruct-A ing andAsolving theAalgebraic numericalAsystemsAofAequations, whichAbecomesA

cumbersome for transient problems as the iterative solution procedure involves repeatedly generated equations systems. The desired solver should exploit efficiently the particular properties of the global FE matrix as discussed in chapter 3. Furthermore, non-linearities inherent to the water table and seepage face iterative updating process, may lead to numerical instabilities. Another major difficulty which is typically encountered in solving groundwater seepage flow in variably saturated flow domains, arises from the strongly nonlinear behavior of the *Richards'* governing flow equation. Also, numerical approximation of the cord slope (tangent of the water retention curve) stemming from the matrix capacitance term is a complicated issue as reported by Paniconi and Putti (1996).

In this chapter the developed numerical approach and its basic concepts which are used to solve the approximate FE matrix equations system derived in the previous chapter are introduced for solving problems with a moving free surface. The developed technique is formally called the *Fasty Updating y Procedure* (FUP). Special consideration is made on computational efficiency in terms of CPU run-time and convergence speed. Care is taken of controlling numerical stability by effective handling of nonlinearities resulting either from difficulties related to estimation of the capacitance matrix coefficients, the chord slope, or from the occurrence of nonlinear boundary conditions (time dependent fixed heads, drainage, seepage, abstraction, etc..). Other essential issues for guaranteying numerical stability will be discussed, such as the performance of the nonlinear iterative solver, the existence of linearized preconditioned conjugate gradient scheme for hexahedral finite elements, and the time stepping scheme.

Several test examples are studied to demonstrate the numerical technique capability of predicting accurate results efficiently. Comparisons are made against available analytical solutions, and other numerical schemes such as the moving mesh method. A comprehensive validation of the model predictions is achieved, by comparing to laboratory experimental measurements of free surface flow in an earth dam model of irregular shape (Baseghi and Desai, 1987). This prob-

lem is rather complex because it allows for real three-dimensional flow and for heterogeneous dam materials.

4.2 The FUP Numerical Technique

This section will focus on the development of the FUP. The method is computationally fast because it avoids systematic reconstruction of the hole set of the FE equations, and does not require recalculating the global matrix entries as given in Equation 3.44. This 'fast' FE matrix reconstruction is performed in two steps. First, the relative hydraulic conductivity values in the conductance matrix terms are updated on an iterative basis, and second, the mass storage entries are approximated automatically from an idealized water retention curve as will be explained in the next two sub-sections. The two steps involve changes in the water suction potential values, and hence updating of the flow field.

4.2.1 Determination of Idealized Relative Hydraulic Conductivity

In the conductance matrix entries in Equation 3.39, two contributions can be recognized, the basis functions derivatives referring to the geometry of the finite elements, while $\mathbf{K}_y$ refers to the hydraulic properties of the medium with respect to water flow. It follows that the coefficients depend upon the position of the water table. In case the nodes position remain fixed, only the effective conductivity will be variable, as some nodes will be situated in the unsaturated zone. G_{ij} can be approximated as proposed by Larabi and De Smedt (1997), as follows

$$G_{ij} \approx k_{ij} \int_V \nabla b_i \mathbf{K}_y \nabla b_j dV = k_{ij} G_{ij}^s \tag{4.1}$$

this means actually, that we assume that the relative hydraulic conductivity between nodes is independent of their positions in space and time, and will depend only on the water status of the region in between as shown in Fig. 4.1(a).

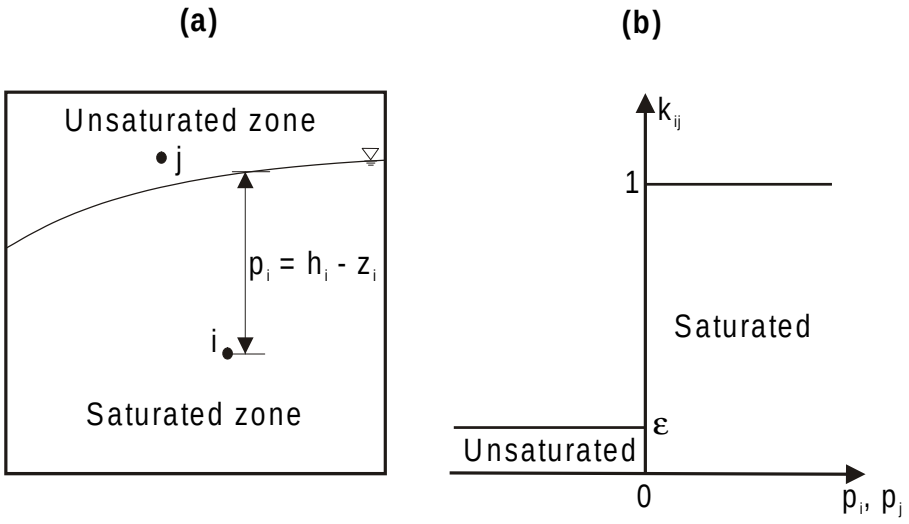

Figure 4.1: (a) Location of a water table between two nodes, and (b) idealized relative hydraulic conductivity curve versus nodal pressure heads (note that $k_{ij} = \varepsilon$ only if both nodes are unsaturated).

Notice that the saturated conductance coefficients, G^s_{ij}, are constant, and hence remain fixed during the solution procedure, such that only the relative conductivities have to be computed again in each iteration. For instance, if nodes i and j are saturated water nodes it follows that $k_{ij} = 1$, otherwise k_{ij} has to be updated. The following method is chosen to achieve this (Fig. 4.1(a))

$$k_{ij} = \begin{cases} 1 & \text{if} \quad p_i \geq 0 \text{ or } p_j \geq 0 \\ \varepsilon & \text{otherwise} \end{cases} \tag{4.2}$$

This is slightly different from the method used by Larabi and De Smedt (1997) for steady state water flow, suggesting k_{ij} to be smoothly updated for a water table region. In contrast, unsteady problems require immediate release of water from unsaturated to saturated nodes, such that small perturbations due to water table retardation effects are avoided. ε is theoretically zero, but chosen here as a small number in order to allow for the finite element equations corresponding to unsaturated nodes to remain in the algebraic equation system, without ob-

structing the numerical solution procedure by making the matrix singular. This also allows a small but negligible amount of water movement in the unsaturated zone, enabling recharge to pass from the soil surface to the water table through the vadose zone.

4.2.2 Idealized Water Retention Curve

Most computer models use various constitutive or characteristic relations describing the soil storage properties. Herein, the updating of the nonlinear storage or time dependent term in the right hand side of Equation 3.44 is evaluated numerically in the FUP numerical technique. The nodal storage variation depends on the water table position, and is evaluated using a mass lumping scheme (Neuman, 1972), such that

$$\int_{V^e} \frac{d\widehat{\theta}}{dh} b_i \, dV \approx \frac{d\theta}{dh} \int_{V^e} b_i \, dV = \frac{d\theta}{dh} V_i \tag{4.3}$$

clear physical interpretation of the mass lumped approximation for unsaturated flow, is that within each element the water content change is independent of the space domain. Whereas in contrast, a mass distributed scheme assumes a trilinear distribution in the element. This is most probably the reason why a mass distributed scheme exhibits numerical oscillations. The ultimate advantage of using a lumped formulation is therefore that it is unconditionally oscillation free (Celia et al., 1990).

The method used to evaluate the derivative term in Equation 4.3 affects significantly the convergence behavior of the iterative schemes, due to steep gradients and discontinuities or points of inflection in the soil curves as shown in Fig. 4.2.

natural choice of an idealized moisture retention curve would be a step function given by

$$\theta(p) = \begin{cases} \theta_s & \text{if } p_i \geq 0 \\ \theta_r & \text{if } p_i < 0 \end{cases} \tag{4.4}$$

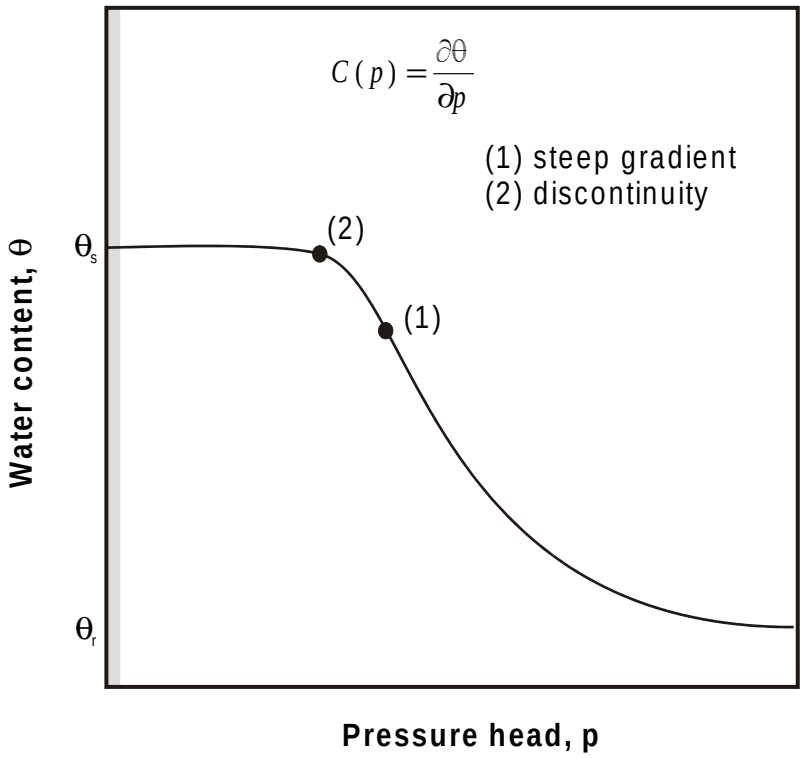

Figure 4.2: Water retention curves for specific soil types, and errors in the water capacity tangent approximation (modified from Istok, 1989).

However, this function suffers from the same disadvantages cited above, especially a discontinuity at the water table position ($p = 0$), hence another method should be adopted. It is of great importance to understand physically the reason of failure of the above mentioned procedure, while it seems to be attractive and simple. Actually, spurious oscillations are observed in cases where there are sharp pressure head variations (near convergence) such that water table movement does not change enough to cross at least one node from top to bottom. In such case, due to a null storage variation, i.e. $[\mathbf{S}] = 0$, a severe cancelation or an eventual jump to steady state flow conditions occurs. Another interpretation of such behavior, is that nodal points are assumed to be physically as either saturated or unsaturated, while the elements have three different water status, i.e., they may be saturated,

unsaturated, or partially saturated as depicted for the element in Fig. 4.3. It turns out that these elements are the source of failure due to neglection of the partially saturated nodes in the formulation of Equation 4.4. An illustrative example is shown in the table at the left side of Fig. 4.3 for the corresponding hexahedral element. The relative position of the water table inside this element to a fictive plane joining specific points at the element z-vertices is depicted. For instance, if the free surface crosses a vertex at a position between this fictive plane and the top element plane, the lower node sharing this vertex will be considered to be saturated while the other node becomes partially saturated. The distance separating a given node from that fictive plane, is interpreted as a sharp depth position from fully saturated or unsaturated state to partially saturated in the node neighborhood; this distance is evaluated as

$$d_i = \frac{\Omega_i}{\Gamma_i} \tag{4.5}$$

where Ω_i is the control volume attributed to node i, and Γ_i is the corresponding FE patch surface in the xy plane.

We define the soil moisture curve used in the described conceptual model as

$$\theta(p) = \begin{cases} \theta_s & \text{if } p_i > +\frac{d_i}{2} \\ \frac{\theta_s - \theta_r}{d_i} p_i + \frac{\theta_s + \theta_r}{2} & \text{if } |p_i| \leq +\frac{d_i}{2} \\ \theta_r & \text{if } p_i < -\frac{d_i}{2} \end{cases} \tag{4.6}$$

and the specific water capacity function as

$$\frac{d\theta S}{dh S}(p) = \begin{cases} \frac{\theta_s - \theta_r}{d_i} & \text{if } |p_i| \leq +\frac{d_i}{2} \\ 0 & \text{otherwise} \end{cases} \tag{4.7}$$

which means that the specific yield is released over the total length of each element if a nodal variation occurs in one node sharing it. Therefore, at least two nonlinear iterations are needed to achieve convergence.

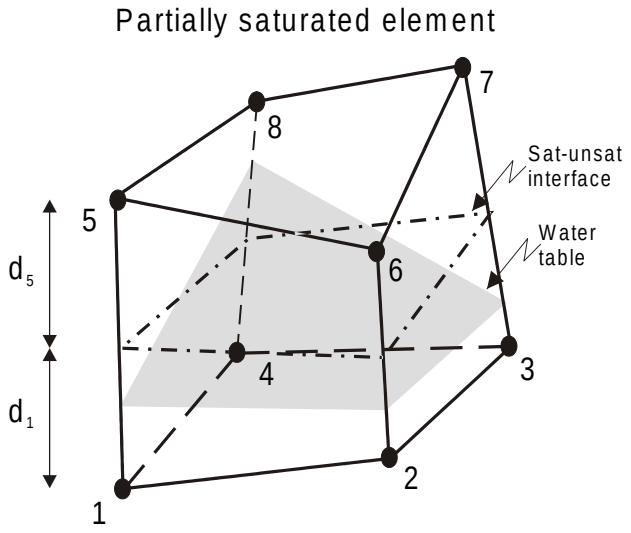

NODE	WATER STATUS
1	P
2	P
3	P
4	S
5	U
6	U
7	U
8	P

P: Partially saturated
S: Saturated
U: Unsaturated

FigureA4.3:AIllustrativewexamplewofwmappingwsaturated,wunsaturatedwandwpartiallyw saturated nodes from a partially saturated element.w

The functionals showed in Fig.A4.4 are used to achieve the numerical differ-A entiation method adopted in this model.A t the beginning of each time step theA differentialAin function (b) is directlyAused to approximate the chord slope, inA the next iterations nodal water content values are relaxed following the functionA (a) definedAexplicitly inAEquation 4.6 and the differential expression is calculatedA thereafter asA

$$\frac{\Delta\theta}{\Delta h} = \frac{\theta(t+\Delta t) - \theta(t)}{h(t+\Delta t) - h(t)} \approx \frac{\theta^m(t+\Delta t) - \theta(t)}{h^m(t+\Delta t) - h(t)} \qquad (4.8)$$

whereAm isAthe iteration level. It can beAnoticed that Equation 4.8AdoesAnot existA whenever$\Delta h(t+\Delta t) = \Delta h(t)$ which is especially the case at the beginning of eachA nonlinear time step. This explains the use of the analytic specific water capacityA as defined in Equation 4.7.A

ThereAremainsAonlyAoneAexceptionAwhenAstartingAfromAdryAconditions, i.e.A when the initial water table position is put exactly at the lower layer of nodes.A UnderAsuch initial conditionsAthe FUP hasAdifficulty to startAup asAthe lowerAnodesA inAtheAfiniteAelement meshAwillAremainApartiallyAsaturated, whichAisAunrealistic.A

possible remedy as adaptation of the idealized water retention curve, by fixing the parameter d_i for such nodes as small as possible ($d_i = \varepsilon \to 0$) and add this same preset value to initial heads ($h_i = z_i + \varepsilon, \forall i$). Another strategy consists in adding another nodal layer beneath the actual mesh. This second choice may involve however an important number of nodes for large applications. However, it is often rare to meet such extreme conditions for large scale groundwater flow models, and this issue is only of importance for local scale simulations and theoretical scenarios.

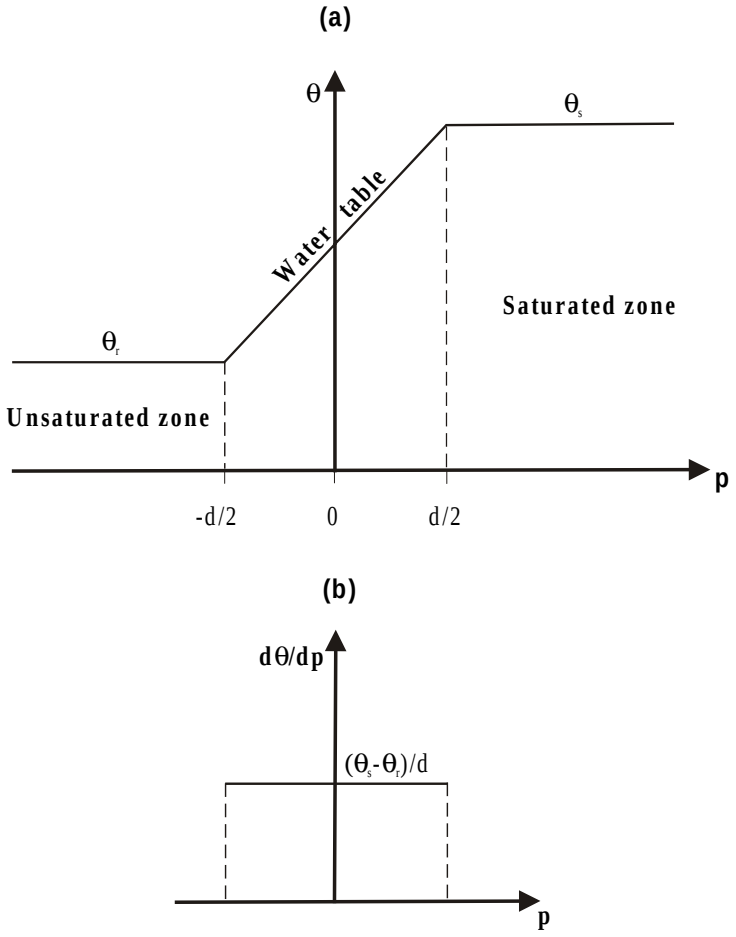

Figure 4.4: Idealized (a) water retention curve, and (b) analytic differentiation of slope tangent at nonlinear first iterate.

4.3 Numerical Solver

Direct solution techniques are not attractive because they cannot handle matrices of large dimensions, and do not make use of the special properties of the conductance matrix. Iterative techniques are more suitable, but it is crucial to choose a good iterative method from the many available, since any one of these methods may solve a particular system in few iterations while diverging for other problems. Hence, preconditioned conjugate gradient methods are preferred, because they are highly successful, reliable and more efficient for solving linear and positive definite symmetric systems, and also because of their reasonable cost per iteration.

4.3.1 Linear Preconditioned Conjugate Gradient (PCG) Solver

Among the existing iterative solvers, the conjugate gradient method (CG) is used mainly to solve positive-definite systems (Hestenes and Stiefel, 1952). This method is very popular for solving FD and FE systems arising from groundwater flow equations. The method does not require the coefficient matrix, only the result of a matrix-vector product is needed. It also requires a relatively small number of vectors to be stored per iteration since its iterates can be expressed by a three-term vector recurrences. The convergence is theoretically guaranteed after n iterations, but in practice the algorithm converges after much less number of iterations. The CG algorithm is given in table 4.1 in which the residual at k^{th} iteration is $\mathbf{r}_k = \mathbf{B}\mathbf{y} - \mathbf{G}\mathbf{h}_k$.

Notice that the algorithm is more efficient when the $\mathbf{G}$ matrix is in particular symmetric and very sparse, because the heaviest operation is the matrix vector multiplication $\mathbf{G}\mathbf{p}_k$ which becomes faster in such case. If the matrix satisfies also the requirements of an M matrix the convergence will be even more faster

(AxelssonAandABarker, 1984).A n important characteristicAofAtheACG algorithmAisA its connection with the Lanczos method which allows to obtain estimates of theA eigenvalues ofAGywith only little work per iteration, in this way Van der VorstA (1988) determined the condition spectral number, which is the ratioAof the highestA and lowest eigenvalues of theAGymatrix, and reported that the CG convergenceA speedAisAdependingAonAthis number. Therefore, theAmoreAGyresembles theAidentityA matrix theAfaster theAconvergence, otherwiseAthe matrix isAill-conditioned andAtheA algorithm requires a substantial number of iterations to converge.ATo overcomeA this problem, a transformation can be applied, which is commonly called scalingA or preconditioning (Van der Vorst, 1989).A

TableA4.1:A*Unpreconditionedyconjugateygradientyiterativeyalgorithmy(BarretyetyaI.,y 1994).y*

Choose an initial estimateA$\mathbf{h}_{04}$

$\mathbf{p}_{04}$=A$\mathbf{By}$– $\mathbf{Gh}_{04}$

Fory$k$ = 0, 1, 2, ... until convergenceA

α_k =A– $\dfrac{\mathbf{r}_k^T \cdot \mathbf{r}_k}{\mathbf{p}_k^T \cdot \mathbf{Gp}_{kd}}$

$\mathbf{h}_{k+14}$=A$\mathbf{h}_k - \alpha_k \mathbf{p}_{kd}$

$\mathbf{r}_{k+14}$=A$\mathbf{r}_k + \alpha_k \mathbf{Gp}_{kd}$

β_k =A– $\dfrac{\mathbf{r}_{k+14}^{Td} \cdot \mathbf{r}_{k+1}}{\mathbf{r}_k^T \cdot \mathbf{r}_k}$

$\mathbf{p}_{k+14}$=A$\mathbf{r}_{k+14}$+ $\beta_k \mathbf{p}_k$

End Fory

4.3.2y Preconditioningy

PreconditioningAacceleratesAgreatlyAthe convergenceAbehaviorAofACG methods, whichAbecomes necessaryAinAdealingAwithApracticalAapplicationsAofAlargeAsize. TheA

idea behind it is to multiply the system by a matrix $\mathbf{C}^{-1/4}$ that resembles $\mathbf{G}^{-1}$. Basically the algorithm does not change except multiplying by $\mathbf{C}^{-1/4}$ whenever this is required. Using initial guess values of the potentials $\mathbf{h}_{0/4} = \mathbf{C}^{-1}\mathbf{B}$ (Gustafsson, 1984; Gambolati, 1988b) leads to the preconditioned algorithm as shown in table 4.2.

Table 4.2: *Preconditioned conjugate gradient iterative algorithm (Barret et al., 1994).*

$\mathbf{p}_{0/4} = \mathbf{C}^{-1}\mathbf{r}_{0/4}$

For $k = 0, 1, 2, \ldots$ until convergence

$\alpha_k = \dfrac{\mathbf{r}_k^T \cdot \mathbf{C}^{-1}\mathbf{r}_k}{\mathbf{p}_k^T \cdot \mathbf{G}\mathbf{p}_{kd}}$

$\mathbf{h}_{k+1/4} = \mathbf{h}_k - \alpha_k \mathbf{p}_{kd}$

$\mathbf{r}_{k+1/4} = \mathbf{r}_k + \alpha_k \mathbf{G}\mathbf{p}_{kd}$

$\beta_{k} = \dfrac{\mathbf{r}_{k+1/4}^{Td} \cdot \mathbf{C}^{-1}\mathbf{r}_{k+1}}{\mathbf{r}_k^T \cdot \mathbf{C}^{-1}\mathbf{r}_k}$

$\mathbf{p}_{k+1/4} = \mathbf{C}^{-1}\mathbf{r}_{k+1/4} + \beta_k \mathbf{p}_k$

End For

The preconditioning matrix $\mathbf{C}$, which is close to $\mathbf{G}$, is considered as a good estimate if it fulfills the following conditions:

- The condition spectral number of $\mathbf{G}\cdot\mathbf{C}^{-1/4}$ is less than that of $\mathbf{G}$;
- The eigenvalue distribution of $\mathbf{G}\cdot\mathbf{C}^{-1}$ is more favorable to the CG algorithm than that of $\mathbf{G}$ itself;
- The coefficients of $\mathbf{C}^{-1/4}$ should be easily determined and $\mathbf{C}$ does not require excessive storage.

However, theseAconditionsArestrictAtheAchoiceAofAaAgoodApreconditioner.ATheA methods proved to be of value when they are used in conjunction with CG likeA methodsAare:AdiagonalAscalingA(DS), incompleteACholeskyAdecomposition A(IC), incomplete factorization (IF), modified incomplete factorization (MIF), and soA on.A ll preconditioners, except DS are derived from the class of incomplete tri-A angularAfactorizationAofA**G**, in this case we set A**C**y=A**L**y**U**y, where A**L**yandA**U**yareAlowerA and upper triangular matrices.A

The choice of the best preconditioner is still a matter of debate, indeed in eachA particularAsituationAoneAmethodAcanAperformAbetterAthanAothers.A ItAwasAalsoA shown that theirAefficiencyAisAhardwareAdependent. DSAisAbestAsuitedAin vectorAcu-A percomputers, while IC is better in scalar distributed memory computers.AThusA there is no general rule of thumb. It is also important to point out that the per-A formance of theseApreconditionersAdependsAon howAtheyAare coded, i.eAvectorized, parallelized, etc.A

TheyIncomplete Factorization Preconditioney

In this study IF preconditioning is preferred, i.eA

$$\mathbf{C}_y = (\mathbf{L}_y + \mathbf{D})\mathbf{D}(\mathbf{L}_y + \mathbf{D})^T \tag{4.9}$$A

whereA**L**yis the strictly lower triangular part ofA**G**, and **D**yis a positive diagonalA matrix, such thatA*diag* [**C**] = A*diag* [**G**] (Meijerink and Van der Vorst, 1977). OnlyA theAentriesAof**D**yneedAtoAbeAcomputed, thus theAmethodAdoesAnot requireAtoo muchA additional storage and computational work.AThe entries of the diagonal matrixA **D**ycan be computed recursively asA

$$D_{ii} = G_{ii} - \sum_{k=1}^{i-1} \frac{G_{ik}^2}{D_{kk}} \tag{4.10}$$A

Larabi andADeASmedtA(1994) concluded after many comparisonsAbasedAon severalA test problems, including hypothetical and field applications, that the precondi-A tioned conjugateAgradient (PCG)AmethodAbasedAon DS is theAmostArobustAbecauseA

it never fails, which is due to the fact that the preconditioning matrix always exists. However, this is not true for other preconditioners. In such cases, the M property of $\mathbf{G}_y$ proves to be a key factor for the successfulness of these solvers (Meijerink and Van der Vorst, 1977), because under this conditions all preconditioners are guaranteed to exist. Therefore, in this study we will use an incomplete factorization preconditioner obtained on the M type transformed conductance matrix as recommended by Larabi and De Smedt (1994).

4.3.3 M-Matrix Transformation Procedure

The flow domain is often divided into irregular finite elements, and leads naturally to a conductance matrix which is not an M matrix. Indeed, the more irregularity in the shape of the elements, the higher the deviation from the M matrix property. This will greatly hamper the numerical solution procedure, because of some constraints related to the existence of preconditioners as discussed in the previous paragraph. Larabi and De Smedt (1994) suggested that for obtaining a preconditioner, $\mathbf{G}_y$ can be transformed to a $\mathbf{G}_M$ M-matrix by maintaining all negative off-diagonal terms of $\mathbf{G}$, while all positive terms of $\mathbf{G}_y$ are added to the diagonal; hence

$$(G_M)_{ij} = \min(G_{ij}, 0) \tag{4.11}$$

$$(G_M)_{ii} = \sum_{j=14}^{nn} \max(G_{ij}, 0) \tag{4.12}$$

In the next paragraph, we will show that $\mathbf{G}_M$ is a good M matrix estimate of $\mathbf{G}_y$ and, that an incomplete factorization preconditioner used in conjunction with the conjugate gradient solver is always guaranteed.

4.3.4 Modified Nonlinear Picard Iteration

Among the most popular linearization schemes are Picard and Newton-Raphson methods (Huyakorn and Pinder, 1983; Istok, 1989), with the Picard method being

more popular because it is easier to implement, cheaper on a single iteration basis and does not need other storage requirements or changes in the system structure. In contrast, the Newton method involves additional costs related to storage and approximation of derivatives of the Jacobian, and leads to an unsymmetrical nonlinear system, which restricts the linear solvers choice. A comprehensive comparison between these two methods with several strategies has been carried by Paniconi and Putti (1996), who concluded that the Newton method is faster in case the initial estimate is good enough, otherwise convergence performance may be poor, and they propose a mixed approach for remedy. Herein, a modified Picard scheme is preferred because we believe that combined to the developed M matrix based linear PCG solver and the FUP, a robust and yet more stable solution method is obtained as will be demonstrated further in this chapter.

To solve the nonlinear FE system of equations 3.41 at time step t_{k+14} starting from the initial potential distribution $h(\mathbf{x}, t_k)$, the modified Picard algorithm involves the following steps described below for $m = 1, 2, ...$

1. The new position of the water table is determined at iterate m, using Equation 3.15, where h^m_{k+1} denotes the m^{th} iterate of $h(\mathbf{x}, t_{k+1})$;

2. The global conductance matrix is adjusted using Eqns 4.1 and 4.2;

3. The capacitance matrix terms are adjusted using Eqns 4.3 and 4.6 to 4.8;

4. The linearized system of FE equations is solved using standard conjugate gradient solvers, preconditioned with point incomplete factorization method enhanced with an automatic M-matrix transformation as described earlier, which yields a potential distribution h^{m+14}_{k+14};

5. For the next iteration, an improved estimate of h is derived from

$$h^{m+14}_{k+14} = \omega^{m+1}(h^{m+14}_{k+14} - h^m_{k+1}) + h^m_{k+14} \qquad (4.13)$$

where ω^{m+14} is an automatic underrelaxation factor used here in order to amortize possible oscillations of the potential iterates. An optimal value of ω^{m+14} is determined upon convergence rate at the previous iteration;

6. The iterative procedure described thought steps 1 to 5 is repeated until the following convergence criterium is satisfied

$$e^{m+14}_{\max 4} = \max \left| h^{m+14}_{k+14} - h^{m}_{k+14} \right| < tolw \qquad (4.14)$$

but, only over nodes lying in the saturated zone domain, while $tolw$ is a prescribed groundwater potential tolerance.

Relaxation Techniquey

Relaxation is suggested to enhance nonlinear iterative schemes as by Cooley (1983) and Huyakorn et al. (1986), this is because iterations could be slow or oscillations my occur. Here we used an adaptation of the Huyakorn's procedure (1996) which quantifies ω^{m+14} as a function of the convergence rate in the previous linear iteration, we suggest the following expression

$$\omega^{m+14} = \max \left[\min \left(\frac{e^{m+14}_{\max 4}}{(\Delta h)_{\max 4}}, 1 \right), \omega_{\min 4} \right] \qquad (4.15)$$

where $(\Delta h)_{\max 4} = \max |h_{\max 4} - h_{\min}|$ is the absolute value of groundwater potential head extremas over all nodal values, and $\omega_{\min 4} (0 < \omega_{\min 4} < 1)$ as a minimal preset value. Typically, this has a greater effect at the beginning of the iterations, and as the solution procedure continues it is obvious that $\omega^{m+14} \rightarrow \omega_{\min 4}$ where $e^{m+14}_{\max 4} \rightarrow 0$, especially when convergence is close. The technique shows to be very effective in accelerating the convergence of the nonlinear iteration by an order of magnitude of few iterations at the beginning of the process.

4.3.5y Timey Steppingy Schemey

The model automatically adjusts time step sizes, in order to avoid possible instabilities during the solution. maximum number of linear iterations; t_{max} is

allowed for each nonlinear time step, and if exceeded without convergence theA solution is recomputed at the current time level 'back stepping' using a reducedA timeAstepAsize.ATheAcomputationAcontinuesAuntilAaAmaximumApresetAtimeAT_{max}.A This time step is calculated using following expressionA

$$\Delta t = \min\left[\frac{S_{ii} tolw}{B_i - \sum_j G_{ij} h_j^{t_k}}\right] \tag{4.16}$$

However, if a fixed time step value Δt_{user} is specified the simulator will assumeA timeAstepAsizesAasAintegerAmultipliersA$(2\Delta t_{user}, 3\Delta t_{user}, ...)$ of this preset value. A If necessary, the time step is adjusted to coincide with a target time value$A t_p$ atA which simulation output is required.A

In conclusion, three nested iterative loops are necessary to build the overallA numerical flow solver.AThey are from the outer to the most inner one, the timeA steppingAloop, theAnonlinearAPicardAiteration, and theAlinearAMAmatrix basedA incomplete factorization preconditioned conjugate gradient method.A

4.4y ModelyValidationyandyApplicationsy

4.4.1 NaturalyDrainageyinyaySoilyColumny

ProblemyDefinitiony

Water drainage in a wet vertical soil column of length L and unit cross sectionA $(S = 1x1\ m^2)$AasAdepictedAinAFig.A4.5AisAinvestigated, assumingAaAhydrostaticA initialApressureAheadAdistributionAinAtheAentireAdomain.A tAt = 0, the pressureA head at the flow outlet becomes equal to zero, the soil column starts draining, andAanAunsaturatedAzoneAwillAdevelopAfromAtopAtoAbottom.ATheAmovingAwaterA table positionA$\zeta(t)$ is predicted using the developed FUP, andAcompared to otherA solutions including the moving mesh solution methodAand the exact analyticalA solution.A

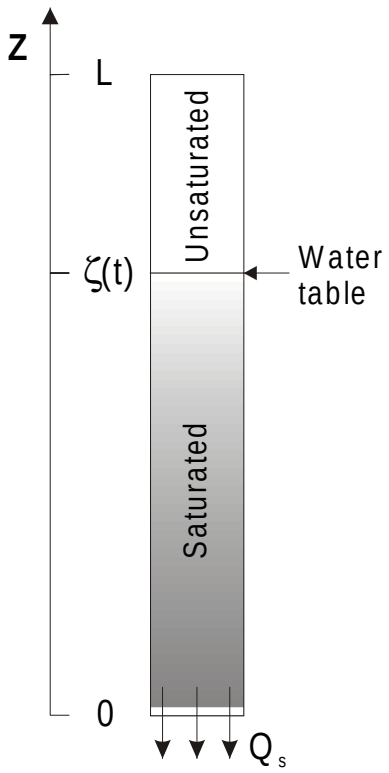

Figure 4.5:ASchematic view of a draining vertical soil column.w

AnalyticalyExpressions

Assuming an instantaneousAdrainageAin theAporous mediumA(*Boussinesq'sy*ap-A proximation), theAdischargeArate throughAtheAsaturatedAsoilAcolumnAengthAsAcon-A stant, and equalsAQ_s =AKS. The drained volume of water at time t is calculatedA equivalently using one of the following expressions given asA

$$V(t) = \int_{04}^{t} \frac{Q_s}{n}\, dt = (\zeta(t) - L)S \tag{4.17}$$

which yields a simple linear decreasing water table heightA

$$\zeta(t) = \text{A} - \frac{K}{n}t \tag{4.18}$$

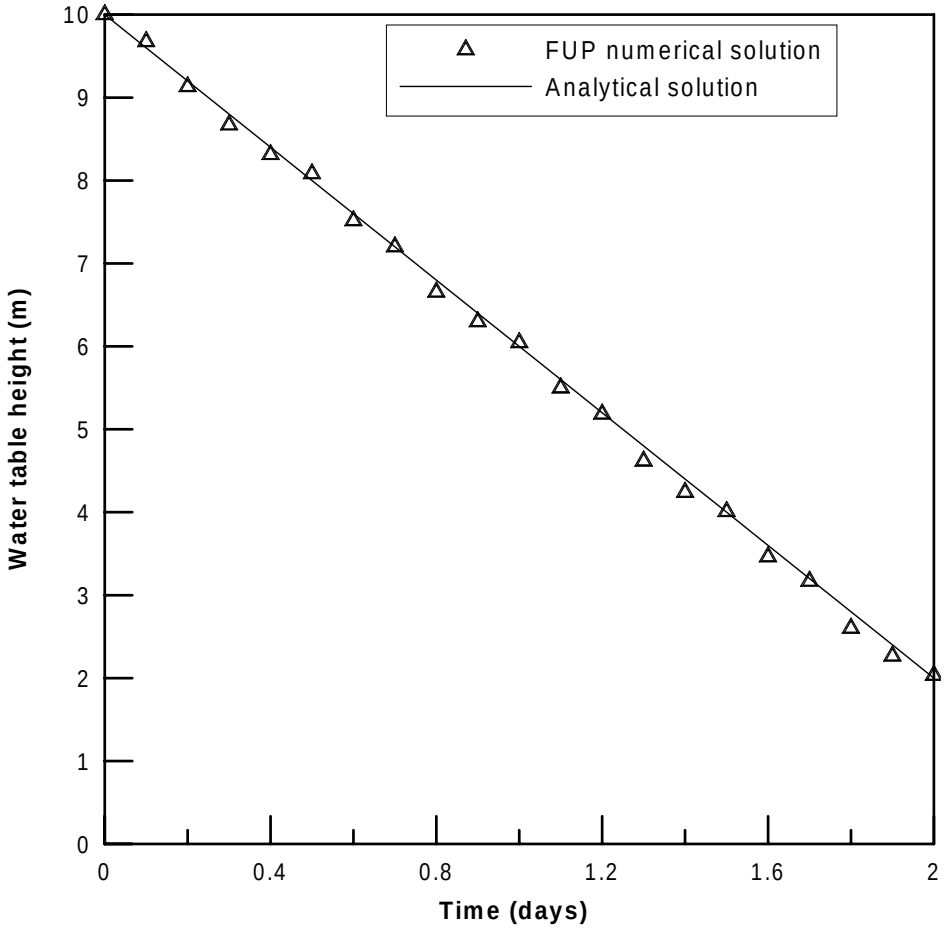

FigureA4.6:AWaterwlevelwdrawdownwlaw $\zeta(t)$;Acomputedwresults withwthewFUPwarew plotted versus analytical solution.w

Numerical Resultsyandy Discussiony

We assume a $10m$ length fine sandy soil column, having a saturated hydraulicA conductivityA$K = 1m/d$ and an effectiveAporosityA$n_e = 0.25$. AlthoughAtheA problem is naturally 1-D, 2 nodes along plane x and y directions are necessaryA toArunAyourA3-DAmodel.ATheAfiniteAelementAmeshAisAcomposedAfromA10AverticallyA orderedAhexahedralAelements, thusA44AnodesAinAtotal.ATheAmodelsAareAexecutedA for 2Adays simulation time, with a user-specified time step of 0.1 days, and aA predefinedA$tolw$ parameter equal to 10^{-3}.A tAeachAtimeAtargetAsolution, sharpA

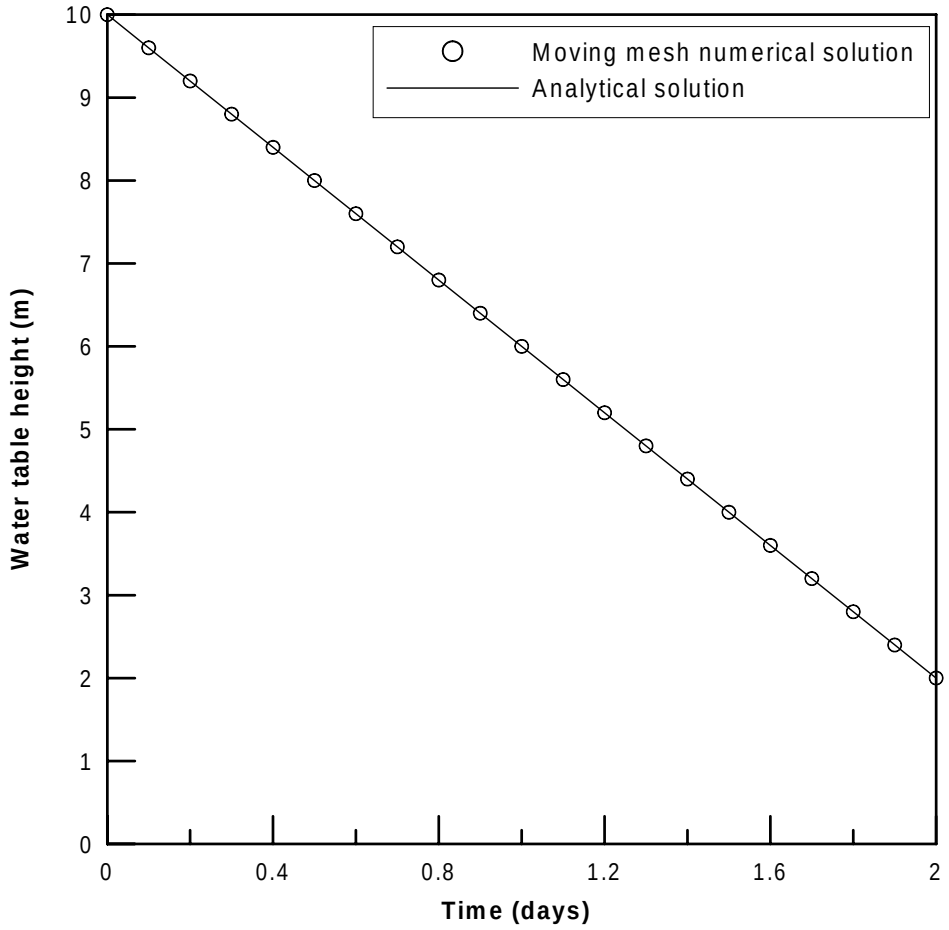

Figure 4.7: Computed sharp water table height $\zeta(t)$ using the moving mesh technique versus analytical results.

water table position occurring at zero pressure head value as linearly interpolated from obtained values at nodal positions.

Decreasing water table heights are plotted in Fig. 4.6 with a time increment of 0.1 days; the numerical solution exhibits very small deviations from the analytical solution, while the moving mesh procedure yields excellent results (Fig. 4.7). This is interpreted as a consequence of discarding the unsaturated zone, because water is released immediately to water table nodes located at the top of the newly adjusted mesh, which somewhat comply with Boussinesq's approximation used to

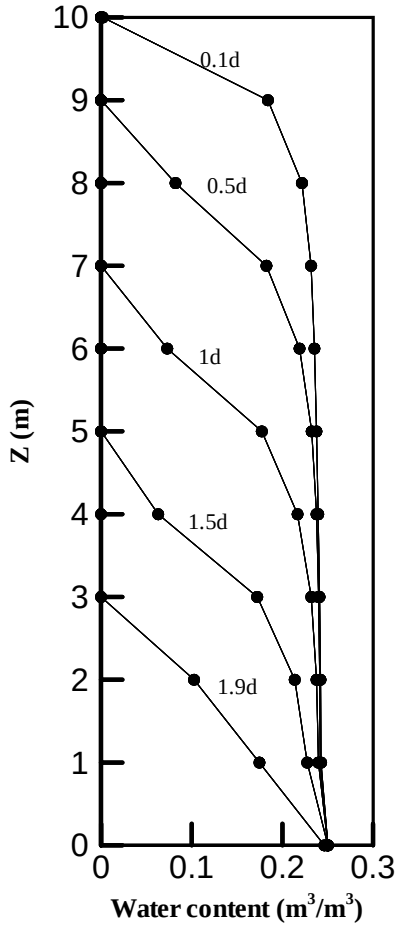

Figure 4.8: Water content profiles at specific target times, dots indicate nodal positions.

derive the Analytic Equation 4.18. Soil moisture content profiles at selected times plotted in Fig. 4.8 show that the desaturation process at a given elevation point is by no means linear in time. One should not confuse the linear water retention curve model which is locally dependent on the moving water table position, and the overall global representation at the end of the solution procedure.

The efficiency of the two calculation methods is investigated in terms of run-time, CPU(s); total number of inner PCG iterations, NI(PCG); and total num-

Table 4.3: *Comparison of the FUP and moving mesh solvers efficiency for testy problem 1.*

	CPU(s)	NI(PCG)	NI(Picard)
FUP	1.1	545	111
Moving mesh method	5.4	725	157

ber of outer Picard iteration loops required to satisfy convergence requirements, NI(Picard)[14]. These values are given in Table 4.3 for the FUP and moving mesh methods. The FUP technique is faster, and requires less number of total PCG iterations and Picard iteration loops, meaning that the successively updated banded matrix equations systems are much easier to solve. However, saving in CPU time is largely due to the implicit reconstruction of the conductance and capacitance matrix terms as explained in Section 4.2.

4.4.2 Drainage of a Soily Column Through a Leaky Outlet

Problem Definition

This problem is taken from Ababou et al. (1998) who solved the same problem with a partially saturated finite volume based approach. This test case is basically similar to the previous example, except that a soil medium of lower hydraulic conductivity $K_b << K$ and small length $b < L$ is placed beneath the original soil column as illustrated in Fig. 4.9.

Analytical Developments

Following again the Boussinesq's approximation, the flow rate remains the same through the upper and lower unit cross-sections of the outlet, such that direct application of Darcy's law at these two cross-sections yields

$$Q_s = K \frac{\zeta - h(b)}{\zeta - b} = K_b \frac{h(b)}{b} \tag{4.19}$$

[1] All test runs in this chapter are executed on a PC platform (Pentiun-166 with Intel CPU-class I, and 64MB RAM).

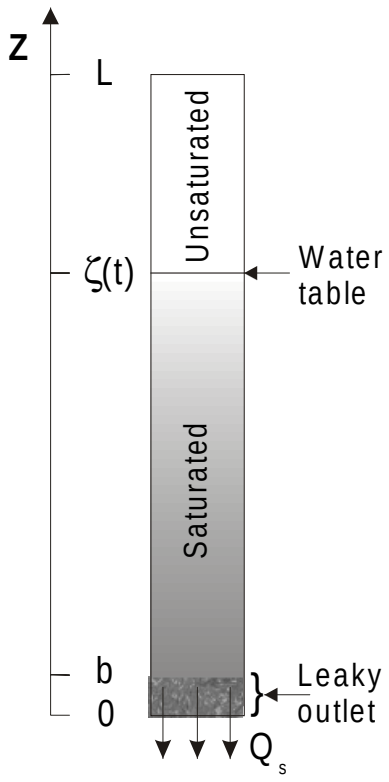

Figure 4.9: Schematic view of a soil column draining through a leaky outlet.w

such that the groundwater potential at the upper outlet section, $h(b)$, can be deduced as

$$h(b) = \frac{(\beta + b)\zeta}{\beta + \zeta} \tag{4.20}$$

where $\beta = b(\frac{K}{K_b} - 1)$. Substitution of Equation 4.20 in one part of Equation 4.19 yields

$$Q_s = K\frac{\zeta}{\beta + \zeta} \tag{4.21}$$

which is a relationship relating the discharge rate at the outlet to the water table height ζ.

Application of Equation 4.17 to the expression derived in Equation 4.21 yields the analytical form of the moving free surface position ζ

$$\zeta + \beta \ln(\frac{\zeta}{L}) = 1 - \frac{K}{n}t \tag{4.22}$$

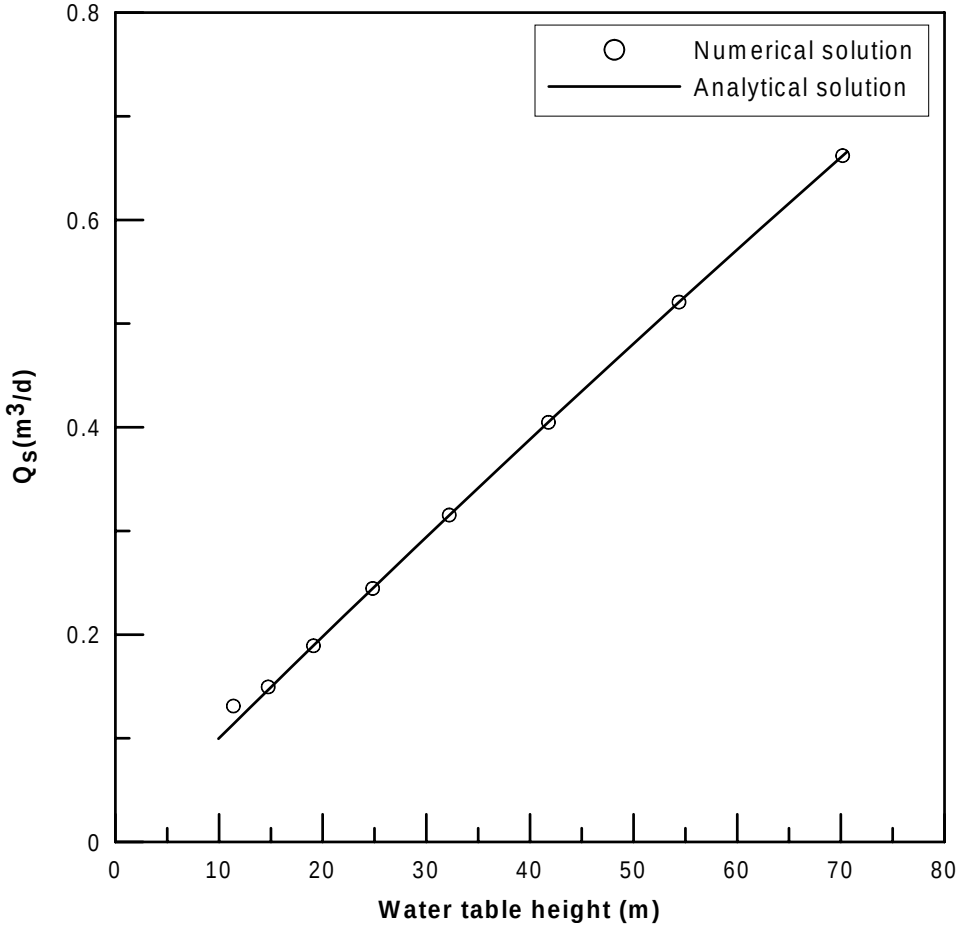

Figure 4.10: Discharge rate-head drop relationship, numerical versus analytical results.

Therefore, the water table height ζ is expected to decrease with a much lower rate than in the first example.

Comparison With Numerical Results and Discussion

Now, we take a soil column of $80m$ length, in which a coarse sandy soil is placed above a $10m$ height clayey outlet. Hydraulic conductivity and effective porosity values are respectively $K = 10m/d$, $n = 0.3$; $K_b = 0.1m/d$ and $n_b = 0.6$ for the macro-porous sand and the leaky outlet. 80 box shaped elements and a total number of 324 nodes are used to approximate the entire domain. The model runs

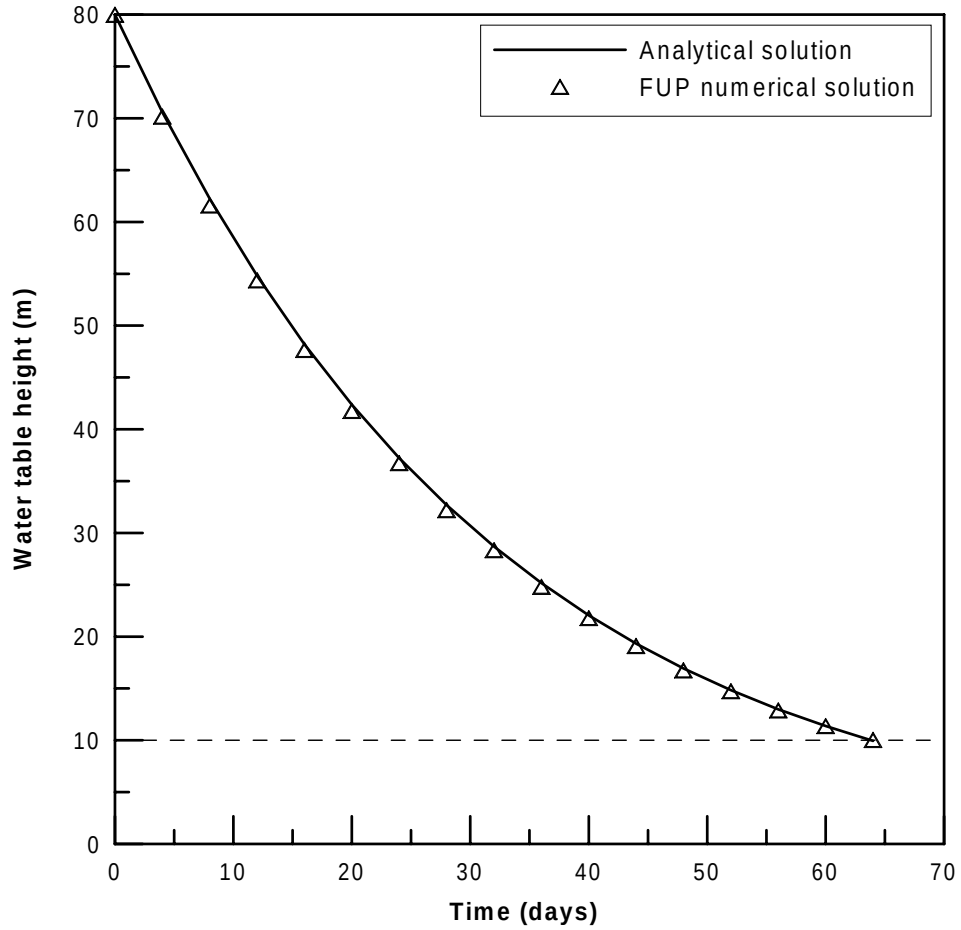

FigureA4.11:AWaterwtablewdrawdownwlaw $\zeta(t)$, FUPwandwmovingwmeshwnumericalw methods are compred to the analytical solution.w

for 80 days with a prescribedA*tolw* parameter equal to 10^{-3}; this time is quiteA sufficient for the soil column to drain completely, as an estimate can be made a-A priori from Equation 4.22 forA$\zeta = 0$. The computational time step is fixed to 0.5A days and the numerical results are obtained within a period of 4 days. PredictedA dischargeArateAvaluesAfitAtheAanalyticalAcurveAperfectlyAasAshownAinAFig.A4.10, except close to the end, when the water table crosses the two mediums interface.A TheAsimulatedAmovingAwaterAtableAfitsAexactly theAanalyticalAoneAasAshown inA Fig.A4.11; such that it can be concluded that the FUP model is able to predictA accurately the time for the sandy soil to become dry.A

The effect of the outlet low permeability on retarding the water table decrease, could be deduced also from soil moisture content profiles at target times shown in Fig. 4.12.

Here again, the FUP based solver performance is checked against the moving mesh method, it is shown from Table 4.4 that still the superiority of the new technique is preserved.

Table 4.4: *Comparison of the FUP and moving mesh solvers efficiency for test problem 2.*

	CPU(s)	NI(PCG)	NI(Picard)
FUP	98.3	13722	791
Moving mesh method	197.3	6620	725

4.4.3 Seepage in a Reservoir from a Semi-Infinite Unconfined Aquifer

Problem Definition

This is another academic test problem: a two-dimensional groundwater flow in a semi-infinite aquifer of rectangular shape. The natural drainage of a water table aquifer starts when the water level in a bounding reservoir is lowered from h_{04} to h_{14} as illustrated in Fig. 4.13. The governing equation in this case is the well-known 1-D *Boussinesq's equation*

$$\frac{\partial h}{\partial t} = \frac{K_s}{n_e}\frac{\partial}{\partial x}(h\frac{\partial h}{\partial x}) \tag{4.23}$$

Initial and boundary conditions are defined in such case as

$$h(x,0) = h_0, \qquad h(0,t>0) = h_{14} \text{ and } h(\infty, t \geq 0) = h_{04} \tag{4.24}$$

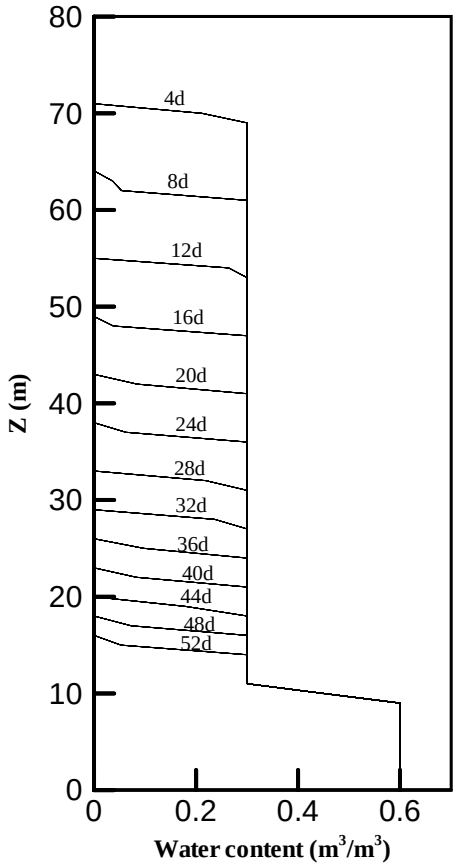

Figure 4.12:AWater content profiles at target times.w

AnalyticalySolutionsy

Several attemptsAwere taken toAderive approximateAandAexact analyticalAsolutionsA for thisAproblem, which can beAfoundAin a numberAofAstandard andAcomprehensiveA textbooks. For instance, solutions given by Bear (1972; 1979) are established byA using linearized forms with respect toAu andAu24as the dependent variable in theA originalAequationA(seeA ppendix A.1).A moreAaccurateAsolutionAwasApresentedA earlier by Polubarinova-Kochina (1962), which is given in the form ofA = A1u, whereAu is a truncatedApowerAseriesAexpansion to theAforth termAofAtheAparameterA

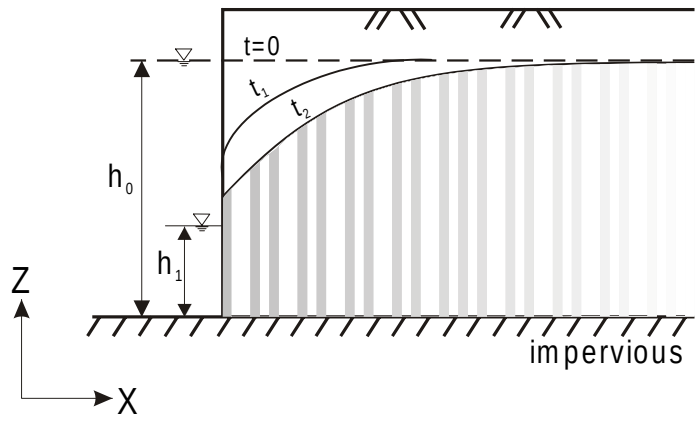

Figure 4.13: Schematic view of test problem 3.

$$l = \frac{h_{04} - h_{14}}{h_{14}}$$

$$u = \sum_{m=0}^{+\infty} l^m u_m \simeq 1 + l u_{14} + l^2 u_{24} + l^3 u_{34} + \ldots \tag{4.25}$$

where u_1, u_2, and u_{34} are functions of the dimensionless parameter $\eta = \frac{x\sqrt{n_e}}{2\sqrt{k h_1 t}}$; analytical expressions of these functions and a set of tabulated numerical values are given in Appendix A.2. However, Equation .5 is not valid for the extreme case of seepage into an empty stream channel, i.e., when $u_{14} = 0$, this is not mathematically neither physically correct. In such situation the following expression was derived alternatively

$$h(\eta, t) = 2.365 h_0 (y - 2y + 3y^{74} - \frac{4}{11} y^{104} - \ldots) \tag{4.26}$$

where $y = 0.4873\sqrt{\eta}$, the discharge flux to the stream is evaluated as

$$q_{x=0} = 0.332 \left(K_s n_e\right)^{1/2} h_0^{3/2} t^{-1/2} \tag{4.27}$$

nother solution based on the *Boltzmany* transformation is recently proposed by Guo (1997), which has the feature of minimizing computational costs in comparison to the Polubarinova-Kochina's solution.

We find it comprehensive to recall some key assumptions under which the *Boussinesq's* equation is derived, namely the horizontal flow or *Dupuit-Forchhemeiry*

approximation, which is known to be not valid near the stream channel where the vertical flow component cannot be neglected (Bear, 1972), this is more obvious as $\frac{h_0}{h_1} >> 1$ or $l >> 1$, and also in case of relatively deep unconfined aquifers. Another limitation of the analytical solution is the inability to predict the seepage face extent. These limitations are not applicable to the numerical model being under study, and differences with the expected numerical results may therefore occur. To be able to interpret these deviations in numerical results, a couple of simulations is performed by disabling and enabling respectively the seepage face detection procedure. The first run is especially chosen to comply with the analytical prescribed head near the stream, while the second simulation is judged to be more realistic as it will occur in either laboratory or field conditions.

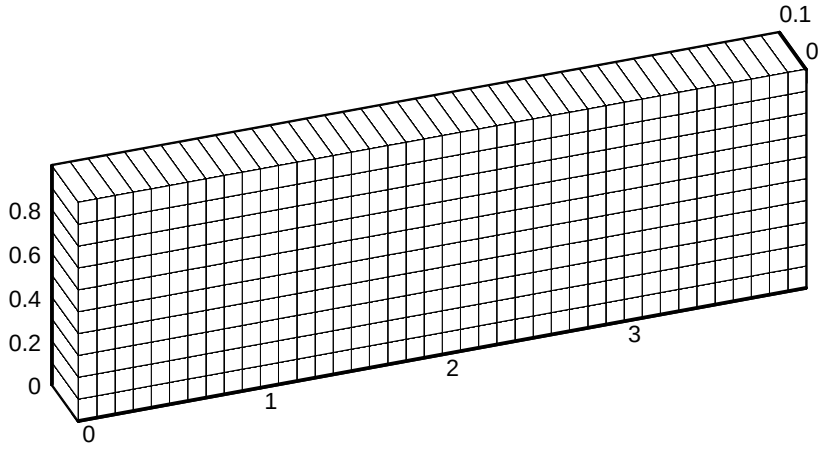

Figure 4.14: Finite element mesh for test problem 3.

Comparison with Numerical Results and Discussion

The parameters for running the numerical simulations are $h_0 = 1m$, $h_1 = 0.5m$, $K = 1m/day$, $n_e = 0.1$; and $1m$ fixed groundwater potential at $4m$ downstream the reservoir, assuming that the flow is stationary landward. The finite element mesh used in this example has a uniform spacing of $0.1m$ as shown in Fig. 4.14.

The total simulation period $T_{\max}$ is 1 day, and the dynamic time step size con-

trol algorithm is enabled. Numerical solutions of the groundwater potential distributions, $h(x,t)$; the free surface positions for runs 1 and 2; and Polubarinova-Kochina's analytical free surface are simultaneously plotted in Fig. 4.15.

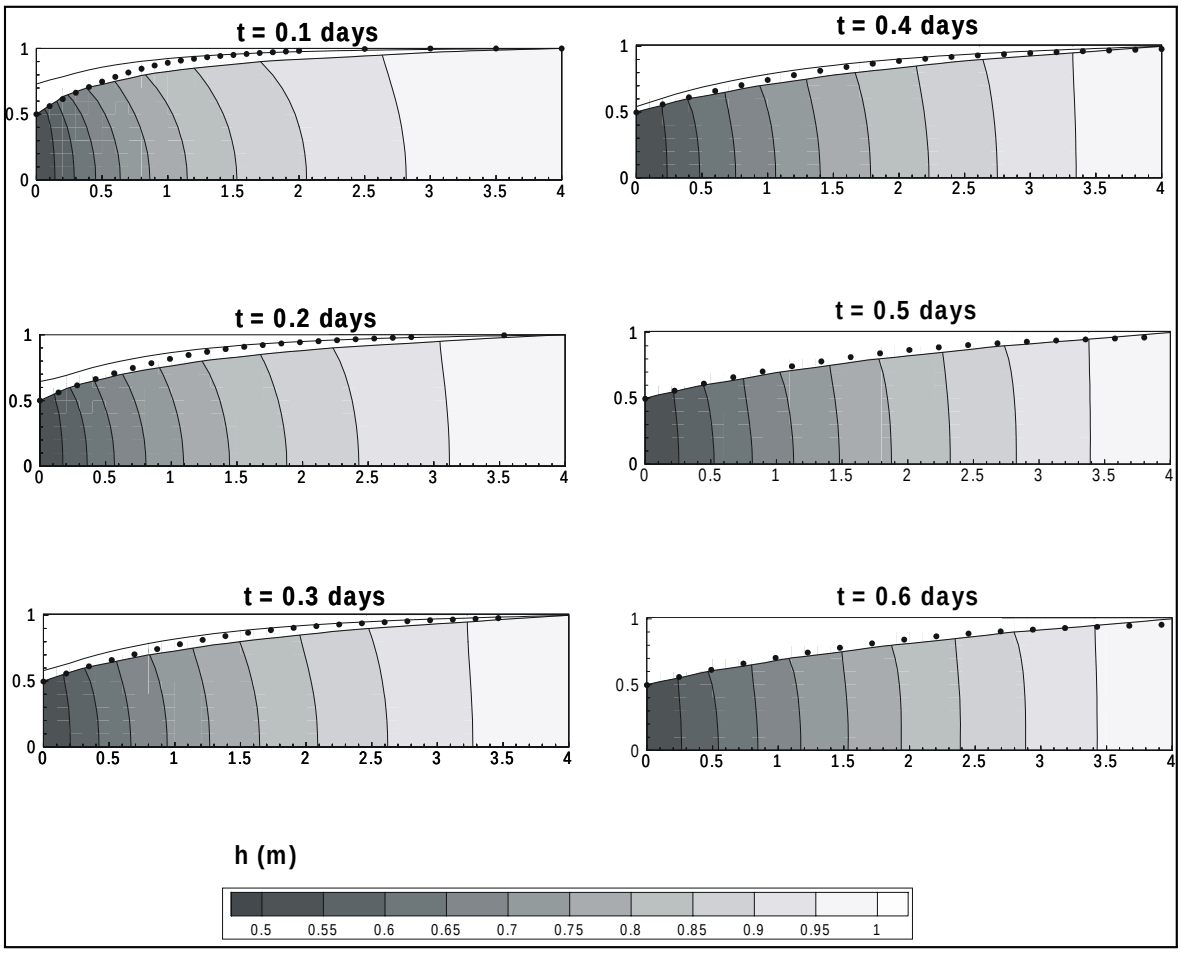

Figure 4.15: Comparison of moving numerical and analytical water tables; coutour heads with an interval of 0.05m are also plotted. Dots represent the analytical solution.

First Run

For the first run no seepage face condition is set at the outlet face. The results show that drainage is faster than expected, especially at starting time levels, but becomes less pronounced as the time increases. Groundwater potential contours

are plotted within a regular interval of $0.05m$, it shows important gradients (and hence velocities) at the outlet boundary of the reservoir, diminishing in time. We can think that not allowing the numerical seepage face existence has led to these difficulties, and explains the motivation for the second run.

Second Run

In this run the seepage face is taken into consideration. It is observed that the newly simulated water tables fit more accurately the analytical solution where the previously simulated ones have the maximum deviations, while deviations near the reservoir are obvious due to the limitation of the analytical solution. These conclusions shed more light on the simplifications of some 'exact' analytical solution, and the superiority of numerical modeling techniques.

The efficiency of the FUP is again investigated for this test problem, these results are shown in Table 4.5. As for the previous examples the FUP is found to be very efficient. Due to sharp water table variations, time steps were automatically adjusted, and the simulations needed additionally 2 time levels (different than output time levels) at $0.02 days$ and $0.0448 days$ which is not excessive but necessary to prevent numerical oscillations around the true solution, which proves that the used time stepping scheme is effective and well implemented.

Table 4.5: *FUP solver performance for test problem 3.*

	CPU(S)	NI(PCG)	NI(PICARD)
FUP (RUN 2)	12.2	360	53

4.4.4 Validation with a Three-Dimensional Laboratory Model

Background and Laboratory Model Description

In general, practical simulations involving moving surface seepage in field conditions are complex due to local medium heterogeneities, non regular geometries,

and time dependencies. Closed form analytical solutions for these problems are hard to formulate and very limited as discussed in the previous section. Hence, to establish a confidence in the numerical model results, validation by using experimental or/and field measurements is an asset for the developed model. In this study, the results of an earlier experimental tests are used to validate the FUP model, these laboratory experiments were carried in department of Civil Engineering and Engineering Mechanics (University of rizona, Tucson) by Baseghi and Desai (1987), which is a useful contribution since it is a unique study that reported laboratory observations on three-dimensional free surface flow.

Laboratory tests were performed on a three-dimensional glass bead model. The model configuration allows for simulation of homogeneous and nonhomogeneous materials such as core in dams, which are simulated by glass beads of different diameters ($1mm$ and $3mm$). Fig. 4.16 shows the 3-D mesh used to approximate the whole domain, in which specific sections are of interest, especially the front section, F; back sections, B_{14} and B_2; and side section S. During the experiments, transient movement of the free surface was recorded photographically along these sections, upon transient (rise, steady-state, drawdown) fluctuations on the upstream section of the earth dam model. These observations are compared to numerical predictions from the presented model.

Model Parameters

Hydraulic conductivity values for granular glass beads are reported by the authors (Baseghi and Desai, 1990), and have been determined using a constant head laboratory test, specific storage coefficients were also calculated. But, neither specific yields or porosities are given for the used materials. This is a limiting factor for the simulations to be performed, but a relatively acceptable estimation of the porosity is found from the Kozny-Carmen equation (Freeze and Cherry,

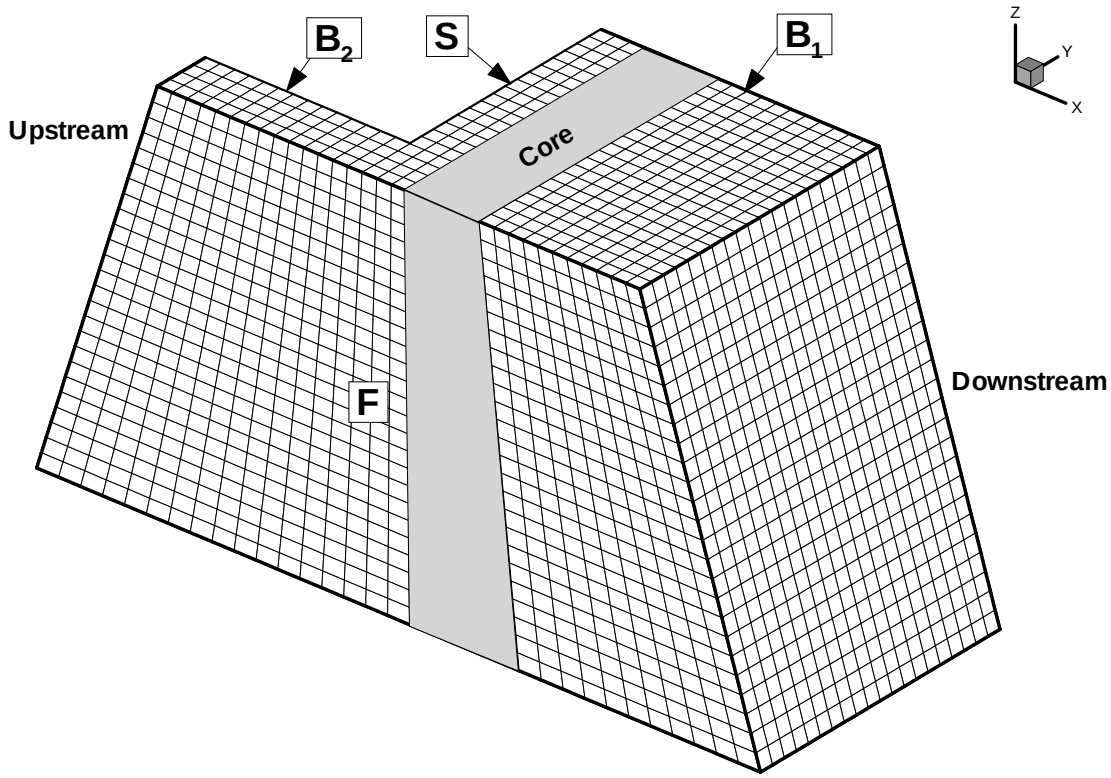

Figure 4.16: Configuration of the laboratory model showing the finite element mesh, the photographed sections, and the core dam location.

1979) relating it to the hydraulic conductivity by

$$K = \left(\frac{\rho g}{\mu}\right) \frac{n^2}{(1-n)^3} \left(\frac{D^2}{180}\right) \tag{4.28}$$

where D is the mean-size granular soil diameter [L]. Equation 4.28 yields the following equation

$$1 - 3n + (3 - \lambda)n^2 - n^3 = 0 \tag{4.29}$$

where $\lambda = \dfrac{(\rho g)D^2}{180K\mu}$, n is therefore the root of the polynomial Equation 4.29 which satisfies necessarily the condition $n \in]0, 1[$.

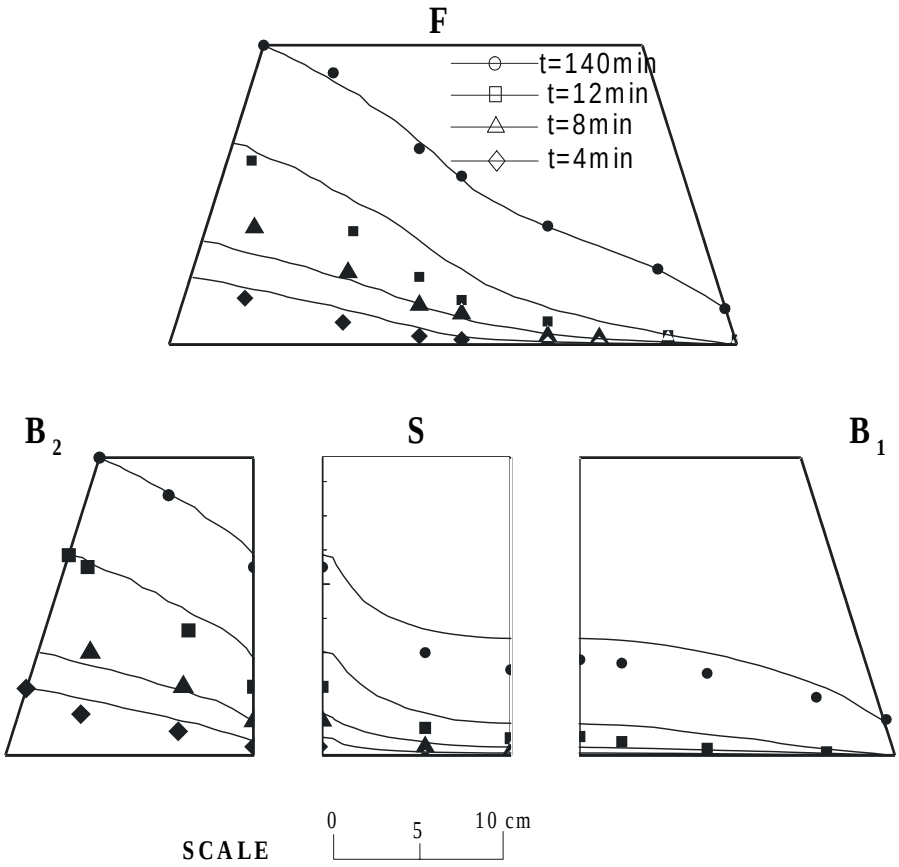

Figure 4.17: Comparison of predicted (continuous lines) and observed free surface during rise and steady state for the homogeneous dam: (F) front section; (B_1, B_2) Back sections; (S) side section.

Comparison of FUPy Numerical Results with Laboratory Observations

Case 1: Homogeneous Dam

Glass beads of $1mm$ diameter are used in this experiment. Starting from dry conditions (e.g. $h = 0cm$ everywhere), the upstream water level is raised to $17.4cm$ in about $20min$, and maintained at that level for about $140min$. The upstream water level is decreased thereafter with a fixed rate of $0.96cm/min$. Measured values were recorded at $4min$, $8min$ and $12min$ for the rising phase, and at $156min$, $158min$, $162min$, and $164min$ for the drawdown stage. So, accordingly these times levels are specified as output in the model. Comparisons

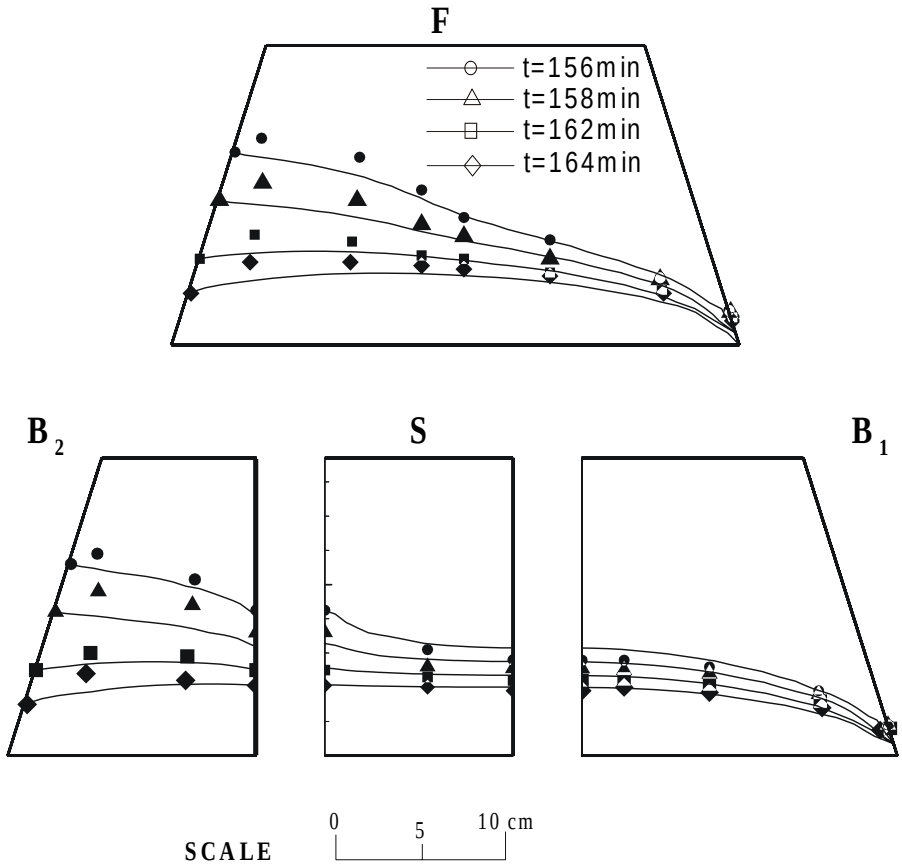

Figure 4.18: Comparison of predicted (continuous lines) and observed free surface during drawdown for the homogeneous dam: (F) front section; (B_1,B_2) Back sections; (S) side section.

between the FUP numerical predictions and the observed water table positions are shown in Fig. 4.17 for the rise and steady state conditions and in Fig. 4.18 for the drawdown stage. It is clear that the developed numerical procedure produces satisfactory predictions of either the free surface or the seepage face height. The observed deviations at given time levels, are due in large extent to inaccurate estimations of the saturated and residual water contents in our models. A parametric study to estimate these values is possible by trial and error calibration procedure with the observed steady state measurements on a long term transient simulation basis, however this would need more effort which is beyond the scope of the present study.

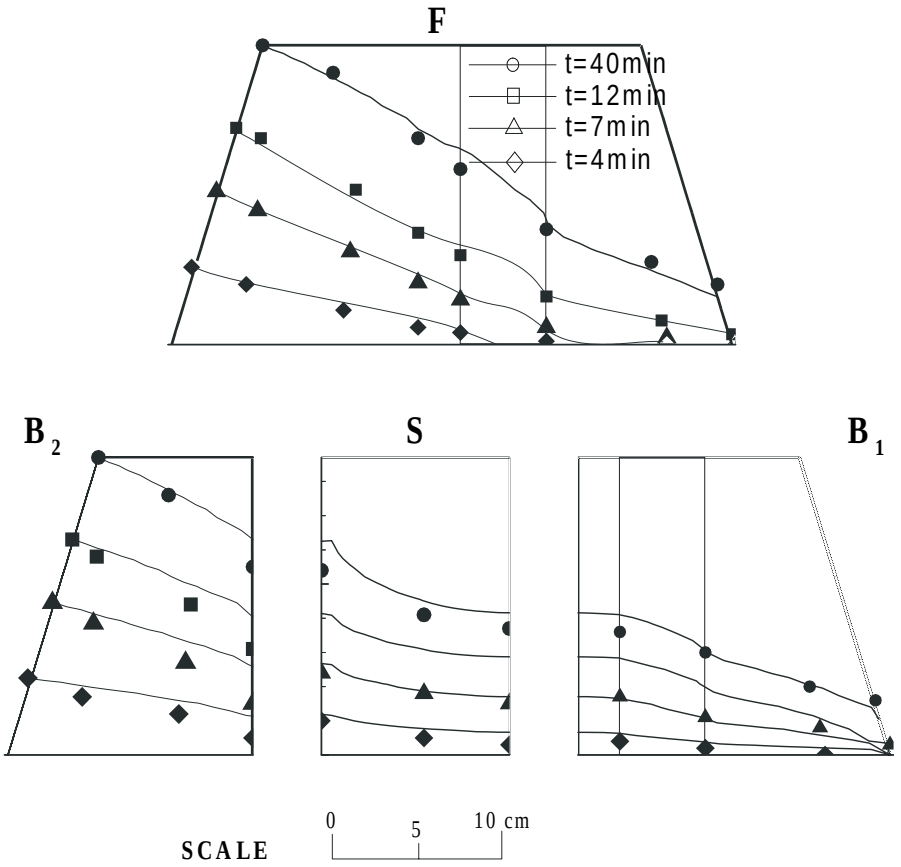

Figure 4.19:AComparisonwofwpredicted (continuouswlines)wandwobservedwfreewsurfacew duringwrisewandwsteadywstatewforwthewheterogeneouswdam:w(F)wfrontwsection;w(B_1,B_2)w Back sections; (S) side section.w

NoteyonyComputer Timey

ItAtookAaboutA33ACPUAsAonAanAaverageAperAtimeAstepAonAa CYBERA205AsupercomputerA of 10 years ago (as reported by the authors) for their 3-D model, andA32 CPU sA for the present FUP model on a simple scalar desktop PC platform.AThis showsA the rapid evolvement of computer hardware and computational methods at theA last era of the current century.A

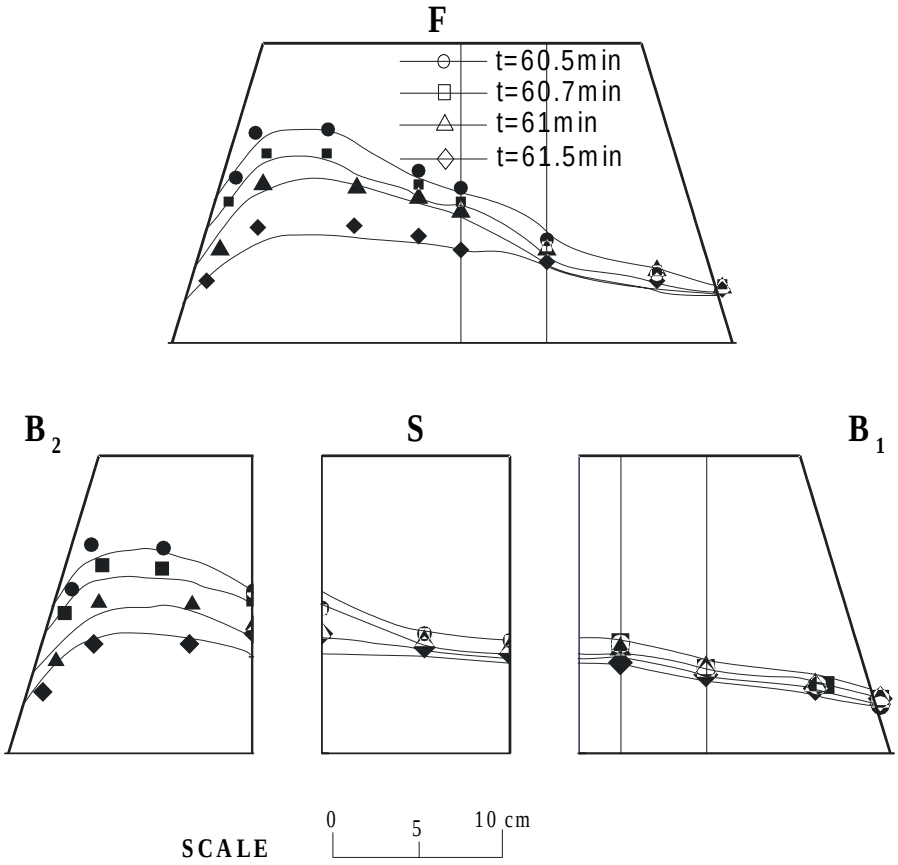

Figure 4.20: AComparisonwofwpredicted (continuouswlines)wandwobservedwfreewsurfacew duringwdrawdownwforwthewheterogeneouswdam:w(F)wfrontwsection;w(B_1,B_2) Back sec- w tions; (S) side section.w

Casey2:yHeterogeneousyDamy

This is a moreAdifficultAand challengingAproblem, because the damAisAsectioned asA shown in Fig. 4.16. InAthe core area the $1mm$ size glass beads are used whileAtheA $3mm$ size beads are placed elsewhere.AThe upstream head variation for the riseA period is similar to the first experiment, the maximum water level is maintainedA for $40min$, andAdecreased at a much faster drawdown rate of $9.33cm/min$. Ob- A served outputs are taken at $4min$, $7min$, and $12min$ for theAwater tableArise, andA at $60.5min$, $60.7min$, $61min$, and $61.5min$ forAtheAdrawdown.ATheAdifficultyAofA this problem arises from the important drawdown for a steep time period, whichA

need special attention.AHere again dynamic time step sizes control is turned on, and very small time steps were needed at the beginning to relax the numericalA solution. ComparisonAbetweenApredictedAandAobservedAvaluesAisAveryAgoodAfor theA two stages, i.e.Arise, steady state andAdrawdown of the free surface as shown inA Figures 4.19Aand 4.20. The seepage face height is also predicted accurately.A

4.5y Summary

computer model forAprediction Aof three-dimensionalAgroundwaterAflow involvingA a moving phreatic boundary is developed based on the Galerkin finite elementA approximation in space and a fully implicit finite difference time approximationA with a mass lumped capacitance term.A

The embedded numerical approach does not completely neglect the flow inA the vadoze zone, but it is assumed to be a small fraction of magnitude as in theA saturated domain. The moving water table boundary is iteratively adjusted basedA onAnodalAwaterAstatusA(i.e. saturated, unsaturated, partiallyAsaturated)Awhich areA deducedAfromAtheArelativeAwaterAtableApositionAwithinAeachAelement.ATheAFUPA technique is shown to be cost-effective and efficient due to inexpensive update ofA the conductanceAmatrix, andAaccurateAestimationAof theAcapacitance terms, whichA are less expensive in comparison with standard approximation methods.A

The overall numerical solver is robust and implements attractive state of theA art features and powerful reputed algorithms, such as the modified incompleteA factorization preconditioner based on a M matrix transformation, a linear con-A jugateAgradient solverAfor theAmostAinnerAloops, and a dynamicAtimeAsteepingA schemeAwithAautomaticAdeterminationAof theAunder-relaxationAfactorAforAupdatingA groundwater heads to avoid possible numerical oscillations and/or instabilities.A The numerical model also enables various types of complex nonlinear boundaryA conditionsA(seepageAface, drainage, timeAvaryingAheads, leakage, abstraction, etc.)A

The usefulness of the FUP approach and the developed model is clearly putA

in evidence, based on a series of test problems.AThese examples are of differentA complexity, dimensions, andAgroundwaterAflowAbehavior.ANumericalAresultsAareA compared toAanalytical solutions whenever they are available, and show very goodA agreement. ComparisonsAare also madeAwithArespectAtoAthe moving mesh method, which is slower in comparison to the FUP for transient nonlinear problems. TheA last test validates the model by comparison with respect to laboratory measure-A ments in a 3-D earth dam model.AThe model structure allows for homogeneousA andAheterogeneousAformationsAwithAcoreAdams. SatisfactoryAagreement isAobservedA in case of rise, steady state andAdrawdown of the free seepage flow for all theseA experiments.A

Chapter 5

A 3-D Sharp Interface Approach for Modeling Seawater Intrusion in Coastal Aquifers

Contents

5.1 Introduction

Coastal aquifers often involve complicated and varying conditions in time and space, owing to the occurrence of a moving fresh-saltwater interface, rather than the natural stationary interface initially existing. Practical examples include pumping stations of variable scheduled withdrawal; artificial recharge for site remediation; construction of cutoff walls and barriers; and other possible scenarios for seawater intrusion control. Moreover, unconfined flow in coastal aquifers

involves additionally a moving water table as discussed in the previous chapter, so adding further complexity.A

Three-dimensional numerical modeling of saltwater intrusion is investigatedA in case of a sharp fresh-saltwater interface approach, neglecting mixing of theA twoAfluids, meaningAthatAtheAtwoAflowAfieldsAbecomeAindependent.A numericalA approachAisAdeveloped toAestimate at theAsame time theAair-freshwaterAfreeAsurfaceA and the fresh-saltwater positions in 3-D space.AThe technique is again based onA a Galerkin finite element scheme and a generalized form of the FUP techniqueA developedApreviouslyAforAtransientAvariablyAunsaturatedAflow.AThe AgeneralizedA FUP accounts for the dual free boundaries separating the freshwater flow fromA the unsaturated zone and the saltwater respectively.AIn contrast to water tableA aquifers only, care is taken to includeAdensity effects in the formulation.A

thorough analysis of this numerical formulation, and assumptions in this ap-A proach are presented first. In particular, the choice of a sharp interface approachA is discussed andAjustified.A fterwards, several validation and application exam-A ples are shown to establish confidence in the obtained numerical results.AtheseA test problems include a number of analytical solutions which have been chosenA carefully, such that the limitations and applicability of the numerical solutionA technique will be highlightedAand explained. An important test case is a three-A dimensional laboratory model (Sugio and Rahim, 1992) which demonstrates theA usefulness of the newly developed numerical procedure, enabling to accuratelyA predict positions of fresh-saltwater interface and free surface in complicate andA irregular configurations.A

TheAdevelopedAthree-dimensionalAgroundwaterAflow andAsaltwaterAintrusionA model '*GEO-SWIM*', is applied to the coastal aquifer of Martil in Morocco, as aA validation of the model package, and also as an example showing the integrationA ofAGISAsupportAtoAprepareAaAbasicAframeworkAforAtheAmodelAapplication.AInitialA conditionsAand some model unknown parameters of the aquifer are found usingA aAtrialAandAerrorAcalibrationAprocedure.AThisAstudyAenablesAtoAunderstandAtheA

aquifer response to changes in recharge and total rate of pumped water, and their effects on seawater intrusion. Different scenarios are investigated for the period of 1966 to 2006, to predict future situations and the salinization risk from seawater intrusion. The obtained results show that the interface will move fast and travel over considerable distances in forthcoming years, and will produce an irreversible degradation of the groundwater quality, especially along the coast and in the center of the Martil plain. An alarming optimal management scheme in the near future is necessary for its safeguard.

5.2 Conceptual Model

In this model, distinction is made of three main areas, namely the unsaturated, the saturated freshwater, and the saltwater zones respectively as shown in Fig. 5.1. The flow hydrodynamics behave differently in each area. In this conceptual problem, only freshwater flow is taken into account, but without excluding completely the other zones from the simulation or the system of FE equations. The unsaturated zone is treated as explained in chapter 4, while the saltwater zone is transformed to an equivalent freshwater zone having the same pressure head distribution as that of the saltwater.

As introduced in chapter 3 this procedure avoids the simultaneous solution of a coupled system of governing differential equations for fresh and salt water zones, or ideally the flow and mass transport equations. The principle consists on dividing the FE domain to three groups of nodes as depicted in Fig. 5.1

1. Unsaturated nodes where the pressure is negative, such that

$$h(\mathbf{x}, t) < z \tag{5.1}$$

2. Saturated fresh water nodes where the pressure should be larger than the pressure in the saltwater zone, assumed to be in hydrostatic equilibrium

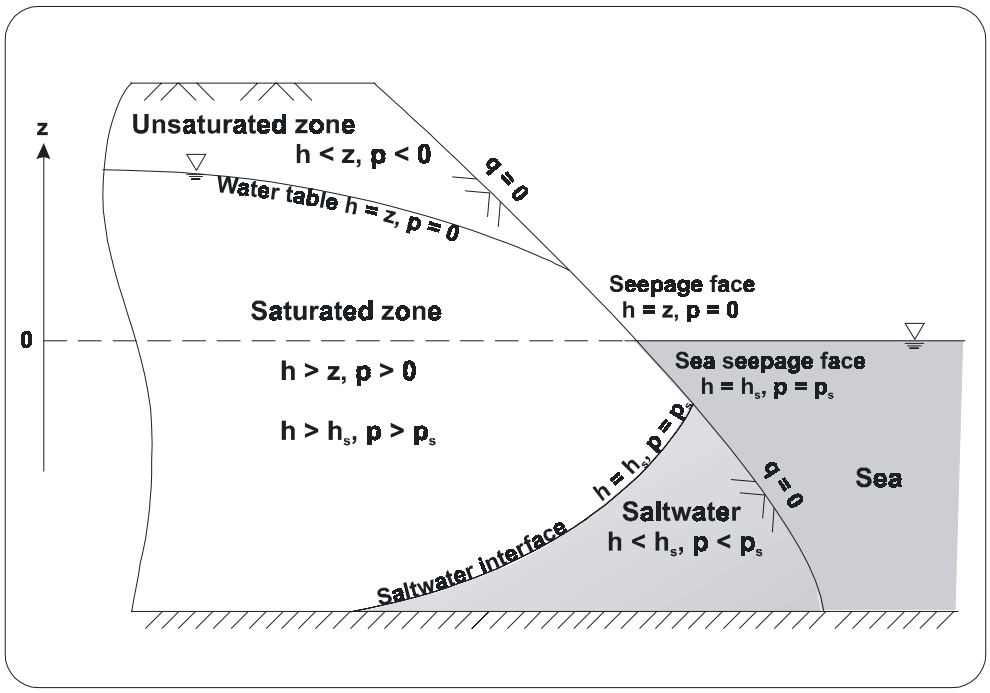

Figure 5.1: Potential pressure conditions along the free boundaries; in the unsaturated, fresh and salt water zones.

with the sea. These nodes satisfy therefore the following equations

$$h(\mathbf{x},t) \geq z \tag{5.2a}$$

$$h(\mathbf{x},t) \geq -\delta z \tag{5.2b}$$

3. Saltwater nodes which necessarily satisfy the condition

$$h(\mathbf{x},t) < -\delta z = h_s \tag{5.3}$$

where h_s [L], is the equivalent saltwater potential at the interface position.

This procedure is implemented on an iterative basis, meaning that the positions of the free and moving boundaries are iteratively changing inside the initial fixed mesh domain, but are not implemented as boundary conditions of the dual problem, and thus avoiding a computational difficulty. Hence, the three different zones are changed accordingly.

This mode permits change of the interfaces in response to boundary conditions applied in the freshwater moving domain. Care should be taken for specification of the boundary condition nodes, which should belong exclusively to the initial and the final freshwater domains. Otherwise, problems may occur during the model execution. This limitation is only applicable to the saltwater zone, because specifying other conditions than the sea outflow face in the salt domain, is not physically acceptable under the sharp interface approximation, and in the specifically designed numerical approach to be explained further in the upcoming section.

clear example is that of an interface dome below a pumping well near the coast, where the appex of the upconing beneath the well crosses the lower well filter section. The only way around this at present is to ensure that the pumping well does not extracts out large amounts of saltwater from the aquifer. Research efforts need to be pursued for developing better and advanced numerical techniques to better include these complicated conditions, which would be feasible in the context of our model. But, in the framework of this study we port much of the developments towards a numerically stable and a mass-conservative solution by extending the scope and the feasibility of the FUP approach as discussed earlier.

5.3 The Generalized FUP Approach

The solution of the FE system for this class of problems is solved in a similar fashion as presented for the variably unsaturated flow equations. However, the numerical techniques needs further modifications and tweaking to comply with physical conditions involved in the saltwater zone. Hence, we take advantage of the FUP procedure which was developed for the case of the free air-freshwater interface, to extend it in cases where dual free boundaries exists in the domain.

5.3.1 RelativeyHydraulicyConductivity

TheArelativeAhydraulicAconductivityAis updatedAdependingAon theArelativeApositionA ofAthe nodesAversusAboth theAwater table and theAsaltwaterAinterface iterativeA positions. The updating process of the relative hydraulic conductivity coefficients, k_{ij}, is therefore generalized asA

$$k_{ij} = \begin{cases} 1 & \text{if} \quad p_i \geq 0 \text{A} \; or \; p_j \geq 0 \\ \varepsilon & \text{otherwise} \end{cases} \text{A} \quad \text{if A } i \text{ and A } j \text{ are apart from the water table A} \tag{5.4}$$

$$k_{ij} = \frac{\eta_i k(\eta_i) - \eta_j k(\eta_j)}{\eta_i - \eta_j} \quad \text{if A } i \text{ and A } j \text{ are apart from the saltwater interface} \tag{5.5}$$

whereAη_i is the distance of nodeAi from the saltwater interface, and given byA

$$\eta_i = z_i + \delta z_i \tag{5.6}$$

$k(\eta)$ is a relative hydraulicAconductivity function, which is defined asA

$$k(\eta) = \begin{cases} 1 & \text{if} \quad \eta > 0 \\ \dfrac{1+\varepsilon}{2} & \text{if} \quad \eta = 0 \\ \varepsilon & \text{otherwise} \end{cases} \tag{5.7}$$

5.3.2y WateryRetentionyCurvey-yDensity Dependencey

The nonlinear storage in time from the right handAside of Equation 3.44 is eval-A uated numerically in the FUP numerical technique.AThe numerical procedure isA similar to that developed in the previous chapter, except that the storage varia-A tions due to changes of the saltwater zone displacement should be included. TheseA changes are evaluated to be equal to the saturated water content, θ_s. However, to ensure numerical stability the variation should be smooth across the nodesA around the salt-freshwater interface.AThis has been performed by modifying theA functionsAin AFig.A4.4Arepresenting AtheAidealizedAwaterAretentionAcurve, andAtheA

water capacity term at the first nonlinear iterate, to the functions represented in Fig. 5.2, which may be expressed as follows

$$\theta(p) = \begin{cases} \theta_r & \text{if } p_i < -\dfrac{d_i}{2} \\ \dfrac{\theta_s - \theta_r}{d_i} p_i + \dfrac{\theta_s + \theta_r}{2} & \text{if } |p_i| \leq +\dfrac{d_i}{2} \\ \theta_s & \text{if } +\dfrac{d_i}{2} < p_i < -\delta z_i - \dfrac{\delta d_i}{2} \\ \dfrac{\theta_s}{\delta d_i} p_i + \dfrac{\theta_s}{2}\left(1 + \dfrac{z_i}{d_i/2}\right) & \text{if } |p_i - \delta z_i| \leq +\dfrac{\delta d_i}{2} \\ 0 & \text{if } p_i > -\delta z_i + \dfrac{\delta d_i}{2} \end{cases} \tag{5.8}$$

and

$$\frac{d\theta}{dh}(p) = \begin{cases} \dfrac{\theta_s - \theta_r}{d_i} & \text{if } |p_i| \leq +\dfrac{d_i}{2} \\ \dfrac{\theta_s}{\delta d_i} & \text{if } |p_i - \delta z_i| \leq +\dfrac{\delta d_i}{2} \\ 0 & \text{otherwise} \end{cases} \tag{5.9}$$

The newly distinguished pressure distribution around the fresh-saltwater interface is smaller in size in comparison with the equivalent pressure distribution existing around the water table, because small variations in the water table position involves greater displacement of the fresh-saltwater interface. And hence, much larger variations in the storage term. The coefficient of proportionality is taken equal to S_s, according to the Ghyben-Herzberg (GH) relationship.

5.3.3 Numerical Solution Procedure

Here again, the same numerical procedures developed in the previous chapter are still applicable in this case, except that changes of the saltwater domain should be accounted for the density variations. Hence, the generalized FUP approach is built around the same nonlinear Picard solver in time, and the inner preconditioned PCG solver as discussed earlier.

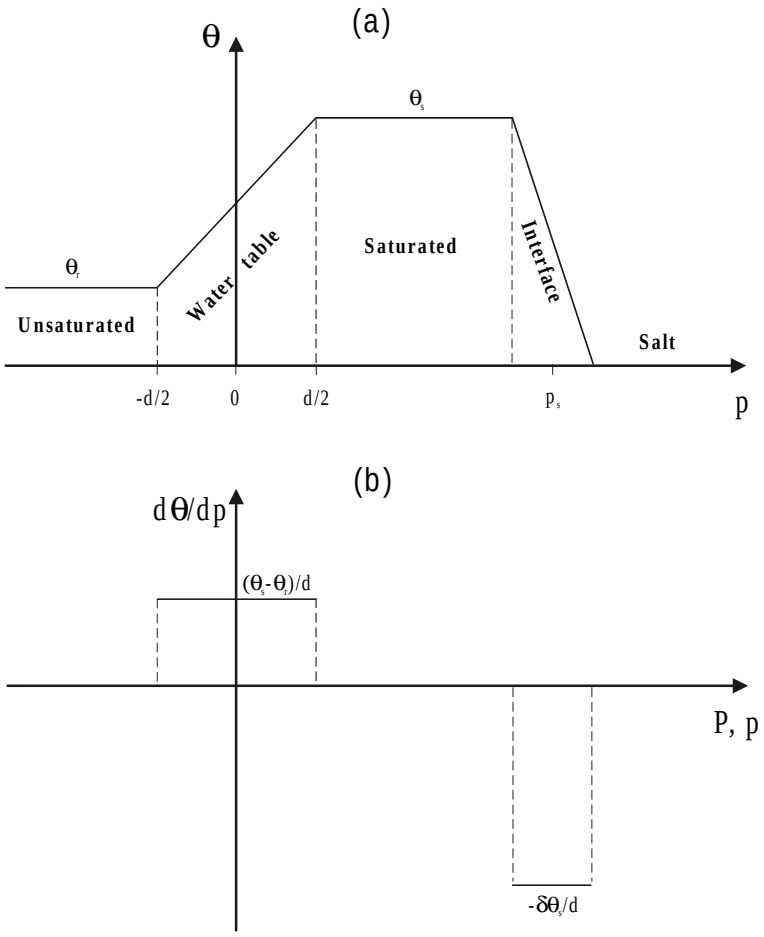

Figure 5.2:AGeneralized (a)w ater retention curve, and (b) analytic differentiation ofw the slope tangents at the nonlinear first iterate.w

greatAfeatureAin this conceptualAgeneralizationAphase, is theAstraightforwardA modularAimplementation usingAexistingAsoftware componentsAdevelopedApreviA ously.A

5.3.4y OtheryFeaturesyofytheyProposedyApproachy

ThoughAthe modelAisAbasedAon an iterativelyAadjustedApositionAof theAfresh-A saltwaterAinterfaceAbasedAon theAGhyben-HerzbergArelation knownAtoAbeAveryA limiting. Approximations and inaccuracies related to this 1-D approach are reA solvedAinAtheAscopeAofAtheApresentedAnumericalAformulation.AInAparticular, theA

geometry of the sea outflow face window boundary condition, to be determined in relation with the freshwater flow behavior in the aquifer system, is automatically adjusted (see Chapter 3 for details). The interface position near the sea shore will not be over-estimated as would be the case within the GH approximation.

Situations involving two moving interfaces in unconfined flow are solved efficiently, these solutions are cheap and run within a minimum hardware requirements. The model has the ability of simultaneous determination of the interface and freshwater potential heads distributions at different time levels. The obtained potentials are continuous across the interfaces, but only potentials comprised between the water table and the fresh-saltwater interface are significant. Hence, a verification model based on measured groundwater heads is still feasible even without taking into account salinity measurements for validating the interface position simultaneously, since piezometric measurements are affected by the existence of the interface. Because, this is a practical limiting factor in many projects in coastal aquifers, the developed model will prove to be useful for representing the global response of the saltwater interface in relationship with the changing freshwater heads conditions.

It will be shown through the field application presented in Section 5.5, that this model is a useful tool for calibration of the groundwater heads. Moreover, the model could be used as a practical tool for providing routinely management support at a professional level, e.g. in a groundwater management office or a governmental department, because of the low requirements in data input as well.

5.4 Validation and Application Examples

In this section, examples are discussed and used as a basis for comparison with the model predictions. The developed model is validated for several situations, involving confined and unconfined aquifer systems, under a variety of physical

boundaryAconditions such as recharge and groundwater abstraction.AIn the ma-A jorityAof theseAtestAexamples, theAproblem accommodateAto an available analyticalA solution. MostAofAtheseAsolutionsAareAlimited toAsteadyAstateAconditions. It isAhardA to find a solution for transient interface flow, and the existing ones lack generalA applicability.ASince this is not always the case for a real case study, a validationA is made with laboratory experiments achieved by Sugio and Rahim (1992) in anA irregularAbox allowingAfor a three-dimensionalAshapeAofAtheAinterface, andAvariableA conditions.

Analytical solutions involving a saltwater interface in confined aquifers areA relatively more encountered, especially if the saltwater is at rest. ThisAis becauseA under such conditions, exact potential functions can be derived separately for eachA region. Strack (1976) has contributed a continuous potential function across theA interfaceAeitherAforAconfinedAflow, orAunconfinedAflowAasAwell.ABut, manyAotherA solutions were also given by Glover (1959), Van der Veer (1977a,b), Van DamA (1982), Haitjema (1991), and Bakker (1998).A

5.4.1 SeawateryIntrusionyinyayConfinedyAquifery

This example concerns steady state seawater intrusion under natural conditionsA (i.e., no recharge and/or pumping conditions exists) in a cross-section of a rect-A angular confined aquifer having a uniform inland horizontal recharge flux, q, asA depictedAinAFig.A5.3.AThisAproblemAisAtakenAfromALarabiAandADeASmedtA(1997)A who used theAsameAproblemAforAvalidationAof theAold computer codeAversion.A It is considered here again, to demonstrate the improvement directlyAobtainedA from the use of the newly implemented solver. Table 5.1 summarize the problemA physical and computational parameters which wereAused toAobtainAthe numericalA solution.A

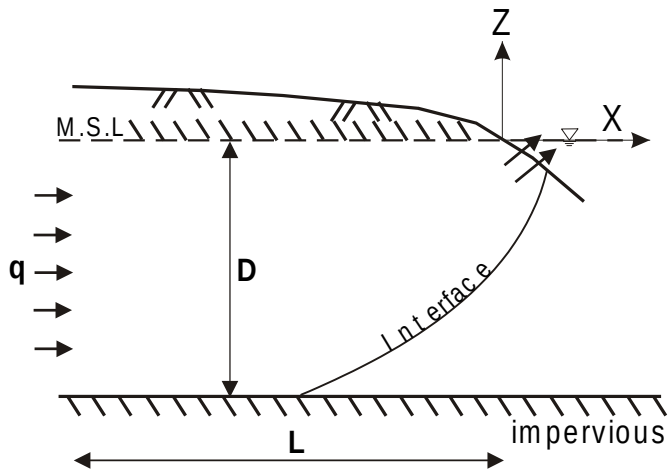

Figure 5.3:ASchematic representation of the Glover's problem (1959).w

Table 5.1:A *Glover'sytestyproblemyphysicalyandycomputationalymodelyparametery values.y*

PARAMETER	VALUE
UpstreamAfixedAflux, q	$3.9\text{cm}^2/\text{s}$A
RectangleAconfinedAaquiferAdimensions, L, D	400cm, 27cmA
GridAdimensionsA	106x2x10A
GridAspacings, $\Delta x, \Delta y, \Delta z$	4cm, 4cm, 3cmA
DensityAdifferenceAratio, δ	0.029A
SaturatedAHydraulicAconductivity, K_s	69cm/sA
StartAupAunderrelaxationAfactor, ω^{04}	0.25A
WaterAtoleranceAparameter, $tolw$	0.02cmA

ComparisonAbetween the twoAsolutionsAisAshown in Fig. 5.4Awhere a veryAgoodA agreement is obtained.ALike in most aquifer systems, the vertical dimension as-A pect ratioAisAincreased toAenable a betterAviewAof theAresults. However, for coastalA aquifers especially, distortion of the figure does not illustrate the orthogonalityA between the groundwater potential isolines and the saltwater interface. Therefore, for the actual problem a zoom is performed on the intrusion zone, while keepingA theAsameAscaleAinAhorizontalAandAverticalAdimensionsA(Fig.A5.5).AGroundwaterA heads are also plotted showing clearly the hydraulicAgradient increase seaward.

AnotherAsubjectAofAinterestAinAthisAtestAexampleAis theAevaluationAof the solverA robustnessAandAefficiency.ASince, steadyAstateAsolutionsAareAcalculated, aAsingleA

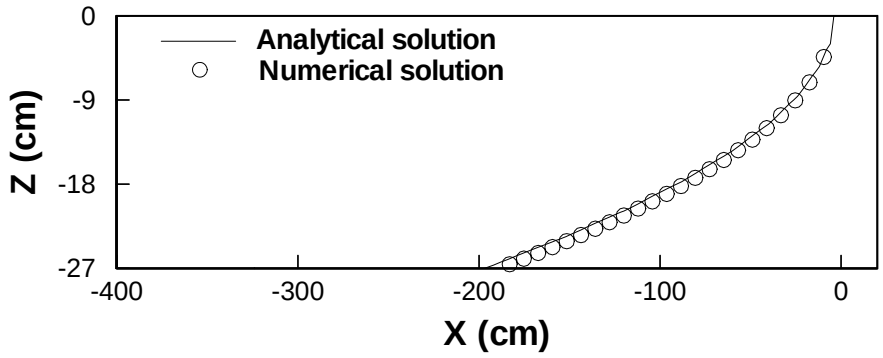

Figure 5.4:AComparison of Glover's analytical solution and numerical results.U

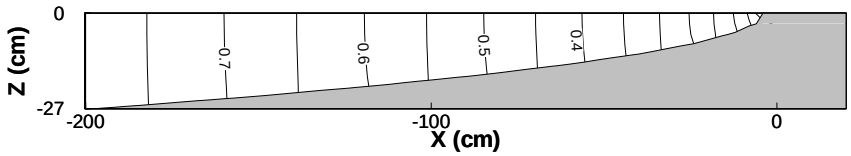

Figure 5.5:AZoom window showingwthewfresh-saltwaterwinterfacewpositionwandwthewfreshw groundwater heads (X and Z axis have the same scale).w

sequenceAofAnonlinearAPicardAiterationsAisAinvolved. Fig. 5.6Aplots theAconvergenceA history of such process, only 7 nonlinear iterations were needed to achieve con-A vergence, withAeachAstepArequiringAanAaverageAofA77APCGAiterations.ATheAmassA balance error acting as an indicator for the quality of the computed results isA equally excellent, $0.135\text{x}10^{-2}\%$.A

5.4.2y SeawateryIntrusionyinyanyUnconfinedyAquifery

ProblemyDescriptiony

Van der Veer (1977) has proposed an analytical solution for the steady interfaceA flowAinAcoastalAaquiferAsystemsAinvolvingAaAphreaticAsurface.AThisAapproachAisA two-dimensional, and assumes the existence of a distanceAL_e between the pointA where the interface and the phreatic surface reach the sea level as shown in FigA 5.7.A

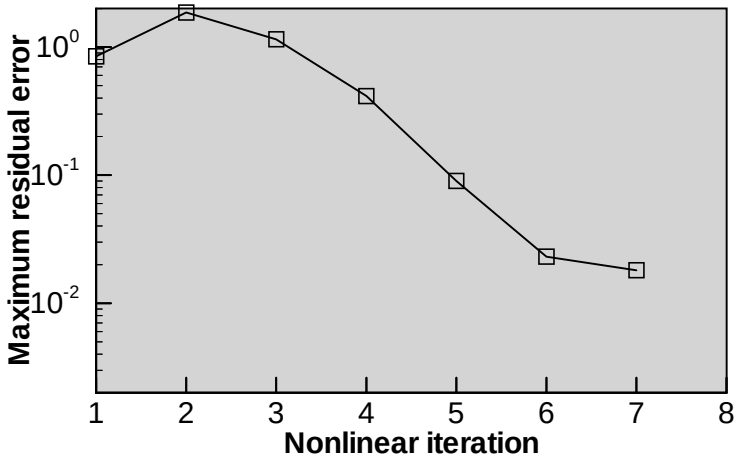

Figure 5.6: Convergence rate history of the modified Picard nonlinear iterations solver for test problem 1.

Analytical Expressions

The analytical solution is derived based on a non-linear algebraic expression in the complex potential Ω, defined by $\Omega \equiv \Phi + i\Psi$, where Φ and Ψ are respectively the velocity potential and the stream functions. Boundary conditions must hold at the interface and the phreatic surface, which gives respectively the position of the interface η and the phreatic surface h as

$$\eta(x) = \left[\frac{-(\frac{N}{K}x^2 + 2\frac{q^*}{K}x)}{(\delta + \frac{N}{K})(\delta + 1)}\right]^{1/24} \tag{5.10}$$

$$h(x) = \left[-(\frac{N}{K}x^{24} + 2\frac{q^*}{K}x)\frac{\delta + \frac{N}{K}}{\delta + 1} - \left(\frac{q^*}{K}\right)^{24}\frac{(1 - [\delta + \frac{N}{K}])}{(\delta + 1)(1 - \frac{N}{K})}\right]^{1/24} \tag{5.11}$$

where N is the effective precipitation, K is the saturated hydraulic conductivity of the homogeneous aquifer, and δ is the density gradient ratio. The x axis origin is taken at the point where the interface reach the sea level, and q^* is a flux

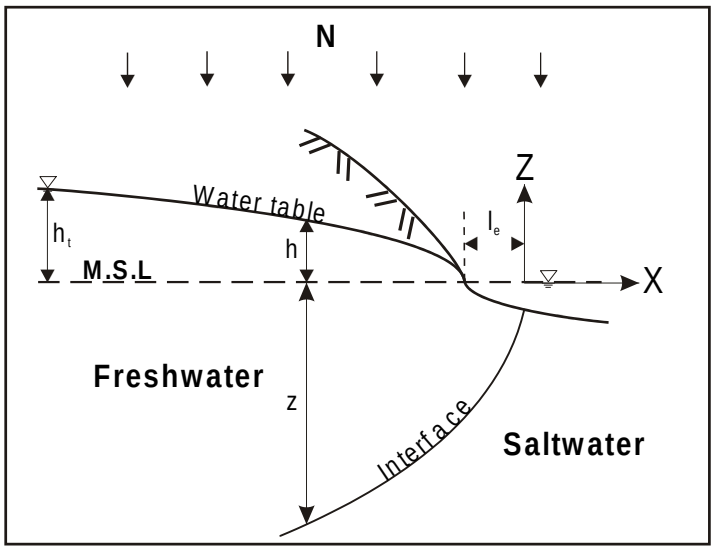

FigureA5.7:AVanwderwVeer'svanalyticalvinterfacevproblemw(1977).w

quantityAdefinedAbyA

$$q^* = Aq + Nl_e \tag{5.12}$$A

whereAq is the outflow of fresh water towards the sea. Note that l_e is calculatedA fromAtheAboundary conditionAz$(-l_e)$A=A0, whichAleadsAtoAtheAfollowingAexpressionsA

$$l_e = A\begin{cases} \dfrac{q^*}{2K}(\dfrac{1}{\delta S}A- 1)A & \text{ifAN} = 0\ A \\ \dfrac{q^*}{N}\left[1 - \left(1 - (\dfrac{N}{K})A\dfrac{1 - [\delta + \dfrac{N}{KS}]A}{(1 - \dfrac{N}{K})(\delta + \dfrac{N}{K})}\right)^{1/2}\right] & \text{ifAN} \neq 0\ A \end{cases} \tag{5.13}$$

There remains only one undetermined variable, q^*.ATwo different situations areA distinguished:A

SymmetricalyFlowinyanyIslandy InAcaseAofAsymmetricalAflow, weAdenoteAbyAl_t theAdistanceAseparating the twoApointsAwhereAtheAinterfaceAintersects theAseaAlevelA at each side, the outflow in steady state is given asAq =AN$(l_t - l_e)$ and it resultsA thatAq* =ANl_t

Non-Symmetrical Flow Another case which can be encountered is a situation where a fixed head value is attributed at the upstream boundary where q is unknown, see Fig. 5.7 for details. In this situation the quantity q^* is calculated analytically from the fixed potential h_t as

$$q^* = a_1 K l_t - [a_1(a_{14} - \frac{N}{K})(Kl_t)^{24} - a_2(Kh_t)^2]^{1/2} \qquad (5.14)$$

where

$a_{04} = (1 - \frac{N}{k})[1 - (\delta + \frac{N}{k})]$, $a_{14} = a_0(\delta + \frac{N}{k})$, and $a_{24} = a_0(1 + \delta)$

Comparison with Numerical Results and Discussion

Two test problems were run to check the model accuracy by comparing the analytical solution and the numerical results. The first example corresponds to the case (N=0) i.e. no precipitation. The fixed finite element mesh used in this example is composed of 211x2x51 nodes respectively along x, y and z coordinate system, which leads to a 3-D mesh of 21522 nodes and 10500 elements. In the FEA mesh the portion above the sea reference is refined to allow for the calculation of the phreatic surface with greater precision. The mesh dimension is 10m and 5m respectively along x and y-directions, while it varies from 1m above the m.s.l to 10m below. Above the sea level all nodes starting from position x=1968m are considered as isolated nodes in the model, because L_e is found to be equal to 32m from Equation 5.13 with L_t=2000m. Additional physical parameters of this problem are K=10m/d, δ=0.002 and h_t(x=0)=10m.

As boundary conditions, an outflow sea boundary condition is attributed to all nodes starting from x=1968m in the plane z=0m, and a fixed head boundary condition h=10m is attributed to all nodes in the plane x=0m. For the second test problem (N=1440mm/year) which impose another fixed flux boundary condition of 0.004m/d at the upper plane (z=10m and x$\leq$1968m). Fig. 5.8 shows simultaneously the obtained numerical results for test runs 1 and 2. The steady fresh-saltwater interface and the phreatic surface positions are compared with

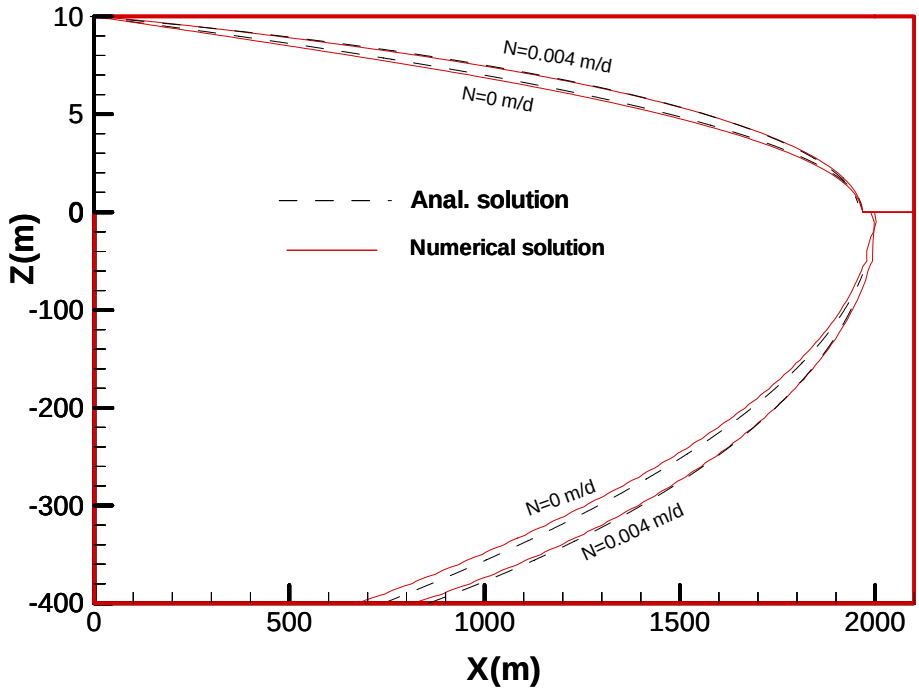

Figure 5.8:AComparison between numerical and Van der Veer's analytical solution.w

the analytical solution, and these comparisons show a good agreement betweenA the two solutions and the model ability to handle situations involving rechargeA conditions.AFig. 5.9Aand 5.10 show the freshwater heads and interface responseA to the recharge boundaryAcondition, the interface moves seawardAdue to moreA steepAhydraulicAgradientsAnearAtheAseaAshore.ATheAlocationAofAtheApointAwhereA the interface reaches the sea level has been determined 'numerically' very closeA to x=2000m for the first problem as expected.A

Here again, itAs instructive toAshowAhowAthe modelAsolver takes controlAofAtheA equations system.AThe nonlinear iterative process for runs 1 andA2 is plotted inA Fig.A5.11.AInAtheAfirstArunA(noArecharge)AaAfewAmoreAiterationsAwereAneededAforA convergence, the two testsAused an averageAof 214, andA223 PCG iterationsArespec-A tively per nonlinear iterative step.ARecorded mass balance errors were satisfyingA the global solution accuracy, they are equal to $0.145\text{x}10^{-1}$% andA$0.733\text{x}10^{-2}$%A

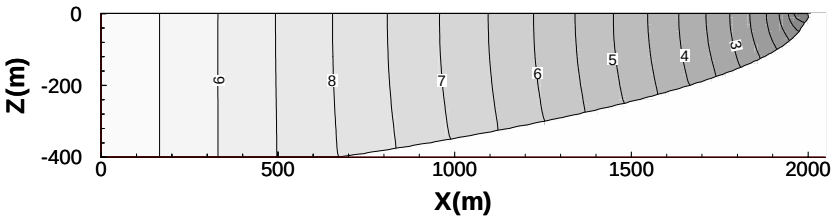

Figure 5.9: Freshwater potential heads distribution for the first run.

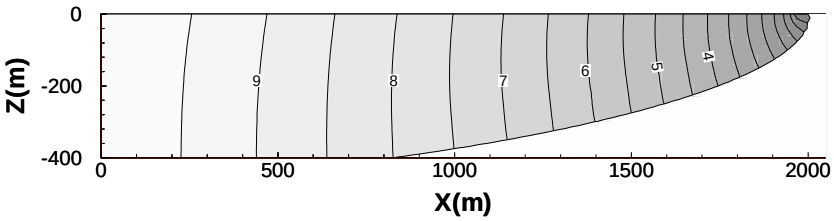

Figure 5.10: Freshwater potential heads distribution for the second run.

respectively.

5.4.3 Plan Seawater Intrusion Control with Artificial Recharge

Problem Description

Seawater intrusion control with pumping or recharge wells is an important issue in field methods and practices for site remediation in coastal aquifers. In particular, artificial injection has been practiced in the field in several projects, with the aim to push the fresh-saltwater interface toward to sea. Two strategies exists: (i) positioning a pumping well field near the coast to withdraw saltwater; or (ii) a battery of recharge wells inland injecting a fixed amount of freshwater, in the later case the injected freshwater is usually of lower quality than that stored in the aquifer. In such situation delineation of the backward movement of the injected water is also important.

In this test example, we consider several wells parallel to the coast line at a fixed distance, d, as represented in Fig 5.12, which are injecting an equal amount

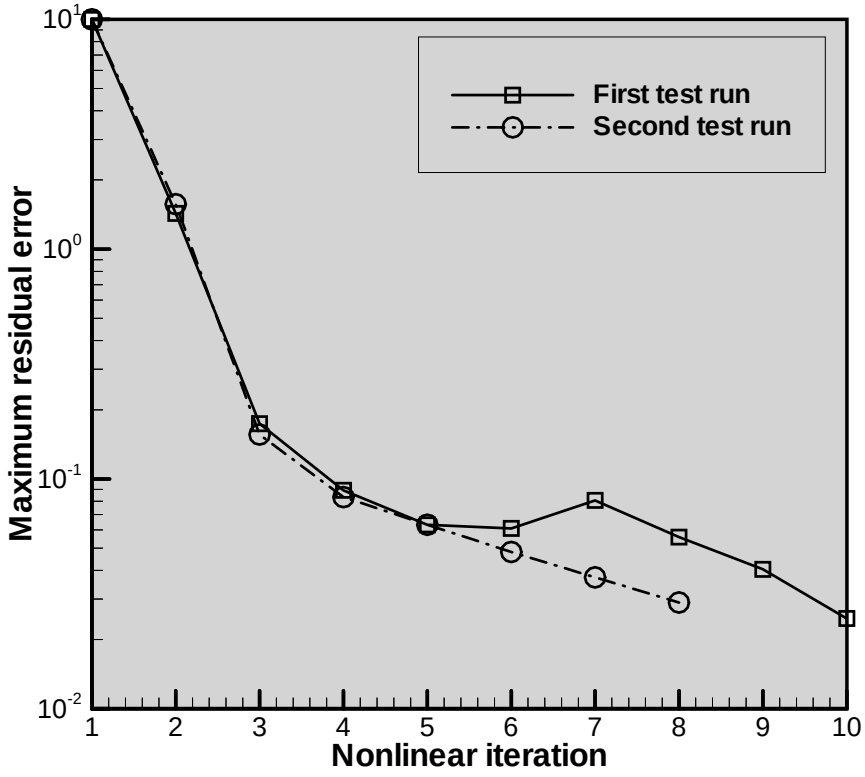

Figure 5.11:AConvergencewratewhistorywofwthewmodifiedw Picard nonlinearwiterationw solver for test problem 2 (runs 1 and 2).w

of water, Q_w, and whereA isAtheAdistanceAseparatingAtwoAsuccessiveAwells.ATheA inland uniform flow rate per unit arc length normal to the coast is denoted byAq.A

AnalyticalySolutiony

steady state analytical solution for this problem is derived by Hunt (1985). ThisA solution accommodates for the case of (i) one inland recharge well; and (ii) anA infinite numberAofArechargeAwells. Herein, theAsecondAsolutionAisAretained, becauseA the first solution implies boundaries at infinity, which can not be handled in theA numerical model.AHence, the second analytical solution was derivedAbased on aA modifiedAformAof theAStrack's (1976)Apotential AforAunconfinedAflowAinAthe complexA plane. The Ghyben-Herzberg approximation was used to locate the interfaceAtoeA

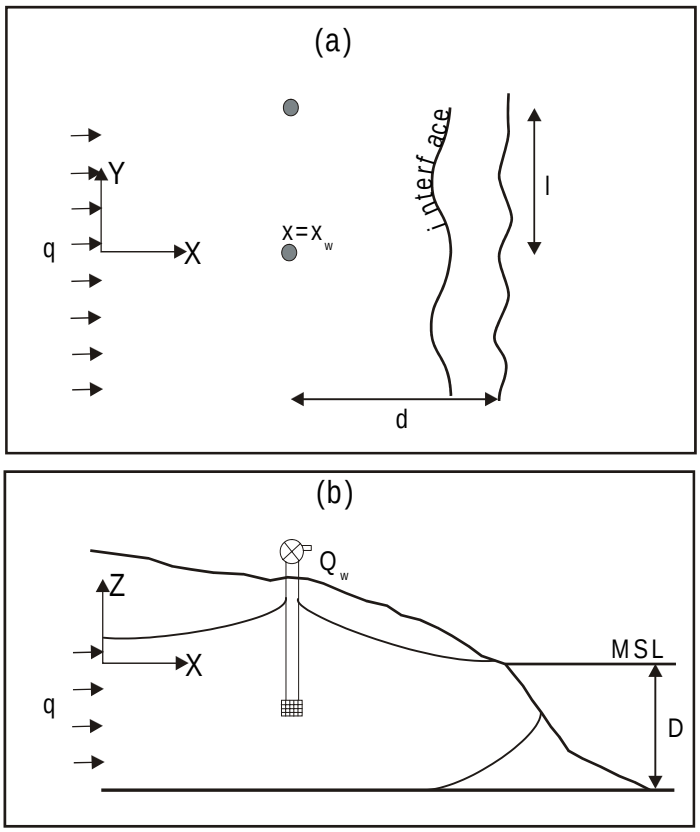

Figure 5.12: Definition of the Hunt's analytical interface problem (1985); (a) plan view, and (b) a cell cross-section profile.

curve for an unconfined aquifer, which has the following equation

$$\frac{KD^2}{2}\delta(1+\delta) = xq + \frac{Q}{2\pi}\ln(r) \tag{5.15}$$

where D is the vertical distance between the mean sea level and the bottom of the unconfined aquifer, and r is given by

$$r^2 = \frac{\sinh^2\pi\left(\frac{x+d}{l}\right)\cos^2\pi\left(\frac{y}{l}\right) + \sin^2\pi\left(\frac{y}{l}\right)\cosh^2\pi\left(\frac{x+d}{l}\right)}{\sinh^2\pi\left(\frac{x-d}{l}\right)\cos^2\pi\left(\frac{y}{l}\right) + \sin^2\pi\left(\frac{y}{l}\right)\cosh^2\pi\left(\frac{x-d}{l}\right)} \tag{5.16}$$

Equation (5.16) has extremas located at $y=0$ and $y=\frac{l}{2}$. For a fixed y value, Equation (5.15) can be solved by a numerical procedure such as *Meuller's method* (See Appendix B) for finding the root of a real function with a single variable.

Comparison withy Numerical Resultsy andy Discussiony

The physical and computational data set used for this test problem are givenA in Table 5.2.AB ecause of the problem symmetry we consider only the half planeA $[0, \frac{l}{2}]$A in theAy-directionAseparating twoAwells, thusAonlyAoneAwellAisA'virtually'A consideredAinAtheAcurrentAmodelingAstudy.ANoticeAalsoAthatAtheAelementsAgridA sizes are uniform, Δx=Δy=10m, and Δz=4m, except for the first element layerA above the water table, Δz=10m, because in this example a detailed water tableA profile is not the main interest. It is assumed also that the wellArecharge occurs forA nodes lying below the sea level, and that the upstream uniform recharge shouldA always adapt to the water table increase/decrease.A

Table 5.2:A*Physicalyandycomputationalymodelyparameteryvaluesyofytheythirdytesty problem.y*

Parameter	Value
UpstreamAfixedAflux, q	$3m^2/dA$
RectangleAuconfinedAaquiferAdimensions, L, D	410m, 40mA
GridAdimensionsA	41x11x12A
DensityAdifferenceAratio, δ	0.025A
SaturatedAHydraulicAconductivity, K_s	10m/dA
WellAinjectionArate, Q_w	$1000m^3/dA$
DistanceAofAwellsAfromAtheAcoast, d	100mA
DistanceAbetweenAtwoAwells, l	200mA
StartAupAunderrelaxationAfactor, ω^{04}	0.25A
WaterAtoleranceAparameter, $tolw$	0.01mA

The maximum seawaterAintrusionAinterface at theAquiferAbottomAisAplottedAinA Fig. 5.13Against theAanalyticalAsolution, andAshows a goodAagreement. AlthoughA differencesAexists, the numericalAsolutionAis acceptableAregarding, firstA(i)AtheA coarse mesh resolution used;Aand secondly (ii) the upstream Neuman boundaryA condition which is applied at a given fixedAlimit, 400m inland, while it existsA 'theoretically' at the infinity, so as a consequence the computed interface has aA tendency to intrude more inland as concluded.A

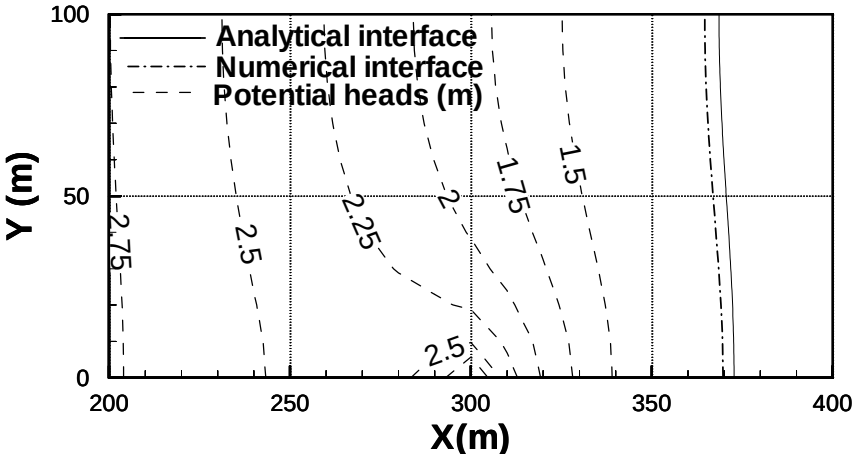

Figure 5.13: Comparison between analytical and numerical results for the hunt's test problem at the aquifer bottom. Results are plotted together with the countour lines of potential heads.

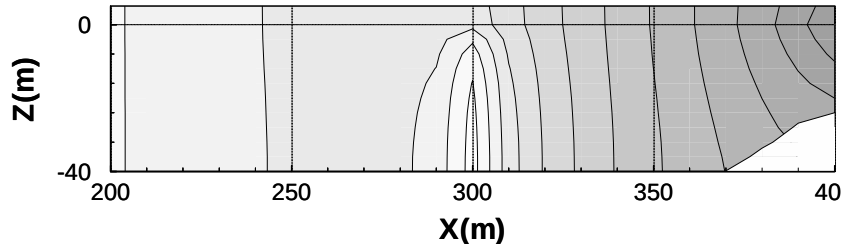

Figure 5.14: Cross-section view of the computed interface and freshwater potential heads along the injection well.

The most seaward interface profile at the plane y=0 is plotted in Fig. 5.14, where the artificial injection through the well location is clearly shown by the potential contour lines. A better 3-D enlarged view of the simulated interface is showed in Fig. 5.15 where intersecting potential iso-surfaces are also plotted, it is noticed that the interface line at the aquifer bottom coincides with the potential isoline h=1m. Convergence within the iterative procedure was achieved within 4 outer iterations, requiring an average of 48 PCG iterations, and performing a mass balance error of $0.176\text{x}10^{-2}\%$.

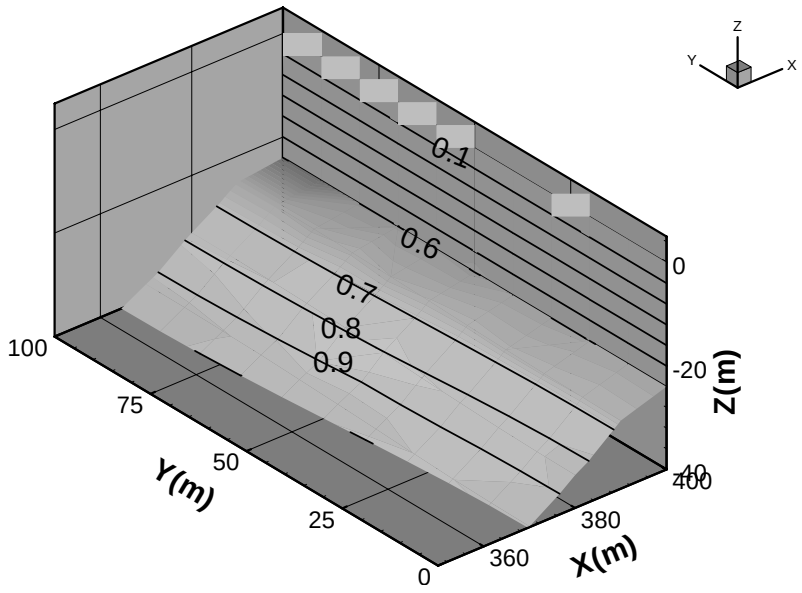

Figure 5.15:AAwzoomwview onwthewinterface,wcrossingwpotentialwisolineswarewshownw alongw ith the outflow to the sea face.w

5.4.4y SaltwateryIntrusionyinyayMultilayeryAquiferySystemy

ProblemyDescription andyBackgroundy

This example is taken fromAHuyakorn et al. (1996) who solvedAtheAsame theoret-A ical problem with their SIMLAS code.AThe test problem involves the simulationA of staggered fresh-saltwater interfaces in a multilayer aquifer system.AFig.A5.16A shows the conceptual problem, in which the chosen parameter values are given, as the hydraulicAconductivities of the upper aquifer, the intermediate thin leakyA layer, andAtheAlowerAconfinedAaquifer, respectively.A ComparisonAisAconductedA against the steady state analytical solution derived by Mualem and Bear (1974).A ItAisAhowverAimportant, toApoint out that thisAsolutionAwasAbasedAon a lin-A earized form of the governing equation, and the use of the*ADupuit-Forchheimery* assumption.AHence, theAanalyticalAsolutionAisAnotAexact, andAthisAwasAgivenAasA an argument by the authors to explain the SIMLAS results deviations from theA analytical results as shown in Fig. 5.17.A

We did run the same problem with the data already given in Fig.A5.16, andA

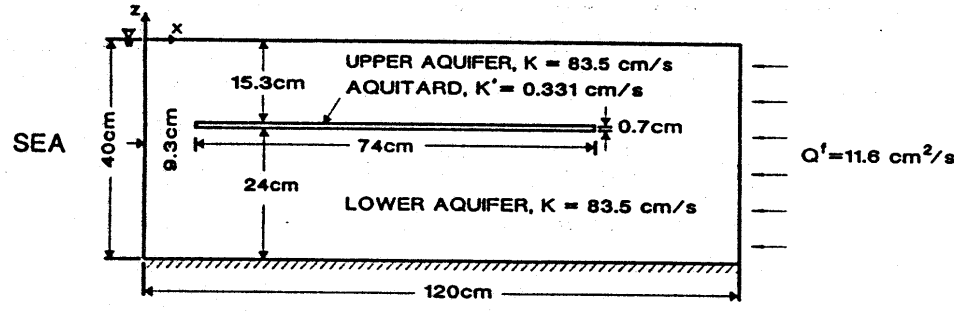

Figure 5.16:ASchematicwrepresentationwandwparameterwvalueswofwthewfourthwtest ex-wample (Huyakorn et al., 1996).w

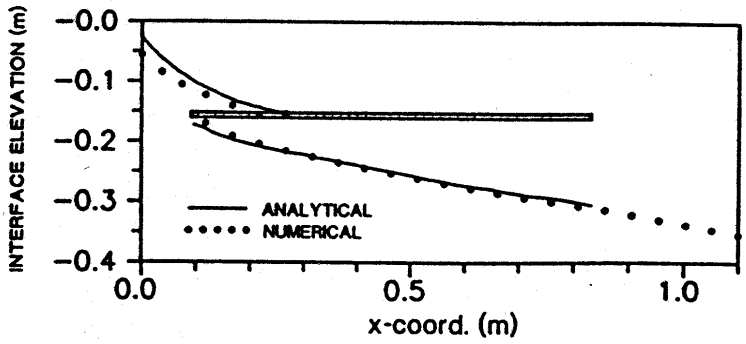

Figure 5.17:AComparisonwofwthewanalyticalwandwnumericalwsolutionswcomputedwbywHuyakorn et al.w(1996).w

using a uniform orthogonal mesh composed of 49x2x21 nodes.AConvergence wasAachieved within 3 nonlinear iterations, and an average of 53 PCG iterations perAeach outerAiterate. ComparisonAbetween analyticalAand numericalAresultsAisAshownAin Fig 5.18.AThe predictions are satisfactory regarding the approximations usedAin the numerical solution, also comparisons could not be performed for the lowerAaquifer unit, outside of the leaky layer extension, because the boundary conditionsAfor theAanalyticalAsolutionAareAspecified at theAquitardAboundaries. Interestingly, GEO-SWIM (Sbai andADeASmedt, 1999;ASbaiAet al. 1998)AandASIMLAS results areAvery close, a comparative study of the two simulators based on other examples, will certainly be fruitful for a wide range of practical applications.A

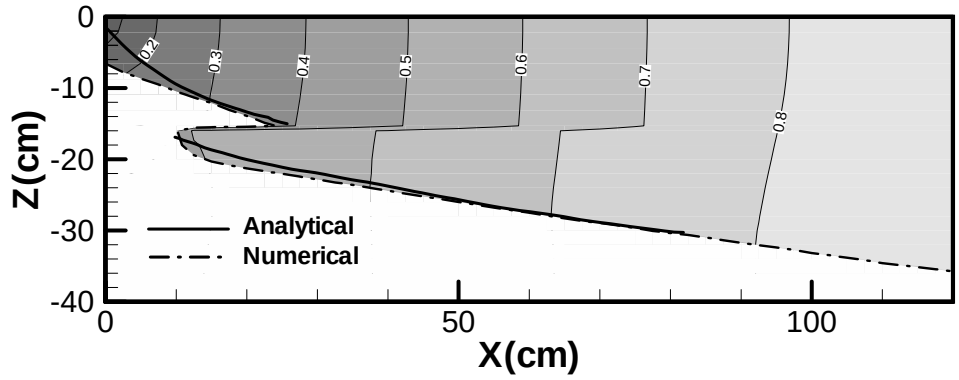

Figure 5.18:AComparisonwofwanalyticalwandwthewnumericalwsolutionwcomputedw ithw GEO-SWIM code, for the fourth test problem.w

5.4.5 MovingySaltwaterYInterface in a 3-DyLaboratory Sandy Box Modely

ToAdemonstrateAthatAthe numericalAmodelAis able to accuratelyAsimulateA3DA groundwater flow problems with a moving freshwater saltwater interface, a com-A putation is made with results from a 3-D sand model (Sugio and Rahim, 1992)A depictedAinAFig. 5.19. The modelAconsistsAof a 3DAsandAbox, 165.8AbyA47.5cm, andA having a width of 63.2cm in the first 82.3cm section, andA30cm in the remainingA part.ADuring the experiment, acrylic plates were placed at upstream andAdown-A streamAsections, whileAthe aqueousAsaltwaterAsolutionAwasAcoloredAbyAdyeAinAorderA to distinguish it from the freshwater part.A

The upstream andAdownstream water levels are 44.15 and 40.67cm respec-A tively; other data are K=1.293cm/s andA$\delta = 0.03$. The behavior of the saltwater A interfaceAwasAmeasuredAonAtheAfront, back, andAbottomAsidesAofAtheAbox forAsteadyA state (initial conditions), and each 30min thereafter, when the upstream head isA reduced to 42.65cm with a linear decrease rate of 0.01cm/min.A

The model is applied by discretizing the box into a total number of 154275A elements, andA30800AinactiveAelementsAwhich areAexcludedAfromAtheAsimulation asA shown in the finite element mesh in Fig. 5.20. The positions of the saltwater in-A

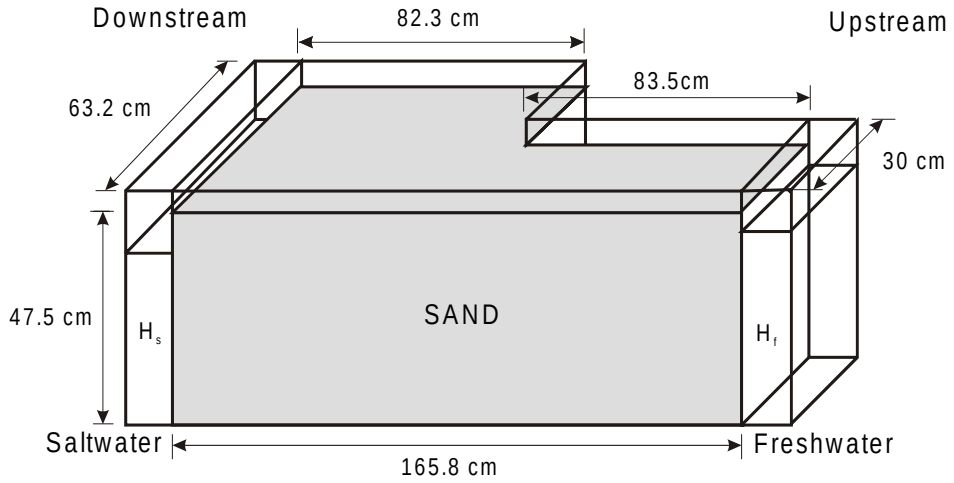

Figure 5.19: Descriptive view of the experimental sand box model used by Sugio and Rahim (1992).

terface are plotted for each section of the model and compared with the numerical results in Fig. 5.21 (a, b and c). These steady and transient interfaces show that the predicted 3D results compare well with the measurements. The interface has a tendency to advance rapidly in the back section than in the front section, this is because of the well pronounced three-dimensional behavior of the flow created by the shorter width section, in which the flow is faster, and the intrusion is likely to be more important. This is better understood from the plotted maximum interface profiles (or interfaces toe positions) shown in the bottom section. It is also worth noting that small variations of the upstream groundwater potentials had led to a noticeable tracking of the salt-freshwater interface; a situation often encountered in practice.

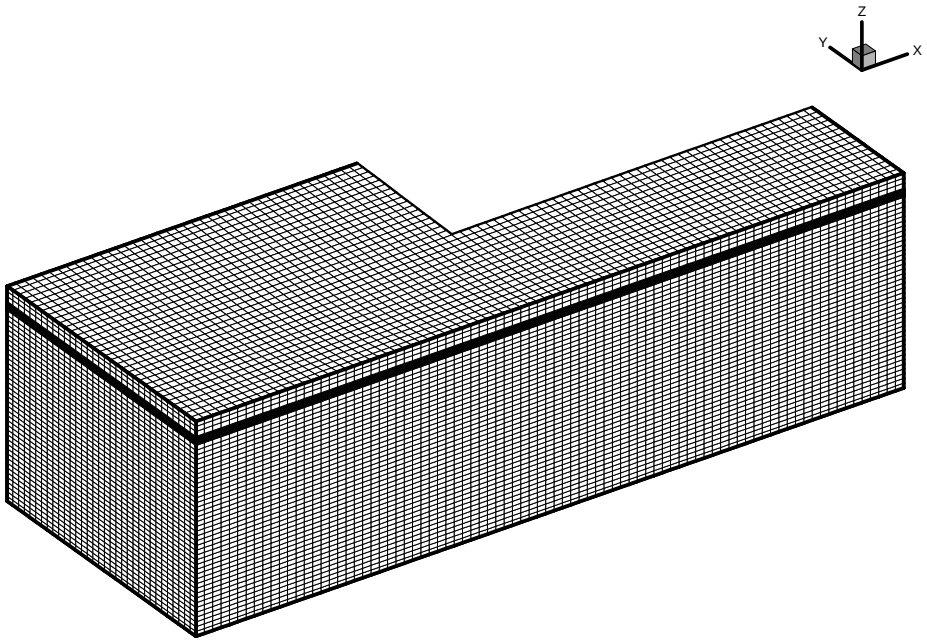

Figure 5.20: Finite element mesh used in Sugio's laboratory sand box model validation.

5.5 Model Application to Seawater Intrusion in Martil Aquifer

5.5.1 General Situation and Background

Aquifer systems in northwestern part of Morocco are known to be of small extension. The Martil aquifer (Fig. 5.22) is not an exception with its 80km^2 surface area (Fig. 5.23). However, it is one of the important local groundwater resources, especially for water supply of Tetouan city, and its industry and irrigated areas located in the center of the plain. In recent years, the aquifer has become vulnerable to potential pollution due to leachate of domestic and industrial wastewater in the Martil river, and also due to seawater intrusion from the Mediterranean sea.

Relevant hydrogeological information on this aquifer is scarce as for many other sites in Morocco, such that before a representative model of this aquifer

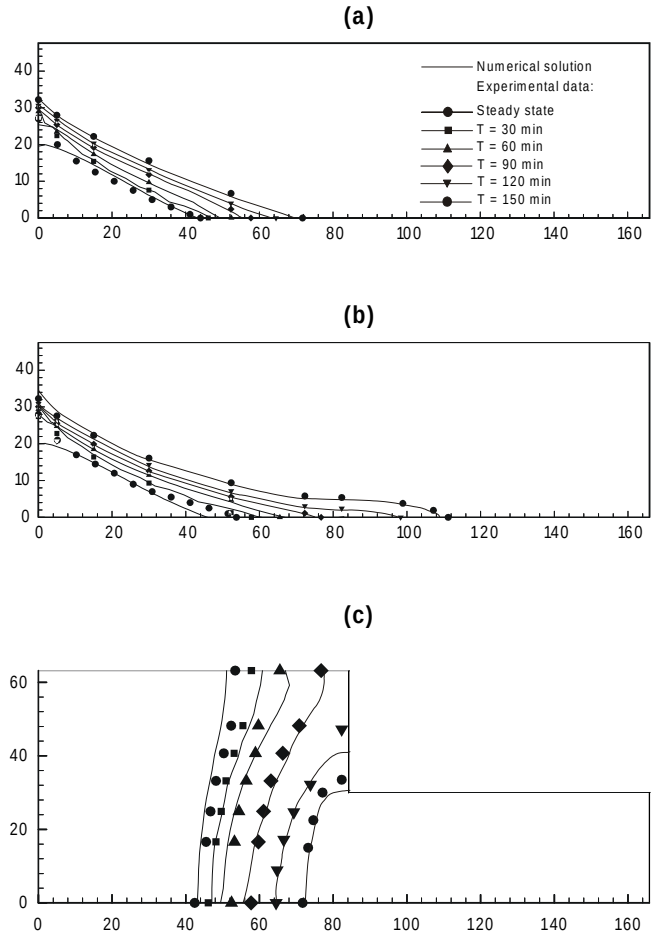

Figure 5.21: Numerical solutions versus laboratory experiments for (a) front section, (b) back section, and (c) bottom section.

can be set up, a significant fraction of the work involves aquifer characterization and reinterpretation of previous measurements. A Combined use of Geographic Information Systems tools (GIS), and developed software interfaces (chapter 7), give consistent support to correlate unavailable data, and a robust approach for its interpretation. A total of 59 boreholes were selected to make digital elevation maps of contacts between different geological layers.

A three-dimensional finite element model for the Martil aquifer is developed using the GEO-SWIM package and associated graphic interface tools. First, a steady-state groundwater flow is simulated. Calibration of this model will

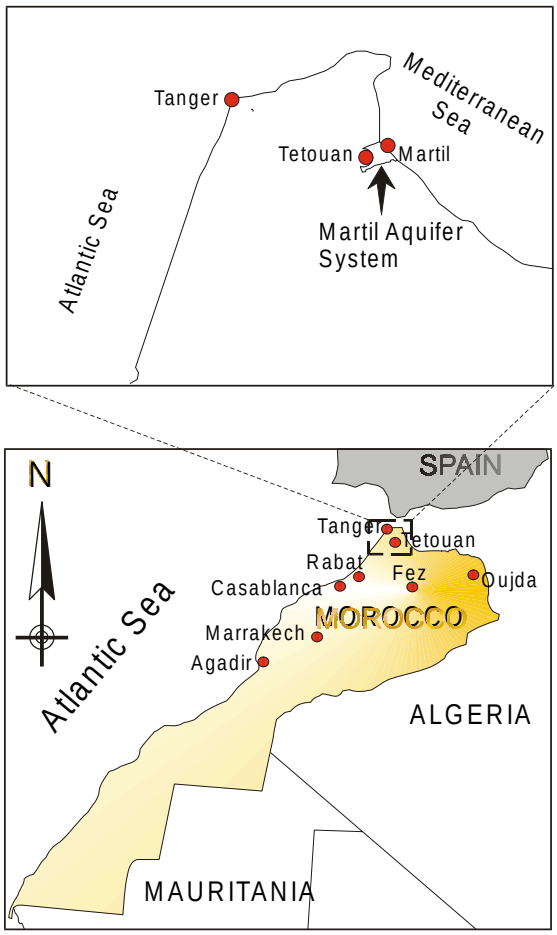

Figure 5.22: General geographic situation map of Martil aquifer.

establish natural conditions and hydraulic conductivity ranges for the different aquifers. Afterwards a transient simulation is performed to predict future lateral extension of the saltwater encroachment due to pumping of groundwater. Future trends of the salinization risk from saltwater intrusion are investigated. This is the first time that a simulation model for groundwater flow and seawater intrusion in the Martil aquifer system is performed.

5.5.2 Data Analysis

Previous studies carried out in the plain (Ennouhi and Melouki, 1984; El Morabiti et Pulido-Bosch, 1993; Larabi et al., 1998) identified two aquifer units, sepa-

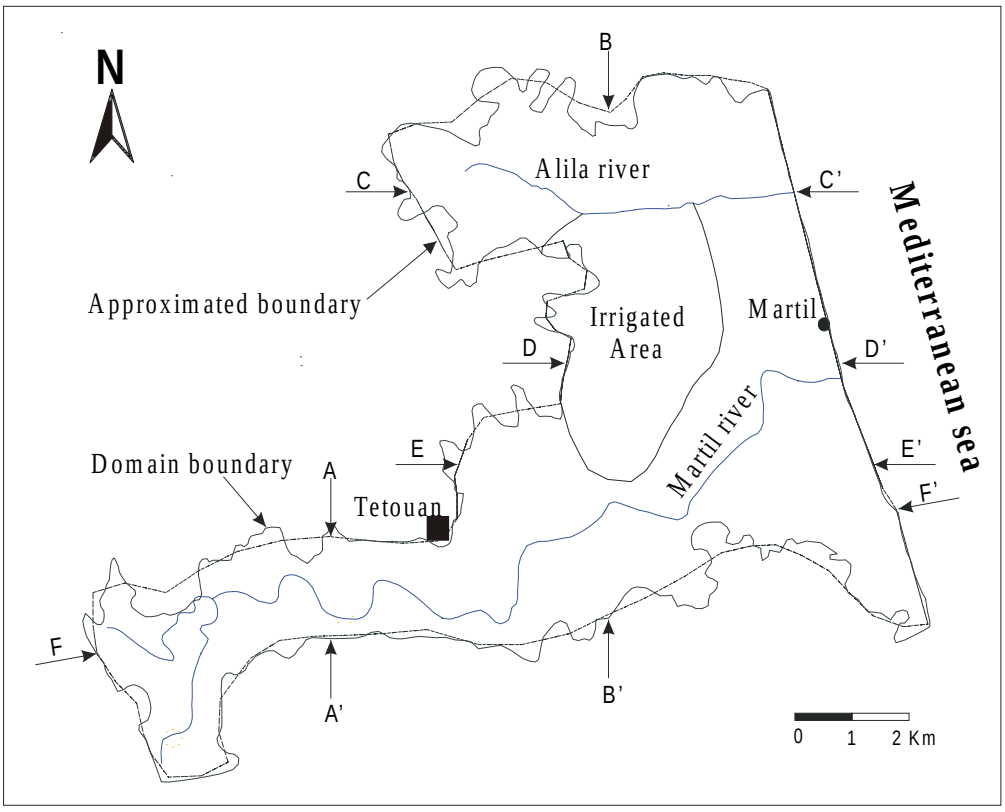

Figure 5.23: Study area and locations of cross-sections of interest.

rated by a leaky aquitard. The upper aquifer is formed from Quaternary alluvial deposits of the Martil river; the lower aquifer unit is composed from sandstone-limestone Pliocene formations, while the aquitard as mainly marl and clay. Variations in thickness are shown to be significant from North to South, and also along the West-East direction. However, this information was not taken into account in studies made in the past. To better characterize the thickness of the three hydrogeological units a reinterpretation of data obtained from a total of 59 wells and boreholes is performed with support of GIS tools.

The aim of this study is to better define the structure of the aquifer system (upper, lower aquifers and aquitard) and their extension. Digital elevation models of these surfaces are shown in Fig. 5.24, and are obtained by interpolating scatter point data sets obtained from contacts between different formations or at the

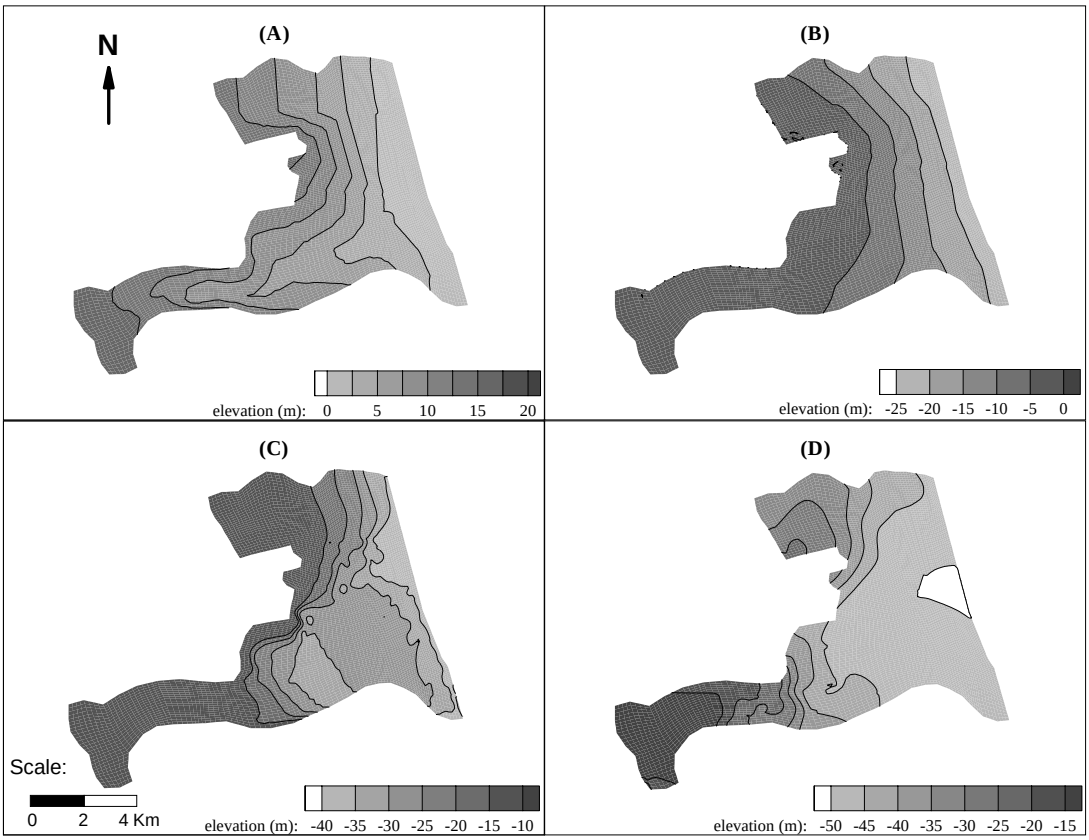

Figure 5.24: Interpolated countour maps of (A) aquifer topography, and bottom of of (B) phreatic aquifer, (C) aquitard and (D) confined aquifer respectively.

surface (topography) of each borehole into a numerical grid (usually the same as used for the numerical FE model). A summary of statistical analysis results of thickness of each of the three units is presented in Table 5.3.

5.5.3 Construction of the Conceptual Model

Model Set Up

The conceptual model used in this study is a multi-layer aquifer system composed of two aquifer strata, separated by an aquitard layer of variable thickness. A structured surface mesh of 93 columns and 121 rows is used to approximate the

Table 5.3: *Information on thickness of model layers.*

	Minimum thickness (m)	Maximum thickness (m)	Mean value (m)
Upper aquifer	8.9	24	16
Aquitard	0.0	28.8	11.5
Lower aquifer	0.0	36.4	17.3

aquifer domain, and some sub-zones are set to be inactive to fit the remaining part at the domain boundaries, especially at the weastern boundary near Tetouan city. In total, the aquifer system is divided into 9 nodal layers, with 88320 hexahedral elements and 101277 nodes.The two-dimensional mesh is projected

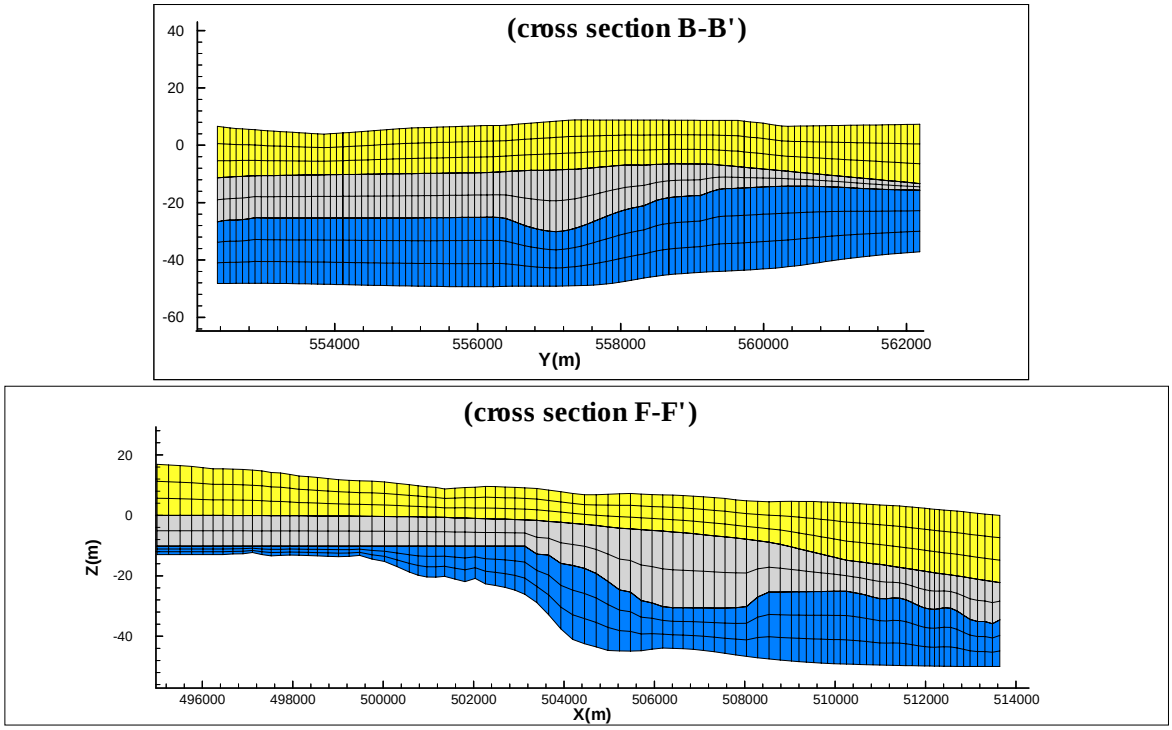

Figure 5.25: S-N and W-E cross-sections of the conceptual model, showing the finite element mesh and soil types distribution.

over the digital elevation maps, including the topography map, as shown in Fig. 5.24. Nodal elevations in intermediate layers are found by linear interpolation from values of existing surfaces above and below. This three-dimensional mesh

conforms to the aquifer configuration and makes it easy to fill in soil types ofA elementsAinsideAeachAof theAmainAthreeAayers. The threeAmodel unitsAare assumedA to be homogeneous and isotropic in this study, to allow for a faster and efficientA calibration.A

Fig.A5.25 shows the finite element mesh used for the numerical simulation ofA theAMartilAaquiferAsystemAwhichAs adjusted toAfit theAstructure andAtheAextensionA ofAtheAhydrogeologicalAlayersA(cross-sectionsAB-B'Aand F-F').ATheAlocationsAofA these cross-sectionsAareAindicatedAnAFig. 5.23. Cross-section B-B'AsAdirectedAS-NA while cross-section F-F' is directed E-W.A

Boundary Conditionsy

Domain boundaries are set impervious, except at the eastern part, which is inA direct contact with the sea. This boundary receives the 'special' sea outflow faceA boundaryAconditionAasAdescribedAinAchapterA3.A TheAextentAofAtheAfreshAwaterA outflow to the sea is therefore automatically determined as part of the results.A Nodes along the rivers paths are taken as fixedAhead with the assumption thatA waterAlevelsAareAequalAtoAtheAelevation. AnotherAconditionAtakenAintoAaccountA is the effective rainfall, which is assumed to be uniformly distributed over theA wholeAsurfaceAbasin.ASaturatedAhydraulicAconductivityAvaluesAareAdeducedAfromA calculated transmissivities of pumping tests analysis, conducted by the RegionalA HydraulicADepartmentAofATetouan.A TheseAvaluesAareAcharacterizedAbyAaAhighA variability, and range between $2.3m/d$ and $4.0m/d$ for the unconfined aquifer;A andA3.5m/d and $4.8m/d$ forAtheAconfinedAunit.AOnlyAaverageAlayerAdepthsAwereA taken into account as a basisAfor thisAestimation, whichAexplainAwhyAtheAobtainedA values should be calibrated afterwards.A

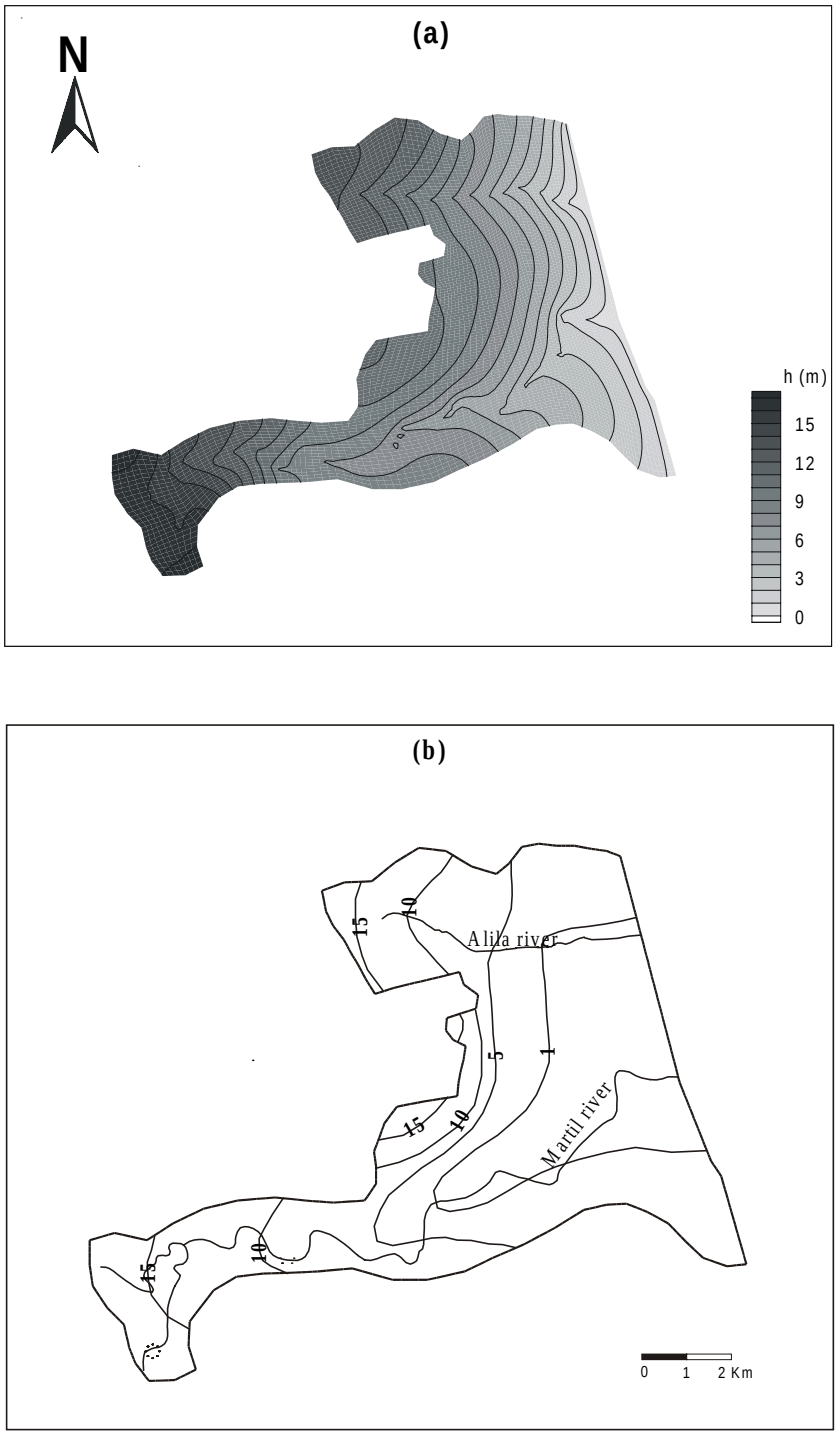

Figure 5.26: Comparison between (a) computed and (b) observed (in 1966, before heave pumping) steady state groundwater potentials (presented as meters above sea level).

5.5.4y ModelyApplicationyandyResultsy

Natural GroundwateryFlowyandySeawateryIntrusiony

first set of steady state simulations is performed under natural conditions (i.e.A noApumpingAwells).ATheAobjectiveAofAthisAcalibrationAprocessAisAtoAreproduceAaA natural groundwater flow pattern of the aquifer system and at the same timeA provide a range of confidence limits for the model parameters, such as hydraulicA conductivity and effective recharge.AThe obtained results for each test run wereA comparedAtoApiezometricAlevelsAmeasuredAinA1966.AItAcanAbeAassumedAthatAtheA aquiferAwasAnotAyetAheavilyApumpedAatAthatAtime.A trialAandAerrorAcalibrationA procedure is used to estimate the hydraulicAconductivity of the different layersA andAtheAnaturalArecharge.AThe AtestsAshowAthatAtheAconceptualAmodelAisAmoreA sensitive to changes in the effective recharge value, moreover varying hydraulicA conductivity values inside a given range for the same recharge does not produceA drastic increase or decrease of the water table.A

ComputedAgroundwater potential heads versus observed values are comparedA inAFig.A5.26, theAfitAisAsatisfactoryAexceptAatAtheAcenterAofAtheAplainAandAnearA theAcoastlineAwhereAdifferencesAareAobvious.A ThereAmightAbeAtwoAreasonsAforA this.A First, theAobservedAvaluesAwereAobtainedAduringAaAperiodAinAwhichAtheA exploitation of the aquifer alreadyAstarted, in a form of pumping for domesticA use andAirrigation in theAcenterAplain. Secondly, theAdifferences mayAbeAexplainedA also by the fact that soil heterogeneity and anisotropy were not included in theA calibrationAprocedure.AHowever,AinAgeneral, theAmodelAisAableAtoAreproduceAtheA same flow pattern, indicating that the main groundwater flow is directed W-E, with some convergence tendency to the rivers.A

In the GEO-SWIM code (Sbai and De Smedt, 1998) the fresh-salt water A interface is computed iteratively in parallelAwithAthe groundwater potential heads, and theAsimulatedAinterfaceAis obtained after convergence.A n enlarged3D view ofA the simulated interface is depicted in Fig. 5.27, showing that preferential pathsA

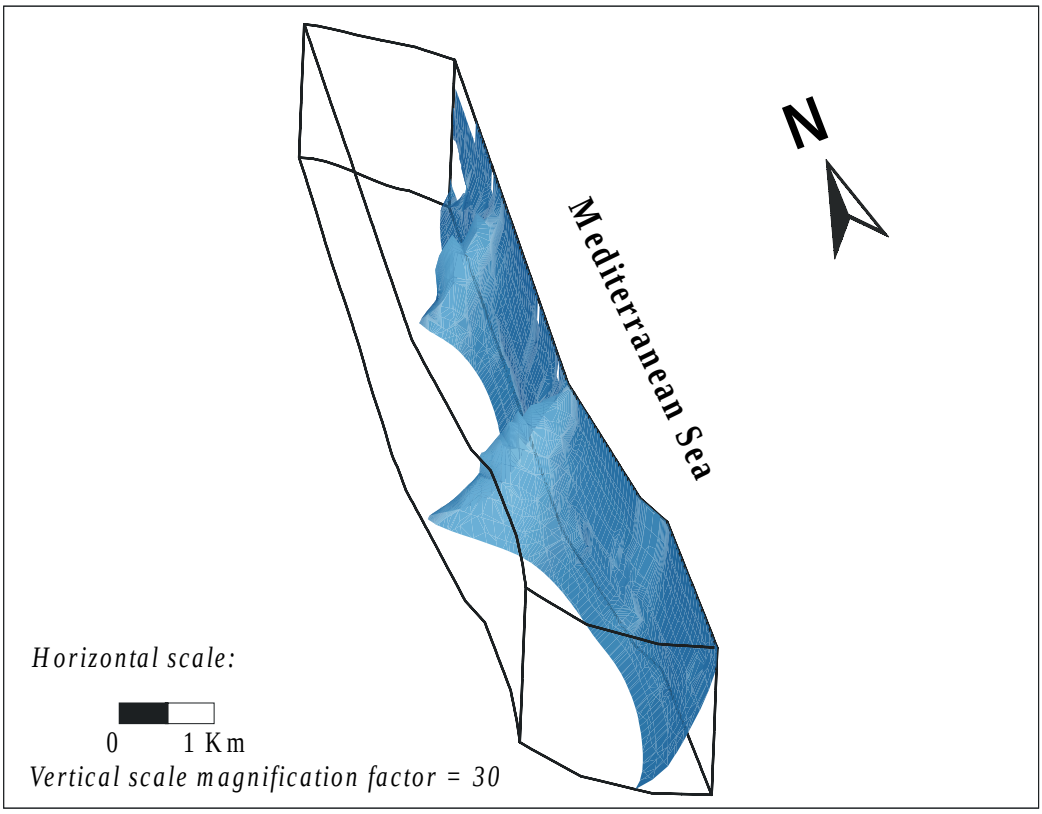

Figure 5.27: Shape and extent of the natural 3-D fresh-saltwater interface.

for seawater intrusion are located along the rivers, especially along the Martil river where the maximum intrusion equals 1100m in the lower aquifer. W-E cross-sections displayed in Fig. 5.28 show the shape of the steady interface and water heads distribution in different parts of the aquifer. By comparing cross-sections C-C' and E-E' which are respectively parallel to the Alila and Martil rivers, it follows that saltwater intrusion is more sensitive along the Martil river as the hydraulic gradient is the smallest due to the flat topography.

Calibration Results

The parameters obtained after calibration are summarized in Table 5.4

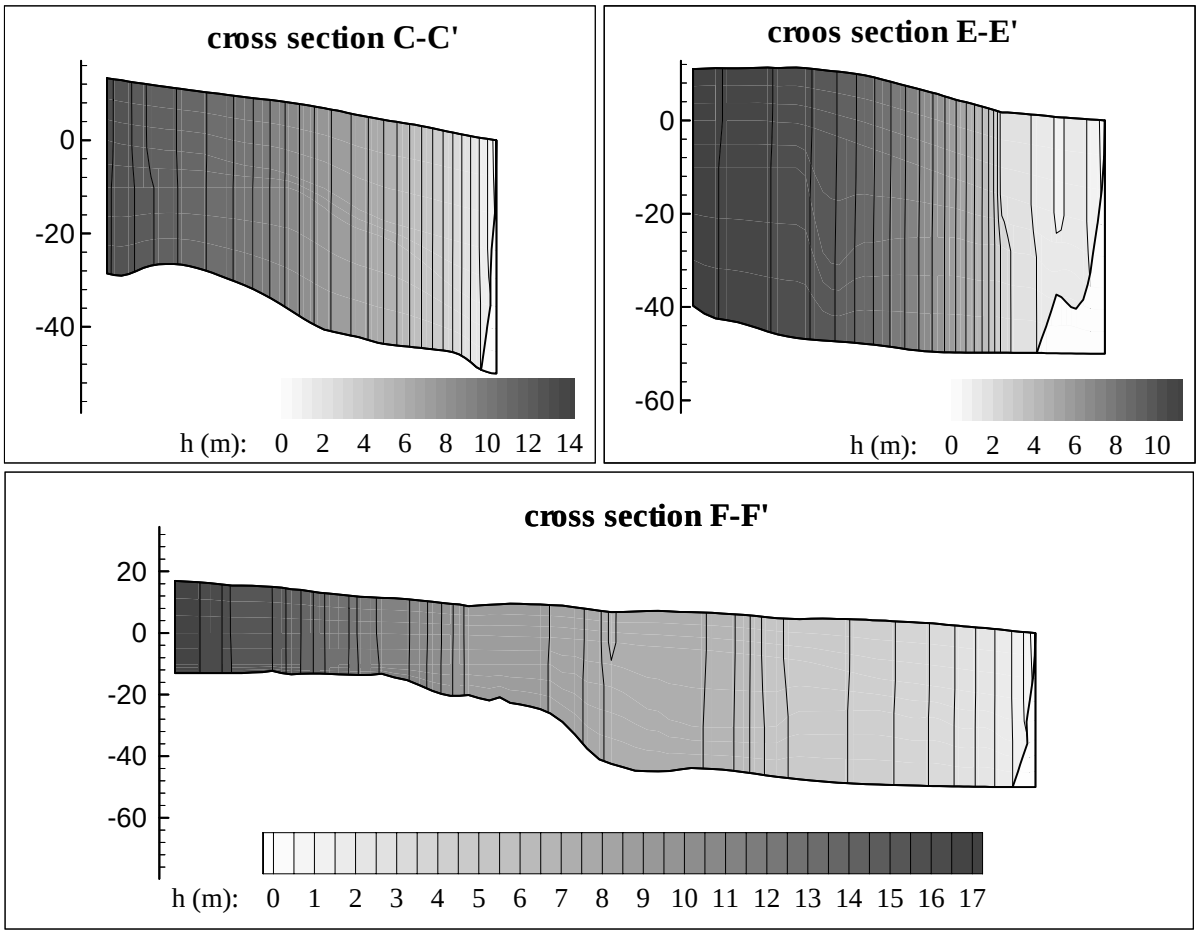

Figure 5.28: W-E cross-sections showing the initial groundwater heads and fresh-saltwater interface position. (The vertical scale magnification factor equals 100 for cross-sections C-C' and E-E', and 66.7 for F-F')

Future Prediction Scenario for Seawater Intrusion

A second set of simulations is performed, to predict the present and future groundwater flow and seawater intrusion in the aquifer. A long-term transient simulation is made of 40 years starting in 1966. The previous calculated heads are used as initial head values.

The pumping of groundwater is assumed to decrease the natural recharge by half during this period, because no other precise information is available about the number of wells and their pumping rates. Fig. 5.29 shows the computed

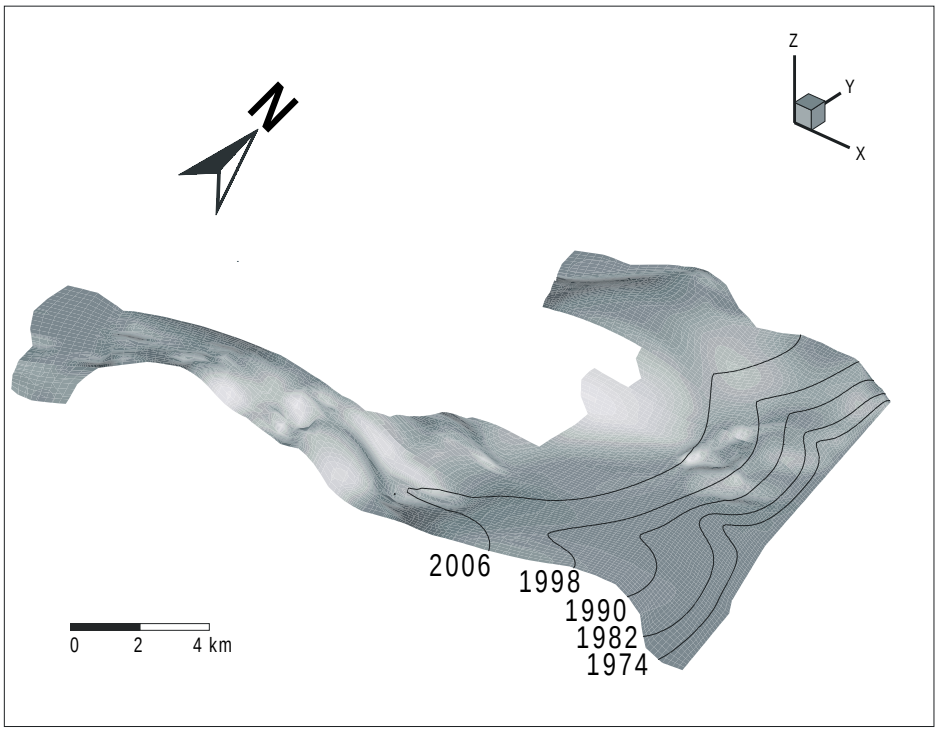

Figure 5.29: Computed moving toe positions of the sharp feshwater saltwater interface each 8 years from 1974 to 2006. The shaded surface represents the bottom of the lower aquifer.

fresh/saltwater interface in the lower aquifer each 8 years from 1974 until 2006. Corresponding positions of the moving interface are also plotted along cross-section F-F' as shown in Fig. 5.30.

Upconing effects due to pumping are negligible, since pumping rates are not concentrated in specific locations as it would be in practice. Also here, the maximum seawater intrusion occurs at the Martil river as clearly shown in Fig. 5.31, where the lateral distance to the coast from the maximum interface toe position versus time is plotted. Three different time periods can be distinguished: before 1986, the interface moves inward linear in time; a second period between 1986 and 1992, when the interface is intruding quadratically in time; and finally after 1992 where the movement is exponential in time.

Table 5.4: *Model calibrated parameters under steady state conditions.*

K_s(M/D)			θ_s			DENSITY	EFFECTIVE
I	II	III	I	II	III	RATIO	RECHARGE (MM/Y)
3.5	0.05	4.5	0.4	0.25	0.25	0.03	50
I : Upper aquifer unit; II : Aquitard unit; III : Lower aquifer unit							

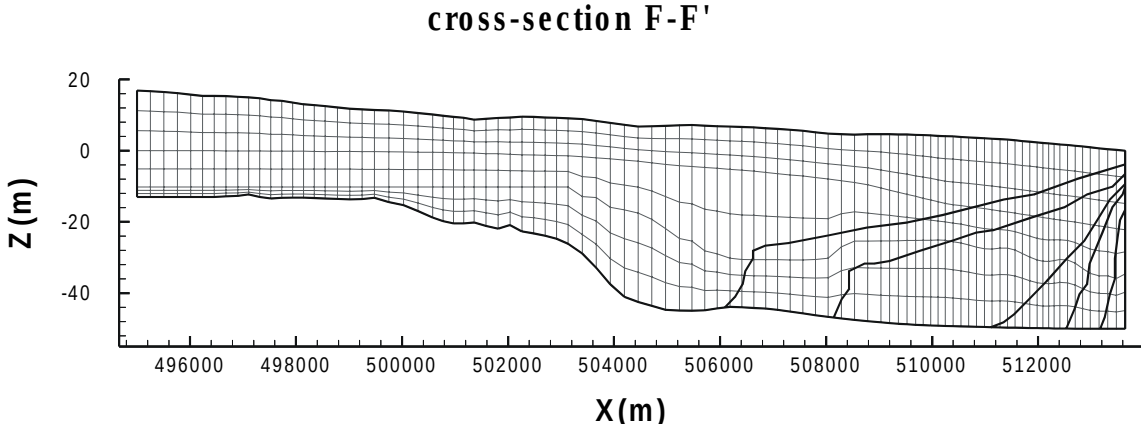

Figure 5.30: Cross-sectional view of the seawater intrusion; simulated moving interface positions from 1974 to 2006 are plotted.

5.6 Summary

A finite element model for simulating seawater intrusion in fully three–dimensional groundwater aquifer systems is developed. This accounts for free and moving boundaries, either between the saturated and unsaturated domains (air-freshwater interface) or between the freshwater and saltwater domains (fresh-saltwater interface). The key assumptions, is an iteratively based Ghyben-Herzberg approximation of the interface position, which permits the flow field to be completely dependent on the governing equations for the freshwater phase. Computer memory and storage savings are not only due to such approach. The presented generalized FUP approach is the second major step for making such economy. The FUP had to adapt for the density difference between the salt and fresh water zones. This was explicitly reflected in the shape of the idealized water retention curve, and in the technique for regenerating the relative hydraulic conductivity at each inner time step. The previously constructed flow solver was smoothly

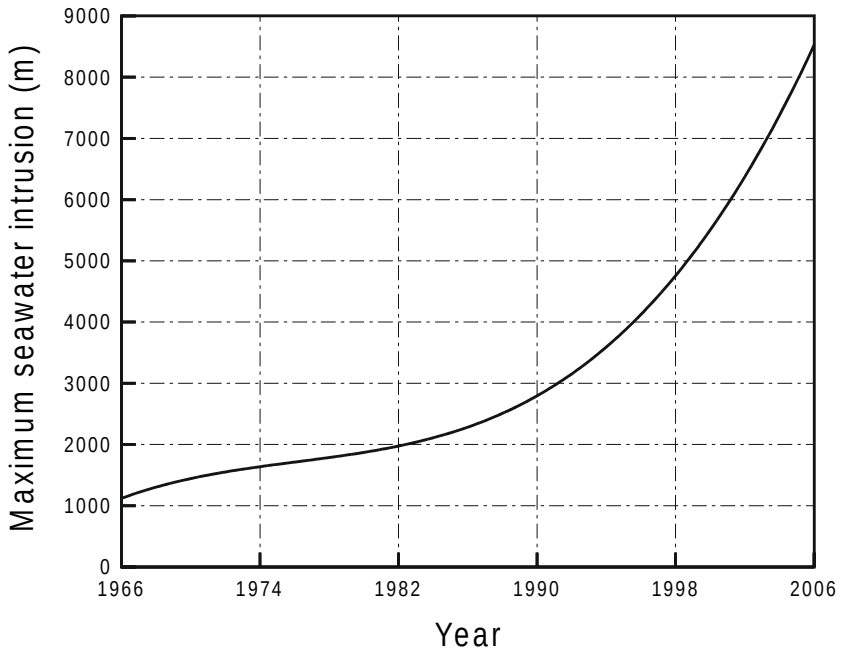

Figure 5.31:AMaximumwinterface toe position of the movingwfresh-saltwater interfacew versuswtime,wthewgraphwshowswevidencewofwoverexploitationwofwthewaquiferwduringwthew nineties.w

implemented in the new model, without further costs, which is a proof for itsA strength and robustness.A

comprehensive set of 5 test problems is provided for validating the numer-A icalAmodel.AThese AexamplesAaccountAforAvariousAanalyticalAsolutions, numericalA results from other models, and measurements performed on a laboratory sand boxA model. Moreover, several types of aquifers were investigated, includingAconfined, unconfined and multilayer aquifer systems.ASeveral kind of boundary conditionsA were tested according to the type of solutions.A ll these tests yield satisfactoryA results regarding the scope of the application, and model specific situation forA each test.A

Finally, a model was set up for the aquifer system of Martil situated in Mo-A rocco usingAtheAGEO-SWIM numericalAcode, in orderAtoAstudyAseawaterAintrusionA effectsAnAtermsAof theAshape andAlateralAextension. First a steadyAstateAmodelAwasA

calibrated to obtain adequate model parameters, such as hydraulicA conductivi-A tiesA andA effectiveA recharge, andA theA naturalA situation. AfterwardsA, aA long-termA transient simulation wasA performed to reproduce actual and future situations, with the aim to analyzeA theA riskA toA salinization from the MediterraneanA sea. It isA concluded thatA withoutA furtherA control theA saltwaterA interfaceA would travelA inlandA overA considerableA distancesA inA theA future.A ControlA ofA saltwaterA intrusionA canA beA obtainedA fromA aA numberA ofA strategies.A TheA bestA oneA isA toA restrictA pumpingA butA this might not be possible from economical and social point of view. However, itA is recommended that this should be a future study, for which the present modelA results could be a starting basis. This present Martil mathematical model is be-A ingA improved asA furtherA dataA areA obtainedA from theA fieldA (distributionA ofA pumpingA well rates at present and in the future, infiltration recharge in the irrigated areaA and better water electrical conductivity values measured with the depth in theA observed wells along the coast that reveal seawater intrusion).A

Chapter 6[0]

Finite Element Modeling of Three-Dimensional Transport using M-Matrix Preconditioners and Nonsymmetric Solvers

Contents

6.1 Introduction

Computational modeling of solute transport is undoubtedly one of the most exciting research areas, for many hydrologists and modelers during the last decades. Pioneering work in this field has been presented by Remson et al. (1971), and Pinder and Gray (1977) who introduce successively applications of finite difference and finite element methods to contaminant subsurface hydrology problems. These

[0] Manuscript submitted for review to *Advances in Water Resources* Journal.

methodsAhaveAgainedAwideApopularityAinside theAgroundwaterAcommunity, andAbe-A come available through famous packagesAand models, such asAMOC (KonikowAandA Bredehoeft, 1978), FEMWASTEA(YehAandAWard, 1981), HST3DA(Kipp, 1987)A and MT3D (Zheng, 1990).AHowever, solving an advective dispersive problem isA traditionallyAsubjectAtoAmanyAsourcesAofApossibleAfailure.ATypicalAerrorsAareAen-A counteredAfor a highAPeclet andACourant numbers, yielding numericalAoscillationsA and/or numerical dispersion, overshooting andAundershooting in case of sharpA concentration fronts, which leads to constraints on the grid size and computa-A tional time step. Other sources of errors or a solution breakdown, depend on theA ability of the numerical solver and the chosen preconditioner to converge.A

With the noticed rapid advances in computer technology, computational speedA and efficiency become affordable, and can be fully used to build complex three-A dimensional models for solving practical contamination problems of large size, such numerical approaches yield large, sparse and nonsymmetric linear algebraicA systems.AThe state of the art in nonsymmetric linear solvers is not yet satisfac-A tory when compared to the highly successful preconditioned conjugate gradientA solver for symmetric problems, such as those arising from the discretization ofA the groundwater flow equation.AHowever, the latest achievements accomplishedA in this discipline are encouraging; modern methods are more reliable, computa-A tionallyAefficient, fastAandAhave a smooth convergenceAbehavior. TheseAtechniquesA knownAasAconjugateAgradient likeAor KrylovAbasedAmethods areAbecomingAincreas-A inglyApopularAinAdealingAwithAnonsymmetricAlinearAsystems. InAthisAclassAof meth-A odsAtheAbiconjugateAgradientAstabilizedAsolverA(BICGSTAB)ApresentedAbyAVanA der Vorst (1992) is reputed to be the most efficient with respect to the trade-offA betweenAstorage and convergence speed. Pini and Putti (1994) reported that theA methodAasAsuperiorAin solvingAfiniteAelement discretizationsAof the two-dimensionalA advectionAdispersionAequation.AGambolatiAetAal.A(1995)AappliedAtheAmethodAtoA solve the partial differential equation of a dual porosity transport model.A

Preconditioning is considered as a key factor in improving the convergenceA

behavior of these solvers, in this study three preconditioning strategies are inves-
tigated in terms of efficiency and computational speed, diagonal scaling (DS) is
the simplest and made always possible by construction. Incomplete factorization
(IF0) which is reputed to be efficient (Larabi and De Smedt, 1994), but can fail
for non M type of matrices. M matrix transformation is then proposed on the
general transport matrix to allow for the IF0 preconditioner existence (De Smedt
and Sbai, 1998). This transformation proves to be very easy to implement and
robust. Its computational efficiency is dependent on the solver used in conjunc-
tion (Sbai and De Smedt, 1997), but in all chosen test problems this scheme is
the most performing.

This paper starts with a brief review of the finite element scheme used in the
presented model to discretize the general three-dimensional advection dispersion
equation. Next, the theory of conjugate gradient like methods for the solution
of nonsymmetric linear systems is highlighted, and algorithms such as minimal
residual (MR) and BICGSTAB methods with some preconditioning strategies are
presented. A comparison between these solvers is performed by test problems,
using preconditioning by three schemes: DS, IF0, and modified incomplete fac-
torization (MIF0).

6.2 Theory

6.2.1 Governing Equations

The equation governing the transient movement of a reactive chemical solute
in three-dimensional groundwater flow systems, taking into account the advec-
tion and dispersion processes, as well as adsorption, first order degradation of
chemicals, and source and sink terms is given by Zheng and Bennett (1995)

$$\frac{\partial}{\partial t}(\theta C + \rho S) = \nabla(\theta \mathbf{D} \nabla C) - \nabla(\mathbf{q} C) - \lambda(\theta C + \rho S) + R_c \qquad (6.1)$$

where θ is the soil moisture content, C is the dissolved concentration [ML^{-3}], ρ is the bulk soil density [ML^{-3}], S is the adsorbed concentration of the solute [M/M], t is time [T^{-1}], $\mathbf{D}$ is the hydrodynamic dispersion tensor [L^2T^{-1}], $\mathbf{q}$ is the groundwater flux vector [LT^{-1}], λ is the first order decay coefficient, R_c is an external source/sink rate term [$MT^{-1}L^{-3}$], and ∇ is the del operator [L^{-1}]. The left hand side of equation (6.1) represents the rate of mass accumulation over a differential volume. In the right hand side, the first term represents the net rate of mass flux due to dispersion and diffusion, the second is the net mass flux due to advection, the third is the degradation rate of the chemical species, and the last term is a source/sink term corresponding to artificial injection and/or withdrawal.

linear isotherm adsorption model is used to couple the concentrations in the aqueous and adsorbed phases, and may be formulated by

$$S = K_d C \tag{6.2}$$

where K_d is the adsorption distribution coefficient [L^3M^{-1}].

Combining equations (6.1) and (6.2) yields a linear partial differential equation as expressed below

$$R\,\frac{\partial C}{\partial t} = \nabla(\mathbf{D}\nabla C) - \nabla(\mathbf{v}C) - \lambda RC + \frac{R_c}{\theta} \tag{6.3}$$

where $R = 1 + \frac{\rho}{\theta} K_d$ is the retardation factor, and $\mathbf{v} = \frac{\mathbf{q}}{\theta}$ is the groundwater seepage velocity [LT^{-1}]. The dispersivity tensor $\mathbf{D}$ includes diffusion coefficient D_0 [L^2T^{-1}], and dispersivity coefficients α_L, α_{Th} and α_{Tv}, respectively the longitudinal dispersivity, the transverse horizontal and vertical dispersivities [L], which multiplied by the different velocity components yield the mechanical dispersion as discussed by Bear (1972).

The groundwater velocity vector is retrieved from a previously computed potential head distribution as

$$\mathbf{v} = -\frac{\mathbf{K}}{\theta}\nabla h \tag{6.4}$$

where $\mathbf{K}$ is the hydraulic conductivity tensor [LT^{-1}], and h is the hydraulic head [L], which is obtained from the solution of the governing equation for the three-dimensional steady state groundwater flow

$$\nabla(\mathbf{K}\nabla h) + Q_h = 0 \quad (6.5)$$

where Q_h is a source/sink flow rate term [LT^{-1}].

Solving equation (6.3) for a well posed initial value problem, requires a prior definition of initial and boundary conditions in the domain being under study.

6.2.2 Initial and Boundary Conditions

Initially, a spatial concentration distribution is known such that

$$C(\mathbf{x}, 0) = C_0(\mathbf{x}) \quad (6.6)$$

where $\mathbf{x} = (x, y, z)$ is the vector position, and C_0 is the initial distribution of concentrations.

Generally, there are three types of conditions used in solute transport models:

(a) Prescribed concentrations, or first type Dirichlet boundary condition

$$C(\mathbf{x}, t)|_{S_D} = C_D(\mathbf{x}, t) \quad t > 0 \quad (6.7)$$

where C_D is a source distribution function specified along the Dirichlet boundary S_D

(b) Fixed dispersive flux, or second type Neuman boundary condition

$$-\theta\mathbf{D}\nabla C|_{S_N} = q_c(\mathbf{x}, t) \quad t > 0 \quad (6.8)$$

where q_c is the solute flux specified along the boundary S_N that is considered impervious for water ($q = 0$)

(c) Fixed total flux, or mixed type, or third type Cauchy boundary condition

$$-\theta\mathbf{D}\nabla C + \mathbf{q}C|_{S_C} = q_c(\mathbf{x}, t) \quad t > 0 \quad (6.9)$$

where q_c is the solute flux specified along the Cauchy boundary S_C.

6.3y Numericaly Modely

6.3.1 They Conformingy Finitey Elementy Methody

Equation (6.3) subject to initial and boundary conditions (eqns 6.6 to 6.9) can be solved numerically with the standard Galerkin weighted residual finite element method (FEM), referred also as the conforming FEM in the literature, and with a fully implicit finite difference time stepping scheme. The finite elements used in this study are isoparametric hexahedral elements. The principle of the method is to subdivide the domain into a given number of conveniently small elements sharing a given number of nodes at their corners. A trial solution is given by interpolating the dependent variable from the corresponding values at the nodal points, using nodal basis functions, such that the approximate solution over the domain becomes

$$\widehat{C} = \sum_{j=14}^{n} C_j b_j \qquad (6.10)$$

where n is the total number of nodes, and b_j is the trilinear basis function associated to node j. To fulfill the weighted residual FE approach, residuals resulting by substitution of equation (6.10) into equation (6.3) are minimized by making them orthogonal to the basis functions, yielding a linear system of algebraic equations at time $t + \Delta t$ ($t \geq 0$), which can be written in matrix form as

$$([\mathbf{Q}] + \frac{1}{\Delta t}[\mathbf{M}])\{\mathbf{C}\}^{t+\Delta t} = \{\mathbf{B}\} + \frac{1}{\Delta t}[\mathbf{M}]\{\mathbf{C}\}^{t} \qquad (6.11)$$

where $[\mathbf{M}]$ is the mass transport matrix, $\{\mathbf{C}\}^{t+\Delta t}$ is the vector of unknown concentrations, $[\mathbf{Q}]$ is the transport matrix, and $\{\mathbf{B}\}$ represents the external effects on the domain namely the boundary conditions and eventual sources and/or sinks. The entries of the given matrices and vectors are

$$M_{ij} = \int R b_i b_j \, dV \qquad (6.12)$$

$$Q_{ij} = \int \nabla b_i (\mathbf{D} \nabla b_j - \mathbf{v} b_j) dV + \int \lambda R b_i b_j dV \qquad (6.13)$$

$$B_i = \int b_i \frac{R_c}{\theta} dV - \int b_i \frac{q_c}{\theta} dS \qquad (6.14)$$

The matrix $\mathbf{G} = \mathbf{Q} + \frac{\mathbf{M}}{\Delta t}$ arising from this FE formulation is highly sparse. It is therefore suitable to use a compact vector form by storing separately the upper and lower triangular parts of the Croute $\mathbf{LU}$ decomposition of $\mathbf{G}$. It is obsolete from (6.13) that the $\mathbf{Q}$ matrix is non symmetrical, a property which restricts the choice of suitable solvers. Indeed, preconditioned conjugate gradient methods which are highly efficient for solving linear symmetric and positive definite systems arising from the groundwater flow equations (Larabi and De Smedt, 1994) cannot be applied.

6.3.2 Iterative Solvers

During the last two decades methods which are specifically developed for solving linear nonsymmetric systems have attracted the intention of many researchers. Efforts were spent on porting the successfulness of the conjugate gradient methods (CG) for solving linear asymmetric systems to the class of nonsymmetric and indefinite systems; these methods are so-called Krylov projection type methods. The literature devoted to this topic is rather huge, and the proposed algorithms can be classified as either orthogonal residual (OR) or minimal residual (MR) based methods (Sleijpen and Van der Vorst, 1993; Barret et al., 1994; Gambolati et al., 1995).

Among the existing up to date MR solvers, the generalized minimal residual method (GMRES) proposed by Saad and Schultz (1986) is successful for solving this kind of problems as noted by Pini and Zilli (1990). The major drawback of the method is the increasing number of vectors and related storage required for each iteration step. GMRES(m) algorithms are therefore constructed in such way that the linear iterations are restarted after m steps. The choice of m is also

a delicate problem since determining an optimal value still relies on the modelerA experience, which needs typically several runs for tuning up this parameter forA eachAspecificAproblem.AThus, theAmethodAisAnotAuserAfriendly, andAespeciallyA cumbersome for large three-dimensional systems.AIn this paper we use the mostA simpleAandAlowestAcostAMRAbasedAmethod.ATheApreconditionedAMRAmethodAisA presented below whereA**P**yis the preconditioning matrix, as explained laterA

Table 6.1:A*TheypreconditionedyMinimumyResidualyiterativeymethody(Barretyetyal.,y 1994).y*

Calculate r$_{04}$=A**b** − **G**$C_{04}$from the initial guessAC_{04}
Fory$i = 1, 2, ...$ until convergenceA
SolveAz fromA**P**z =Ar
α_i =A$\frac{r_i^T \mathbf{G}z_i}{\| \mathbf{G}z_i \|^{25}}$
C_i =AC_{i-14}+ $\alpha_i z_{id}$
r_i =Ar_{i-14}+ α_i **G**z_{id}
End Fory

The biconjugate gradient method (BCG) introduced by Lanczos (1952) wasA considered as a first natural extension of the three-term short recurrences biorthog-A onalAalgorithms, requiringAlessAstorage and computationalAworkAperAiterationAstep.A However, an erratic convergence behavior or an eventual breakdown can be ob-A served for ill-conditioned systems. The explicit use ofA**G**^{T} in the algorithm makeA it also inappropriate to use for many practical applications.ATo overcome theseA limitations the conjugate gradient squared method (CGS) has been developedA by Sonneveld (1989).AThe method is quite competitive, because it preserves theA low cost per iteration and avoids the multiplication with the matrixA**G**^{T}. It isA A reported that the method converges two times faster than BCG whenever thisA one converges, but asAnotedAby Van der VorstA(1992)AitsAconvergenceAbehavior canA beAworseAthanABCGAdueAtoAlocalAinstabilitiesAresultingAin failure. TheAbiconjugateA

gradient stabilized method was proposed as a smoother variant of CGS, but the convergence can still oscillate remarkably for difficult problems having complex eigenvalues with big imaginary parts as noticed by Sleijpen and Fokkema (1993) and later by Pini and Putti (1994). The preconditioned BICGSTAB seems to be the most attractive OR method with respect to computer storage and convergence speed. Below, are depicted the iterative steps involved in the preconditioned BICGSTAB method, where $\mathbf{P}y$ is again a preconditioning matrix.

Table 6.2: *The preconditioned BiCGSTAB iterative method (Barret et al., 1994).*

Calculate $r_{04} = b - \mathbf{G}C_{04}$ from the initial guess C_{04}
Choose an arbitrary vector $\tilde{r}_{04}$ such that $\tilde{r}_{04}^T r_{04} \neq 0$ (e.g. $\tilde{r}_{04} = r_0$)
Initialize the iterative parameters:
$\rho_{04} = \alpha = v_{04} = 1$
$p_{04} = v_{04} = 0$
For $i = 1, 2, ...$ until convergence
$\rho_i = \tilde{r}_{04}^T r_{i-1}$
$\beta = (\rho_i / \rho_{i-1})(\alpha / \omega_{i-1})$
$p_i = r_{i-14} + \beta(p_{i-14} - \omega_{i-1} v_{i-1})$
solve y from $\mathbf{P}y = p_i$
$\alpha = \rho_i / r_{04}^T v_i$
$s = r_{i-14} - \alpha v_i$
solve z from $\mathbf{P}z = s$
$t = \mathbf{G}zS$
$\omega_i = s^T t / t^T t$
$C_i = C_{i-14} + \alpha y + \omega_i z$
$r_i = s - \omega_i t$
End For

Gutknecht (1993) has refined this algorithm for the case of complex eigenvalues, which leads to better convergence behavior. He showed that the later is a combination of BCG and GMRES(2). This point of view was generalized by Sleijpen and Fokkema (1993) who describe how to derive a BICGSTAB variant of order l: BICGSTAB(l), and give a practical implementations for low orders.

ThisAisAusuallyAusedAasAanAalternativeAwheneverABICGSTABAstagnatesAorAfailsA toAconverge.AHowever, highAorderAvariantsAincreasinglyArequireAmoreAworkAperA iteration.A

6.3.3y PreconditioningyMethodsy

Preconditioning is a key factor to the successfulness of any iterative solver, espe-A cially when dealing with practical applications of large size. The state of the artA isAstillAnotAsatisfactory, because muchAeffortAwasAgiven forAdevelopingAmoreArobustA solvers at a first stage.AThe idea behind it is to transform the original system ofA equations by multiplying withA$\mathbf{P}^{-1}$, such that the new system is easier to solve, which implies that the preconditioning matrixA$\mathbf{P}$yshould resembleA$\mathbf{G}$yas close asA possible.A goodApreconditionerAproducesAenoughAgainAinAconvergenceArateAtoA overcomeAtheAextraAcostArelatedAtoAitsAownAconstruction.AForAaAmoreAdetailedA discussion in this subject we refer to Barret et al.A(1994).A

Three preconditioning schemes were implemented in this study to seek theA performance of the selected solvers:A

1.ADiagonal scaling (DS):A$\mathbf{P}$y=A$diag[\mathbf{G}]$, point Jacobi preconditioning is theA easiestAtoAimplement since there is no extraAstorageAbeyond that ofA$\mathbf{G}$. One A canAnoticeAtheAunconditionalAexistenceAofAthisAtransformation.AByAscalingA the original matrix the spectrum becomes smaller, and thus the convergenceA rateAisAimproved. Unfortunately, in manyAtestAcases, itAisAobservedAthatAthisA preconditionerAdoes notAdrasticallyAimproveAtheAsolverAperformance, andA the convergenceAmight beAslow.A moreApowerfulApreconditioningAscheme isA therefore needed for such problems.A

2.APoint incompleteAfactorizationAofAorderAzeroA(IF0): theApreconditioningAma-A trix isAoftenAformulatedAin theAformA$\mathbf{P}$y= $(\mathbf{L}+\mathbf{D})\mathbf{D}^{-1}(\mathbf{D}+\mathbf{U})$, whereA$\mathbf{L}$yandA $\mathbf{U}$yare respectively the strictly triangular lower and upper parts ofA$\mathbf{G}$, and A $\mathbf{D}$yis a positive diagonal matrix, such thatA$diag[\mathbf{P}] = diag[\mathbf{G}]$. The essenceA

of the method is to prohibit fill-in positions where $g_{ij} = 0$ during the factorization. Meaning that, $\mathbf{L}_y$ and $\mathbf{U}_y$ have the same sparsity pattern as $\mathbf{G}$. An attractive feature of the method as to its reasonable construction cost since only $\mathbf{D}_y$ diagonals are needed and no other extra storage is required. The entries of $\mathbf{D}_y$ can be computed recursively

$$D_{ii} = G_{ii} - \sum_{k=1}^{i-1} \frac{G_{ik}\, G_{ki}}{D_{kk}} \tag{6.15}$$

3. Point modified incomplete factorization of order zero (MIF0): $\mathbf{P}_y$ has the same form as an IF0 except that $\mathbf{D}_y$ is constructed in such way as to preserve the row sum constant, the entries of $\mathbf{D}_y$ are computed in this case as

$$D_{ii} = G_{ii} - \sum_{k=1}^{i-1} \sum_{j=k+1}^{n} \frac{G_{ik}\, G_{jk}}{D_{kk}} \tag{6.16}$$

For a more practical implementation the entries of D are calculated as (Beauwens, 1990)

$$U_i = \sum_{j=1}^{n} G_{ij} - \sum_{k=1}^{i-1} \frac{G_{ik}\, U_k}{D_{kk}} \tag{6.17a}$$

$$D_{ii} = U_i - \sum_{k=i+1}^{n} G_{ki} \tag{6.17b}$$

The preconditioners IF0 and MIF0 only work when the obtained diagonals are positive, and it turns out that there are cases for which IF0 and MIF0 are not guaranteed to exist. Meijerink and Van der Vorst (1977) proved that preconditioning by IF0 is possible only if $\mathbf{G}_y$ satisfies the requirements of an M matrix ($G_{ii} > 0$, and $G_{ij} < 0$ for $i \neq j$, and $\mathbf{G}_y$ is non singular). However, for MIF0 the existence is even not guaranteed, Beauwens and Quenon (1976) noticed that such factorization exists for diagonally dominant matrices. Hence, for many practical applications these kind of methods may fail. To overcome this drawback we suggest the use of the following M matrix approximation $\mathbf{G}_M$ of $\mathbf{G}$, such that

$$(G_M)_{ij} = \min(G_{ij}, 0) \tag{6.18}$$

$$(G_M)_{ii} = \sum_{j=1}^{n} max(G_{ij}, 0) \tag{6.19}$$

Practically, the global matrix is lumped by moving positive off-diagonals to the diagonal position while keeping negative off-diagonals, such that row sums are kept constant. The proposed method was successfully used by Larabi and De Smedt (1994) to solve linear systems stemming from three dimensional hexahedral finite element discretizations of the steady state groundwater flow equation. The previously presented algorithms and preconditioners are efficiently implemented in a user friendly numerical tool kit, which is integrated to GEO-PROF numerical code (De Smedt, 1996).

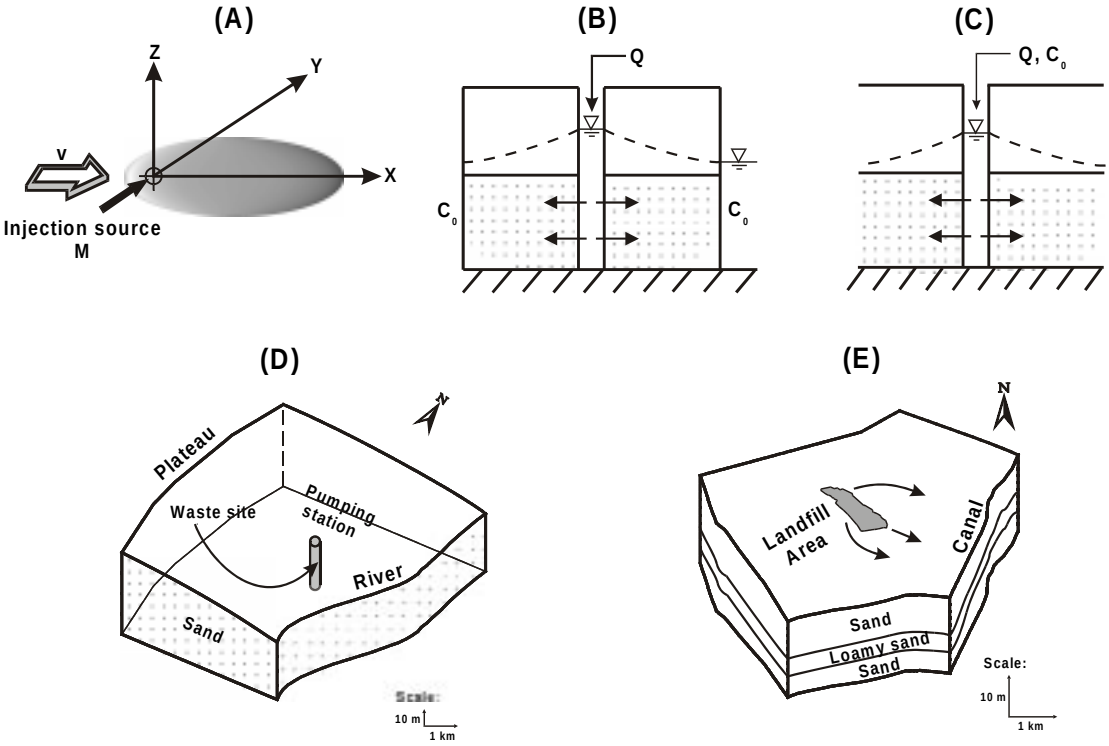

Figure 6.1: Schematic representation of the test problems; (A) Injection in a uniform flow field; (B) Radial injection with equilibrium counter dispersion; (C) Radial injection; (D) Field problem 1; and (E) Field problem 2.

6.4 Results and Discussion

Five test problems are selected to investigate the solvers and preconditioners performance. These examples include 3 theoretical and 2 field applications illustrating a diversity of physical situations as shown in Fig. 6.1. Table 6.3 shows several of the numerical features of the studied examples, as the total number of nodes and elements used in the problem discretization, the shape of the elements, the degree of sparsity of the G-y matrix, the maximum Peclet and Courant numbers, and if the M matrix requirement is satisfied or not. Additionally, physical parameters of the test problems used to run the models are given in Table 6.4. The numerical results are obtained by executing the numerical models on a Sun UltraSparc 2 desktop workstation. For each test problem, the tolerance related to the convergence stopping criterion (sum of squared residuals) is denoted by *tol* parameter, this is either previously specified or determined automatically by an internal routine implemented in the models. The obtained results in terms of total number of iterations required to achieve the convergence criterion, and the used CPU calculation time are also checked.

In the remainder we denote by I the solution procedure without preconditioning, and by ILUF0-M and MILUF0-M the incomplete factorization preconditioners with M matrix transformation, as proposed in equations 6.18 and 6.19.

Table 6.3: *Numerical features of the test problems.*

Test No.	No. of nodes	No. of elements	Element shape	Degree of G Sparsity (%)	M matrix	Pe	Cr
1a	50000	54756	box	99.97	Yes	4	-
1b	50000	54756	irregular	99.97	No	4	-
2a	672	300	wedge	99.98	No	1	-
2b	6432	3000	wedge	99.98	No	2	-
3	1608	600	wedge	99.98	No	1	5
4	21000	16284	irregular	99.94	No	37	-
5	77964	69696	irregular	99.93	No	48	-

Table 6.4:A*Physicalyparametersyofytheytestyproblems.g*

PHYSICAL PARAMETERS	TEST PROBLEMS						
	1	2	3	4	5		
					Layer 1 !	Layer 2 !	Layer 3 !
K!(m/d)!	10!	5!	10!	12!	3.4	0.5!	3.1!
α_L (m)!	5!	5!	0.1	100!	20!	20!	20!
α_{Th} (m)!	0.5!	5!	0.1	33	5!	5!	5!
α_{Tv} (m)!	0.5!	5!	0.1!	0.33!	0.5!	0.5!	0.5!
$D_{04}(m^2/d)$!	0	0!	0!	10^-	0	0	0!
n	0.25!	0.35!	0.387!	0.25!	0.3!	0.45!	0.3!

6.4.1 TestyProblemy1:y ContinuousyPointyInjectionyinyay UniformyFlow Fieldy

The first test example is based on an available three-dimensional analytical so-A lution from Hunt (1978) for steady state solute transport in a uniform flow fieldA from a continuous point injection source, and given byA

$$C = \frac{M}{8\pi nRD_T}\exp\left(\frac{vx}{2D_L}\right)\left[\exp\left(\frac{-Rv}{2D_L}\right)\operatorname{erfc}\left(\frac{R-vt}{2\sqrt{D_L t}}\right) + \exp\left(\frac{Rv}{2D_L}\right)\operatorname{erfc}\left(\frac{R+vt}{2\sqrt{D_L t}}\right)\right] \quad (6.20)$$

whereA$R = \sqrt{x^2 + (y^2 + z^2)\frac{D_L}{D_T}}$ [L], M isAthe massAinjectionArateA[MT^{-1}], v isAtheA uniform groundwater flow velocity [LT^{-1}] along the longitudinalAdistanceAx, D_L andAD_T are the longitudinal and transverse dispersion coefficients respectivelyA [L^2T^{-1}], and erfc is the complementary error function.A

In the present test example the pollution plume is simulated for a constantA groundwaterAvelocityAofA$0.5m/d$ and a massAinputArateAofA$1000kg/d$; otherAparam-A etersAareAgiveAinATableA6.4.ATheAmodelAregionAisAreducedAtoAoneAquadrantAwithA the solute source injection point at the origin. Two test runs are conducted withA different meshesAtoAstudyAtheAeffectsAofAtheAMAmatrix transformation. TheAfirstArunA (1a) is done by discretizing the domain into box sized elements of 4x2x2m^3. WhileA in the second test (1b) the previous mesh is modified by adding or substractingA a constant value of $0.5m$ randomly to the coordinates of all interior nodes.ATestA

problem (1a) yields a M matrix, while problem (1b) is non M matrix.7

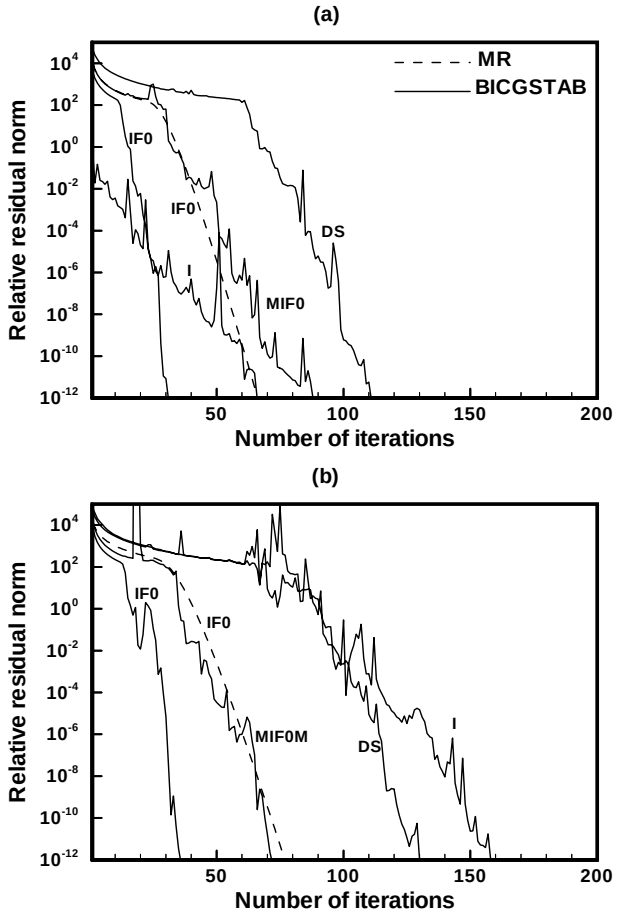

Figure 6.2:AConvergence history analysis of test problems (a) 1a and (b) 1b.w

The obtained results are shown in Table 6.5.AIn the table are indicated:AtheA number of iterations needed to obtain convergence, NI; the total runtime, CPU(s);A the solute mass balance error, MBE expressed in percentage, and the maximumA error between calculatedAand exact concentrations over the hole mesh, excludingA theAinjectionApoint.ATheAhighestAerrorsAareAfoundAatAtheAmodelAboundaries, asA theAanalyticalAsolutionAisAestablishedAassumingAinfiniteAspacialAdimensions.ATheA total mass balance error is somewhat higher for the unpreconditioned methods, nevertheless all are satisfactory.

All algorithms except MIF0 converge for test problem 1a, and an M type ofA

transformation is unnecessary. Obviously, the MR method preconditioned with IF0 is the fastest, although more iterations are needed compared to BICGSTAB. For the other preconditioners BICGSTAB is the fastest. The convergence behavior of the different solvers is illustrated in Fig. 6.2(a). Obviously, IF0 enables a steady decrease in the relative residual norm. The same convergence behavior was observed for the second run 1b, as can be concluded from Fig. 6.2(b). For this case, the IF0 preconditioner unexpectedly exists, and turns out to be the most efficient solver, while M transformation requires a little less iterations but somewhat more execution time.

6.4.2 Test Problem 2: Steady State Transport in a Radial Flow Field with Counter Dispersion

recharge well is injecting clean water in an initially polluted aquifer. A fixed concentration boundary condition is imposed at a distance R from the well, such that steady state advection and dispersion act in inverse directions. By neglecting sorption and decay mechanisms, the steady state transport equation simplifies to

$$\frac{\partial^2 C}{\partial \rho^{24}} = \frac{\partial C}{\partial \rho S} \tag{6.21}$$

where $\rho = \frac{rS}{\alpha_L}$, and r is the radial coordinate $[L]$. Equation 6.21 is easily solved for the boundary condition

$$C = C_{04} \qquad \text{at } r = R \tag{6.22}$$

such that

$$\frac{C}{C_{04}} = \exp\left(\frac{r - R}{\alpha_r}\right) \tag{6.23}$$

Assuming a well radius of $0.1m$, a discharge rate of $15m^3/d$, a radius R of $100.1m$, with a unit upstream fixed concentration, i.e. $C_{04} = 1$, this problem is solved

Table 6.5:A*Solveryperformancesforytheyfirstytestyproblem.g*

Test	Solver	Preconditioner	NI	CPU(s)	MBE	Error
(a)!	MR!	I!	1025!	696.2!	1.17!	1.467!
		DS!	799!	369.5!	0.85!	1.467!
		IF0!	67!	64.6!	0.15!	1.467!
		MIF0!	*!	*!	*!	*!
		IF0-M!	–!	–!	–!	–!
		MIF0-M!	–A	–A	–!	–!
	BICGSTAB!	I!	144	111!	0.27!	1.467!
		DS!	138.7!	133.9!	0.05!	1.467!
		IF0!	31!	74.3!	0.14	1.467!
		MIF0!	*!	*!	*!	*!
		IF0-M!	–!	–!	–!	–!
		MIF0-M!	–!	–!	–!	–!
(b)!	MR!	I!	960!	665.6!	1.02!	
		DS!	735!	359.5!	0.65!	
		IF0!	77!	63.45!	0.11!	
		MIF0!	*!	*!	*!	*!
		IF0-M!	73!	64	0.12!	
		MIF0-M!	460!	448.6!	0.54	
	BICGSTAB!	I!	159!	142.3!	0.21!	
		DS!	129!	155.6!	0.03!	
		IF0!	36!	83.4	0.09!	
		MIF0!	*!	*!	*!	*!
		IF0-M!	38!	90.9!	0.07!	
		MIF0-M!	72!	309.5!	0.05!	
–!Solver!not!executed!						
*!Residual!stagnates!before!maximum!number!of!iterations!(10000)!was!reached!						

using aA$\frac{\pi}{4}$Awedge andAadopting two mesh configurations. Test runs (2a)Aand (2b)A use respectively 21x16x2 andA201x16x2 nodes along a three-dimensional radialA coordinate system. For test run (2a) the spacing along the radial axis is $5m$ andA forA(2b) itAisA$3m$ exceptAforA$30m$ aroundAthe well centerAwhereAthe nodalApositionsA follow an exponential sequence in incremental order starting form $0.045m$ at theA well.A

For the first run with the coarse mesh and using a tolerance of 10^{-124}all pre-A conditioned algorithms perform very well and need very few iterations to convergeA

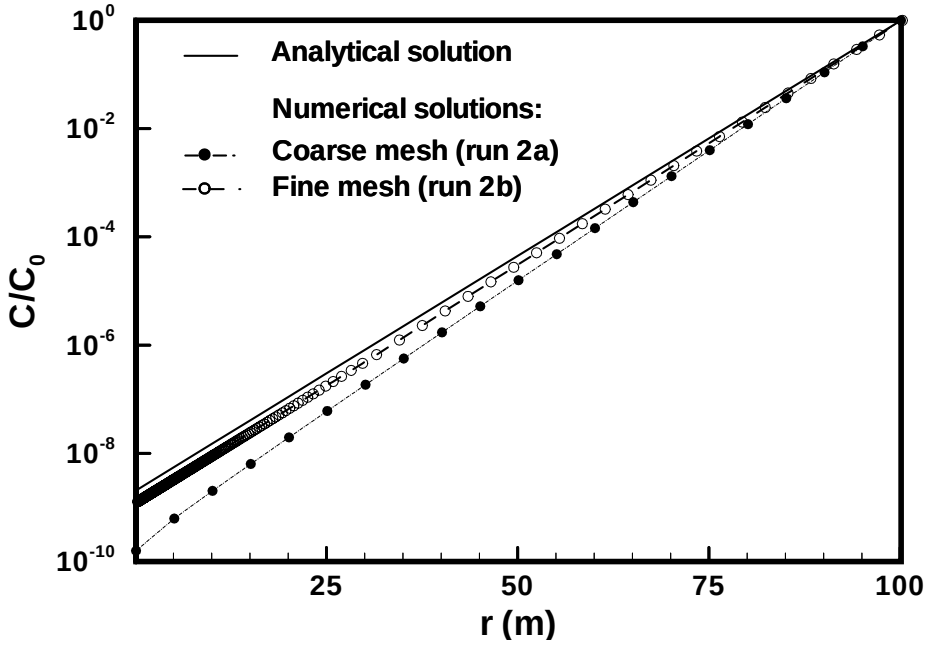

Figure 6.3: Comparison of analytical and numerical solutions of normalized concentration versus radial distance for test examples 2a and 2b.

as shown in Fig. 6.4(a). Surprisingly, the obtained numerical results are not very accurate as demonstrated by the comparison versus analytical results shown in Fig. 6.3. Especially close to the well, the computed results deviate noticeably; this lack of accuracy results from the fact that the advective component of the solute transport is very important in this region, such that element velocities need to be approximated more accurately.

For the second run the different solvers and preconditioners are tested with the fine mesh and severe convergence criteria ($tol = 10^{-30}$). The performance of the different solvers are presented in Table 6.6, showing that all MR based methods fail to converge; in this case the iterative process either stagnates, as for DS, IF0 and IF0-M, or eventually breaks down as for MIF0 and MIF0-M. The same convergence behavior is observed for the BICGSTAB based methods, except for IF0 and IF0-M, which are the only successful methods (Fig. 6.4(b)). The error norm over the hole mesh becomes very small, and the obtained results of the

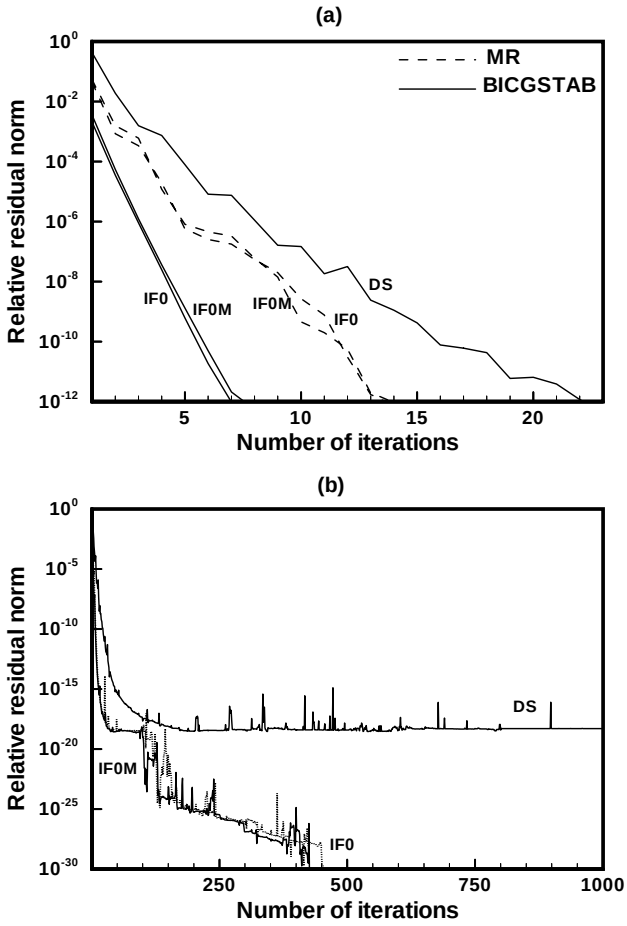

Figure 6.4:AConvergence history analysis of test problems (a) 2a and (b) 2b.w

numericalAsolution are muchAmoreAaccurateAthanAnAtheAfirstArun, asAshown in Fig.A 6.3.AHowever, stillAsomeAdeviationsAwithAtheAexactAsolutionAremain, indicatingA that this seemingly simple problem is rather difficult to solve numerically.A

6.4.3 TestyProblemy3:y TransientyTransportyinyayRadialy Velocity Fieldy

The radialAdispersion problem is typical for describing the movement of a tracer, injected from a recharge well of finite radius. Several authors have analyzed thisA problem by deriving approximate and exact analytical solutions, such as Tang andA

Table 6.6:A*Solveryperformancesyforytestyproblemy2b.g*

Solver	Preconditioner	NI	CPU(s)	Error(10^{-2})
MR!	I!	#!	#!	#!
	DS!	*!	*!	*!
	IF0!	*!	*!	*!
	MIF0!	#!	#!	#!
	IF0-M!	*!	*!	*!
	MIF0-M!	#!	#!	#!
BICGSTAB!	I!	#!	#!	#!
	DS!	*!	*!	*!
	IF0!	452!	208.35!	1.36!
	MIF0!	#!	#!	#!
	IF0-M!	426!	173.4	1.36!
	MIF0-M!	#!	#!	#!
*!Residual!stagnates!before!maximum!number!of!iterations!(10000)!was!reached! #!Iterations!stopped!when!division!by!zero!was!encountered!				

Babu (1979), Hsieh (1986) and Yates (1988), who gives also additional solutionsA for variable boundary conditions at the well.AThe same problem was also solvedA by Hoopes and Harleman (1967) using a finite difference based model.A

finite element wedge of 600 elements in 3 layers composed of 200 elementsA along theAradialAdirection, with uniform nodalAspacingAofA0.1m isAadopted. ModelA parameters and analytical solution values usedAforAcomparisonApurposeAare takenA fromASegolA(1994).A user-specifiedAtimeAstep of 0.01day is used for computing theA solution atA$t = 0.1$ and 1day.ACorresponding numerical and analytical solutionsA -in terms ofAC/C_{04}versus radialAdistance- are plotted in Fig. 6.5 showing a fairlyA good agreement.A fixed tolerance of $10^{-54}$was used to obtain these results.

All test runs except BICGSTAB preconditioned with IF0-M fail to converge.A The solution obtained with BICGSTAB is computed in about 547.3 CPU sAandA 439AtotalAnumberAofAiterations.A llAotherAsolversAexhibitAaAtypicalAoscillatoryA convergence behaviorAin time which fails to converge before the maximum numberA ofAallowedAiterationsA10000AisAreached.A Hence, alsoAthisAtestAproblemAisAveryA difficult to solve numerically.A

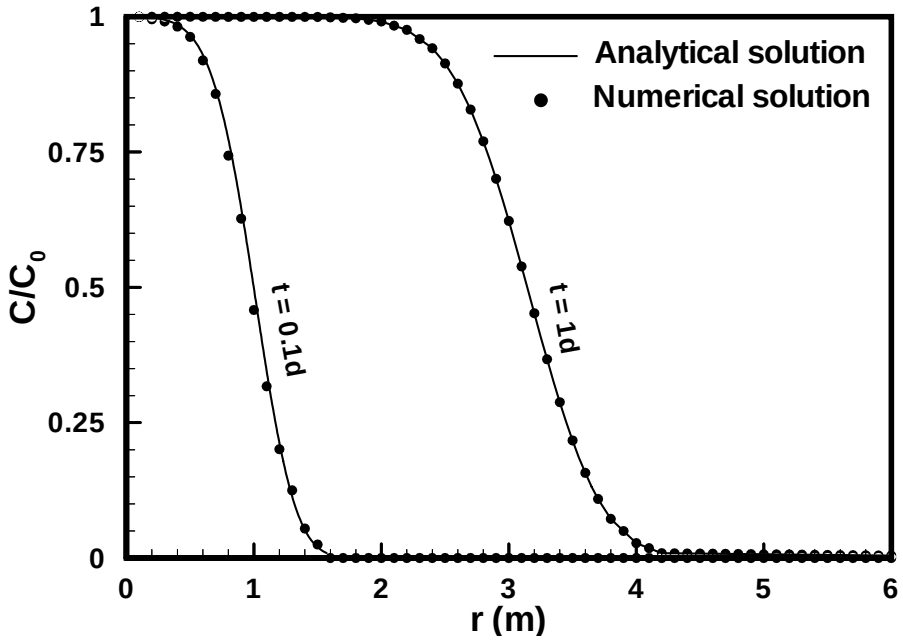

Figure 6.5:AComparison of analytical and numerical solutions of normalized concen-w trationwversuswradialwdistancewforwtestwexamplew3.wOutputswarewplottedwatwtimewlevelw 0.1day and 1day.w

6.4.4y TestyProblemy4:yFirstyFieldyExampley

The objective of this field application study is to predict the possible contami-A nationAofAaAwellAfromAaAnearbyAwasteAdisposalAsite.ATheAwaterAabstractionArateA at the groundwater pumping station equals $12000m^3/d$ and a pollution injectionA rate of $100kg/d$ is infiltrating from the waste site as depicted inAFig. 6.1(d). TheA velocity fieldAis obtained by solving the groundwaterAequation by an adaptiveA moving mesh procedure such that only the saturated part of the domain is con-A sidered. TheAwater table position fits exactly with the iteratively adjusted upperA meshAlayer asAshown inAFig. 6.6(a), whereAalsoAso-potential surfaces andAvelocityA vectors at theAwater tableAareAshown, clearlyAindicating theAradialAconvergent flowA nearby the well.AThe element velocity extrema is found to be equal to $6.17m/d$ near the well location, which results in a high Peclet number of approximatelyA 37 for this problem.ATest runs are performed for the steady state transport sit-A

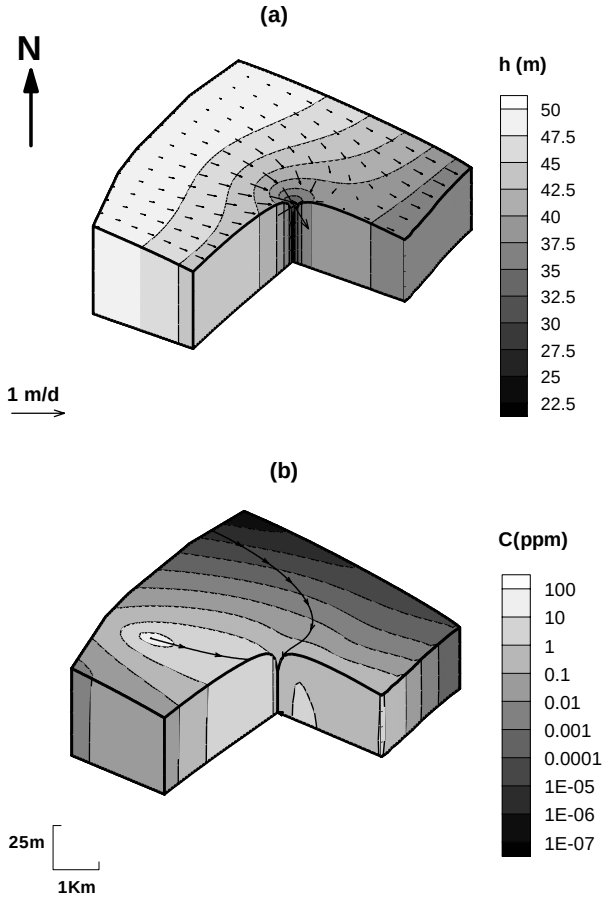

Figure 6.6: Simulated steady state (a) potentials, water flow velocities, and (b) concentration iso-surfaces for test problem 4.

uation, and solver performances corresponding to $tol = 10^{-12}$ are presented in Table 6.7. Most solvers fail, except when DS preconditioned or M matrix preconditioned. The successful preconditioned MR based methods are slow, while the IF0-M preconditioner needs less number of iterations compared to DS. The successful preconditioned BICGSTAB methods show a very important speed-up and less number of iterations. We can also notice the good performance of DS for this problem, but IF0-M is exceptionally good, while MIF0-M has a poor performance in comparison. As an illustration, numerical results are visualized in Fig. 6.6(b), with iso-concentration surfaces, showing the extent of the pollution

plume at steady state.

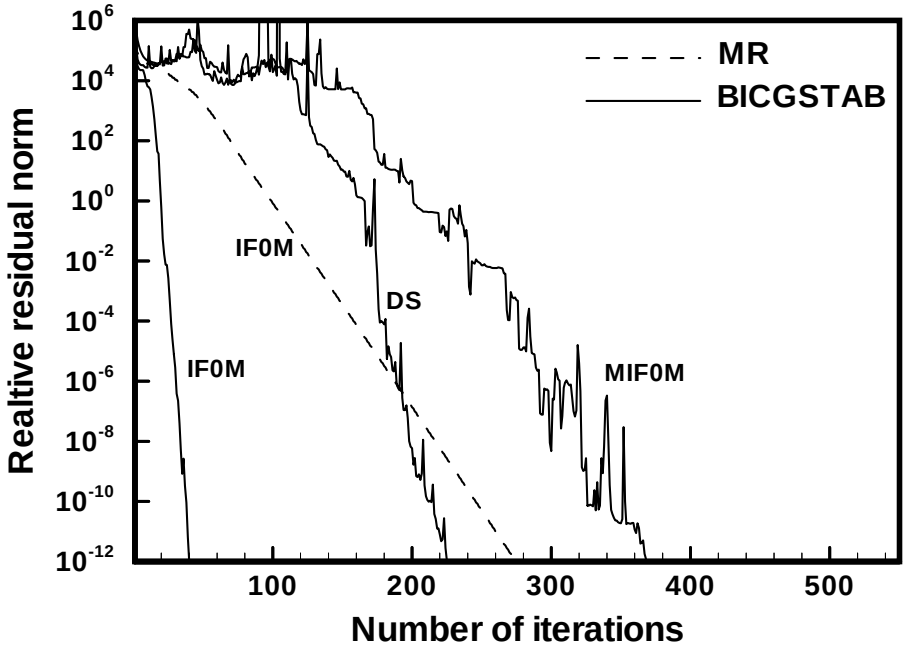

Figure 6.7:AConvergence history analysis of test problem 4.w

6.4.5y TestyProblemy5:ySecondyFieldyExampley

The pollutant transport from a landfill area of irregular geometry is studied inA a phreatic aquifer system with three different lithologic layers.AThe landfill is inA contact with the waterAtable, such thatAas a boundary condition the concentrationA at theAwaterAtable areAconsideredAtoAbeAfixed. TheAgroundwater movement passesA through andAunderneath the landfill, flowing to a nearby canal.A lso, recharge isA added to theAaquiferAdiluting theApollution plume. The transportAis calculatedAun-A til steady state is reached.A three-dimensional finite element mesh is designedA consistingAofA73x89x12Anodes.AFig.A6.8AshowsAsimultaneouslyAtheAgroundwaterA heads isolines, and the direction andAmagnitude of the velocity vectors drivingA

Table 6.7:A*Solveryperformancesforytheyforthytestyproblem.g*

Solver	Preconditioner	NI	CPU(s)
MR!	I!	*!	*!
	DS!	542!	141.4
	IF0!	x!	x!
	MIF0!	x!	x!
	IF0-M!	275!	118.2!
	MIF0-M!	*!	*!
BICGSTAB!	I!	*!	*!
	DS!	225!	41!
	IF0!	x!	x!
	MIF0!	x!	x!
	IF0-M!	41!	37.7!
	MIF0-M!	368!	323.6!
*!convergence!not!achieved!after!maximum!number!of!iterations!(10000)!was!reached! x!preconditioner!does!not!exist!			

theAsteadyApollutionAplumeAatAtheAaquiferAbottom.ATheAspecifiedAtoleranceAforA convergence was chosen as$A tol = 10^{-124}$and numerical results are presented inA Table 6.8. Exceptionally, the IF0 preconditioning exists although the problem isA nonAMAmatrix type. TheAmostAimportant findingAsAthatABICGSTABAbased meth-A ods are faster, and that DS shows to be competitive when used in combinationA with a robust solver.A

By comparing all previous results, an immediate conclusion is that the BICGSTABA method is more efficient than MR, because it requires less computational timeA andAisAalwaysAtheAfastest.AForAproblemsA2AandA3AwhereAMRAfailsAwithAallAtheA preconditioners, BICGSTAB is still successful with some of the studied precon-A ditioners.AUnpreconditioned algorithms do not converge except for test problemA 1a, because the elements have a simple and regular geometry such thatAGyiis anA M matrix. WithArespect to theApreconditioners, one can notice thatADS convergesA for all tests except for problem 2bAandA3, but is much slower than IF0. However, DS could be more efficient in massively parallel computers, since it is the onlyA

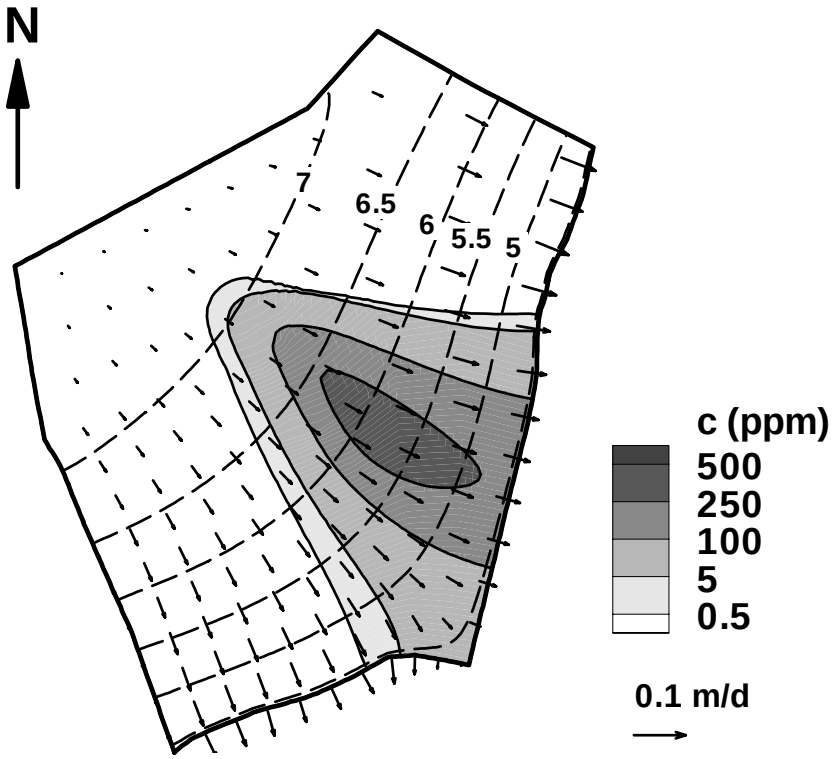

Figure 6.8: An illustrative plan view of the computed head and velocity fields and the pollution plume at the base of the lower aquifer unit.

preconditioner that can be parallelized easily. Also, it is very robust and always exists. Clearly, IF0 and especially IF0-M perform very well, and in combination with BICGSTAB yield the most efficient and fastest solver. MIF0 and MIF0-M preconditioning strategies are less efficient due to the related expensive cost per iteration, this is in agreement with the conclusions obtained by Jacobs (1984) and Larabi and De Smedt (1994) for preconditioned conjugate gradient methods.

The results arising from runs (1a) and (1b) show that the loss of the desirable M matrix property does not affects the rate of convergence of the solvers, and the superiority of each method is preserved. It is also instructive to notice that the MIF0 preconditioner does not exist for test problems 1b, 2b, and 5, but that an IF0 decomposition exists even for a non M matrix. This is not surprising since the M condition is a sufficient but not essential condition for the existence

Table 6.8: *Solver performances for the fifth test problem.*

SOLVER	PRECONDITIONER	NI	CPU(S)	ERROR(10^{-2})
MR	I	*	*	*
	DS	1544	772.2	0.437
	IF0	166	257.5	0.567
	MIF0	x	x	x
	IF0-M	184	288.9	0.597
	MIF0-M	#	#	#
BICGSTAB	I	#	#	#
	DS	106	150.2	1.73
	IF0	35	126.1	0.635
	MIF0	x	x	x
	IF0-M	37	152.9	0.9
	MIF0-M	#	#	#

*! Residual stagnates before maximum number of iterations (10000) was reached!
#! Iterations stopped when division by zero was encountered!
x! preconditioner does not exist!

of the IF0 decomposition (Meijerink and Van der Vorst, 1977). However, in problems having irregular and wedge shaped elements, preconditioning and MA matrix transformation are essential. The BICGSTAB solver preconditioned by IF0-M shows to be the most efficient, and proves to be of value in repeatedly long-term transient simulations, as in case of problem 3. Indeed, in case of the MRA solver, IF0-M and DS are quite comparable, but for BICGSTAB preconditioning by IF0-M results in an important speedup. One can also observe that the repeated oscillatory changes of the residual norm for the BICGSTAB applications becomes less pronounced when preconditioned by IF0, and that MR preconditioned by IF0 has in contrast a smoother convergence behavior, and shows to be competitive. However, for all cases BICGSTAB preconditioned with IF0-M performs always the best.

6.5y Summary

Three-dimensional numerical modeling of pollutant transport in aquifer systemsA by the finite element method leads to large linear systems that are sparse andA nonsymmetric. TheAglobal transport matrix arising from the discretization usingA hexahedral elements does not in general satisfy the requirements of an M ma-A trix, which is a very desirable property with respect to the numerical solutionA procedure.AThe efficiency of preconditioned conjugate gradient like solvers suchA asAMRAandABICGSTABAwasAinvestigated. FiveArepresentative testAexamplesAwereA selected as a basis for this comparison, and several strategiesAwereAdopted to con-A ductAdifferent numerical simulations, based on the implementedApreconditioners, stopping convergence criteria, and solutions benchmarks when an exact solutionA was available.A

Preconditioners as diagonal scaling, incomplete factorization, and modifiedA incompleteAfactorizationAwereAtested. AnAMAmatrix transformationAisAproposedA whichAguaranteesAtheAexistenceAofAincompleteAfactorization, the mostAefficientA preconditionerAsoAfar.ATheAnumberAofAiterations, andACPUAcostAwereAusedAasAaA basis for these comparisons, also a series of benchmarks for all succeeded testsA were performed for problems, which could be solved analytically, to ensure theA accuracy of the obtained results.A

It is found that BICGSTAB preconditioned by incomplete factorization per-A formsAwellAfor allAtestAproblems. However, forAdifficultAproblemsAsuchAfactorizationA is unlikely to exist, and the proposed M matrix transformation proves to be ef-A fective, leading to the guaranteed existence of a robust and efficient solver.A

Chapter 7

Software Development and GUI For Models Support

Contents

7.1 Introduction

In this chapter we shall discuss issues which are more relevant to software engineering development, rather than the models concepts, mode of functioning, and implemented approaches themselves. These aspects are reported herein, because they are valuable tools to support some of the models already discussed in the previous chapters, and take effective role in a number of ways for a model setup, run and analysis.

The following descriptions are restricted to the saltwater intrusion model GEO-SWIM. However, pre and post-processor modules are shared within GEO-PROF numerical code for which the models described in chapter 4 and 6 are the newly implemented pieces, contributed in the framework of this work.

7.2y GeneralyOverviewy

new system for finite element modeling of three-dimensional groundwater flowA andAsaltwaterAintrusionAinAaquiferAsystemsAisAdeveloped.AGEO-SWIMA(Geohy-A drologicalASaltwaterAIntrusionAModel)Ahas several features including flexibility, computationalAefficiency, portability, andAhandling a largeAvarietyAofAphysicalA conditions, makingAitAsuitableAfor a wideArangeAofApracticalAandArealAlife ap-A plications.A SteadyAstateAasAwellAasAtransientAproblemsAcanAbeAinvestigatedAinA three-dimensions, forAheterogeneousAporous media. TheAsoftwareAisAbuildAupAfromA differentAmodules, includingApre-processorAandApost-processorAmodules.AImple-A mented numerical algorithms are efficiently coded to optimize computer storage, memoryAmanagement, andAcomputingAtime.AVisualAsupportAtoAinputAdata, andA output results, is given through an integrated program that interfaces in differ-A ent ways with the simulators, andAotherAdeveloped GUI (GraphicAUser Interface)A tools.A

ModelingAofAgroundwaterAflowAtakingAintoAaccount variationsAinAdensityAisA traditionallyAprerequisiteAwhenAaquiferAsystemsAareAin directAcontact withAtheA sea.AFiniteAdifferenceAandAfiniteAelementAcomputerAcodesAhaveAbeenAdevelopedA for such applications, such as SWIM (Sa da Costa and Wilson, 1979); SUTRA (Voss, 1984);ASHARPA(Essaid, 1990a);AMAGNASA(HuyakornAetAal., 1994Aa,b);A and SIMLAS (Huyakorn et al., 1996).ASharp interface models are yet the mostA common, economicalAandApracticalAforAtheseAtypesAofAsimulations.AMostAofAtheA existing modelsAin this category areAeitherA2DAorAquasi-3DAandAhaveAlimitedAbuilt-A in GUI and visualization capabilities, except for SUTRA, recently supported byA a number of 2D visual routines in Argus ONE (Voss et al., 1997). Driven by theA need for a fully three-dimensional sharp interface model, GEO-SWIM has beenA developedA(SbaiAandADe Smedt, 1998)AincludingApre-processor andApost-processorA packagesAthatAcommunicateAwithAtheAsimulatorsAthroughAinterfaceAcalls.A TheA developed system is highly efficient, simple in use, portable, interactive in a wayA

to provide modular and user-friendly tools to handle separate modeling tasks, and open to other software packages leading in their field.A

7.3y GEO-SWIMyArchitecturey

Before presenting the general structure of the developed software packages, howA they interface and inter-depend, the objectives are discussed first.A

7.3.1 DesignyGoalsy

The following were design goals for GEO-SWIM with their motivation and im-A plications.A

HighyNumerical Performancey

GEO-SWIM takes advantage from latest developments and approaches for solv-A ing the sharp fresh-salt water interface, by avoiding solving the equivalent twoA fluid flow problem.AThis was achieved by transforming the saltwater (and even-A tually the unsaturated) part of the domain, to an equivalent freshwater domainA having the same pressure distribution as in the saltwater domain. Also, numer-A ical difficulties prone to the non-linear discrete Richards equation are handled. Another reason forAsuch numericalArobustnessAisAdueAtoAtheAefficiency and level ofA optimizationAin coding. As an example, an important improvement wasAobservedA when converting many parts of the code from FORTRAN 77 to FORTRAN 90A language, by usingAdynamicAmemoryAallocation, intrinsicAarrayAfunctions, andA modules for organizing data structures, objects and shared variables, and avoid-A ing the use of obsolescent FORTRAN 77 features.A

Portability

GEO-SWIMAwasAdesigned toArun under anyAplatformAandAoperatingAsystem. TheA code was tested on the following systems:A

- Dos/Windows95/98/NT for Intel based PCs,
- UNIX-based Solaris for SUNSPARC workstations,
- UNIX-based IRIX for SGI.A

Numerical models areAported successfully, at no cost. ThereAs only an excep-A tion for Windows based interfaces, because such tools use windows 32-bitAbasedA GUIAandAgraphicAlibraryAcalls, which areAnotAeasilyAported toAotherAenvironments.A

Simple ProgrammingyInterfacey

ItAwasAdecidedAtoAuseA NSIAFORTRANA90AasAaAprimaryAlanguageAtoAdevelopA all packages.AFor instance, all numerical routines used to buildAdifferent modelsA were developed from scratch, making the numerical codeAself-dependent, or onA the other handAindependent of any hardware, compilerAdirective or system specificA library calls.AWe preferred also to keep each program independent of others, toA have a programming layout as simple as possible, which allows a user with anA average programming knowledge, the ability to navigate through and change codeA partsAaccording to hisAspecific need. However, thisAgivesAnowever moreAflexibility, butAlessAsecurity.ABut, accordingAtoAtheApreviousAgoalAthisAwasAallowedAinAthisA release. AnotherAstrategyAis toAlock access to theAuserAtoAprevent possibleAdamageA by providing a set ofA PI (Application Programming Interface) calls to built-inA libraries.AThis issue may be considered in the next release.A

Highly InteractiveyResearchyTooly

RecentlyAdevelopedAGUIAandAgraphicalApackages, aim at providing a highlyAinter-A activeAandAvaluableAresearchAtool.ATheseAprogramsAareAdevelopedAinAaAmodularA way, which implies an easier level of maintenance.A

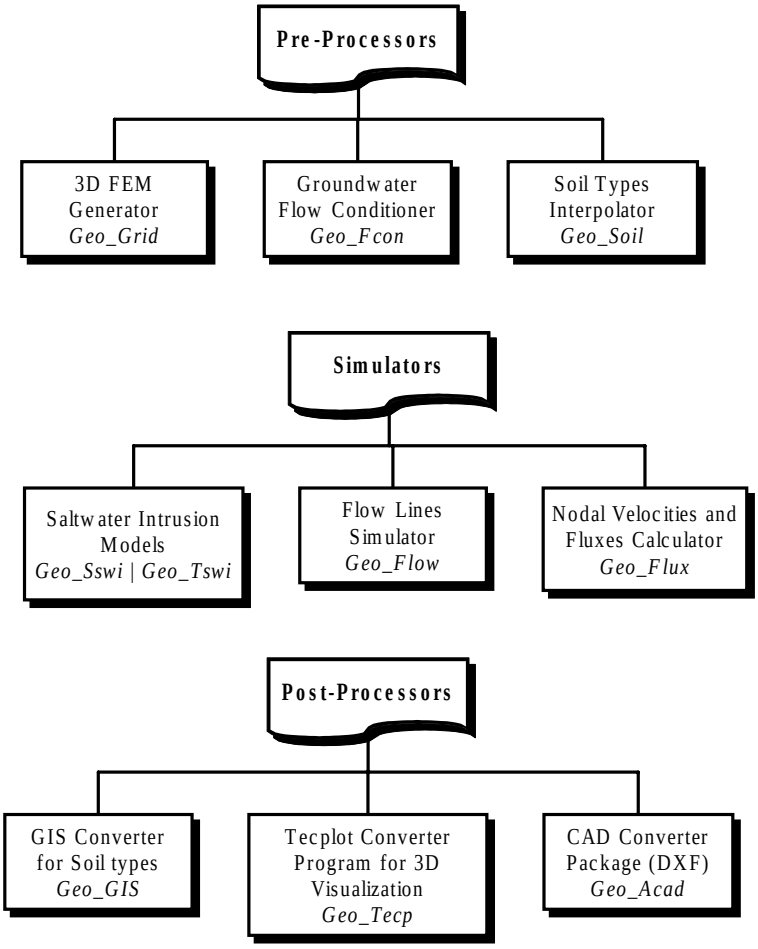

Figure 7.1:AGEO-SWIM modules.w

7.3.2y Structurey

GEO-SWIM is composed from different packages as depicted in Fig.A7.1.AtheyA are classified as pre-processors, post-processors or models, which constitutes theA core system component.A

Pre-Processor Packagesy

typicalAfiniteAelement simulation.An GEO-SWIMAstartsAby constructing a three-A dimensional mesh of the aquifer system, and attributing soil types and relatedA physicalAparametersAtoAt.AThisAfirstAtaskAcanAbeAaccomplishedAusingAtheAGEO-A

GRID mesh generator for making structured grids from irregular hexahedral finiteA elements, and GEO-SOIL a soil types interpolator package, which attributes soilA types to all elements from an initial number of given vertical geological cross-A sections.A

Boundary conditions on external boundaries and/or internal nodes (e.g. waterA abstraction nodes) are then specified prior to run the saltwater intrusion model.A The package GEO-FCON handles this task andAadditionally a user-friendly win-A dows GUI version of this package was designed to facilitate user input.A

Twelve typesAof nodalAboundaryAconditionsArepresenting a wideArangeAofApossi-A bilitiesAencounteredAinApractice areAallowedAin GEO-FCON.AItAhas alsoAthe abilityA to specify soil types as conditions confined to elements based on structured sub-A zones of the whole mesh, this option is not powerful as the use of GEO-SOIL, but it is faster in case of simple situations (e.g. horizontally layered aquifers).A

SaltwateryIntrusion Modelsy

Two models are included in the software package, plus two other auxiliary pro-A grams for tracking flow lines, and velocity calculation.A

GEO-SSWI:Ais theAsteadyAstateAsaltwaterAintrusion model, whichAisAbasedA on a symmetric conjugate gradient flow solver, preconditioned with a modifiedA M-matrix incomplete factorization.AThe conductance matrix coefficients are im-A plicitly corrected, depending on the nodal water pressure status.A

GEO-TSWI: simulates the moving salt-fresh water interface in groundwaterA aquiferAsystems.AThisAprogramAusesAaAfiniteAdifferenceAapproximationAinAtimeA and a finite element discretization in space.AIn each time step a modified PicardA iteration schemeAis adoptedAto solve theAnon-linear set of equations. An idealizedA soil characteristic curve is used, and proves to be very efficient in enhancing theA behavior of the numerical model, by eliminating irregularities encountered whileA solving standard non-linear equations.A

GEO-FLOW:AThisAprogramAtrack flowAlinesAindividually, untilAleaving theA

flow domain, or arriving in elements with zero soil type (inactive elements), or when the flow time becomes larger than a pre-set maximum simulation time. The mobile water fraction parameter has an important effect here, since it represents the fraction of the groundwater that is considered to be effectively flowing.

GEO-FLUX: This program produces a continuous nodal flow velocity field, the corresponding nodal flux vectors are also calculated. A lumped formulation is used to solve the finite element equations obtained from post processing the simulated groundwater potential heads.

Post-Processors

This group includes converter programs, which converts GEO-SWIM data sets to files format compatible with third party software. GEO-GIS program converting user specified slice cuts to readily post-processed GIS compatible files. Other programs in this category are GEO-TECP a converter for visualization with external software: Tecplot^{TM}[14], and GEO-ACAD a CAD converter.

7.4 Visualization Tools

Another alternative for post processing GEO-SWIM data sets, is the use of the integrated modelling environment (Fig. 7.2), which has been developed recently. The motivation for developing such program is to provide a number of routines for visualizing the model input and results, which will enable easy verification and calibration of the model. At the same time, a significant environment for building easily groundwater models for practical and field studies is obtained, without tremendous effort, such that the modeler will concentrate mainly in using the model and interpretation of the obtained results.

The developed user interface can run under Win[32][4] operating systems, such as Windows 95/98/NT. It is a configurable windows menu-driven interface, with

[1] Tecplot is a trademark of Amtec Engineering Inc.

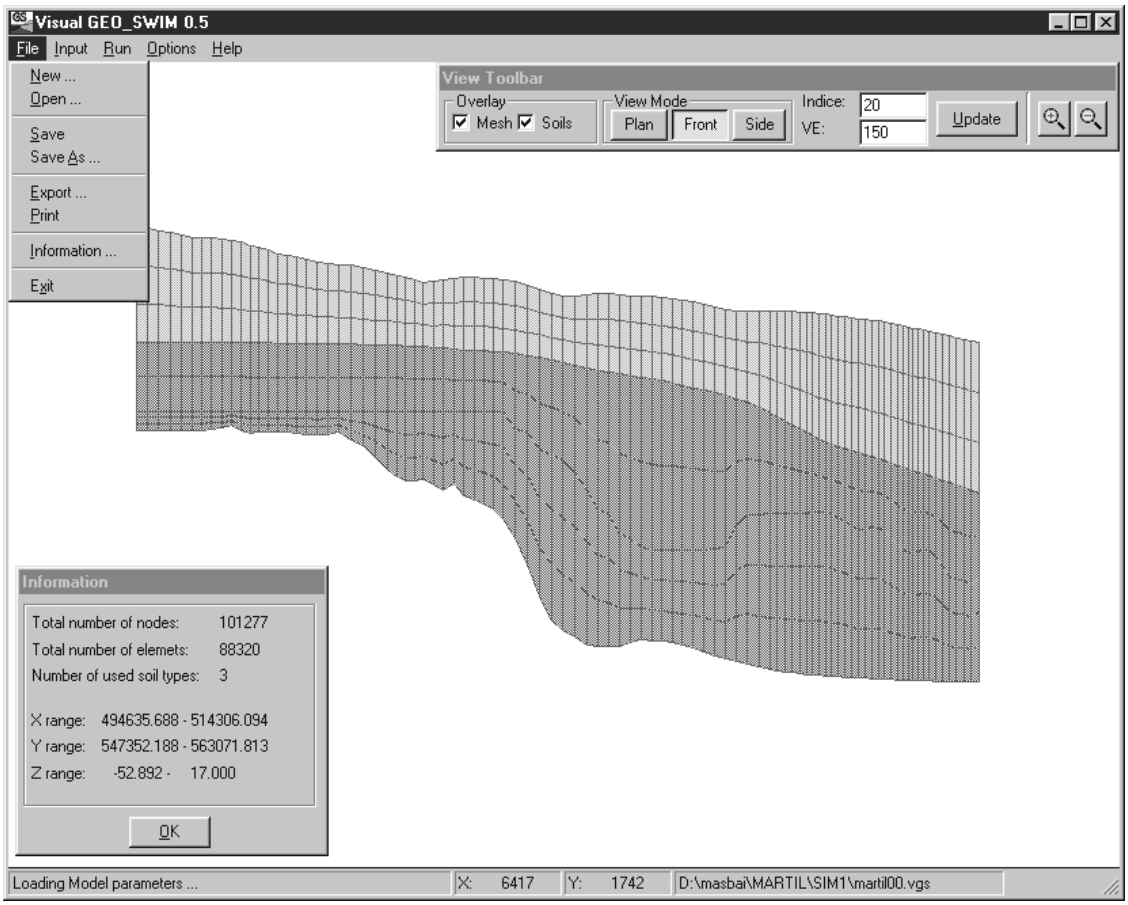

Figure 7.2: Visual GEO-SWIM interface: A sample front section view, mesh and soil types are overlayed.

many significant characteristics and implemented packages. Some of these pack-ages give GUI support for previously described programs such as GEO-FCONA and GEO-TECP. Other built-in packages include:

Cross-Sectional Cutter Package

2D cross sectional cutter package for previewing cross-sectional or plan views of the loaded model, this package has the ability to view model features e.g. mesh, soil types as separate layers of information, such that it works as a true Geographic Information System. The list of information overlays includes: soil types, simulated groundwater potentials, pressures, and fresh/saltwater interface.

MapsyExport Packagey

This package enables exporting displayed maps to popular raster and vector for-A mats (e.g.A utoCAD DXF, Windows Metafile, PostScript) which can be used inA third party CAD and engineering graphic programs.A

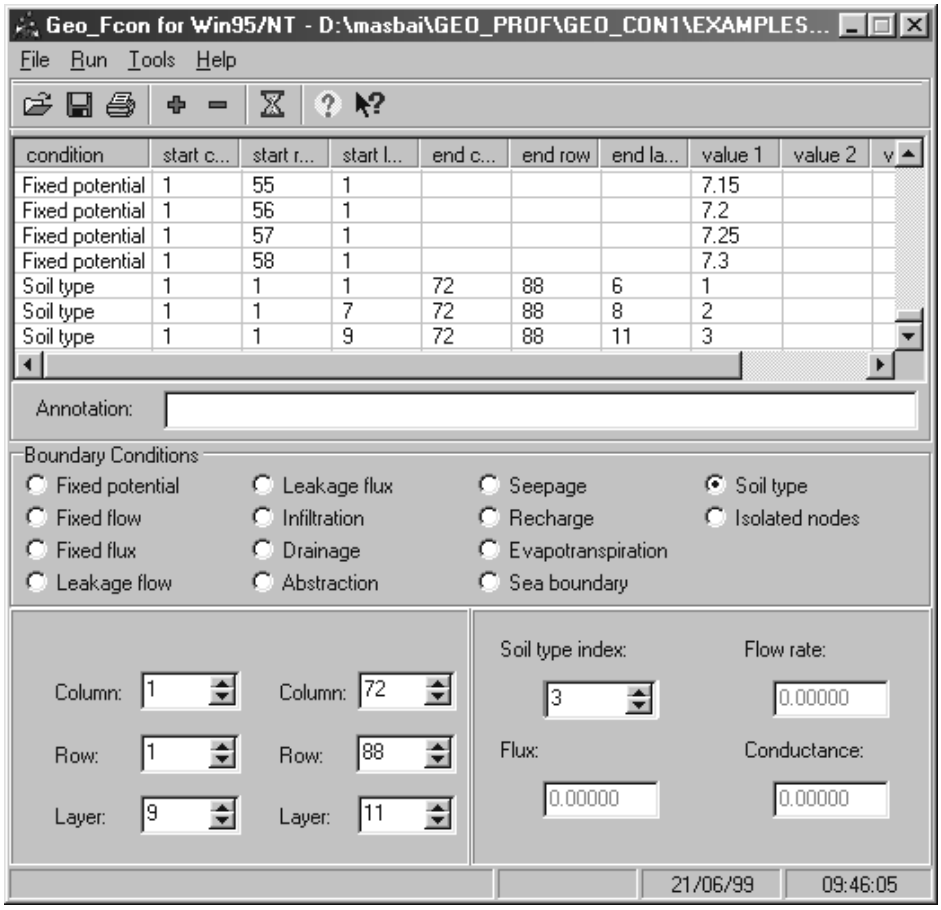

Figure 7.3:AFlow conditionerwpackage:wUpperwlist shows boundarywconditionswused forw the processed case study.w

FlowyConditions Packagey

ThisApackageAis a comprehensiveAGUIAversionAof theApreviously AdescribedAground-A water flow conditioner program (Fig. 7.3). The interface works in a similar way asA for the batch program version, and enables to speed up this process for practicalA

applications.A

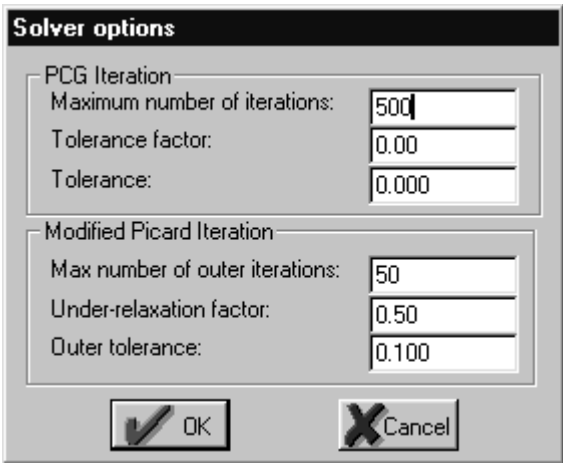

Figure 7.4:AOptions of GEO-SWIM solver package.w

ModelsyInterface Packagey

This package is a collection of interactive dialog boxes and tools for collectingA model input parameters e.g.Adensity, soil types parameters, solver options (Fig.A 7.4), time dependent parameters, etc.AThe collectedAdata is translated to GEO-A SWIM specific format, as required by the models.AThis makes the modelAdevel-A opment independent of thatAof theAnterface andAenables theAater toAnaveAsupportA for other groundwater flow models if required, eliminating the need to write an-A otherAspecificAcodeAforAt. WhenAdirectoriesAofAprogramsAexecutables areAdefinedAnA theAnterfaceAenvironment optionsAasAdisplayedAn Fig. 7.5, severalAmodelAversionsA can run from the same box. A

GEO-SWIMyto TecplotyConverter Packagey

ThisAisAaAGUIAprogramA(Fig.A 7.6)AspecificallyAdevelopedAtoAenableAeasyAandA automatic production of high quality presentation graphics with the help of theA TecplotAvisualizationAsoftwareA(AmtecAEngineeringAnc., 1996). AlthoughA, priorA knowledge of how to manipulate different data sets for best visualization resultsA

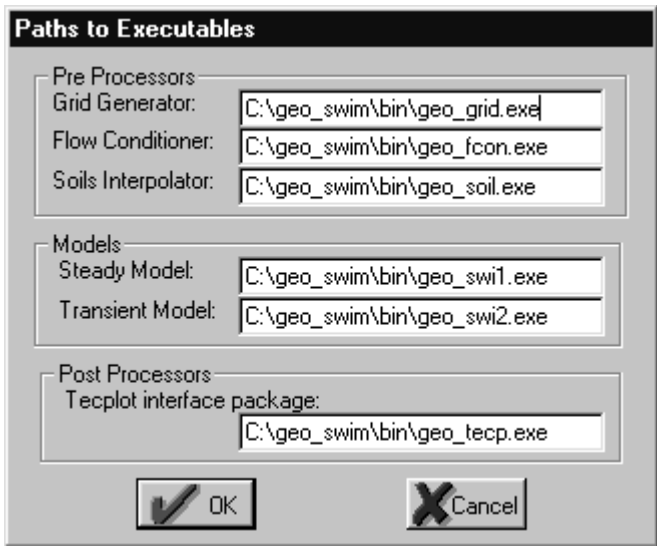

Figure 7.5:AExecutable program paths interface.w

with this powerful software is necessary, this program acts as a simple generatorA toAbuildAcustomAdata setsAwhichAcouldAbe usedAdirectlyAfromAwithinATecplot, thus transforming data formats from GEO-SWIM. The transformation is doneA smoothlyAin different ways, and a varietyAofAdataAformatsAareAsupported;Aso ASCIIA andABinaryATecplotAfileAformatsAareAsupported, theAlaterAversion couldAbeAof choiceA whenAdataAsetsAareAlargeA(i.e.AexcessiveAnumberAofAnodesAand/orAtransientAdataA sets).AThisAenablesAmakingAfilesAofAhighAcompressionAratios, whichAresultsAinAaA significantAstorageAmediaAsavingAandAsmallerAaccessAtimesAtoAtheAfiles.A SCIIA data sets are useful only for small size problems, such as theoretical ones, forA which immediate checking of the results is faster through immediate viewing ofA theA SCII Tecplot file.A

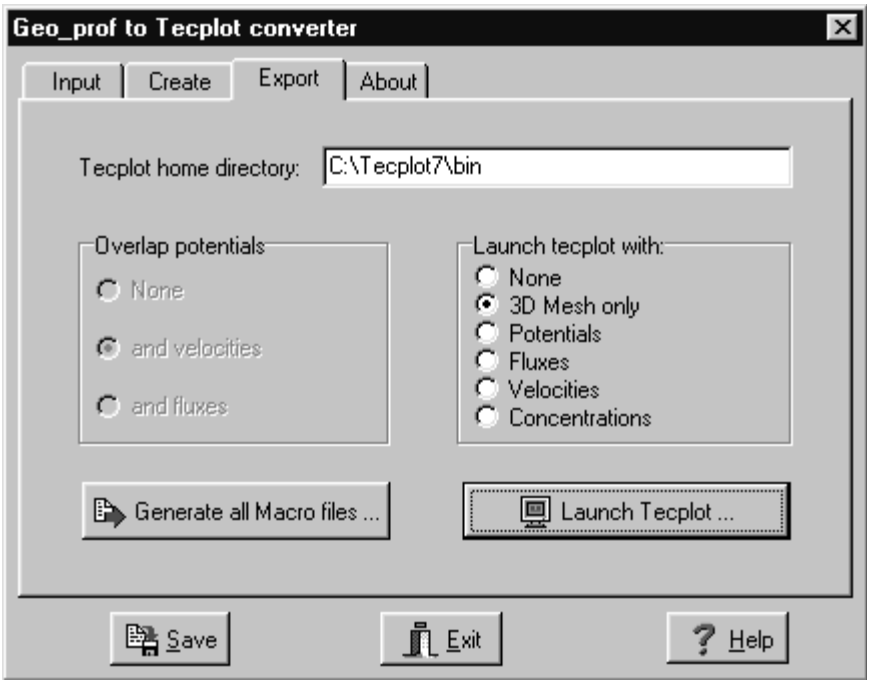

Figure 7.6:AA Tab view of the GEO-SWIM to Tecplot converter GUI package.U

Chapter 8

Conclusions and Recommendations

Contents

8.1 Conclusions

The results and significant findings are summarized in the sub-sections given below, following the order at which they were discussed earlier.

8.1.1 Variably Saturated Groundwater Flow Problems

computer program for modeling time dependent, and three-dimensional variably saturated groundwater flow has been developed based on several numerical techniques, enabling great savings in computer time, and giving rise for running large problems of billion of unknowns, efficiently on cheap desktop workstation or PC's. The model uses a Galerkin finite element approximation in space and a fully implicit finite difference time approximation with a mass lumped storage term. It features the following items:

- Automatic location of the moving water table boundary, based on the FUP technique found to be excessively cheap in comparison to the standard finite element method. The water table location is based on the changing nodal water status which are mapped from the relative water table position within each hexahedral element;

- Other non-linearities related to the difficulty in estimating the soil characteristic curves are tackled using nodal specific idealized water retention curves, by taking into consideration the saturated and the residual water contents for each soil type exclusively. This approach is found to be useful, and very attractive especially in combination with the solver;

- The implemented numerical solver shows to be very efficient, stable, and mass conservative. The embedded methods which largely contribute to such robustness are: the modified incomplete factorization preconditioner, with an M matrix transformation, the inner linear conjugate gradient solver, and the dynamic time marching scheme with automatic under-relaxation;

- Special attention was paid to complex and nonlinear boundary conditions, such as, seepage face, drainage, time varying heads, leakage and abstraction, these conditions are effectively implemented and tested on several application samples, thus providing a meaningful way to build applications with many levels of complexities.

The model is verified and validated using 4 test examples. Numerical results are compared versus analytical, measured results, and other numerical techniques such as the moving mesh method. For all these test problems, a good agreement is obtained. The most important test validates the model by comparison with respect to laboratory measurements in a 3-D earth dam model (Baseghi and Desai, 1987). Numerical experiments were carried out in case of rise, steady state and drawdown of the free seepage flow, which allow for modeling heterogeneities

represented by coarse sand materials. The model was able to predict accurately the moving water table location and seepage face extent.

8.1.2 Saltwater Intrusion Problems

Simulation of the saltwater encroachment in 3-D aquifer systems was studied based on a newly developed finite element based computer code: GEO-SWIM. This model can handle difficult cases where two free and moving boundaries exist in the domain, e.g. in coastal unconfined aquifers. An iteratively based Ghyben-Herzberg approximation was implemented, and thus avoiding the solution of the coupled two-phase governing equations simultaneously. Instead, the saltwater zone is replaced with an equivalent freshwater zone having the same pressure distribution as in the saltwater. Other achieved developments are classified as follows:

- The FUP numerical technique was generalized for the case of dual moving boundaries, especially explicit modifications are performed for the shape of the idealized water retention curve, showing its dependence on the density difference ratio;
- The model uses the same numerical solver, and time marching scheme developed for the variably saturated groundwater flow model.

Five test problems are provided to support the numerical model. Various solution types (analytical, numerical, and experimental) are adopted for comparison purposes. The behavior of the saltwater encroachment has been studied in confined, unconfined and multilayer aquifers with different complexities and conditions. All these tests yield satisfactory results regarding the scope of the application, and model specific situation for each test.

The GEO-SWIM numerical code is applied to study saltwater encroachment in the coastal aquifer system of Martil situated in the northern part of Morocco. The

detailed three-dimensional geometry of the aquifer was reconstructed from the available data sets as a further step to pursue the modeling study. A calibrated steady model shows that sensitivities are more relevant to the natural recharge, in comparison to other parameters such as hydraulic conductivity and the saltwater density. Afterwards, a long-term transient simulation was performed to reproduce actual and future situations, with the aim to analyze the risk to salinization from the Mediterranean sea. It was concluded that without further control the saltwater interface would travel inland over considerable distances in the future.

8.1.3 Solute Transport Problems

In spite of the investigated three-dimensional groundwater flow class of problems, numerical modeling of pollutant transport in aquifer systems by the conforming finite element method leads to large linear systems that are sparse and nonsymmetric. However, compared to the flow conductance matrix, it is observed that the global transport matrix arising from the discretization using hexahedral elements is not an M matrix, which is a very desirable property guarantying the numerical stability of the solution procedure. Therefore, several issues were investigated to overcome this difficulty, such as:

- The efficiency of preconditioned conjugate gradient like solvers such as MR and BICGSTAB;

- Preconditioners as diagonal scaling, incomplete factorization, and modified incomplete factorization were tested. An M matrix transformation is proposed which guarantees the existence of incomplete factorization, the most efficient preconditioner so far. The number of iterations, and CPU cost were used as a basis for these comparisons, also a series of benchmarks for all succeeded tests were performed for problems, which could be solved analytically, to ensure the accuracy of the obtained results.

Five representative test examples were selected as a basis for this comparison, and several strategies were adopted to conduct different numerical simulations, based on the implemented preconditioners, stopping convergence criteria, and solutions benchmarks when an exact solution was available.

It is found that BICGSTAB preconditioned by incomplete factorization performs well for all test problems. However, for difficult problems such factorization is unlikely to exist, and the proposed M matrix transformation proves to be effective, leading to the guaranteed existence of a robust and efficient solver.

8.2y Recommendationsy

General guidelines for suggested future research are given herein. Throughout several possibilities and directives, we recommend either an extension of this work or other alternatives and complementary developments, which may take profit from this thesis findings. We think at present that future modifications and/or extensions of the existing computer packages and models is manageable to success any of these suggestions.

- ±The developed FUP numerical technique for free and moving interfaces, including the water table and the salt-freshwater interface was tested on problems all constructed on structured meshes. However, we should keep in mind that, this is not a restrictive condition with respect to the numerical approach since the FUP involves updating nodal storage and conductance with respect to the hexahedral element behavior. We expect the numerical scheme to work for problems with unstructured 3-D problems using exclusively hexahedrals. This could prove to be useful for a particular class of problems where local refinement is advised;

- ±Under tidal conditions in the sea, the pressure distribution in the saltwater zone may become important, and hence it is advised that the coupled

system of freshwater and saltwater equations are solved simultaneously in time;

- More detailed probes are needed for the evaluation of the vertical flow components. In case of the moving interface flow, this will be very useful for proper adjustment of the boundary conditions at wells which may withdraw saltwater;

- For the preconditioning methods (either for the flow or the transport problems) discussed in this work, the ability of each method to adopt to a particular hardware is dropped. In particular, the cost and ease of the implementation in parallel architectures are not discussed. Parallelization of computer codes is considered as one of the most exiting research topics in development in today's software engineering market. The promising new generation of programming languages, optimized compilers, and operating systems will provide a solid platform for an integrated development of automatic parallel codes generation. However, the best results are obtained through a direct implementation at the computer code level;

- We are aware that for many situations where there exists a strong dependence of the water density upon the solute concentration, the solution of coupled flow and transport problems is necessary. To solve effectively these class of problems, it is often assumed that spatial differences in the mass of pure water per unit volume due to variations of pressure are negligible in comparison. Particularly, in case of unsaturated transport a robust fully coupled solver may be based on the FUP technique. In this context, and more precisely in case of highly advective flow, a second order accurate CVFE approach could be more feasible in solving solute transport equations. The latest developments are still not satisfactory for 3-D domains, especially for hexahedral elements (most of the existing formulations as only

for 2-D triangular elements), these new strategies should take into account the cost of the developed numerical engine, as in 3-D these are expected to be very high;

- Unstructured meshes are efficiently designed, if they effectively minimize the overall solver time for the same number of nodes. This is achieved in particular for a number of problems, using at least a combination of two elements (triangles and quadrilaterals in 2-D, and hexahedrals and tetrahedrals in 3-D), the possible extension of the M matrix transformation to other kinds of elements can provide challenging applications to be performed efficiently;

- The visual interface program presented in chapter 7 is an attempt to give a sufficient level of support for the models being developed. As the software development was academically and research oriented, the program can be used as a learning tool for postgraduate level and training on finite element groundwater flow principles. To boost the practical use of the program, we strongly recommend its continuous development and support, for a wider range of models.

ENDd

REFERENCES

Ababou, R., G.ATregarotA&A .ALarabiA(1998), PartiallyAsaturatedAhydrologicalA flows: numerical experiments and analyses, *inj*XIIAnt.Aconf. of comp. meth-A ods in Water Resour.', pp. 529–536.

Amtec Engineering, Inc. (1996), *Tecplotyversiony7,yProductiveypoweryforydatayvi-y sualization,yUser'syManual*, Bellevue, Washington, DC.

Anderson, M.AP.A(1976), 'UnsteadyAgroundwaterAflowAbeneathAstripAoceanicAis-A lands', *WateryResour.yRes.y*1**2**(4), 640–644.

Anderson, M. P. & W. W. Woessner (1992), *Appliedygroundwaterymodeling:ySim-y ulationyofyflowyandyadvectiveytransport*, cademic Press, Inc., New York.A

xelsson, O.A&AV. A.ABarkerA(1984), *Finiteyelementysolutionyofyboundary valuey problems,ytheory andycomputation*, cademic Press.A

Baden-Ghyben, W.A(1888), NotesAon theAprobableAresultsAofAwellAdrilling nearA amsterdamA(inADutch), TechnicalAReportA21, Tijdschrift Van hetAKoninklijkA Inst. Van Ing., The Hague.A

Bakker, M.A(1998), 'Transient dupuitAinterfaceAflowAwithApartiallyApenetratingA features', *WateryResour.yRes.y***3**4(11), 2911–2918.A

Barret, R., M. Berry T. Chan J. Demmel J. Donato J. Dongarra V. Eijkhout R.A Pozo C. Romine & H. Van der Vorst (1994), *Templatesyforytheysolutionyofy linearysystems:ybuildingyblocksyforyiterativeymethods*, SIAM, Philadelphia.A

Baseghi, B. & C. S. Desai (1987), Three-dimensional seepage through porous mediaA with the residual flow procedure, Technical Report 85721, Dept. of CivilA Eng. and Eng. Mech., University ofA rizona, Tucson.A

Baseghi, B.A& C. S.ADesaiA(1990), 'LaboratoryAverificationAofAtheAresidualAflowA procedureAforAthree-dimensionalAfreeAsurfaceAflow', *WateryResour.yRes.y* **26**(2), 259–272.A

Bear, J. (1972), *Dynamicsyofyfluidsyinyporousymedia*, Elsevier, New York.A

Bear, J. (1979), *Hydraulicsyofygroundwater*, McGraw-Hill, New York.A

Bear, J.A& A.AVerruijtA(1987), *Modelingygroundwateryflowyandypollution*, Reidel A Publishing, Dordrecht, Holland.A

Bear, J. & G. Dagan (1964), 'Moving interface in coastal aquifers', *J.yHydraul.y ASCEy***90**(90), 193–216.A

Beauwens, R.A(1990), *LectureyNotesyinyMathematics*, Springer-Verlag, chapterA ModifiedAincompleteAfactorizationAstrategies, PreconditionedAConjugateA Gradient Methods, pp. 1–16.A

Beauwens, R.A&AL. QuenonA(1976), 'Existence criteriaAforApartial matrixAfactoriza-A tions in iterative methods', *SIAMyJ.yNumer.yAnal.y***13**, 615–643.A

Brezzi, F.A&AM. FortinA(1991), *MixedyandyhybridyfiniteyelementymethodsSpringer-A* Verlag, Berlin.A

Brooks, R.AH. & C. T. CoreyA(1964), 'UnsaturatedAflow in groundwater hydraulics', *Hydr.yDiv.yJ.,yAm.ySoc.yCiv.yEng.y***90**(5), 121–127.A

Celia, M.A .A&AE.AT.ABouloutasA(1990), 'A general mass-conservative numericalAso-A lutionAfor the unsaturatedAflowAequation', *WateryResour.yRes.y***26**(7), 1483–A 1496.A

Celia, M.A .A&AP.ABinningA(1992), 'A mass conservative numericalAsolutionAfor two-A phase flow in porous media with application to unsaturated flow', *Watery Resour.yRes.y***28**(10), 2819–2828.A

Chesshire, G.A& W. D.AHensaw (1990), 'Composite overlapping meshes for theA solutions of partial differential equations', *J.yofycomp.yphys.y***90**, 1–64.A

Chesshire, G.A&AW.AD.AHensawA(1994), 'A schemeAforAconservativeAinterpolationA on overlapping grids', *SIAMyJ.ySci.yandyStat.ycomp.y***15**(4), 819–845.A

Chu, W. S. & R. Willis (1984), 'An explicit finite difference model for unconfinedA aquifers', *GroundyWatery***22**(6), 728–734.A

Clement, T.AP., W.AR.AWiseA&AF.AJ.AMolzA(1994), 'A physicallyAbased, two-A dimensional, finiteAdifferenceAalgorithmAforAmodelingAvariablyAsaturatedA flow', *J.yofyHydrology* **161**, 71–90.A

Cooley, R.AL.A(1983), 'Some newAproceduresAfor numericalAsolutionAofAvariablyA saturated flow problems', *WateryResour.yRes.y***19**(5), 1271–1285.A

Cordes, C.A&AM.APuttiA(1997), 'FiniteAelement approximationAof theAdiffusionA operator on tetrahedra', *Submitted to SIAM J. Sci. Comp.* (to appear).A

Croucher, .AE.A&AM.AJ.AO'SullivanA(1995), 'TheAhenryAproblemAforAsaltwaterA intrusion', *WateryResour.yRes.y***31**(7), 1809–1814.A

Crowe, .AS., S.AG.AShikazeA&AF.AW.ASchwartzA(1998), 'A gridAgeneratingAalgo-A rithm for simulating a fluctuating water table boundary in heterogeneousA unconfined aquifers', *Adv.yWateryResour.y***22**(6), 567–575.A

Custodio (1987), *Groundwateryproblemsyinycoastalyareas*, contributionAtoAtheA International Hydrological problems, Elsevier.A

De Smedt, F. (1995), *GEO-PROF:yAynumericalysimulationyprogramyforygroundy wateryflowyandypollutionytransport*, version 1.0 edn, Laboratory of Hydrol-A ogy, Pleinlaan 2, B-1050, Brussels, Belgium.A

De Smedt, F. (1996), 'Grondwaterstromingsmodel GEO-PROF', *Watery* **90**, 222– A 228.A

DeASmedt, F.A&AM.A .ASbaiA(1998), GroundwaterApollutantAtransportAmodelingA based on the finite element technique with m-matrix preconditioning, *iny* B.et al., ed., 'XII Int. conf. of computational methods in water resour.', Vol. 2, Computational Mechanics Publications, pp. 601–608.A

Desai, C. S., J. G. Lightner & S. SomasundaramA(1983), 'A numerical procedureA for three-dimensional transient free surface seepage', *Adv.yWateryResour.y* **6**, 175–181.A

Douglas, J., R.AE.AEwingA&AM. F.AWheelerA(1983), 'ApproximationAof theApressureA by a mixed method in the simulation of miscible displacement', *R.A.I.R.Oy Anal.yNum.y* **17**, 17–33.A

Durlofsky, L. J. (1993), 'A triangle based mixed finite element-finite volume tech-A nique for modeling two phase flow through porous media', *J.yComp.yPhys.y* **105**, 252–266.A

Durlofsky, L.AJ.A(1994), 'AccuracyAofAmixedAandAcontrolAvolumeAfiniteAelementA approximationsAtoAdarcyAvelocity andArelatedAquantities', *WateryResour.y Res.y* **30**(4), 965–973.A

ElAMorabiti, K.A&A .APulido-BoshA(1993), 'HydrogeologyAofAtheAmartil-alilaA aquifer', *Hydrogéologiey* **1**, 21–33.A

Ennouhi, M. & M. Melouki (1984), Etude hydrogéologique et hydrologiqueAdesA bassins côtiersAmediterraneensAlao, martil, smir, negro, Master's thesis, Ecole MohammadiaAd'Ingénieurs, B.P. 765, gdal, Rabat, Morocco.A

Essaid, H. I. (1990), 'A multilayered sharp interface model of coupled freshwaterA andAsaltwaterAflowAin coastalAsystems: ModelAdevelopment and application', *WateryResour.yRes.y* **26**(7), 1431–1454.A

Fetter, C. W. (1998), *Groundwatery contamination*, Prentice Hall, Inc.A

Forsyth, P.A .A(1989), controlAvolumeAfiniteAelementAmethodAforAlocalAmeshA refinement, p. paper SPE 18415.A

France, P. W. (1974), 'Finite element analysis of three-dimensional groundwaterA flow problems', *J.yHydrology* **21**, 381. A

Freeze, R. A. (1971), 'Three-dimensional transient saturated-unsaturated flow inA a groundwater bassin', *WateryResour.yRes.y***7**(2), 347–366.A

Freeze, R. A. & J.A . Cherry (1979), *Groundwater*, Pentice Hall, Inc., EnglewoodA Cliffs, New Jersy.A

Fuentes, C., R. Haverkamp & J. Y. Parlange (1992), 'Parameters constraints onA closed form soil water relationships', *J.yofyHydrology* **134**, 117–142.A

Galeati, G., G.AGambolatiA& S.AP. NeumanA(1992), 'CoupledAandApartiallyAcoupledA eulerian-lagrangian model of freshwater-seawater mixing', *WateryResour.y Res.y***28**(1), 149–165.A

Gambolati, G., G. Pini & G. Verri (1988a), SimulationAof regional subsurface flowA byAfiniteAelement models, *iny*D.OuazarA&ACA .Brebbia, eds, 'ComputerA methods and water resources, Groundwater and aquifer modelling', Com-A putational Mech. Publication, Spring-verlag, pp. 107–116.A

Gambolati, G., G.APiniA&AG.AZilliA(1988b), *Numericalycomparisonyofyprecondi-y tioningyforylargeysparseyfiniteyelementyproblems*, JohnAWileyA Sons, Inc, pp. 139–157.A

Gambolati, G., M. Putti & C. Paniconi (1995), 'Projection methods for the finiteA element solution of the dual-porosity model in variably saturated porousA media', *Adv.yinyGround.yPol.yCont.yandyremed.y*A

Glover, R.AE.A(1959), 'TheApatternAofAfreshwaterAflowAin a coastal aquifer', *J.y Geophys.yRes.y***64**(4), 439–475.A

Gottardi, G.A&AM.AVenutelliA(1993), 'A control-volumeAfinite-elementAmodelAforA two-dimensional overland flow', *Adv.yWateryRes.y***16**, 277–284.A

Gray, W. G. (1984), *Comparisonyofyfiniteydifferenceyandyfiniteyelementymethods*, pp. 899–952.A

Guo, W. (1997), 'Transient groundwater flow between reservoirs and water-tableA aquifers', *J.yofyHydrology* **195**, 370–384.A

Gureghian, A.AB.A(1978), 'SolutionAofAboussinesq'sAequationAforAseepageAflow.', *WateryResour.yRes.y***14**(2), 231–236.A

Gustafsson, I. (1984), *ModifiedyincompleteyCholesky (MIC)ymethods*, Gordon andA Breach, Science Publisher, New York, pp. 265–293.A

Gutknecht, M.AH.A(1993), 'VariantsAofABI-CGSTABAforAmatricesAwithAcomplexA spectrum', *SIAMyJ.ySci.yComp.y*1**4**, 1020–1033.A

Hantush, M.AS.A(1968), 'Unsteady movement ofAfreshwaterAin thick saline aquifers', *Bull.yInt.yAssoc.ySci.yHydrol.y*1**3**, 40–60.A

Harbaugh, .AW.A&AM.AG.AMcDonaldA(1996), User'sAdocumentationAforA MODFLOW-96, an update to theAu.s.AgeologicalAsurvey modularAfinite-A difference groundwater flow model, Open-File Repport 96-485, U.S.G.S.A

Harr, M.AE.A(1962), *Groundwateryandyseepage*, DoverAPublications, Inc. NewAYork.A

Haverkamp, R., F.ABouraouiAF.AZammitA& Angulo-JaramilloA(1999), *Theyhand-y bookyofygroundwateryengineering*, CRC Press, chapter Soil properties andA moisture movement in the unsaturated zone, pp. 5–1–5–50.A

Herzberg, . (1901), 'Die wasserversorgung einiger nordseebader', *J.yGasbeleucht.y Wasserversorgy*4**4**, 815–819, 842–844.A

Hestenes, M.A& E. StiefelA(1952), 'MethodsAofAconjugateAgradients forAsolvingAlinearA systems', *J.yRes.yNat.yBur.yStandardsySect.y*pp. 409–436.A

Ho-Le, K. (1988), 'Finite element mesh generation methods: a review and classi-A fication', *ComputeryAidedyDesigny*2**0**, 27–38.A

Hoopes, J.A .A&AD.AR.AF.AHarlemanA(1967), 'DispersionAinAradialAflowAfromAaA recharge well', *J.yGeophys.yRes.y*7**2**(14), 3595–3607.A

Hsieh, P. A. (1986), 'A new formula for the analytical solution of the radialAdis-A persion problem', *WateryResour.yRes.y*2**2**, 1597–1605.A

Hubbert, M. K.A(1940), 'The theoryAofAground-water motion', *J.yGeol.y*4**8**(8), 785–A 944.A

Hunt, B.A(1978), 'DispersiveAsourcesAinAuniformAflow', *J.yHydraul.yDiv.y*1**04**, 75–85.A

Hunt, B. (1985), 'Some analyticalAsolutionsAforAseawater intrusionAcontrolAwithA recharge wells', *J.yofyHydrology* **80**, 9–18.A

Huyakorn, P. S., B. Geofery Jones & P. F. Andersen (1986), 'Finite element algo-A rithmsAforAsimulating three-dimensionalAgroundwaterAflow andAsoluteAtrans-A port in multi-layer systems', *WateryResour.yRes.y*2**2**(3), 361–374.A

Huyakorn, P. S., E.AP.ASpringerAV.AGuvanasenA& T.AD.AWadsworthA(1986), 'A three-dimensionalAfiniteAelement modelAforAsimulatingAwaterAflowAin variablyA saturated porous media', *WateryResour.yRes.y*2**2**, 1790–1808.A

Huyakorn, P. S.A&AG.AF.APinderA(1983), *ComputationalymethodsyinysubsurfaceyflowA*, Academic, San Diego, Calif.A

Huyakorn, P. S., S.AD.AThomasA&AB.AM.AThompsonA(1984), 'TechniquesAforAmakingA finite elements competitive in modeling flow in variably saturated porousA media', *WateryResour.yRes.y***20**(8), 1099–1115.A

Huyakorn, P. S., S. Pandy & Y. S. Wu (1994), 'A three-dimensional multiphase flowA model for assessing NAPL contamination in porous andAfractured media', *J.yContam.yHydrol.y***16**, 109–130.A

Huyakorn, P.AS., Y.AS.AWuA&AN.AS.AParkA(1994), 'AnAimprovedAsharp-interfaceA model for assessing NAPL contamination and remediation of groundwaterA systems', *J.yContam.yHydrol.y***16**, 203–234.A

Huyakorn, P. S., Y.AS.AWu & N. S.AParkA(1996), 'Multiphase approach to theA numerical solution of a sharp interface saltwater intrusion problem', *Watery Resour.yRes.y***32**(1), 93–102.A

Iribar, V., J. Carrera E. Custodio & A. Medina (1996), 'Inverse modelling of seawa-A ter intrusion in the liobregat delta deep aquifer', *J.yofyHydrology* **198**, 226– A 244.A

Istok, J. (1989), *Groundwatery modelingyby theyfiniteyelementymethod*, MonographA 13, merical Geophysical Union, Washington, DC.A

Jacobs, D.A .AH.A(1984), *Preconditioningymethods,ytheory andyapplications*, ScienceA Publisher, chapter Preconditioned conjugate gradient algorithms for solvingA finite difference systems, pp. 509–535.A

Jie, S.A&AN.AvanAQuyA(1992), newAmethodAforAreducingAnumericalAaccumula-A tion andAdispersion application toAenhanced oil recovery, *inyProceedings ofA* ECMOR III', Delft University Press.A

Kaasschieter, E. F. (1995), 'Mixed finite elementsAfor accurateAparticle trackingAinA saturated groundwater flow', *Adv.yWateryResour.y***18**(5), 277–294.A

Kipp, K.AL.A(1987), HST3D:A computerAcodeAforAsimulationAofAheatAandAsoluteA transportAin three-dimensionalAgroundwaterAflowASystems, TechnicalAreport, U.S. Geol. Surv. Water Resour. Inv. Rep.A

Kishi, Y.A&AY. FukuoA(1977), 'StudiesAon salinizationAofAgroundwater, i. theoreticalA consideration on theAthree-dimensional movement of theAsaltAwaterAinterfaceA caused by the pumpage of confined groundwater in fan-shaped alluvium', *J.yofyHydrology* **35**, 1–29.A

Knupp, P. & S. Steinberg (1993), *Fundamentalsyofygridygeneration*, Buca Raton, CRC Press.A

Konikow, L. F.A&AJ.AD.ABredehoeft (1978), Computer code of two-dimensionalA solute transport and dispersion in groundwater, Technical report, U.S. Geol.A Surv. Water Resour. Inv. book 7.A

Kresic, N. (1997), *Quantitativeysolutionsyinyhydrogeology andygroundwaterymodel-y ing*, Lewis Publishers, Boca Raton, New York.A

Lanczos, C. (1952), 'Solution of systems of linear equations by minimized itera-A tions', *J.yRes.yNat.yBur.yStandard.y***49**, 33–53.A

Lapidus, L. & G.APinder (1982), *Numericalysolution ofypartialydifferentialyequationsy inysciencesyandyengineering*, Wiley-interscienceAPublication, JohnAWileyA Sons.A

Larabi, .A&AF.ADeASmedtA(1993), NumericalAfiniteAelement modelAforA3-dAphreaticA flowAin porous media, *in*yL.AC.WrobelA&AC.A .Brebia, eds, 'Free andAmovingA Boundary problems', Computational Mechanics Publications, pp. 49–56.A

Larabi, .A&AF.ADeASmedt (1994*a*), 'Solving three-dimensionalAhexahedralAfiniteAel-A ement groundwaterAmodelsAbyApreconditioned conjugateAgradient methods', *WateryResour.yRes.y***30**(2), 305–321.A

Larabi, .A&AF.ADeASmedtA(1994*b*), Three-dimensional finite element model forA saltwaterAintrusionAinto aquifers, *in*ye.Aa.Peters, ., ed., 'XAInt.Aconf.AofA comp.AmethodsAinAwaterAresour.', KluwerA cademicAPublishers, pp.A1019–A 1026.A

Larabi, .A&AF.ADeASmedtA(1997), 'NumericalAsolutionAofA3-dAgroundwaterAflowA involvingAfreeAboundariesAby a fixedAfiniteAelement method', *J.yofyHydrology* **201**, 161–182.A

Larabi, ., M. Hilali & M.A . Sbai (1999), Investigation of the groundwater salin-A ization in the martil coastal aquifer (tetouan-morocco), *in*yW.De BreuckA & L.Walschot, eds, 'Proceedings of the 15th salt-water intrusion meeting', Ghent University, Flemish J. of Nat. Sci., pp. 263–267.A

Mahesha, A.A(1995), 'ParametricAstudiesAonAtheAadvancingAinterfaceAinAcoastalA aquifersAdueAtoAlinearAvariation of theAfreshwaterAlevel', *WateryResour.yRes.y* **31**(10), 2437–2442.A

McDonald, M.AC.A& A.AW.AHarbaughA(1988), MODFLOW:A modularAthree-A dimensionalAfiniteAdifferenceAground-waterAflowAmodel, TechnicalAReportA 83-875, U.S.G.S.A

Meijerink, J. A. & Van der Vorst H. A. (1977), 'An iterative solution method forA linear systems of which the coefficient matrix is a symmetric m-matrix', *MathematicsyofyComputationy*pp. 148–162.A

Meissner, U. (1972), 'A mixed finite element model for use in potential flow prob-A lems', *Int.yJ.yNum.yMethodsyEng.y***6**, 467–473.A

Motz, L. H. (1992), 'Salt-water upconing in an aquifer overlain by a leaky confiningA bed', *GroundyWatery***30**(2), 192–198.A

Motz, L.AH. (1997), 'Comment onA"multiphaseAapproachAtoAthe numericalAsolutionA of a sharp interface saltwater intrusion problem" by p. s. huyakorn, y. s.A wu, and n. s. park', *WateryResour.yRes.y***33**(11), 2617–2618.A

Mualem, Y.A&AJ.ABearA(1974), 'TheAshapeAofAtheAinterfaceAinAsteadyAflowAin aA stratified aquifer', *WateryResour.yRes.y***10**(6), 1207–1215.A

Nawalany, M. (1986), Numerical model for the transport velocity representationA of groundwater flow, *iny*VI Int. conf.on finite element in water resources'.A

Neuman, S. P. (1973), 'Saturated-unsaturated seepage by finite elements', *ASCEy J.yHydrau.yDiv.y***99**(12), 2233–2251.A

Neuman, S.AP.A&AP. A.AWitherspoonA(1970), 'VariationalAprinciplesAforAconfinedA and unconfined flow of groundwater', *WateryResour.yRes.y***6**(5), 1376–1382.A

Paniconi, C., . A. Aldama & E. F. WoodA(1991), 'Numerical evaluation of iter-A ative and noniterative methods for the solution of the nonlinear richardsA equation', *WateryResour.yRes.y***27**(6), 1147–1163.A

Paniconi, C.A&AM.APuttiA(1994), 'A comparisonAofApicardAandAnewtonAiterationA inAthe numericalAsolutionAof multidimensionalAvariablyAsaturatedAflowAprob-A lems', *WateryResour.yRes.y***30**(12), 3357–3374.A

Park, N. & Y. S. Wu (1994), Evaluation of vertical leakage schemes for multilayerA sharp-interface saltwater-intrusion models, *iny*e.Aa.Peters, ., ed., 'XAInt.A conf.AofAcomp.AmethodsAinAwaterAresour.', KluwerA cademicAPublishers, pp. 1027–1034.A

Pinder, G. F. & W. G. Gray (1977), *Finiteyelementsyinysurfaceyandysubsurfacey hydrology.*A

Pini, G. & G. Zilli (1990), 'On vectorizing the preconditioned conjugate gradientA residual methods', *Int.yJ.yComputeryMath.y***33**, 195–207.A

Pini, G.A&AM.APuttiA(1994), Krylov methodsAinAtheAfiniteAelement solutionAofA groundwaterAtransportAproblems, *in* A.Ae.Aa.Peters, ed., 'XAInt.Aconf.AOfA comp.AmethodsAinAwaterAresour.', KluwerA cademicAPublishers, pp.A1431–A 1438.A

Polo, J. F.A&AF.AJ.AR.ARamisA(1983), 'SimulationAofAsaltAwater-freshAwaterAinterfaceA motion', *WateryResour.yRes.y*1**9**(1), 61–68.A

Polubariva-Kochina, P.Y. (1962), *Theory ofygroundwaterymovement*, TranslatedA from Russian by J.N.R. de Wiest. Princeton University Press, Princeton, NJ.A

Reilly, Thomas E. & Alvin S. Goodman (1985), 'Quantitative analysis of saltwater-A freshwater relationships in groundwater systems - a historical perspective', *J.yofyHydrology* **80**, 125–160.A

Remson, I., G. M. Hornberger & F. J. Molz (1971), *NumericalyMethodsyinySub-y surfaceyHydrology*, Wiley-Interscience.A

Richards, L.A .A(1931), 'CapillaryAconductionAofAliquidsAthroughAporousAmedia', *Physicsy*1, 318–333.A

Rubin, J. (1968), 'Theoretical analysis of two-dimensional transient flow of waterA in unsaturated and partly saturated soils', *SoilySci.ySoc.yAm.y***32**(5), 607–A 615.A

Sa Da Costa, .A . & J. L. Wilson (1979), numerical model of seawater intru-A sion in aquifers, Technical Report 247, Ralph Parson Lab., Mass. Inst. ofA Technol., Cambridge.A

Saad, Y. (1994), *SPARSKIT:yaybasicytoolykityforysparseymatrix computations*, ver- A sion 2Aedn.A

Saad, Y.A&AM.AH.ASchultzA(1986), 'GMRES:A generalizedAminimumAresidualA algorithmAforAsolving nonsymmetricAlinearAsystems', *SIAMyJ.ySci.yStat.y Comput.y*7, 856–869.A

Sbai, M.A ., A. LarabiA& F. De Smedt (1998), Modeling saltwater intrusion by a 3dA sharp interface finite element model, *in*'Computational Methods in WaterA Resources XII', Computational Mechanics Publications, pp. 201–208.A

Sbai, M.A .A&AF.ADeASmedtA(1997*a*), FiniteAelement transportAmodeling usingA preconditioned biconjugate gradient stabilized methods, *in*'Proc. Of BHSA 6th National Hydrology Symposium', Salford University, pp. 3.9–3.15.A

Sbai, M.A . & F. De Smedt (1999), 3-d finite element model for simulation ofA the moving fresh-salt water interface, *iny*W.De Breuck & L.Walschot, eds, 'ProceedingsAofAtheA15thAsalt-waterAintrusionAmeeting', UniversityAofAGhent, Flemish J. of Nat. Sci., pp. 91–97.A

Sbai, M.A. & F. De Smedt (1997*b*), 3d sharp interface finite element model forA simulation of saltwater intrusion, Progress report 95-96 of avi-73 project, Laboratory of Hydrology, Free University Brussels.A

Segol, G. (1994), *ClassicyGroundwaterySimulations:yProvingyandyImprovingyNu-y mericalyModels*, Prentice Hall, Inc.A

Segol, G., G.AF.APinderA&AW.AG.AGrayA(1975), 'A galerkin-finiteAelement techniqueA for calculating theAransient positionAof the saltwaterAfront', *WateryResour.y Res.y***11**(2), 343–347.A

Simon, H.AD.A(1989), DirectAsparseAmatrix methods, *iny* J.AC.AlmondA&A D. M.Young, eds, 'Modern numerical algorithms for supercomputers', TheA UniversityAofATexasAat Austin, CenterAforAhighAperformanceAcomputing, ustin, pp. 325–444.A

Sleijppen, G.AL.A&AD.AR.AFokkemaA(1993), 'BICGSTAB(L)AforAlinearAequationsA involving unsymmetric matrices with complex spectrum', *Elec. Trans.yNum.y Anal.y*pp. 11–32.A

Sonneveld, P.A(1989), 'CGS, a fastAlanczos-typeAsolverAforAnonsymmetricAlinearA systems', *SIAMyJ.ySci.yStat.yComput.y***10**, 36–52.A

Spitz, Karlheinz & Joanna Moreno (1996), *Aypracticalyguideytoygroundwateryandy soluteytransportymodeling*, John WileyASons, Inc., 605, Third Avenue, NewA York. NY 10158-0012.A

Strack, O.AD.AL.A(1976), 'A single-potentialAsolutionAforAregionalAnterfaceAproblemsA in coastal aquifers', *WateryResour.yRes.y***12**(6), 1165–1174.A

Sugio, S.A&A .AM.ARahimA(1992), ProtectionAofAaAcoastalAaquiferAfromAsaltwaterA intrusionAby artificialArecharge, *iny*ProceedingsAofA12thASaltAwaterAntrusionA meeting', Barcelone, pp. 319–331.A

Sugio, S. &AC. S. Desai (1987), 'Residual flowAprocedure for seaAwaterAntrusion inA unconfined aquifers', *Int.yJ.yforyNum.yMeth.yinyEng.y***24**, 1439–1450.A

Tang, D.AH.A&AD.AK.ABabuA(1979), 'AnalyticalAsolutionAofAaAvelocityAdependentA dispersion problem', *WateryResour.yRes.y***15**, 1471–1478.A

Thompson, J. F., Z. U. A. Warsi & C. W. Mastin (1985), *Numericalygridygenera-y tion:yfoundationsyandyapplications*, Elsevier, North-Holland, New York.A

Tracy, F.AT.A(1994), comparisonAofAFEAandAFVAsolutionsAforAunsaturatedAflowA and contaminant transport in groundwater, *in* A. e. a.Peters, ed., 'X Int.A conf. of comp. methods in Water Resour.', KluwerA cademic Publishers.A

VanADam, J.AC.A&AP.AC.ASikkemaA(1982), 'ApproximateAsolutionAofAtheAproblemA of the shape of the interface in a semi-confined aquifer', *J.yofyHydrology* **56**, 221–237.A

Van der Veer, P.A(1977*a*), 'AnalyticalAsolutionAforAaAtwo-fluidAflowAinAaAcoastalA aquiferAinvolving a phreaticAsurfaceAwithAprecipitation', *J.yofyHydrology* **35**, 271–278.A

Van derAVeer, P.A(1977*b*), 'AnalyticalAsolutionAforAsteadyAinterfaceAflowAin a coastalA aquiferAinvolving a phreaticAsurfaceAwithAprecipitation', *J.yofyHydrology* **34**, 1–11.A

VanAderAVorst, H. A.A(1988), ConjugateAgradientAtypeAmethodsAandAprecondi-A tioning, *iny*'NewADevelopmentsAin GroundwaterAModeling', InternationalA Groundwater Modeling Center, Delft, The Netherlands, IHE Delft.A

VanAderAVorst, H. A.A(1989), 'ICCGAandArelatedAmethodsAforA3-dAproblemsAonA vector computers', *Computeryphysicsycommunicationsy*(53), 223–235.A

Van der Vorst, H. A. (1990), 'Iterative methods for the solution of large systemsA of equations on supercomputers', *Adv.yWateryResour.y***13**(3), 137–146.A

Van der Vorst, H. A. (1992), 'BI-CGSTAB:A fast and smoothly converging variantA of bi-CG for the solution of nonsymmetric linear systems', *SIAMyJ.ySci.y Stat.yComput.y***13**, 631– 644.A

VanAderAVorst, H. A.A&AT.AF.AChanA(1998), LinearAystemAsolvers:AsparseAterativeA methods.A

VanAGenuchten, M.ATh.A(1980), ' closedAformAequationAforApredictingAtheAhy-7 draulicAconductivity of unsaturated soils', *SoilySci.ySoc.yAm.yJ.y***44**, 892– A 898.A

Van Genuchten, M. Th & D. R. Nielsen (1985), 'On describing andApredicting theA hydraulic properties of unsaturated soils', *Ann.yGeophys.y***3**, 615–628.A

Volker, R. E. (1980), Predicting the movement of seawater into a coastal aquifer, TechnicalAReportA51, ustr.AWaterAResour.ACounc., Dept.AofANat.ADevel.A and Energy, ustr. Gov. Publ. Serv., Canberra.A

Volker, R. E. & K. R. Rushton (1982), 'An assessment of the importance of someA parametersAforAseawaterAintrusionAin aquifers and a comparisonAofAdispersiveA and sharp-interface modelling approaches', *J.yofyHydrology* **56**, 239–250.A

Voss, C.A.A(1984), QUIFE-SALTAA finite element modelAfor aquiferAcontaining aA seawater interface, Technical Report Water Resources Investigations ReportA 84-4369, U.S.G.S.A

Voss, C.A., D.ABoldtA&A .AM.AShapiroA(1997), graphical-userAinterfaceAforAtheA u.s.AgeologicalAsurvey'sASUTRA codeAusingAargusAONEA(forAsimulationAofA variable-densityAsaturated-unsaturatedAground-water flow with solute or en-A ergy transport), Technical Report Open-File report 97-421, U.S.G.S.A

Wise, W. R., T. P. Clement & F. J. Molz (1994), 'Variably saturated modeling ofA transient drainage: Sensitivity to soil properties', *J.yofyHydrology* **161**, 91– A 108.A

Xue, Y., C.AXieAJ.AWuAP.ALiuAJ.AWangA&AQ.AJiangA(1995), 'A three-dimensionalA miscible transport model for seawater intrusion in china', *WateryResour.y Res.y*3**1**(4), 903–912.A

Yates, S.AR.A(1988), 'Three-dimensionalAradialAdispersionAin a variableAvelocityAflowA field', *WateryResour.yRes.y*2**4**(7), 1083–1090.A

Yeh, G.AT.A&AD.AS.AWardA(1980), FEMWATER:A finiteAelementAmodelAofAwa-A terAflowAthroughAsaturated-unsaturatedAporousAmedia, TechnicalAReportA ORNL-5567, Oak Ridge National Laboratory, Oak Ridge, Tennessee.A

Yeh, G.AT.A&AD.AS.AWardA(1981), FEMWASTE:A finiteAelementAmodelAofA wasteAtransportAthroughAsaturated-unsaturatedAmedia, TechnicalAreport, Oak Ridge National Laboratories, Oak Ridge, Tenn.A

Yeh, G. TA., J. R. Cheng HA. R. 2Cheng J. Hsin-Chi R. D. Richards C. A. Talbot A &AN.AL.AJonesA(1997), FEMWATER:A three-dimensionalAfiniteAelementA computerAmodelAforAsimulatingAdensity-dependent flowAandAtransportAinA variably saturated media, Technical Report CHL-97-12, Dept. of Civil Eng., Pennsylvania State University.A

Zheng, C. (1990), MT3D:A modular three-dimensional transport model for sim-A ulation of advection, dispersion and chemical reactions of contaminants inA groundwater systems, Technical Report 170, U.S. EPA Report.A

Zheng, C. & Gordon D. Bennett (1995), *Appliedycontaminantytransportymodeling:y theory andypractice*, Van Nostrand Reinhold, New York.A

Zienkiewics, O.AC.A&AR.AL.ATaylorA(1989), *Theyfiniteyelementymethod*, Vol. 1A, McGraw-Hill.A

Zijl, W.A&AM. NawalanyA(1993), *NaturalyGroundwateryFlow*, LewisAPublishers, Boca Raton.A

Appendix AG

Analyticalysolutionsyforytransienty seepagey

A.1 Linearizationytechniquesy

The Dupuit theory simplifies the governing groundwater flow equation, but doesA notAremoveAallAtheAnonlinearity.ATheAcommonAmethodsAofAlinearizationAseekAtoA escape from this difficulty by transforming the original governing equation to anA equivalent form, which can be directly solved using standard applied mathemat-A ics.AForAtheAsakeAofAsimplicity, theAtechniqueAwillAbeAbrieflyAdescribeAinAcaseAofA 1-D Boussinesq's equation, with no sources/sinksA

$$\frac{\partial h}{\partial t} = \frac{k}{n_e}\frac{\partial}{\partial x}(h\frac{\partial h}{\partial x}) \qquad (A.1)$$

1.AThe simplest idea consists on approximating the dependent variable by anA averaged value $\overline{h}$ in the right handAside of equation A.1, such thatA

$$\frac{\partial h}{\partial t} \approx \frac{k\overline{h}}{n_e}\frac{\partial^2 h}{\partial x^2} = \frac{\overline{T}}{n_e}\frac{\partial^2 h}{\partial x^2} \qquad (A.2)$$

where $\overline{T}$ is the apparent transmissivity.AEquationA .2 is equivalent to theA famous heat conduction PDE for which a known space of basic solutionsA isAavailable, e.g.AtheAerrorAfunction.AHowever, theAapproximationAusedAinA equationA .2 remains valid for small variations in the flow field, otherwiseA errors are significant.A

2. A second method assumes $\frac{kh}{n_{ed}}$ asAconstant, such thatAequationA .1Abecomes linear withAh^2.7

ItAhasAbeenAdemonstrated that theAsecondAmethodAisAmoreAaccurateAthanA the first one, because the linearization inAh^{24}preserves somewhat the nonlinearA behavior of the original equation (Polubarinova-Kochina, 1962; Guo, 1997)A

A.2y Polubarinova-Kochina'syseriesyfunctionsy

The analyticalAsolutionAprovidedAnASectionA4.3Aisagiven in a formAof an expansionA series, whose first three terms are evaluated by Polubarinova-Kochina asA

$$u_1(\eta) = \frac{2}{\sqrt{\pi}} \int_{04}^{\eta} e^{-t^2} dt = \operatorname{erf}(\eta) \qquad (A .3) \qquad A$$

$$u_2(\eta) = \frac{1}{\pi}(1 - e^{-2\eta^2}) - \frac{1}{\sqrt{\pi}} \eta e^{-\eta^2} u_{14} - \frac{1}{2} u_{14}^{34} + (\frac{1}{2} - \frac{1}{\pi}) u_{14} \qquad (A.4)A$$

$$\begin{aligned} u_3(\eta) \;=\; & \frac{1}{2} u_{14}^{34} + \frac{9}{4\sqrt{\pi}} \eta e^{-\eta^2} u_1^{24} - \frac{1}{2\sqrt{\pi}} \eta^3 e^{-\eta^2} u_{14}^{24} + \frac{3}{\pi} e^{-\eta^2} u_{14} - \frac{1}{\pi} \eta^2 e^{-2\eta^2} u_{14} - \qquad (A.5) \\ & \frac{1}{\pi\sqrt{\pi}} \eta e^{-\eta^2} - \frac{1}{2\pi\sqrt{\pi}} \eta e^{-3\eta^2} - \frac{3\sqrt{3}}{4\pi} u_1(\eta\sqrt{3}) + (1 - \frac{2}{\pi}) u_{24} + (\frac{3\sqrt{3}}{4\pi} - \frac{1}{2}) u_{14} \end{aligned}$$

Tabulated values of this functions for values of η fromA0 toA4 areagivenAin tableA .1A below.AOneAmayAnoticeAhowever Athat Aby Atruncating Athe Apower Aseries Aexpansion A in equation (4.25) to the second term, the solution simplifies toA

$$h(\eta, t) = h_1(1 + l \operatorname{erf}(\eta)) = h_{14} + (h_{04} - h_1) \operatorname{erf}(\eta) \qquad (A .6) \qquad A \quad A$$

whichAis theAsolutionAof theAinearizedABoussinesqAequation using theAfirstAmethodA (Bear, 1972).A

TableA .1:A*Coefficientsyofyseriesyusedyinytheyolubarinova-Kochina'syanalyticaly solution.y*

η	u_{14}	u_{24}	u_{34}
0	0A	0A	0A
0.1A	0.1125A	+0.0141A	-0.0039A
0.2A	0.2227A	+0.0160A	-0.0081A
0.3A	0.3286A	+0.0073A	-0.0090A
0.4A	0.4284A	-0.0092A	-0.0049A
0.5A	0.5205A	-0.0300A	+0.0039A
0.6A	0.6039A	-0.0519A	+0.0159A
0.7A	0.6778A	-0.0718A	+0.0280A
0.8A	0.7421A	-0.0874A	+0.0373A
0.9A	0.7969A	-0.0975A	+0.0422A
1.0A	0.8427A	-0.1017A	+0.0418A
1.1A	0.8802A	-0.1004A	+0.0368A
1.2A	0.9103A	-0.0946A	+0.0281A
1.3A	0.9340A	-0.0855A	+0.0194A
1.4A	0.9523A	-0.0744A	+0.0078A
1.5A	0.9661A	-0.0626A	-0.0011A
1.6A	0.9764A	-0.0510A	-0.0079A
1.7A	0.9838A	-0.0394A	-0.0125A
1.8A	0.9891A	-0.0310A	-0.0147A
1.9A	0.9928A	-0.0232A	-0.0151A
2.0A	0.9953A	-0.0169A	-0.0141A
2.5A	0.9996A	-0.0024A	-0.0047A
3.0A	0.9999A	-0.0002A	-0.0006A
3.5A	1A	-0.0000A	-0.0001A
4.0A	1A	-0.0000A	-0.0001A

Appendix By

Meuller's methody

B.1 Synopsisy

This methodAfinds a zero of a real functionAf(x) = 0. An initial approximationA to the zero must be given.A

ThisAuses an interpolatingApolynomialAP(x)AofAdegree two, by usingAthreeA approximate values for a root and approximates $f(x)$ near the root to be obtained.A One of the roots for AP(x) A 0Ais taken as the next approximate root of Af(x).AInA this way iteration is continued.AThis algorithm has the following featuresA

- Derivatives ofAf(x) are not requiredA
- The function is evaluated only once at each iterationA

B.2y Descriptiony

LetAα be a root ofAf(x) and let three values Ax_{i-24} x_{i-14}andAx_i be approximationsA to the root (See later explanation for initial values Ax_{14}, x_{24}andAx_3). According toA Newton'sAnterpolation formula ofAdegree two, $f(x)$ is approximatedAby using theA three values described above as followsA

$$P(x) = f_i + f[x_i, x_{i-1}](x - x_i) + f[x_i, x_{i-1}, x_{i-2}](x - x_i)(x - x_{i-1}) \qquad \text{(B.1)}$$

A

where $f_i = f(x_i)$, and $f[x_i, x_{i-1}]$ and $f[x_i, x_{i-1}, x_{i-2}]$ are the first and the second order divided differences of $f(x)$, respectively, and are defined as follows

$$\begin{aligned} f[x_i, x_{i-1}] &= \frac{f_i - f_{i-14}}{x_i - x_{i-14}} \\ f[x_i, x_{i-1}, x_{i-2}] &= \frac{f[x_i, x_{i-1}] - f[x_{i-1}, x_{i-2}]}{x_i - x_{i-24}} \end{aligned} \tag{B.2}$$

$P(x) = 0$ is then solved and the two roots are written as

$$\begin{aligned} x &= x_i - \frac{2f_i}{\omega \pm \{\omega^2 - 4f_i f[x_i, x_{i-1}, x_{i-2}]\}^{1/2}} \\ \omega &= f[x_i, x_{i-1}] + (x_i - x_{i-1})\, f[x_i, x_{i-1}, x_{i-2}] \end{aligned} \tag{B.3}$$

Of these two roots for $P(x) = 0$, the root corresponding to the larger absolute value of the denominator in the second term of equation (B.3) is chosen as the next iteration value x_{i+1}. This means that x_{i+1} is a root closer to x_i. In equation (B.1), if the term of x^2 is null, i.e., if $f[x_i, x_{i-1}, x_{i-2}] = 0$, the following equation is used in place of using equation (B.3)

$$\begin{aligned} x &= x_i - \frac{f_i}{f[x_i, x_{i-1}]} \\ &= x_i - \frac{x_i - x_{i-1}}{f_i - f_{i-1}} f_i \end{aligned} \tag{B.4}$$

This is the secant method.

In equation (B.1) also, if both terms x and x^2 are null, $P(x)$ reduces to a constant and the algorithm fails. (See later explanation.)

B.3 Algorithm

- Initial values x_1, x_2 and x_3

The three initial values are set as follows: Let x be an initial value set by the user in the input parameter X.

When $x \neq 0$

$x_1 = 0.9x$

$x_{24} = 1.1x$

$x_{34} = x$

When $x = 0$,

$x_{14} = -1.0$

$x_{24} = 1.0$

$x_{34} = 0.0$

- When $f(x_{i-2}) = f(x_{i-1}) = f(x)$

This corresponds to the case in which both terms x and x^{24} in equation (B.4) are null, so Muller's method cannot be continued.

The subroutine changes x_{i-24}, x_{i-1}, and x_i and tries to get out of this situation by setting

$x'_{i-24} = (1 + p^n)x_{i-24}$

$x'_{i-14} = (1 + p^n)x_{i-14}$

$x'_i = (1 + p^n)x_i$

where $p = u^{-1/10}$, u is the unit round off and n is the count of changes. Muller's method is continued by using x'_{i-24}, x'_{i-1}, and x'_i. When more than five changes are performed the subroutine terminate unsuccessfully.

B.4 Convergence criteria

The following two criteria are used.

Criteria I. When the approximate root x_i satisfies $f(x_i) \leq \varepsilon$ the x_i is taken as the root.

Criteria II. When the approximate root x_i satisfies $|x_i - x_{i-1}| \leq \gamma.|x_i|$ the x_i is taken as the root. When the root is a multiple $|x_i|$ root or very close to another root, γ must be set sufficiently large. If $0 \leq \gamma < u$, the subroutine resets $\gamma = u$.